



## **Evolving microfluidics: Moving towards clinical applications**

**Shah, Pranjul Jaykumar**

*Publication date:*  
2011

*Document Version*  
Publisher's PDF, also known as Version of record

[Link back to DTU Orbit](#)

*Citation (APA):*  
Shah, P. J. (2011). *Evolving microfluidics: Moving towards clinical applications*. Technical University of Denmark.

---

### **General rights**

Copyright and moral rights for the publications made accessible in the public portal are retained by the authors and/or other copyright owners and it is a condition of accessing publications that users recognise and abide by the legal requirements associated with these rights.

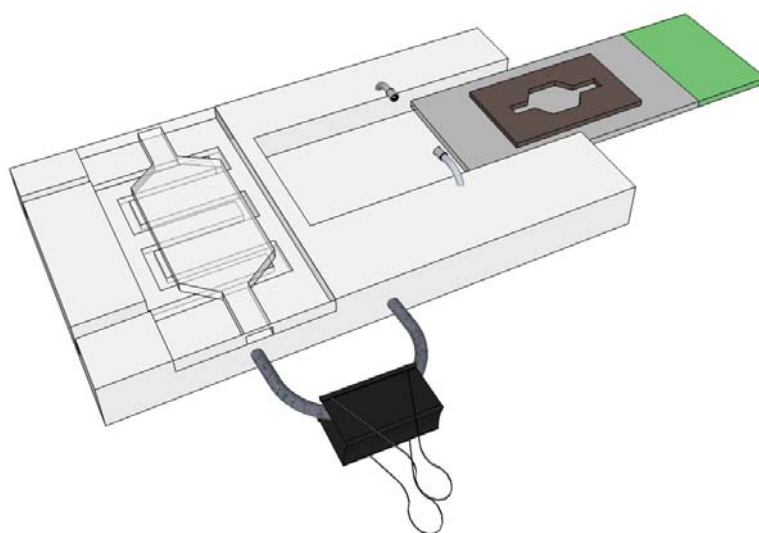
- Users may download and print one copy of any publication from the public portal for the purpose of private study or research.
- You may not further distribute the material or use it for any profit-making activity or commercial gain
- You may freely distribute the URL identifying the publication in the public portal

If you believe that this document breaches copyright please contact us providing details, and we will remove access to the work immediately and investigate your claim.

# Evolving microfluidics: Moving toward clinical applications

---

Pranjul Shah



PhD Thesis

Nano-Bio Integrated Systems Group  
Department of Micro and Nanotechnology  
Technical University of Denmark

**January 2011**

*The efforts of most human-beings are consumed in the struggle for their daily bread, but most of those who are, either through fortune or some special gift, relieved of this struggle are largely absorbed in further improving their worldly lot.*

*Beneath the effort directed toward the accumulation of worldly goods lies all too frequently the illusion that this is the most substantial and desirable end to be achieved; but there is, fortunately, a minority composed of those who recognize early in their lives that the most beautiful and satisfying experiences open to humankind are not derived from the outside, but are bound up with the development of the individual's own feeling, thinking and acting.*

*The genuine artists, investigators and thinkers have always been persons of this kind. However inconspicuously the life of these individuals runs its course, none the less the fruits of their endeavors are the most valuable contributions which one generation can make to its successors....*

**-Albert Einstein in Emmy Noether's obituary (1935)<sup>1</sup>**

***To my family and mentors***

## Preface:

This thesis has been submitted as a partial fulfillment of the requirements for obtaining a Ph.D. degree from the Technical University of Denmark (DTU). The research for the Ph.D. project was conducted at DTU-Nanotech, Department of Micro and Nanotechnology, from January 2007 to December 2010.

This project was supervised by Associate Professor Winnie Svendsen, group leader of the Nano-Bio Integrated Systems (NaBIS) group in the Self-Organizing Materials for Nanotechnology (NanoSOM) section. The project was co-supervised by Associate Professor, Fridolin Okkels group leader of the Theoretical Microsystems Optimizations Group and Assistant Professor Maria Dimaki from NaBIS group.

The project formed an integral part of the Chromosome Total Analysis project (c-tas) funded by research grants from FTP and Lundbeck along with 3 other Ph.D. projects. The overall aim of the C-TAS project was to create a total analysis system to identify translocations in patient samples. This research was conducted in close collaboration with Prof. Niels Tommerup and Asso. Prof. Asli Silahtaroglu from the Wilhelm Johanssen Centre of Functional Genomics at The Panum Institute and Prof. Zeynep Tumer from the Kennedy Institute.

Mid-way through the project, I had an opportunity to spend 6 months in US as a Kauffman Global Scholar and observe some of the pioneers of 'User-driven innovation' - focusing on the imminent needs of the end-users. This immerse program allowed me to interact these thought leaders at MIT (Sloan Business school, Media Labs, D-labs), Olin College of Engineering (Prof. Lynn Stein), Harvard (Whitesides group, Diagnostics for All), Stanford University (Biodesign Program), IDEO, among many others and followed by an internship at DEKA Research and Development, arguably one of the most innovative companies around. This experience changed my attitude towards research and to a greater extent even challenged the views I had adhered to in my earlier work. They pushed me to focus more on 'what is needed' than 'what is possible'. The difference between 'invention' and 'innovation' were crystal clear in my head. In line with DEKA's guiding motto "FAIL FAST AND SUCCEED SOONER", I focused more on the result driven development track than lingering on dead ends or delaying issues.

As a result, apart from the work included in this thesis, the project has also been instrumental in discovering a number of inventions which are currently under patent review and hence could not be included in this thesis due to confidentiality issues. A



chapter describing these inventions briefly has been appended to the thesis. Papers not included in the description of the thesis have been put in a separate appendix.

In general, this thesis applies to readers with prior knowledge in micro and nanofabrication, simulations, microfluidic theory and some basic genetic and biological analysis experience. As this project was a multidisciplinary endeavor, there is a hope that biologists as well as geneticists will find it informative. Major emphasis of this work was on optimization of the current microfluidic toolkit to enable rapid integration and development of various existing and developed microfluidic platforms into commercially viable and readily deployable cytogenetic solutions.

Kgs. Lyngby 2800

Pranjul Shah

## Abstract:

The field of microfluidics faces significant challenges in order to achieve wide-spread usage of microfluidic devices. Among the biggest challenges, there is an imminent need to develop microfluidic systems which are reliable, robust, user-friendly, reconfigurable, versatile, flexible, possibly automated, disposable, low cost and above all solving real problems.

Taking microfluidics and miniaturized analytical systems a step further, this thesis is focused on achieving the vision of a chromosome total analysis system (C-TAS). The aim of this thesis was to develop a  $\mu$ TAS system with functional integration to enable it to analyze chromosomes for possible chromosomal rearrangements called translocations. To realize such a C-TAS, the key challenge is to integrate various pre-processing steps (cell culture, cell lysis, chromosome extraction, chromosome isolation and waste manipulation) and finally the analysis (FISH) on a single chip. Hence, the biggest motivating factor for this research was the fact that we could power a chip to analyze rapidly and effectively human chromosomes and screen them for any possible translocations. This could prove to be a big leap forward in the field of cytogenetics and clinical diagnostics.

In the beginning of the project, the focus was on developing a modular microfluidic platform for integrated sample handling and analysis, but later the focal point was shifted on realizing integrated solutions to lessen the complexities of existing protocols. In the course of the project, a first substrate independent versatile microfluidic motherboard was developed allowing easy interfacing of microfluidic modules via plug and play functionality. The integrated fluidic and electrical network in the motherboard provided users with substrate and design independence at the expense of size and position of fluidic and electrical interconnections. Our attempts to adapt the modular motherboard into C-TAS system provided significant insights into the existing work routines of the central labs. This led to the transition of development efforts from the 'modular approach' towards a more 'integrated approach'.

In an effort to tackle challenges with respect to identification of unknown chromosomal translocations, this thesis focused on developing a novel toolkit of miniaturized devices providing the features of cell culture, slide preparation and Fluorescence *In-Situ* Hybridization (FISH) analysis.

The key objectives included:

- Development of a novel approach for culture of non-adherent cells such as peripheral T-lymphocytes.
- Integration of a slide preparation protocol with the cell culture device, leading to a minimal handling device for sample pretreatment and slide preparation.
- To complete the puzzle, the first miniaturized protocol for performing metaphase FISH analysis on chip was developed.
- A novel FISH cartridge was developed to automate the FISH analysis and create a minimal handling integrated device for metaphase FISH analysis.
- Finally, a strategy to integrate the new toolkit into a C-TAS was devised as a step towards development of a clinically viable system ready for deployment in genetic labs.

Together with the development of the C-TAS, many efforts have been put into solving practical issues hampering progress of microfluidic technologies into commercial and clinical applications. Novel interconnection techniques were invented for rapidly interfacing microfluidic devices with the macro world. In brief:

- The plug and play socket based approach was developed for the interfacing of various modules with the modular motherboard.
- Spring actuated interconnections were developed to create the first self-actuated self-sealing microfluidic interconnect technology providing multiple, parallel, reusable, aligned and bonding-free interconnections demonstrated in both planar as well as vertical formats [Patent pending].
- Quickfix interconnects for adhocly attachable fluidic connections were devised in an attempt to create ultra low cost, reusable interconnects for easy interfacing with microfluidic devices [Patent – in process].
- Novel O-rings with functional scaffolds for microfluidic devices for neuronal and cell culture applications [Patent – in process].

Clinical validation and testing of applicability of the presented systems in relevant areas is currently underway through collaborators. The focus in the near future will be towards wide scale clinical implementation of this microfluidic toolbox.

## Abstract in Danish:

Microfluidics-feltet står overfor omfattende udfordringer for at opnå udbredt brug af *mikrofluidiske devices*. Blandt de største udfordringer er et presserende behov for udvikling af *mikrofluidiske systemer* som er pålidelige, robuste, brugervenlige, *rekonfigurerbar*, alsidige, fleksible, muligvis automatiserede, beregnede til engangs-brug, billige og frem for alt i stand til at afhjælpe faktiske problemer.

Denne afhandling tager *mikrofluidiske* og *miniaturiserede analytiske systemer* ét skridt videre, idet fokus er opnåelsen af visionen om et *kromosom total analyse system* (C-TAS) [www.c-tas.dk]. Målet for projektet var udviklingen af et  $\mu$ tas system med funktionel integration der skulle gøre det i stand til at analysere kromosomer for mulige *kromosom omlejring*er som kaldes *translokationer*. For at opnå et sådan *kromosom total analyse system*, er den væsentligste udfordring integrationen af forskellige *forbehandlingsstrin* (celledyrkning, celle *lysis*, kromosom udvinding, kromosom *isolation* og behandling af spildprodukter) og selve analysen (FISH) på en enkelt chip. Derfor har den væsentligste motivation for dette forskningsarbejde været ønsket om at gøre en chip i stand til hurtigt og effektivt at analysere menneskelige kromosomer, og *screen*e dem for samtlige mulige translokationer. Dette ville kunne betyde et stort spring fremad indenfor feltene cytogenetik og kliniske diagnostik.

I begyndelsen af projektet fokuseredes på udvikling af en modulopbygget *mikrofluidisk* platform til integreret prøvehåndtering og -analyse, men senere rettedes fokus mod opnåelse af integrerede løsninger med henblik på reduktion af kompleksiteten i eksisterende protokoller. I løbet af projektet udvikledes et første substrat-uafhængigt, alsidigt *mikrofluidisk motherboard* som muliggør let tilkobling af *mikrofluidiske* moduler via *plug-and-play* funktionalitet. Det integrerede *fluidisk* og elektriske netværk i *motherboard*'et gav brugeren uafhængighed af substrat og design på bekostning af fastlåste størrelser og positioner for de *fluidiske* og elektriske forbindelser. Vores forsøg på at tilpasse dette modulære *motherboard* i C-TAS gav væsentlig indsigt i de arbejdsrutiner, som pt er etableret i centrallaboratorierne. Dette førte til at udviklingsindsatsen flyttedes fra en "modulær tilgang" hen mod en mere "integreret tilgang".

I et forsøg på at tackle udfordringerne vedrørende identifikation af ukendte *kromosom translokationer*, har projektet fokuseret på udvikling af et nyt sæt af redskaber bestående af *miniaturiserede devices* med *funktioner* der omfatter celledyrkning, *objektglas klargøring* og Fluorescence *In-Situ* Hybridization [FISH] analyse.

- Udvikling af en ny tilgang til kultur af ikke-klæbende celler såsom perifere T-lymfocytter.
- Integration af et objektglas klargøringsprotokol med cellekultursenheden, hvilket fører til en minimal håndteringsenhed for prøve forbehandling og objektglasklargøring.
- Til at færdiggøre puslespillet, var den første miniaturiserede protokol for udførelse af metafase FISH analyse på chip udviklet.
- En ny FISH patron blev udviklet for at automatisere FISH analyse og skabe en minimal håndterings integreret enhed for metafase FISH analyse.
- Endelig en strategi for at integrere den nye værktøjskasse med C-TAS-systemet blev udtænkt, som vil resultere i en klinisk bæredygtigt system klar til indsættelse i genetiske laboratorier.

Sammen med udviklingen af C-TAS, har vi også bestræbet os på at løse praktiske problemer, som hindrer fremskridt af teknologien mod kommercielle og kliniske anvendelser. Nye sammenkoblingsteknikker blev opfundet for hurtigt at kunne koble mikrofluidiske systemer med makro-verdenen. Kort sagt:

- Plug and play stik blev udviklet til at koble forskellige moduler med motherboardet.
- Sammenkoblinger baseret på fjeder-princippet blev udviklet til at skabe den første selvaktiverede og selvlukkende sammenkoblingsteknologi, der giver flere parallelle, genanvendelige, afrettede og limningsfrie sammenkoblinger. Dette er blevet demonstreret i både plane såvel som vertikale formater [Patentanmeldt].
- QuickFix sammenkoblinger til ad-hoc fluidiske forbindelser er blevet udviklet i et forsøg på at skabe billige, genanvendelige sammenkoblinger for nemme forbindelser med mikrofluidiske systemer [Patent - i processen].
- Nye O-ringe med funktionelle platformer for neuron- og cellekultur anvendelser [Patent - i processen].

Klinisk validering og afprøvning af anvendeligheden af de forelagte ordninger inden for de relevante områder er i øjeblikket i gang gennem samarbejdspartnere. I den nærmeste fremtid vil vi rette fokus mod den kliniske afprøvning af denne mikrofluidiske værktøjskasse.

## Acknowledgements:

This thesis marks the end of my life-long quest for education (for now). Through all its struggles and triumphs, it has been the most remarkable 4 years of my life. I couldn't have done this all alone, and I would like to take a moment to thank all those who have contributed to this feat.

First and foremost, I would like to thank the two pillars of my life - **Niki** and **Kiah**, you have been my inspiration, motivation and constant source of support and love. Although it has been a constant struggle, we have persevered and grown closer in the process. Thank you for letting me chase my personal goals and bearing my long disappearances.

Working on this thesis has been a privilege and many thanks go to my supervisor, **Winnie Svendsen** for putting her faith in me and standing by me through the ups and downs of this project. I sincerely appreciate the excellent learning environment you have provided me with and congratulate you for bringing together such an excellent group of talented people. I am extremely grateful for your ability to tackle difficult situations and admire your courage at going to all lengths to solve issues for your students. Much of the accomplishments and awards received as part of this project wouldn't have been possible without your supportive and open nature towards new and even crazy ideas. Thank you for expanding my scientific imagination and innovative capacity.

I would like to specially thank **Maria Dimaki** for her continuous guidance and supervision throughout the project. I am deeply grateful for all your help with the thesis. Without you, I could have never managed this work.

I am particularly grateful of my co-supervisor, **Fridolin Okkels** for his supervision, guidance and discussion of the results and support with the theoretical and simulations aspect of this project.

I would like to personally thank the entire **NaBIS group** for making sure that the cake never ran out and for their collective enthusiasm, social and scientific environment. I have been incredibly fortunate to be continually surrounded by amazing people throughout my PhD. You have influenced me and this project, in numerous ways.

I am grateful of **DTU-Nanotech**, to provide me with the state of the art facilities and making this research possible. And everyone at Nanotech, you have been my extended family for the last 4 years.

Without expert and efficient administrative assistance provided by **Jette, Anne-Line, Peter, Dorthé, Birgitte, Pernille, Michael, Nathalie, Rolf** and others, the project would have not run as smoothly as it did. I tried my best to bring you as many challenges as I could, but you have continually showed me that we have one of the most competent admin groups at Nanotech.

And finally my comrades, who deserve a special mention:

**Indu** – For all those weekends, late nights and evenings you put aside for helping me bring the project back on track. Thank you.

**Dorota** – For joining the pursuit, it was good to have you on board late than never.

**Romen** – For helping me through the final experiments and being the ‘tovholder’ of the impedance project.

**Lars** – For bringing the much needed biological expertise to the group and your assistance with CFSE experiments.

In the end, most importantly, my parents who let me sail 8 years ago on this wonderful journey, which has brought me here today. Thank you for your love and blessings.

## Publications:

### *Patents:*

[2009, Application # 09169729.2-2404] Multiplex Analyte Concentration Measurement

[2010, Application # 10159494.3-2320] Radial peristaltic pump

[2010, Application # 10159495.0-2315] Multi-infusion pump

[2010, Application # 10164907.7-1270] Spring Actuated Microfluidic Interconnects

[2011, In process] Sandwiched membranes

[2011, In review] Adhocly attachable microfluidic interconnections

### *Peer-Reviewed Journals:*

[In preparation: To be submitted to Interface] Novel scaffolds for microfluidic cell and neuronal cultures

[In preparation: To be submitted to Lab Chip] QuickFix Interconnects: One step fluidic and electrical interconnections for microfluidic applications

[In preparation: To be submitted to Lab Chip] FISH reagent cartridge: Minimal handling Fluorescence *in-situ* Hybridization

[In preparation: Book Chapter for Cytogenetics book (InTech Publishers)] Cytogenetics meets microfluidics

[In preparation: To be submitted to Integrative Biology] Microfluidics evolving Cytogenetics

[Submitted: Invited Review to BioEssays] Dorota Kwasny, Indumathi Vedarethinam, **Pranjul Shah**, Maria Dimaki, Asli Silahtaroglu, Zeynep Tumer, Winnie E. Svendsen. *Advanced microtechnologies for detection of chromosome abnormalities*.

[Submitted to Biomicrofluidics] **Pranjul Shah**, Romén Rodriguez-Trujillo, Maria Dimaki, Winnie E. Svendsen. *Versatile motherboard enabling substrate independent plug and play microfluidics*.

Winnie Svendsen, Jaime Castillo-Leon, Jacob Lange, Luigi Sasso, Mark Olsen, Mohammed Abaddi, Lars Andresen, Simon Levinsen, **Pranjul Shah**, Indumathi Vedarethinam, Maria Dimaki. *Micro and Nano-Platforms for Biological Cell Analysis*. Sensors and Actuators A: Physical (2011), doi: 10.1016/j.sna.2011.02.027.



**Pranjul Shah**, Indumathi Vedarethinam, Dorota Kwasny, Lars Andresen, Maria Dimaki, Søren Skov, Winnie Svendsen. *Microfluidic Bioreactors for culture of non-adherent cells.*, Sens. Actuators B: Chem. (2011), doi:10.1016/j.snb.2011.02.021.

**Pranjul Shah**, Indumathi Vedarethinam, Dorota Kwasny, Lars Andresen, Søren Skov, Asli Silahatoglu, Zeynep Tümer, Maria Dimaki, Winnie E. Svendsen. *FISHprep: A novel integrated device for metaphase FISH sample preparation*. Micromachines 2, no. 2: 116-128 (2011).

Vedarethinam I. \*, **Shah P.**<sup>1</sup>, Dimaki M., Tumer Z., Tommerup N., Svendsen W.E. *Metaphase FISH on a Chip: Miniaturized Microfluidic Device for Fluorescence in situ Hybridization*. Sensors 2010; 10(11):9831-9846.

Casper Hyttel Clausen, Jacob Moresco Lange, Linda Boye Jensen, **Pranjul Jaykumar Shah**, Maria Ioannou Dimaki, and Winnie Edith Svendsen. *Scanning Conductance Microscopy Investigations on Fixed Human Chromosomes*. Biotechniques: Volume 44 (2), p 225-228, 2008.

Maria Dimaki, Casper Hyttel Clausen, Jacob Moresco Lange, **Pranjul Jaykumar Shah**, Linda Boye Jensen, Winnie Svendsen. *A micro-fabricated platform for chromosome separation and analysis*. In Proceedings of the 17th International Vacuum Congress/13th International Conference on Surface Science/ International Conference on Nanoscience and Technology, Johansson, L. S. O.; Andersen, J. N.; Gothelid, M.; Helmersson, U.; Montelius, L.; Rubel, M.; Setina, J.; Wernersson, L. E., Eds. 2008; Vol. 100.

## ***Peer-Reviewed Conference Proceedings:***

**Pranjul Shah**, Indumathi Vedarethinam, Romén Rodríguez-Trujillo, Maria Dimaki and Winnie E. Svendsen, *Versatile microfluidics for Democratizing Microfluidics*, Advanced Microfluidics Nanofluidics and Asia-Pacific Lab on Chip Conference 2011.

**Pranjul Shah**, Maria Dimaki, Winnie Edith Svendsen, *A novel passive microfluidic device for preprocessing blood for point of care diagnostics*, Transducers 2009, Denver, Colorado.

**Pranjul Shah**, Maria Dimaki, Winnie Edith Svendsen, *An integrated microfluidic system to isolate leukocytes from whole blood*, MMB2009, Quebec, Canada.

**P. J. Shah**, J. M. Lange, C. H. Clausen, M. Dimaki, L. B. Jensen, M. H. Jakobsen, O. Geschke and W. Svendsen, *Fabrication of polymeric microstructures to capture chromosomes on monolayer of antibodies*, MicroTAS 2007, Paris.

**Pranjul Shah**, Remma Sridhar, Maria Dimaki, Fridolin Okkels, Winnie Svendsen, *Spatially optimized mixers to enhance mixing of whole blood with water to lyse red blood cells*, NanoBioEurope, Barcelona, 2008

---

<sup>1</sup> (\* - Joint first authors)

## ***Conference Proceedings:***

**Pranjul Shah**, Maria Dimaki, Winnie Edith Svendsen, *Smart Microfluidic Blood Preprocessing Devices*, National Seminar on Nanoscale Science and Technology 2009, Ghaziabad, India 2009

**Pranjul Shah**, Maria Dimaki, Winnie Edith Svendsen, *Smart Microfluidic Blood Preprocessing Devices*, International Conference on Biomedical and Genomics Research 2009, Ahmedabad, India

**Pranjul Shah**, Remma Sridhar, Maria Dimaki, Fridolin Okkels, Winnie Svendsen, *A microfluidic lyser to extract blood cells*, Northern Nanotech Europe, Copenhagen, 2008

**Pranjul Shah**, Remma Sridhar, Maria Dimaki, Fridolin Okkels, Winnie Svendsen, *Spatially optimized mixers to enhance mixing of whole blood with water to lyse red blood cells*, Nano2Life Scientific Meeting, Crete, 2008

## ***Awards:***

- Danish Ministry of Sci., Tech. and Innovation Award: *Innovation Award*
- Kauffman Global Scholars Program - Scholarship 2010: *Erhvervs og Byggestyrelsen (DKK 120000)*
- Danish Proof of Concept Consortium: *Seed Grant, DKK 1.2 million*
- INCUBA Science Park Special Prize: *IDEA to Concept Award*
- Venture Cup Denmark Finals 2009: *3rd Prize Winner*
- The Mai Bangkok Business Challenge @ Sasin 2009: *Winner (Grand prize & Best pitch)*
- Venture Cup Copenhagen Finals: *Winner*
- Symposium for Biological Research 2008: *Most Innovative Project Award –Danisco Award*
- Northern Nanotech Europe Conference 2008: *Best Poster Award*
- Nano2Life Scientific Meeting 2008: *Best Poster Award*
- European Scientific Writing for the Public: *2nd Place Award*

## ***Travel Bursaries:***

Otto Monsteds Fond, Oticon Fond, Lundbeck Fond, Nano2Life Mobility Fund, Politiken-Fonden, Augustinus Fond, Thriges Fond, Tranes Fond, Lauritz Andersens Fond and Jorcks Fond.

# Contents:

## Chapter 1: Introduction

1.1 Microfluidics: The journey	2
1.2 Incompatible domains	5
1.3 Need for a new approach: The road ahead	7
1.4 A step in the right direction: New objectives and end-goals	11
1.5 Advanced microtechnologies for detection of chromosome abnormalities	12
1.6 Thesis Overview	24

## Chapter 2: Modular C-TAS

2.1 C-TAS: The vision	26
2.2 C-TAS: The challenge	28
2.3 Impending decisions	30
2.4 Versatile motherboard for substrate independent plug and play microfluidics	34
2.5 Outlook	49

## Chapter 3: Integrated C-TAS

3.1 Integrated C-TAS System: Needs and Approach	54
3.2 Microfluidic Bioreactors for culture of non-adherent cells	57
3.3 FISHprep: A novel integrated device for metaphase FISH sample preparation	72
3.4 Metaphase FISH on a chip: Miniaturized microfluidic device for FISH	84
3.5 AutoFISH: FISH Reagent cartridge for minimal handling FISH	99
3.5 Outlook	106

## Chapter 4: Side projects

4.1 The Quest of the Lymphocytes	108
4.2 Integrating Continuous Flow Separation Systems	108
4.3 Pinch flow fractionation (PFF)	110
4.4 Dual pinch flow fractionation (DPFF)	113
4.5 Microfluidic FACSlyser: Lysing based isolation of lymphocytes	118

4.6 Hydrodynamic cell traps	126
4.7 Gravitational conditioning of cells	129
4.8 Continuous gravitational fractionation of lymphocytes	135
4.9 Antibody based trapping of chromosomes	138

## **Chapter 5: Methods**

5.1 Simulations	142
5.2 Cleanroom fabrication protocols	144
5.3 Polymer fabrication protocols	148
5.4 Bonding	152
5.5 Device Recipes	154
5.6 Biological Protocols	161

## **Chapter 6: Patents**

6.1 Multiplexed Analyte Concentration Measurement	168
6.2 Radial Peristaltic Pump	176
6.3 Multichannel infusion pump	177
6.4 Spring Actuated Microfluidic Interconnects	178
6.5 Sandwiched membranes	179
6.6 Adhocly attachable microfluidic interconnections	180

## **Chapter 7: Conclusions**

## **Bibliography**

## **Appendices**

A: A microfluidic system to capture single cells	200
B: Other publications	206
C: Errata	235

# List of figures

**Figure 1.1:** The modular C-TAS system

**Figure 1.2:** Typical goals for microfluidic platforms development

**Figure 1.3:** Modular microfluidic motherboard with 3 sockets for C-TAS modules. The pictures show meandering channel for the integrated mixer and circular rotors for fluid valving.

**Figure 1.4:** An interphase nuclei (blue) (A) and metaphase spreads (B) with X centromeric FISH probes (green dots)

**Figure 1.5:** The cytogenetics analysis protocol. Blood sample is collected from the patient (A). The collected blood (B) is cultured in a medium for 3 days at 37 °C (C). Colchicine is added at the end of the culture period to arrest the cells in metaphase. Followed by hypotonic treatment, the cells are splashed on a glass slide (D) to obtain metaphase chromosome spreads (E). At this point the chromosome spreads can either be analyzed by banding or FISH.

**Figure 1.6:** Fabricated bio-cell chip slide. (A) A PDMS layer with 96 wells for multiple cell analysis. (B) A glass slide with a gold pattern for sample numbering (used with permission from Lee et al, 2007)

**Figure 1.7:** (A) The mask layouts and dimensions of an integrated FISH microchip. The microchip includes a reagent multiplexer, a cell chamber with an integrated thin-film heater, and a peristaltic pump. (B) Image of a complete integrated FISH chip (used with permission from Sieben et al, 2008)

**Figure 1.8:** Microfluidic device for miniaturized FISH. (A) Diagram of the microfluidic PDMS pad with inlet and outlet connected by a straight channel. (B) Complete structure of the FISH device with the PDMS pad assembled with a TiO<sub>2</sub> functionalized glass slide (used with permission from Zanardi et al, 2010)

**Figure 2.1:** The vision of the C-TAS system

**Figure. 2.2:** The C-TAS protocol and original modules

**Figure 2.3:** Modular motherboard and the development challenge

**Figure 2.4:** Design specifications & schematic drawing for motherboard socket and modules (Red dots depict electrical connections and the white dots depict positions of fluidic interconnects. Size is not to scale (2x).

**Figure 2.5:** Designs specifications for the motherboard modules (Red dots depict 6 electrical connections and white dots depict the 6 fluidic connections). Overall dimension 20 x 20 mm.

**Figure 2.6:** Schematic of the motherboard

**Figure 2.7:** Steps of motherboard fabrication and assembly

**Figure 2.8:** (Top) Schematic of the PDMS Lid mould (3 layers put together by screws in the blue slots towards the end)(Bottom) Schematic of a moulded Pluggable interfacing lid

**Figure 2.9:** (Left) Laser ablated double sided tape (Centre and Right) Pluggable module consisting of impedance chip bonded together with Pluggable by means of a double sided tape.

**Figure 2.10:** Schematic of the measurement setup for the impedance cytometer chip

**Figure 2.11:** Rotor assembly on motherboard with integrated O-rings for leak proof interconnections

**Figure 2.12:** Fully assembled motherboard

**Figure 2.13:** (Left) Mold for curing PDMS based Pluggable with alignment pins for through holes. (Right) PDMS Moulded Lid – Pluggable

**Figure 2.14:** (Top-Left) Electrodes on Pyrex wafer (Top-Right) Moulded Lid showing the PDMS channel structure and through holes for interconnections. (Bottom) Impedance chip after oxygen plasma bonding.

**Figure 2.15:** (Left) One touch plug and play assembly (Centre) Assembled motherboard with electrical contacts and external fluidic connection to the syringe. (Right) Impedance chip plugged on the motherboard showing 3 electrical spring pins connecting to the impedance chip. (The fluidic connections are difficult to visualize due to channel width being 10  $\mu\text{m}$ ).

**Figure 2.16:** (Left) Motherboard with integrated electrical connections on test setup with modulation board (Right) Data acquisition setup for simultaneous recording of images and impedance detection of passing beads.

**Figure 2.17:** Beads transiting through the 10  $\mu\text{m}$  channel across the detection zone

**Figure 2.18:** Graph of beads transiting across the detection zone.

**Figure 2.19:** Enlarged image of one transition from the fig. 2.18.

**Figure 2.20:** Comparison of traditional culture plate with pipette and the complex motherboard based protocol needing syringe pumps (not shown in image) for actuation. Apart from complexities related to extra modules, the handling on the motherboard is also much complicated compared to the pipette based traditional protocol.

**Figure 3.1:** Schematic of the integrated C-TAS system. The schematic highlights proposed step by step approach for developing an integrated C-TAS system. The results are depicted in (a) Section 3.2: Cell culture, arrest and fixation device (b) Section 3.3: Metaphase spread preparation device and (c) Section 3.4: FISH analysis device are presented. (d) Automation of the reagents injection (AutoFISH protocol) by means of FISH reagent cartridge.

**Figure 3.2:** Schematic of the  $\mu$ BR. (Top) culture chamber (bottom) perfusion chamber (middle) sandwiched PC membrane

**Figure 3.3:**  $\mu$ BR with the interconnections

**Figure 3.4:** The diffusion of KCl through the membrane for complete media exchange in the culture chamber. Diffusion occurs both through the perfusion channel/membrane interface and through the culture chamber.

**Figure 3.5:** Cells on day 1 on the membrane

**Figure 3.6:** Proliferated cells on the membrane on day 4. It was difficult to focus on the membrane on day 4 due to multiple layers of cells

**Figure 3.7:** Control and PHA stimulated growth count for 3 days culture in culture flask and on chip

**Figure 3.8:** (Left) metaphase spreads from control samples (Right) metaphase spreads from  $\mu$ BR samples

**Figure 3.9:** PHA stimulated growth count for 3 days T-lymphocytes culture on a reused chip.

**Figure 3.10:** Exploded view of the FISHprep device top and bottom part. A polycarbonate membrane is sandwiched between the two parts to form the barrier between the culture chamber and perfusion meander.

**Figure 3.11:** (a) Bonded FISHprep device (b) FISHprep device depicting paper clip based valving procedure.

**Figure 3.12:** (a) Paper clip valve of the external U-section: Isolation of flow from culture chamber to splashing chamber (b) Flow through culture chamber on to the splashing chamber on opening of the paper clip valve (Leakage in the device at 500  $\mu$ L/min flow rate).

**Figure 3.13:** FISHprep culture (a) Cells on Day 0 (b): Cells on Day 3 (background shows pores in the PC membrane). (Inset—Enlarged cytoplasm on Day 3).

**Figure 3.14:** CFSE proliferation assay results. Count of cells vs. the fluorescence intensity of CFSE stained cells analyzed by fluorescence cytometer. (Control experiments relate to negative control of cultures on FISHprep device without PHA stimulation).

**Figure 3.15:** (a) (Top) Chromosome spreads prepared using the FISHprep device (b) (Bottom) Chromosome spreads achieved using the manual dropping technique. Offset pictures present high magnification images

**Figure 3.16:** FISH analysis on the FISHprep samples (The FISH signals indicate the presence of two X-chromosomes in the chromosome spreads and cells).

**Figure 3.17:** Schematic Protocol for splashing the metaphase spreads followed by rapid assembly of the microFISH device.

**Figure 3.18:** Glass slide with laser ablated tape stencil

**Figure 3.19:** The splashing device fabricated with two layers of PMMA.

**Figure 3.20:** (a) Master for moulding PDMS microFISH device lid fabricated in SU-8 photoresist over silicon wafer; (b) PDMS microFISH device lid moulded using PDMS elastomer.

**Figure 3.21:** (a) Peeling off top cover of the double-sided tape stencil to expose the silicone adhesive layer (b) Assembled microFISH device by bonding the microFISH device lid on to the silicone adhesive layer.

**Figure 3.22:** Fully assembled microFISH device with interconnects and tubings to connect it to the syringe pump.

**Figure 3.23:** (a) Sliding of the glass slide with stencil into the splashing device; (b) Splashing device with glass slide. The stencil is positioned under the syringes for splashing glacial water followed by fixed mitotic cells for spreading.

**Figure 3.24:** (a) Metaphase spreads stained with DAPI on the control slides prepared using the traditional dropping method (Inset—40× resolution); (b) Metaphase spreads stained with DAPI on the test slides prepared using splashing protocol (Inset—40× resolution).

**Figure 3.25:** (a) FISH analysis on the control slide. The two green dots highlight the two X chromosomes in the female sample; (b) FISH analysis on the test slide. The two green dots highlight the two X chromosomes in the female sample.

**Figure 3.26:** (Left) AutoFISH device designed in COC with 3 inlets (extra inlet for probe) (Right) Glass slide with tape stencil to spread metaphase chromosomes and bond the COC lid to create an AutoFISH device.

**Figure 3.27:** Loading of reagents on the FISH cartridge with air spacers to separate the reagents.

**Figure 3.28:** Testing of AutoFISH device with reagent cartridge (showing interconnections for rapid connection of the FISH cartridge)

**Figure 3.29:** FISH signals on interphase cells (Green circles highlight the interphase signals)

**Figure 4.1:** A typical continuous flow separation procedure: sample is injected continuously together with a carrier liquid into a wide separation chamber, a force acts at an angle to the direction of flow and sample components are deflected from their flow path and thus spatially separated.

**Figure 4.2:** The model of the pinch flow fractionation system



**Figure 4.3:** Ratio of Flow rates compared to the intersection width ratio assuring aligning of the particles to the channel walls in the pinch segment

**Figure 4.4:** Concept of blood sorting via DPFF

**Figure 4.5:** Concept of blood filtration on Dual Pinch flow fractionation device.

**Figure 4.6:** Illustration of DPFF model. The central channel collects only the WBCs, while the outer channels will collect most of the WBCs and RBCs.

**Figure 4.7:** Tunable DPFF to tune the sorting of particles based on selection of different outlets at the time of application.

**Figure 4.8:** Flow profile of the separation experiment. The flow rates were  $0.8 \mu\text{l}/\text{min}$  for the particles solution and  $20 \mu\text{l}/\text{min}$  for the aligning flow. Channel height is  $31 \mu\text{m}$ . Pictures are edited by adding dots to outline the flow not clearly visible in the picture.

**Figure 4.9:** Microparticles extracted out of the DPFF system central outlet containing particles larger than  $3 \mu\text{m}$ .

**Figure 4.10:** (a) Stroock's design (b,c) Yang's designs 1 and 2 (Bottom) Our proposed design

**Figure 4.11:** Improved vorticity in our design (b) compared to the Stroock's Design (a)

**Figure 4.12:** (Left) Mixing in one cycle of our design with herringbone ridges (Right) Mixing in our one cycle of our design with herringbone grooves. (Red indicates concentration of 0 and blue indicates concentration of 1)

**Figure 4.13:** Figures show the simulations of concentration-diffusion profiles of the cross section after one mixing cycle. (a) Stroock's design (b) Yang's design1 (c) Yang's design 2 (d) Our design with ridges (e) Our design with grooves. (Note: (a, b, c, e) show the contour of the groove and (d) doesn't have a black outline of the groove as it has been simulated with a ridge to compare the difference in mixing (also shown in Fig 4.12(Left)))

**Figure 4.14:** Schematic of the microfluidic FACSLysing principle and Laser ablated FACSLyser.

**Figure 4.15:** (Left) Blood at inlet focused by DI water streams (Right) Blood at outlet focused by PBS solution.

**Figure 4.16:** Trypan blue based viability testing for cells collected from FACSLyser. The background shows debris of the lysed erythrocytes.

**Figure 4.17:** Colorimetric Cell Proliferation WST-1 assay for validating the viability and expansion of Leukocytes after 3 days culture [Section 5.6.11].

**Figure 4.18:** Quantification of lysing on chip and comparison with traditional FACSLysing technique for different lysing solutions.

**Figure 4.19:** The schematic of the trapping system with inset pictures focussing on the positioning of cell traps before meanders and depicting the trapping mechanism of a cell in the cell trap.

**Figure 4.20:** (Left) one trap system (Right) Equivalent electrical circuit diagram based on hydrodynamic resistances of the one trap system

**Figure 4.21:** 10  $\mu\text{m}$  polystyrene beads trapped in the cell traps (Image courtesy: Jacob Lange)

**Figure 4.22:** Jurkat cells (15  $\mu\text{m}$ ) squeezing through a 5  $\mu\text{m}$  cell trap

**Figure 4.23:** Schematic of design 1.

**Figure 4.24:** Sedimentation of cells from loading channel into concentration channel via the sedimentation channel

**Figure 4.25:** Cells concentrated in the concentration channel after 1 and 3 min of the concentration protocol relating to the first and third cycle of the protocols respectively.

**Figure 4.26:** Grooved chamber for gravitational concentration of cells. The cells are perfused from A to B i.e. perpendicular to grooves leading to sedimentation of the cells in the grooves on stopping of the flow and subsequent trapping in the convection free zone on restarting of the flow.

**Figure 4.27:** (Left) Simulation of flow across the grooves showing convection above the groove and diffusion in the grooves (Right) Stop and Flow based gravitational trapping of cells

**Figure 4.28:** Time lapse of concentration of cells using gravitational sedimentation into convection free zone of the grooved chamber.

**Figure 4.29:** (Left) Magnified image of concentration showing multiple layer buildup of cells and (Right) Higher concentration of cells in the edge of the grooved chamber due to unbalanced hydrodynamic resistances due to clogging in the middle of groove.

**Figure 4.30:** Operation of Ficoll-Paque based isolation of blood sub-types. ([www.ge.com](http://www.ge.com))

**Figure 4.31:** Depicting normal flow of cells without including gravitational sedimentation

**Figure 4.32:** High throughput gravitational hydrodynamic sedimentation designs

**Figure 4.33:** High throughout gravitational sedimentation of erythrocytes

**Figure 4.34:** Depicting isolation of lymphocytes due to floatation in Ficoll-Paque medium.

**Figure 4.35:** Fabrication of PDMS membranes to act as stencil for selective surface activation for antibody binding.

**Figure 4.36:** Process of surface passivation, selective activation and subsequent trapping of the antibodies

**Figure 4.37:** (Left) Anti-CENP A patterning showing clear defined edge of coating (Right) Showing unspecific binding of chromosomes on both the sides of the dotted line demarking the edge of the CENP-A coating.

**Figure 5.1:** (Left) Micromilling process (Right) Tools used for micro milling (Courtesy: Janpo)

**Figure 5.2:** (Top) Typical Gaussian profile of structures (under 400  $\mu\text{m}$ ) ablated in PMMA with fewer than 60% laser power (Bottom) Typical profile of a large channel structure (wider than 1 mm) made in PMMA with 50% laser power. Another typical effect observed in channel structures made with laser ablation is the edges near the channel sides on both sides (marked with dotted circles). This is believed to be mostly the result of re-solidification of ablated polymer or cold fracture at the interface

**Figure 5.3:** Rotors assembly on motherboard for flow routing

**Figure 5.4:** (Top) Schematic of the PDMS Lid mould layers (put together by screws in the blue slots towards the edges) (Bottom) schematic of moulded Pluggy

**Figure 5.5:** Splashing device with two sets of inlets (typically splashing device has only one set of needles)

**Figure 5.6:** Interconnections of FACSllyser with press fitted silicone tubing inserts and needles

**Figure 5.7:** PFF devices bonded onto Si wafer.

**Figure 5.8:** (Left) Tracking 10 generations of cells using CFSE stain [279] (Right & Top) Schematic of the CFSE staining and related signals for 3 generations of a cell (Right & Bottom)  $\mu\text{BR}$  testing via CFSE staining.

**Figure 5.9:** Validation of WST-1 assay with Jurkat cells test assay

**Figure 6.1:** Steps of ELISA based techniques

**Figure 6.2:** Steps of our technology

**Figure 6.3:** Comparison of our technology with ELISA.

**Figure 6.4:** Principle of impedance based protein concentration measurement

**Figure 6.5:** Principle of multiplexed protein concentration measurement

**Figure 6.6:** Multiplexed impedance based simultaneous sizing and protein concentration measurement

**Figure 6.7:** Principle of differentiation of dimers (bead-bead conjugates) from monomers (unbound beads).

**Figure 6.8:** Multiplexing of bead-bead conjugates by means of differentiating the transition times.

**Figure 6.9:** *Differentiation of beads of 3 and 5  $\mu\text{m}$  sizes using an impedance cytometer.*

**Figure 6.10:** *Differentiation of metallic beads and polystyrene beads using an impedance cytometer.*

**Figure 6.11:** *(Left) Transition times of dimers and two unbound single particles (Right) Corresponding image of a dimer and two unbound single particles across the detection zone.*

**Figure 6.12:** *(Left) View of fluidic connection holder with a microfluidic chip. (Right) View of the electrical connections on a silicon nanowire chip with alignment accuracy down to 25  $\mu\text{m}$ .*

# List of tables

**Table 2.1:** Evolution of the C-TAS modules and their final versions

**Table 3.1:** Cell culture protocol for  $\mu$ BR with state of valves at each stage and inlet/outlet operation type. \*The time of culture is dependent on the cell type and length of experiment (generally ranges between 48 h and 3 weeks).

**Table 3.2:** Recipe for fabrication of SU-8 mould using negative photolithography process.

**Table 3.3:** Comparison of conventional FISH method and microFISH protocol showing over 23 fold reduction in total reagents used and a 2 fold reduction in the probe volume (highlighted in yellow) which is the most expensive reagent for conducting FISH analysis. All steps of the FISH protocol are presented and in case of the microFISH protocol the flow rates used for the FISH reagents are also presented.

**Table 3.4:** Average number of metaphase spreads found in the microFISH chamber ( $3 \times 3 \text{ mm}^2$ ) using manual dripping method and our splashing device protocol

**Table 3.5:** Comparison of time and reagent volume used for performing traditional FISH protocol compared to the microFISH protocol (Only the time of the protocol is indicated but the time with respect to handling can differ from person to person)

**Table 3.6:** Comparison of microFISH and the current version of AutoFISH protocol.

**Table 5.1:** Parameters used for theoretical analysis of various microfluidic systems

**Table 5.2:** SU-8 master fabrication recipe

**Table 5.3:** Process flow for fabricating Silicon Master with KOH wet etch process

**Table 5.4:** Process flow for creating electrodes on a Pyrex wafer.

**Table 5.5:** PDMS Replica Moulding

**Table 5.6:** Process flow for bonding PDMS to other substrates using Plasma oxidation

**Table 5.7:** Laser ablation parameters of FACSlyser in PMMA. Passes means number of runs per design feature. Power means % power from the total power, Resolution means dots per inch of the marking.

## List of abbreviations

7up	98% sulphuric acid and ammonium sulphate
μBR	Microfluidic Bioreactors
μTAS	Micro-Total Analysis Systems
BAC	Bacterial Artificial Chromosomes
CENP-A	Centromeric Protein A
CFSE	Carboxyfluorescein succinimidyl ester
CGH	Comparative Genomic Hybridization
COC	Cyclic Olefin Copolymer
C-TAS	Chromosome-Total Analysis System
DAPI	4',6-diamidino-2-phenylindole
DEP	Dielectrophoresis
DPFF	Dual pinch flow fractionation
ELISA	Enzyme-Linked Immunosorbent Assay
ID	Inner Diameter
IPA	Isopropyl alcohol
FBS	Fetal bovine serum
FISH	Fluorescence <i>In-Situ</i> Hybridization
LOC	Lab On Chip
MEMS	Micro Electro-Mechanical Systems
OD	Outer Diameter
PBS	Phosphate buffer saline

PDMS	Polydimethylsiloxane
PEG	Polyethylene Glycol
PFF	Pinch flow fractionation
PGMEA	Propylene Glycol Methyl Ether Acetate
PHA	Phytohemagglutinin
PMMA	Polymethylmethacrylate
RBC	Red blood cells
RPMI	Roswell Park Memorial Institute medium
SSC	Saline sodium-citrate buffer
TLs	T-Lymphocytes
TsT	triazine, 2,4,6-trichloro-1,3,5-triazine
WBC	White blood cells
WJC	Wilhelm Johannsen Centre for Functional Genome Research
YAC	Yeast Artificial Chromosomes



# CHAPTER 1

# INTRODUCTION

While looking at the phenomenal progress that microfluidic technology has made in making inroads to various scientific disciplines, this chapter also introduces the background to the experimental work described further in this thesis which mainly concerns the development of a novel microfluidic toolkit for on-chip FISH analysis.



## 1.1 Microfluidics: The journey

Microfluidics is an area of microfabrication that currently mainly focuses on the miniaturization of fluid-handling systems. For nearly two decades, microfluidics continued to be a part of the MEMS revolution and was initially considered a mere added functionality on integrated MEMS called 'BioMEMS'. Incidentally, all throughout the 80's, microfluidic development was mostly only focused on adding functionality to MEMS based Si devices. It was not until the early 90s, that microfluidics started to emerge as a major research direction. Only after Manz *et al.* coined the term ' $\mu$ TAS', when they published their theoretical work on what they called "Miniaturised total chemical analysis system" in 1990, microfluidics and miniaturized analytical systems started to gain emphasis [1, 2]. In coming years, due to increasing funding support from DARPA, the term "Lab on Chip" was coined to include the efforts made towards miniaturizing lengthy laboratory protocols in miniaturized devices[3].

While the concept of a micro-total analysis systems ( $\mu$ TAS) and Lab on Chip (LOC), where sample transport and manipulation (including mixing, reaction, separation, and manipulation of chemicals and particles) take place on a miniaturized scale, has only recently caught interest, the underlying idea of shrinking chemical and biological analyses and reactions dates back to 1959. Richard Feynman professed the potential of miniaturization in the physical sciences in his now celebrated lecture "There is plenty of room at the bottom" [4]. Two decades later, Stephen Terry and co-workers fabricated and tested a gas chromatograph on a planar silicon wafer in what was the first ever publication of an integrated microfluidic gas chromatograph [5]. That was soon followed by IBM Inkjet Printer in 1979 [6-8], integrated miniaturized microconduits system for flow injection analysis in 1983 [9-11] and fluid dynamics study for miniaturized flow injection analysis in 1986 [12, 13].

Much of this work went unnoticed and it was only after the publication of the conceptual  $\mu$ -TAS paper that there was an explosion of developments and discoveries in microfluidics[1]. Manz *et al.* suggested extending MEMS technologies to biology and chemistry [1, 2]. Another major event at the same time was the shifting focus of the microfluidics community from silicon to polymer based devices. Emergence of soft lithographic principles based on primarily PDMS material was instrumental in moving the fabrication process out of the cleanroom to lab benches [14-18]. This was a welcome change for chemists & biologists and this began to attract people from diverse fields to microfluidics and its possible applications, which continue even today.

Today, biological applications of microfluidic research seem to be the most promising commercially. The explosion of publications, patents and startups catering for *in vitro* and point of care diagnostics, drug discovery, high throughput screening, sequencing, among many others profess a promising journey ahead for biomicrofluidics [19-31]. The ability to devise systems at scales mimicking the natural habitat of cells is a fascinating pathway microfluidics has brought us to.

Recently, microfluidics has been instrumental in first demonstrations of micro-scale systems capable of manipulating, organizing and handling single cells precisely [32-36]. The ability to probe cells and control their microenvironment in microfluidic systems has provided better tools for attempting to understand the complexities of nature. Since DNA was discovered, man has been accumulating vast amount of data through explorations in genomics, proteomics, biology, protein chemistry, etc in a quest to understand nature better. Until microfluidics, the toolkit for probing cells continued to be manual, semi-automated, low throughput and expensive for studying complex phenomena occurring at cellular dimensions.

During the last decade, microfluidics has reaped the benefits of the miniaturization drive and has rolled out integrated analytical systems which are scaled down versions of the standard analytical systems found in central labs. These systems are equipped with sampling, pre-processing, analysis and detection units which function impeccably with the help of micro-sized pumps, valves, mixers and reservoirs, and perform the same analytical operations with comparable and often better sensitivity and much higher throughputs than lab based equipments [37-40].

### **Where to next?**

Successful demonstrations of countless applications of microfluidic based technologies have flooded the literature [41] and patents space [42, 43]. But most of these attempts have ended up being mere toolkits for research and have failed to enter the commercial space. As a result, the public visibility of microfluidics based products is still very low [44, 45]. Hence, there is a constantly growing segment in the clinical user's community and venture capital industry, who are starting to feel that microfluidics technology will only remain a toy for research and fail to cross the "Valley of Death" [46]. Of course there have been exceptions to this, but they have mostly been with respect to platforms developed for performing microfluidic unit operations mostly helpful in research space and not with actual end-user products [44, 45]. Today, most of the revenue in the field of microfluidic lab on chip systems continues to come from business-to-business trade and not from business-to-consumer space [19].

Microfluidics has shown promising potential for a wide range of applications in the field of genetics, genomics, proteomics, cell biology, biomedical analysis, chemical analysis, high throughput screening, drug discovery, polymer spinning, among countless others [38, 39]. But the significant lag in the commercialization of these applications has now become a cause for concern [47]. Microfluidics has been facing great hurdles in commercializing the university research demonstrators and turning them into end-user products partly due to high initial investments and high fabrication costs, but mostly due to the technology itself being immature and not ready to compete with the advance liquid handling platforms which continue to be the industry standard [48]. The hype generated around microfluidic technology and its potential applications is slowly starting to wither with the complexities of enabling and mainstreaming such systems becoming rapidly apparent. This is the classic pattern following the “Gartner Hype Cycle” and the first wave of microfluidic hype has seemed to pass over the research and microfluidic industry and in due time we will ride yet another wave, but hopefully this time with subtle moderation with the established benchmarks of commercial viability and applicability [47, 49].

But the recent down path (failure of multiple startups to kick off and their subsequent folding) has clearly opened some eyes and in microfluidic circles, the need for redefining the development strategies is becoming increasingly evident [50]. Simultaneously there is a significant push for aligning future development efforts with the end-user expectations [51, 52]. Nevertheless, microfluidics revolution is here to stay for a long time [19]. In years to come it will change the fundamental way of performing fluid-based analysis. But significant hurdles remain before microfluidic technologies and applications can be mainstreamed into commercial end-user products. Firstly, there is a need to standardize and thereby reduce the costs and time associated with development of microfluidic systems. But most importantly, the quest should be to solve the inherent issues [practicality, interoperability, compatibility with other analytical systems] with microfluidics deterring wide adoption and deployment of microfluidic technologies into the world outside research labs.

This thesis forms a part of such translational efforts aiming to bridge the gaps between the microfluidic research and development at typical microfluidic labs like the one at DTU-Nanotech and the targeted users. This work originated from a research project targeted at developing a lab-on-chip system for detection of chromosomal translocations. Using this research project as a starting point and a typical case, this thesis aims to highlight the underlying issues with the current microfluidic development efforts when aiming to solve other similar biological conundrums. In an effort to push research closer to expectations of the end-users, this thesis presents a novel microfluidic toolkit aiming to highlight and tackle

some critical challenges ahead for the microfluidic community which are currently delaying the wide scale adoption of microfluidics into clinical and industrial space.

## 1.2 Incompatible domains:

Microfluidics is in numerous ways unifying worlds. People from various backgrounds and disciplines are trying to work together in order to solve problems inherently spanning across multiple sciences. Microfluidics has now become the underlying enabling technology which has now sprawled into countless fields of applications. While microfluidics seems very compatible and readily amenable to accommodate complex problems in various fields, the practical issues concerning using microfluidics technologies widely and adopting microfluidics- based solutions in daily routines is in fact not that simple.

Researchers (biologists, chemists, environmental researchers, toxicologists, etc) unanimously agree that they see potential in miniaturizing their current experimental setups and use microfluidics to provide them numerous benefits by reducing reagent costs, sample volumes, analysis time and providing them higher throughput. This simple realization has attracted scores of researchers to attempt blending their research domains with microfluidics. Without any doubt, it is indeed a fascinating technology with huge potential and it's a great opportunity to do things very differently than they are done currently in many fields.

But then why hasn't the potential of this technology materialized? A critical look at the current microfluidic research activities can show why the potential of this technology has not been materialized.

- **The quest of a killer application**

While the quest for a killer application continues, researchers continue to push and extend the boundaries of microfluidics technologies every day [52]. Papers depicting numerous versions of similar or slightly varying devices providing applications in cell biology, PCR, cell trapping, chemical analysis, genomics, gradient analysis, etc among others have sprawled the microfluidic literature space [42]. But the inherent lack of these devices to transcend the boundaries laid by end-users on counts of applicability, usability and viability has indeed moved us away from the actual path of discovery of the killer application.

- **Lack of standardization**

The mammoth task of replacing the petri dishes and titer plates in clinical labs cannot be accomplished if the newer microfluidic formats do not interface with the rest of the clinical equipments. The need for standardizing size and material of microfluidic devices has been continually ignored and has significantly affected the onset of adoption of microfluidic based clinical devices [51]. There has been an increased demand for standardizing the development efforts synonymous to the standards adopted by the semiconductor industry earlier on leading to the phenomenal success of the semiconductor industry.

- **Lack of direction**

Identifying the real needs of the end-users which demand a microfluidic solution is a first step in mainstreaming microfluidics. In many cases, development efforts are directed at miniaturizing existing lab scale setups into micro-sized devices. The process of identification of actual user needs is often ignored in lieu of benefits microfluidics will provide them in cost, time, sensitivity, etc. Hence, most attempts at creating miniaturized microfluidic versions of existing protocols fail miserably to account for existing work routines, interfacing to rest of the clinical environment, end-user ability and most importantly to provide any real incentive which can justify changing to microfluidic based devices. But the problem is in the assessment of needs and verifying applicability of targeted solutions[50]. It is equally important to match expectation of the end-user in terms of functionality, simplicity, ease of handling and adaptability to their existing daily routine[53].

**Microfluidics is not a miniaturization exercise.. don't make it one!**

## 1.3 Need for a new approach: The road ahead

This PhD project was part of a larger research project titled “Chromosome Total Analysis System” which aimed to detect chromosomal translocations or alterations on a lab-on-chip setup. The vision was to create a modular microfluidic system capable of handling various sequential steps of the Fluorescence *In-Situ* Hybridization protocol [Fig. 1.1], which will be described in detail in chapter 2.

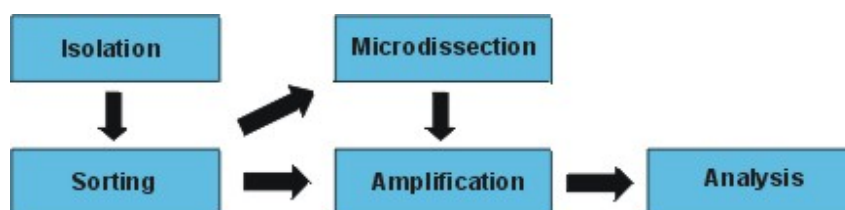


Figure 1.1: The modular C-TAS system

Researchers for many years have focused on developing microfluidic platforms to replace the classical fluid-handling platforms [pipetting robots]. The goal has generally been to benefit from miniaturization and provide to end-users the benefits that typically are proclaimed for microfluidics based systems [Fig 1.2].

- Low cost per test
- Faster analysis
- Smaller setups
- Higher sensitivity
- Parallelization (capability to handle massively parallel experiments. i.e. up to  $10^6$ )
- Laminar flow (providing gradients and control down to single cell level)
- Serial handling of samples, reagents and droplets in plug-based microfluidics.

Figure 1.2: Typical goals for microfluidic platforms development

But if these goals were accurate, all microfluidic device manufacturers would be selling platforms but as the case is currently most revenue for microfluidic companies comes from chip based sales. And as it also appears the emerging formats in microfluidics industry for high throughput devices are also geared towards making use of existing analysis and fluid handling setups i.e. devices in titer plate formats [45].

Hence, there is clearly a difference in the market expectation and the research direction. These widely proclaimed expectations have been benchmarked into every microfluidic researcher's mind and this project started with the same goals to build a microfluidic platform to allow integration and seamless functionality of various modular units for performing a biological analysis.

Coming back to the C-TAS project, our challenge was to build a motherboard to allow for sample preparation (cell isolation, cell capture, cell culture, fixation, chromosome extraction) and subsequent analysis of a patient sample for possible translocations. A group of PhD students with multi-disciplinary backgrounds were put together and assigned the following projects based on the vision of C-TAS system [Fig. 1.1].

**Project 1: Isolation of chromosomes from whole blood**

**Project 2: Sorting of chromosomes**

**Project 3: Fluorescence *In-Situ* Hybridization**

**Project 4: Integration into a C-TAS system**

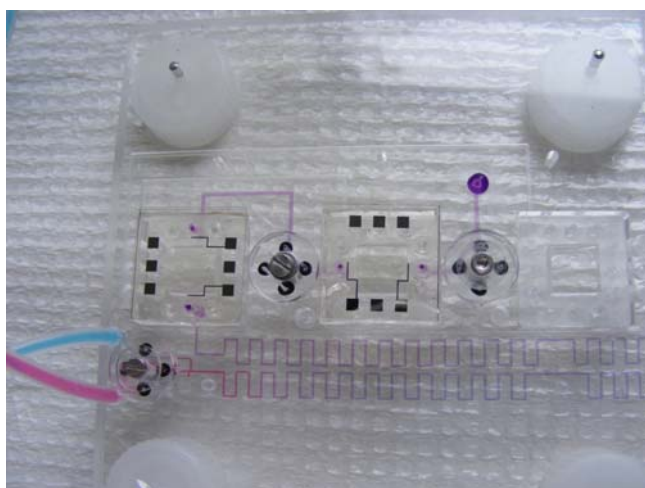
As generally happens, a miniaturizing exercise was initiated and the projects went through a phase targeted at imitating the standard traditional lab protocols in their miniaturized microfluidic versions. After many design iterations and couple of years, the result was a modular microfluidic motherboard with integrated fluidic and electrical connections, which interfaced with a cell culture chip, a dielectrophoresis (DEP) based chromosome sorting device and a FISH on chip module [Fig. 1.3]. This research or rather re-search endeavor encompassing 8 man-years of work was met with skepticism and general criticism with respect to the complexity of the handling protocol and difficulties in terms of integrating the microfluidic motherboard in clinical settings. The consensus was that it would not only be difficult to integrate such a platform in existing work routines at central labs, but will also be almost impossible to train technicians to shift to the new protocol. Unless fully automated, we concluded that our platform was not feasible for implementation in clinical labs.

These complexities stemmed from the fact that the project had clearly focused more on the descriptions of existing protocols and not on end-users needs. We had succeeded in our project requirements, but failed to breach the most common barrier hurting wide-scale microfluidic adoption – change. The biggest difficulty for microfluidics in breaching the barriers of medical devices and diagnostics markets is unwillingness and inflexibility of end-



users to adopt newer technologies which don't comply with existing work routines and protocols.

At this stage, the end-users were put into the equation and attempts were made to bridge the gap in our knowledge of the existing work routines in the labs and identifying the real needs of the intended end-users. It was simply an eye opening experience. And it became apparent that too much focus on miniaturization had led us to a mere microfluidic version of the current solution. While the resultant solution did reduce volume of reagents, analytes, costs per test, among others, but the real challenge in central labs was not just the time of analysis and cost of the reagents. The fact that the manual protocol kept the technicians occupied for 4 days was a greater issue than the expenses and time related to the tests. Hence, we had clearly missed the need to first optimize and possibly minimize the handling time of the protocol by some level of automation, even before attempting to miniaturize the protocol.



**Figure 1.3:** Modular microfluidic motherboard with 3 sockets for C-TAS modules. The pictures show meandering channel for the integrated mixer and circular rotors for fluid valving.

Identifying actual user needs is a process of interacting with the end-user, observing their work routines, probing details of every step of the existing protocols to figure out minor and often hidden details ignored on protocol descriptions. This exercise gives you a better understanding of finding the right balance between what is microfluidically possible and figuring out what is actually needed in terms of development to push applications and products based on microfluidic technologies into commercial space. Following such a needs definition exercise for the C-TAS project, it was discovered that while above goals are partially correct and applicable to few applications [Fig. 1.2], but there was an urgent need to tailor the future microfluidic development efforts towards:



- **Portability** (as point-of-care assays are touted to be the biggest market segment for microfluidic applications [19]),
- New techniques for efficient **sample preparation, separation and analysis**
- **Low cost high volume production**
- **Automation** (with reagents and sample handling providing sensitivity matching the industry standards or better)
- **User-friendliness** (in comparison to the ability of targeted end-user, in our case a regular lab technician working in central lab).
- The creation of a library of **compatible materials and their properties and their compatibility with various cell types** (and preferably force suppliers to adhere to the standards as materials routinely vary from batch to batch)
- **A fixed standard size for future devices (based on standardized toolkit of methods for fabrication of devices)** analogous to standards that were created for the semiconductor industry [51, 54]

This revelation also opened new venues and project ideas for individual C-TAS projects which lead to a new roadmap and project goals for designing the C-TAS system. In close collaboration with technicians at our collaborating clinical labs, we designed a new strategy and goals for the C-TAS system to make it:

- **Simple and easy to handle**
- **Integrated**
- **Possibly automated or needing minimal handling (self sufficient)**
- **Compatible with existing equipment (slide-sized)**
- **Needing minimal change in existing work routines.**

While developing the C-TAS system with above goals was the core focus of this project, the need for a flexible microfluidic toolkit which solves the practical issues and concerns of end-users in widely adopting microfluidic technologies had become very apparent. As a result, lot of attention was allocated to practical issues like bubble traps, interconnections, bonding and assembling techniques, among others to add flexibility and versatility to the microfluidic toolkit. Multiple inventions providing novel solutions for critical microfluidic applications have been discovered during this project, which has resulted in numerous patents which are described in Chapter 6.

## 1.4 A step in the right direction: New objectives and end-goals

Understanding the end-user's current challenges not only helped us redefine our end-goals but also made more sense of our earlier blunders. Observing the technicians in action provided us greater insights into the existing standard protocols and related minutiae which play a big role in the technician's final choice of technique. The modular schema of the C-TAS protocol complicated the existing work routines and also created additional technical challenges in form of needs for integrating new functionality. [For e.g. cell trapping, cell sorting, need for concentration of cells due to dilution, among others – see Chapter 2].

Hence, the following new project objectives based on a **step-by-step approach** leading to a **simple integrated solution for performing FISH on chip** were adopted.

- To design a **sample preparation module** to perform cell culture, arrest and fixation of blood sample, which can later be integrated with a FISH module [Paper 1].
- To realize a separate approach for **splashing based spreading of metaphase chromosomes** [Paper 2].
- To demonstrate a novel protocol for performing **FISH on a chip** [Paper 3].
- Finally, to merge the sample preparation, spreading device and the FISH chip into a **monolithic integrated FISH device with minimal handling**, providing **the possibility to automate**.

All throughout this development work, the underlying goal and efforts were to provide the end-user with simplicity and ease of handling matching and in-line with their existing work routines. We hope that someday the results of these efforts will be welcomed through the doors of clinical labs. As the majority of experiments in this thesis are directed towards advancing of traditional cytogenetic techniques, the next section will describe the standard cytogenetic techniques with the present state of the art which is in the process of being redefined by the work presented further in this thesis.

## 1.5 Advanced microtechnologies for detection of chromosome abnormalities<sup>1</sup>

Dorota Kwasny, Indumathi Vedarethinam, [Pranjul Shah](#), Maria Dimaki, Asli Silahtaroglu, Zeynep Tumer, Winnie E. Svendsen

The overall goal of cytogenetic analysis is to detect chromosome abnormalities in patient samples. This analysis is a standard procedure for prenatal as well as postnatal diagnosis and cancer detection. Cytogenetic techniques such as karyotyping by banding have been for the last years complemented by molecular cytogenetic techniques such as fluorescent *in situ* hybridization (FISH). FISH is recently evolving towards on chip detection of chromosome abnormalities with the development of microsystems for FISH analysis. The challenges addressed by the developed microsystems are mainly the automation of the assay performance, reduction in probe volume, as well as reduction of assay time. The recent focus on the development of automated systems for performing FISH on chip is summarized in this review.

**Keywords:** Fluorescent in situ hybridization, FISH on chip, microsystems, cytogenetic analysis

### Introduction

Conventional methods for disease diagnosis are based on analysis of cells, biochemical pathways, and infectious agents. Chromosome studies provide cytogenetists with valuable information as chromosome disorders are a major category of genetic disease [55]. The incidence of chromosome abnormalities in live births is around 0.7 % [56]. Specific chromosome abnormalities are responsible for more than 100 identifiable syndromes, thus an understanding of cytogenetics and chromosome disorders is important [55]. The rapidly growing field of biomedicine focuses on detecting the genetic causes of diseases by means of molecular diagnostics. This involves studying of DNA and RNA as diagnostic targets. Cytogenetics is a study that concentrates on cell analysis with special focus on chromosomes. The conventional cytogenetic analysis known as chromosome analysis or karyotyping is based on the analysis of metaphase chromosomes through banding techniques and microscopy. The typical resolution is in the range of 5 – 10 megabases and depends on the compaction of the chromosome and number of bands. Karyotyping is still a gold standard for

---

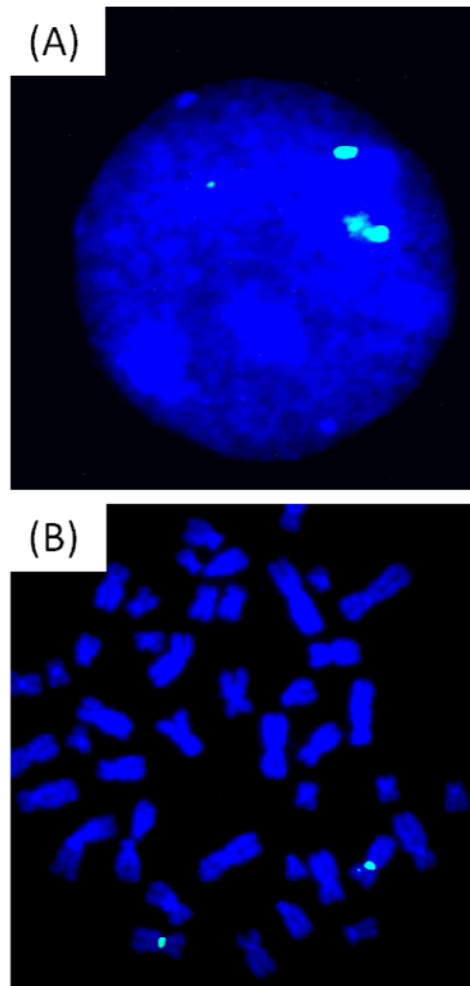
<sup>1</sup> Excerpt of an Invited review: Submitted to BioEssays. This section will introduce the basic cytogenetic techniques setting the premises for the rest of the thesis.

cytogenetics; however, new technologies have been developed to improve the resolution power of chromosome abnormalities detection. One of the mostly used techniques in molecular cytogenetics is fluorescence in situ hybridization, which has been a bridge between cytogenetics and molecular genetics. Even though preparation of FISH analysis is laborious it has grown in popularity in cytogenetic laboratories all over the world. However, to make the analysis a more standard procedure in genetic diagnostics some efforts need to be done to automate the protocol. Nowadays researchers focus on the development of integrated, miniaturized systems for more sensitive and rapid analysis of biological samples at low cost. Recently some efforts have been made towards fabrication of systems for analysis of chromosome abnormalities with the goal being a reduction of costs, sample volume, and hybridization time related to FISH analysis, and automation of assay. In this paper, we review the current state of the art of the microsystems developed for abnormalities detection.

## **Chromosome abnormalities**

Chromosomes are nuclear structures composed of DNA and proteins. Their structure and number are highly preserved in different organisms with a typical human cell containing 46 chromosomes. Conventional and molecular cytogenetic techniques are used to study the structure and number of chromosomes and to detect chromosome abnormalities [57]. A chromosome abnormality may be numerical or structural. Numerical abnormalities such as Down syndrome (three copies of chromosome 21), Turner syndrome (X chromosome monosomy) occur when an atypical chromosome number is present in the cell. Structural abnormalities can be balanced rearrangements, such as inversions or translocations; or unbalanced, such as deletions and duplications. Depending on the nature and size of the chromosome abnormality, different cytogenetic and molecular cytogenetic techniques are employed. Chromosome abnormalities are often associated with congenital anomalies, dysmorphic features, growth retardation and learning disabilities [58].

Furthermore, numerical chromosome abnormalities, deletions and translocations are also associated with cancer [59, 60]. Over the years cytogenetic analysis has become an integral part of genetic disorders and myeloid malignancies diagnosis. Genetic material is available in cell nucleus in different forms depending on the cell cycle phase. During interphase cells do not divide, the DNA in the form of chromatin is enclosed in a nuclear membrane with the chromosomes visible but not detectable as single entities [Fig. 1.4 A]. The most condensed and highly coiled form of DNA – metaphase chromosomes - is visible during a metaphase, with the chromosomes still enclosed in a nuclear membrane [Fig. 1.4 B].



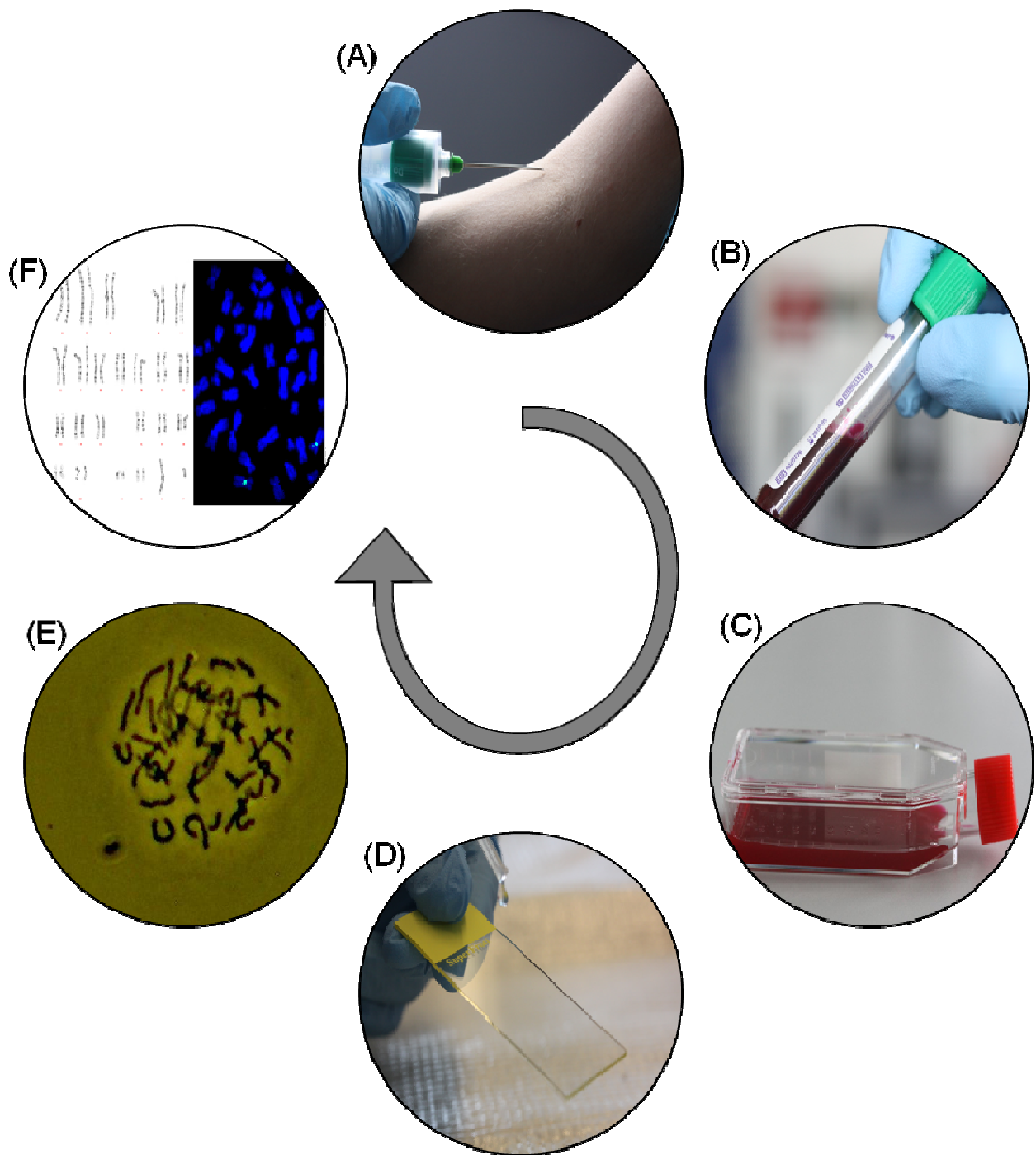
*Figure 1.4: An interphase nuclei (blue) (A) and metaphase spreads (B) with X centromeric FISH probes (green dots).*

## Classical and molecular cytogenetics

Any cytogenetic analysis starts with obtaining the cells as a chromosome source. The most commonly used cells for cytogenetic analysis are peripheral T-lymphocytes, because they can be obtained from peripheral blood samples [Fig. 1.5 A, B]. To perform analysis on metaphase chromosome the cell culture is required to increase the amount of cells in metaphase [Fig. 1.5C], which is not necessary for interphase analysis. Phytohemagglutinin is a typically used chemical to stimulate cell division during a 72 hours T-lymphocytes culture. A minimum of

20 cells needs to be fully analyzed to obtain reliable results [61]. A mitogenic stimulation with colchicine is further performed to arrest the cells in metaphase and thus increase the number of metaphase spreads for the analysis. After treatment with hypotonic solution, the cells are splashed on the glass slide with ice-cold water [Fig.1.5 D] to obtain the metaphase spreads [Fig.1.5 E]. The karyotyping by banding relies on staining such chromosomes fixed on a surface and then further analyzing these under a microscope, while FISH requires a use of fluorescently labeled probes [Fig. 1.5F]. FISH is based on the hybridization between two DNA sequences, a fluorescently labeled probe and its complementary sequence on a chromosome. The fluorescent microscopy visualization of a hybrid between a probe and genetic material reveals the presence, number and distinct location of targeted sequences [62, 63].

Over many years cytogenetic techniques have been evolving enabling more accurate and faster detection of chromosome abnormalities. Nevertheless, the conventional karyotyping by banding technique is still a standard procedure in cytogenetic laboratories over the world despite the need for trained technical staff [64-66]. Such a simple, but time-consuming analysis, allows for inexpensive diagnosis of numerical and structural chromosome aberrations at a limited resolution [67-69]. The main advantage of karyotyping by banding is that it is a whole genome screening technique, where the entire genome can be visualized at once [57]. The requirement for high quality metaphase chromosome spreads for karyotyping is challenging as some cells, such as solid tumor cells, cannot produce good spreads [66]. To overcome issues with the limited resolution of karyotyping, the requirement for dividing cell population and good quality metaphase spreads; a FISH technique is often used. The conventional banding analysis can only be carried out on metaphase chromosomes, while FISH may be performed both on metaphase and interphase chromosomes. Introduced over 30 years ago, the FISH technique commenced a new era in the cytogenetic studies providing greater resolution than was possible with the karyotyping by banding technique [58, 64, 70, 71]. The typical resolution obtained with FISH is in the range of 10-100 kilo bases sequences while karyotyping by banding has a resolution of 5-10 mega bases [64, 67, 71, 72]. FISH provides a simple, fast and reliable means to assess genetic instability in cancer [59, 60, 73, 74]. Despite many advantages of performing FISH, it is not an alternative to karyotyping but a complementary technique.



**Figure 1.5:** The cytogenetics analysis protocol. Blood sample is collected from the patient (A). The collected blood (B) is cultured in a medium for 3 days at 37 °C (C). Colchicine is added at the end of the culture period to arrest the cells in metaphase. Followed by hypotonic treatment, the cells are splashed on a glass slide (D) to obtain metaphase chromosome spreads (E). At this point the chromosome spreads can either be analyzed by banding or FISH.



## Conventional FISH analysis

For the cases involving chromosome abnormalities that need a higher resolution or analysis on non-dividing cells FISH is often applied. After fixing metaphase chromosomes or interphase nuclei to the glass slide FISH analysis starts. Firstly, chromosomes are washed, dehydrated through a series of alcohol washes and air-dried. A probe solution is then prepared by mixing it with a hybridization buffer containing formamide, salt and dextran sulfate [75]. After that both, the chromosomes on a glass slide and the probe solution are heat denatured. The probe in solution is placed immediately on ice and then applied directly to the slides. They are incubated overnight at 37°C in a moist chamber. After several washing steps to remove the unbound or nonspecifically adsorbed probe the slides are incubated in a dye solution (e.g. DAPI) to label the chromosomes. Stained chromosomes are visualized under an epifluorescent microscope with an appropriate set of filters to observe the probe signal and the chromosomes [76].

FISH complements karyotyping by banding, thus is often prepared as a second step to enhance diagnostic efficiency [61, 63, 77, 78]. Moreover, FISH enables identification of numerous microdeletions and microduplications syndromes that are not generally detectable by classical cytogenetics. Thus, it is often applied for cases with a visibly affected phenotype and apparently normal karyotype to identify otherwise undetectable chromosome abnormalities. Although, one of major limitations of FISH is that it can only be used to detect known abnormalities. It depends on a probe targeting a specific DNA sequence, e.g., to detect known translocations, microdeletions or specific chromosomes and hence can only be used to address questions for which DNA probes are available.

## FISH techniques

One of the attractive features of FISH is that it can be performed both on metaphase spreads but also on interphase nuclei fixed on a glass slide providing valuable information about chromosome abnormalities [67, 74]. Interphase FISH has a great potential for screening large number of cells, as well as for examining archival samples. Interphase FISH is applicable for testing solid tumors as it eliminates the need for dividing cell population. It can also be performed very rapidly within 24 hours, as no cell culturing is required. Tumor cells often show numerical or structural changes in chromosomes that may provide information about the changes that initiated tumor formation. The analysis of metaphase chromosomes in solid tumors is hampered, as extensive culturing is necessary to obtain sufficient number of mitotic



cells, which in few cases may induce additional chromosomal changes. Furthermore, the metaphase spreads obtained from solid tumors have poor quality that makes their proper analysis troublesome [71, 79, 80]. Interphase FISH is used to identify numerical abnormalities as well as specific structural abnormalities, by targeting them with a specific DNA probe.

On the other hand, metaphase chromosomes are widely used in cytogenetic analysis for standard karyotyping and FISH analysis. FISH can be used in metaphase cells to detect specific microdeletions at high resolution. It is also applicable in cases where it is troublesome to determine whether a chromosome has a simple deletion or is involved in some more complex rearrangement. Using metaphase spreads for analysis is beneficial as one can visualize the entire genome at once. Applying whole chromosome FISH probes, a complex mixture of sequences from the entire length of specific chromosomes available for all human chromosomes, enables detecting abnormalities at the genome level [81]. Simultaneous visualization of spectrally distinct fluorophores enabled the representation of different chromosomes with a unique fluorescent signature with a potential application to reveal complex structural abnormalities [57, 65, 67, 69, 74, 82, 83]. By performing such analysis we can obtain information about the unknown translocations between chromosomes at higher resolution than achievable by karyotyping by banding [74, 84-86]. However, such method requires specialized computer software, expensive equipment, and complex analysis by skilled technicians that can interpret the obtained data [57]. Moreover, limited use of FISH is also attributed to the high cost of FISH probes necessary to detect the chromosome abnormalities.

Generally speaking, FISH techniques are utterly useful for the confirmation of chromosome abnormalities suspected based on previous findings, with the use of specific DNA probes. Its main advantage lies in the analysis that can be performed on both interphase and metaphase chromosomes depending on the specific disorder to be detected. Interphase FISH can be performed very fast, but metaphase FISH offers observation of the entire genome that may enable identification of complex rearrangements at a genome level. These techniques present many opportunities; however, their major disadvantage is the cost of reagents (mainly probes) and the requirement for an expensive high-resolution microscope. Development of novel micro assays could significantly increase the usage of these assays broadening our knowledge on chromosome abnormalities.

## **FISH techniques worldwide application**

For the FISH techniques to be used routinely in the laboratories all over the world certain challenges need to be addressed. As stated above the FISH techniques are continuously evolving, however their use is still limited due to high cost and long experimental time. Their use is sometimes advantageous as they are capable of detecting chromosome abnormalities at a higher resolution than karyotyping by banding.

The major drawback of FISH analysis is the cost of the reagents used for the assays, mainly the fluorescent probes. In standard lab protocols 10-15  $\mu$ l of probe are used per slide containing metaphase spreads or interphase nuclei [73]. Such analysis is normally performed on a single patient's sample, thus the cost of a single analysis is extremely high. The development of a high throughput device for metaphase or interphase FISH analysis would reduce the volume of the probe used per single sample, at the same time reducing the cost of an experiment. Also, addressing the need for reduction in probe volume for single analysis would greatly increase the application of FISH in routine analysis.

Another bottleneck of the analysis is the long experiment time. To perform a complete FISH analysis, even well trained technicians spend several hours in sample preparation as well as the waiting time in between each pre- and post- hybridization washes. There are at least 12-15 different washes in a standard routine test that in total takes about 45 minutes. Apart from the cell culture work, the hybridization time is a very long process. At minimum, performing a FISH analysis with centromeric probes (repetitive sequences), will take 2 to 4 hours. Furthermore, in some FISH experiments the hybridization of a probe requires overnight incubation. The automation of sample preparation, probe delivery, imaging and analysis would result in molecular cytogenetic analysis to be performed routinely at the doctor's office as a point-of-care diagnosis.

For metaphase FISH analysis it is necessary to culture cells for three days. The disadvantage of such a culture method is the large volume of medium used and the fact that handling of suspension cells is tedious. This issue was currently addressed by developing a membrane based microfluidic bioreactor for suspension cell cultures, which makes preparation of chromosome spreads much easier [87, 88]. The proposed diffusion based microreactor facilitates culturing of lymphocytes but also expansion, hypotonic treatment, and fixation of cells with the possibility to avoid several tedious centrifugation steps [87]. Svendsen *et al.* developed a bioreactor for a suspension cells culture on the membrane with a microfluidic

channel for media perfusion. The continuous flow ensures all the necessary nutrients to be delivered from the medium to the cells by diffusion. It enables fast solution changes for expansion and cell fixation to obtain high quality metaphase spreads. Separation of culture chamber by a membrane from the channel is beneficial as it protects the cells from air bubbles formed in the flowing medium and allows the perfusion to be started even before the cells settle on the membrane. Shah *et al.* modified the media perfusion channel to ensure more thorough transport of nutrients across the membrane to the resting cells [87]. Moreover, by performing CellTrace™ CFSE cell staining protocol it was demonstrated that cell proliferation on chip is better than in control experiment in a well plate culture.

One of the many advantages of microdevices for complete chromosome analysis is the possibility to perform high throughput analysis. In cytogenetic laboratories chromosome analysis is performed several times a day on different patient samples. High throughput automatic devices for cell culturing, preparation of chromosome spreads or interphase nuclei, followed by detail FISH analysis would drastically speed up the process and provide fast results.

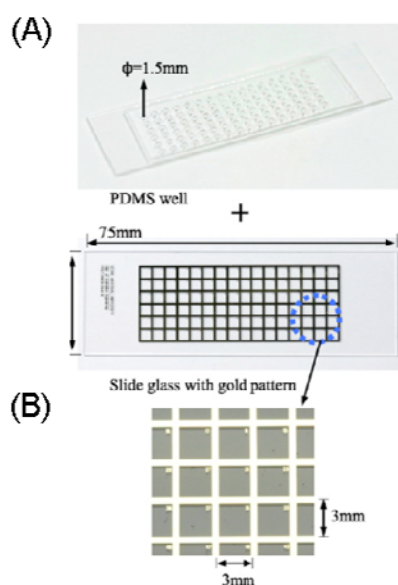
### **Microsystems developed for FISH analysis**

In recent years the integration and automation of cytogenetic techniques has gained more attention. Most reports in this field focus on the development of an integrated microfluidic chip for interphase FISH analysis. This article reviews the recent developments in the field of microcytogenetics that address the need for automation, time and cost reduction in chromosome analysis.

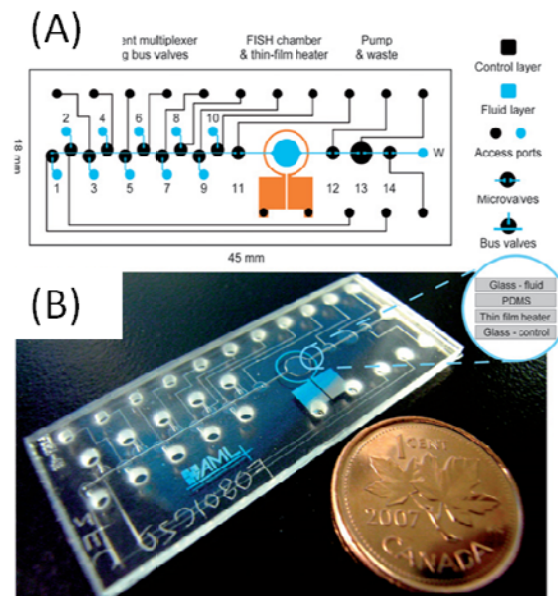
In 2007, Lee *et al.*, presented one of the first examples of miniaturized devices for performing FISH analysis [89]. The presented work allows for high throughput FISH analysis on a cell array. The typically performed analysis lacks the possibility of conducting high throughput analysis as there is limited amount of samples available. To address this problem, the authors showed the possibility to array cells by spotting the small amounts of cell specimens onto a supporting matrix, which enables high throughput analysis. For the preparation of the chip, a glass slide was used as a supporting matrix. 1 mm thick perforated PDMS was bonded to a glass slide to form 96 cavities of 1.5 mm in diameter for spotting cells [Fig.1.6]. To enable microscopic cell identification a matrix corresponding to the 96 PDMS wells was microfabricated by photolithography on a glass slide. They have showed that 1 µl samples were spotted onto each PDMS well followed by air drying, removal of PDMS cover and

performing conventional FISH protocol. In this way, only 10  $\mu\text{l}$  of probe were used to analyse 96 specimens. The device is very useful in mass sample analysis for the same kind of samples, in which the probe reduction is relevant. The authors have mentioned the probe volume reduction, but other major issues such as manual intervention and time consumption were not stated.

The first implementation of FISH on chip was showed in 2007 by Sieben, *et al.* [80]. They have adapted the conventional FISH except the cell immobilization step, where cell immobilization was achieved using temperature. They also investigated a method to reduce hybridization time by probe recirculation with on-chip peristaltic pumps, and electro-kinetic transport of probes by introducing the electrodes into the end-wells. By these two methods, they found out that electro-kinetic transport of the probes was slightly better than recirculation method. In addition, the electro-kinetic chip design is simpler than the recirculating micropump, which involves valves and complex micro fabrication. Nevertheless, by performing the analysis at microfluidic volumes, they were able to achieve a tenfold reduction in DNA probe reduction per test, with equivalent the cost reduction from \$90 for 10  $\mu\text{L}$  of probe, to \$9 for 1  $\mu\text{L}$ .

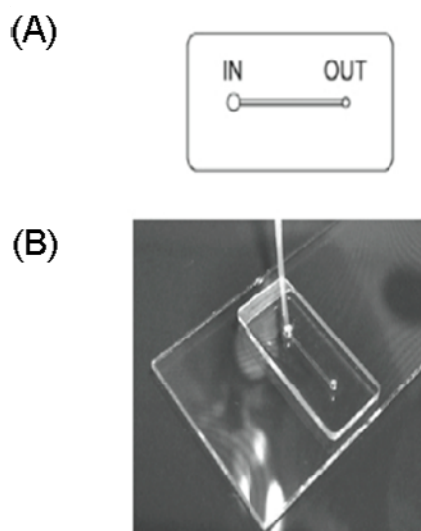


**Figure 1.6:** Fabricated bio-cell chip slide. (A) A PDMS layer with 96 wells for multiple cell analysis. (B) A glass slide with a gold pattern for sample numbering (used with permission from Lee *et al*, 2007)



**Figure 1.7:** (A) The mask layouts and dimensions of an integrated FISH microchip. The microchip includes a reagent multiplexer, a cell chamber with an integrated thin-film heater, and a peristaltic pump. (B) Image of a complete integrated FISH chip (used with permission from Sieben *et al*, 2008)

In 2008, Sieben, *et al.*, published another paper in which all previously performed steps with microfluidic FISH were integrated onto one chip and automated [90]. Similar to the recirculating design, the new chip consisted of a PDMS layer sandwiched between two glass layers, one of which carried fluids, while the other transmitted air pressure for valve control, e.g. for peristaltic pumping, which is a very complex fabricated system. With the valves operated by computer, preloaded reagents could be multiplexed through the hybridization chamber at appropriate intervals for each step of FISH. A copper thin-film heater was built into the design as well, for the cell-immobilization and denaturation steps [Fig.1.7]. Unlike the previous designs, this new device did not focus on the reduction in hybridization time, but instead focused mainly on minimizing the labor time and automation of the microfluidics FISH chip. One of the issue with the conventional FISH, which takes more than an hour of on-and-off attention of a skilled technician, using their time inefficiently, whereas the automated microfluidic FISH device would reduce human intervention and only involve the technicians work during reagent preparation, and image analysis .



**Figure 1.8:** Microfluidic device for miniaturized FISH. (A) Diagram of the microfluidic PDMS pad with inlet and outlet connected by a straight channel. (B) Complete structure of the FISH device with the PDMS pad assembled with a  $\text{TiO}_2$  functionalized glass slide (used with permission from Zanardi *et al*, 2010)

The most recent advances in integrated interphase FISH analysis were presented in 2010 by Zanardi, *et al* [78]. They focused on the development of an analytical tool for performing interphase FISH on both living and fixed cells. The application of microfluidic technologies might reduce costs and improve assay performance by development of microchannels for easy reagent loading and cell immobilization. However, the fluid flowing in the microchannels causes intense shear stress on cells; this may result in their disruption or detachment from the surface. In this paper the authors' addressed this particular problem in the application of microfluidics for FISH. By changing the surface chemistry they enhanced the cell immobilization on the surface that significantly reduced the cells detachment due to shear stress. In this article, the entire glass slide is coated with nano structured  $\text{TiO}_2$  using cluster beam technology which adds significant costs to the device owing to the need for access to cleanroom and costs of additional metal deposited. Moreover, routine genetic labs do not necessarily have access to cleanroom facilities, which makes the method very difficult to implement on a larger scale. The top cover bonded to the modified glass slide contains a microfluidic channel that is used for loading cells and other reagents in FISH protocol [Fig.1.8]. Such a simple design facilitates handling of the fluids without generating bubbles that could affect assay performance.<sup>2</sup>

<sup>2</sup> As described in section 1.5, in recent years interphase FISH has received much attention and has successfully been implemented on a chip, but due to complexities of the protocol, metaphase FISH remains complicated to be miniaturized. This is one major goal of this thesis i.e. to make a miniaturized device to perform metaphase FISH on chip.

## 1.6 Thesis Overview

Primarily work described in this thesis is targeted towards development of translocation analysis technologies supported by microfluidics-based techniques which can be used in clinical settings for standard cytogenetic analysis.

**Chapter 1** discussed the phenomenal success of microfluidics as a research tool for multiple disciplines. Finally, using this research project as an example, this chapter highlights the common problems with microfluidic research approaches which are continually moving microfluidic applications away from the wide scale implementation and public adoption.

**Chapter 2** introduces the concept and vision of a modular C-TAS system with development of a modular microfluidic motherboard.

**Chapter 3** highlights our step by step efforts towards reaching the goal of an integrated C-TAS system.

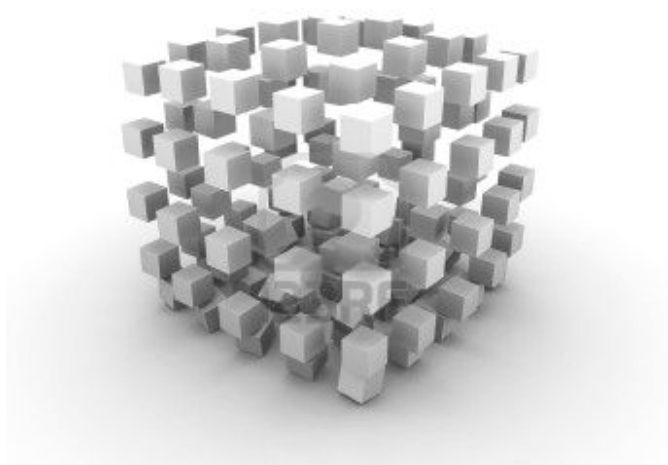
**Chapter 4** is dedicated to describing side projects attempted related to the C-TAS system and other projects for developing a microfluidic toolkit for biological analysis in general.

In **Chapter 5** methods of simulation, fabrication, analysis and characterization related to the development of the microfluidic devices are presented in more details then described in earlier chapters. The reader is asked to refer to this chapter for more details of methods used.

**Chapter 6** provides a brief summary of the patents filed or in process concerning the discoveries and inventions made as part of this PhD project.

Finally, **Chapter 7** concludes the thesis with discussion of overall results.





## CHAPTER 2

# MODULAR C-TAS

This chapter introduces the C-TAS protocol which has been the primary goal of this PhD project. We will also describe the development of a modular motherboard providing substrate independent plug and play functionality. Finally, the experiments done on motherboard with an Impedance cytometer are extensively described.



## 2.1 C-TAS: The vision

The C-TAS project was focused on achieving the vision of a miniaturized platform for performing chromosomal analysis [91]. Specifically, the critical mission was to design a microfluidic system capable of handling a patient blood sample and performing in sequence - a controlled cell culture based expansion and arrest of cells in metaphase, followed by isolation of T-lymphocytes (TLs), extraction of chromosomes, sorting of chromosomes, fixation of chromosomes on substrate, ending with a Fluorescence *In-Situ* Hybridization based detection of any chromosomal translocations on the patient's sample [Fig. 2.1, courtesy: Winnie Svendsen]. Such a device could provide many benefits to the cytogeneticists for diagnosis of various diseases caused by chromosomal translocation i.e. by truncation or deletion of critical function genes [92].

Chromosome translocations are part of a major category of genetic disorders. The incidence of chromosome abnormalities is rapidly emerging as a common occurrence in the population. Hence, their early prognosis, diagnosis and treatment of related diseases are now a routine part of major genetic clinics. Chromosome translocations related cases are now forming big part of the cases involving spontaneous abortuses; congenital malformations, mental retardation, infertility, gonadal dysgenesis and for couples with repeated spontaneous miscarriages. Additionally, the field of cytogenetics is becoming very important in the workup of patients with hematologic/oncologic disorders. In congenital disorders these rearrangements have led to identification of novel disease genes. Hence, cytogenetic testing is extremely important for diagnosis, classification of disease, help with decisions about treatment and to monitor disease status and recovery. Thus, our motivation was to provide the cytogeneticists with tools and strategies as part of the C-TAS system to minimize their existing workload by automating the entire diagnostic protocol and providing them the benefits of low cost, sensitive, minimal handling and automated system to perform translocation analysis followed by isolation of the translocated chromosomes for further molecular characterization via breakpoint analysis.

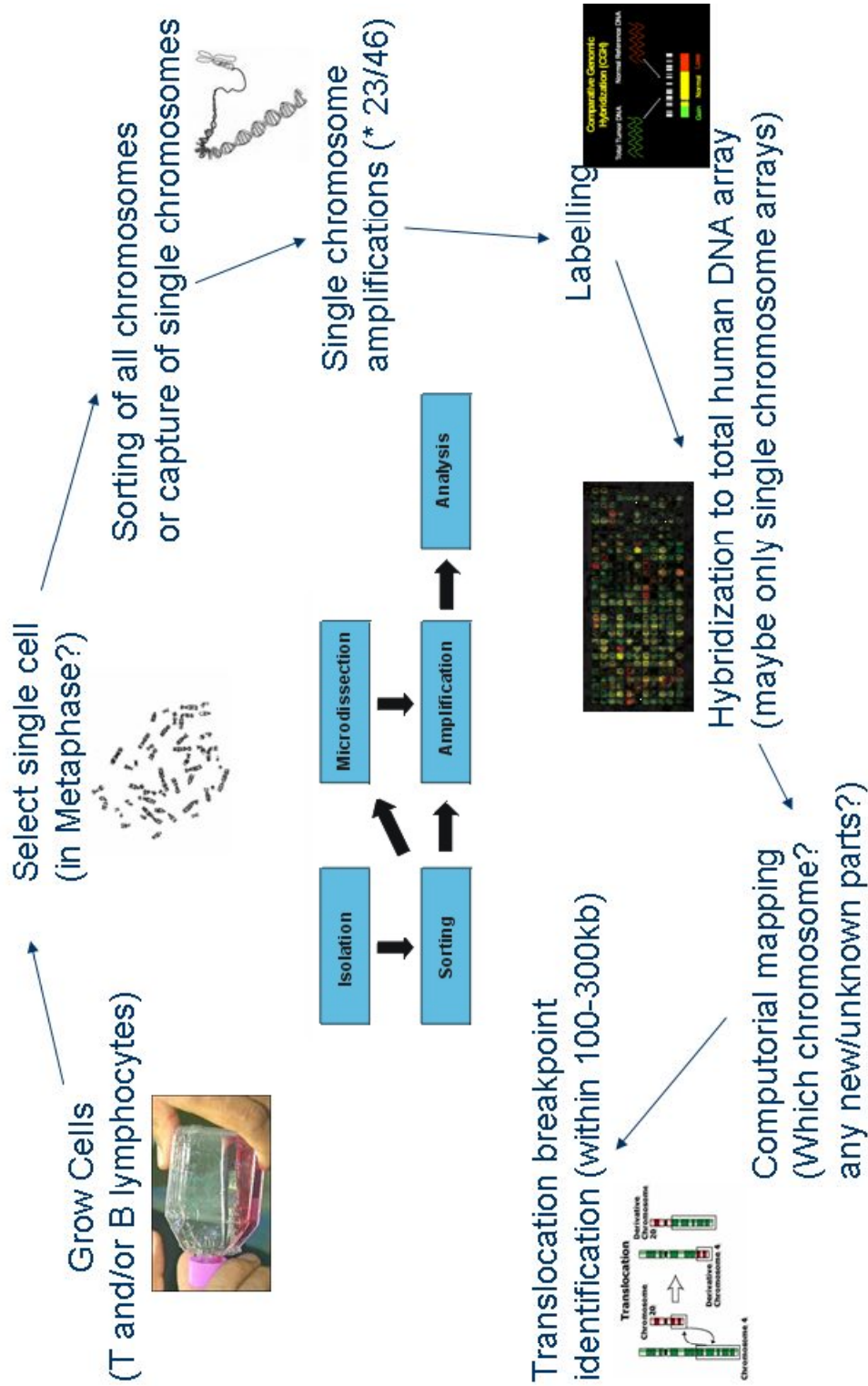
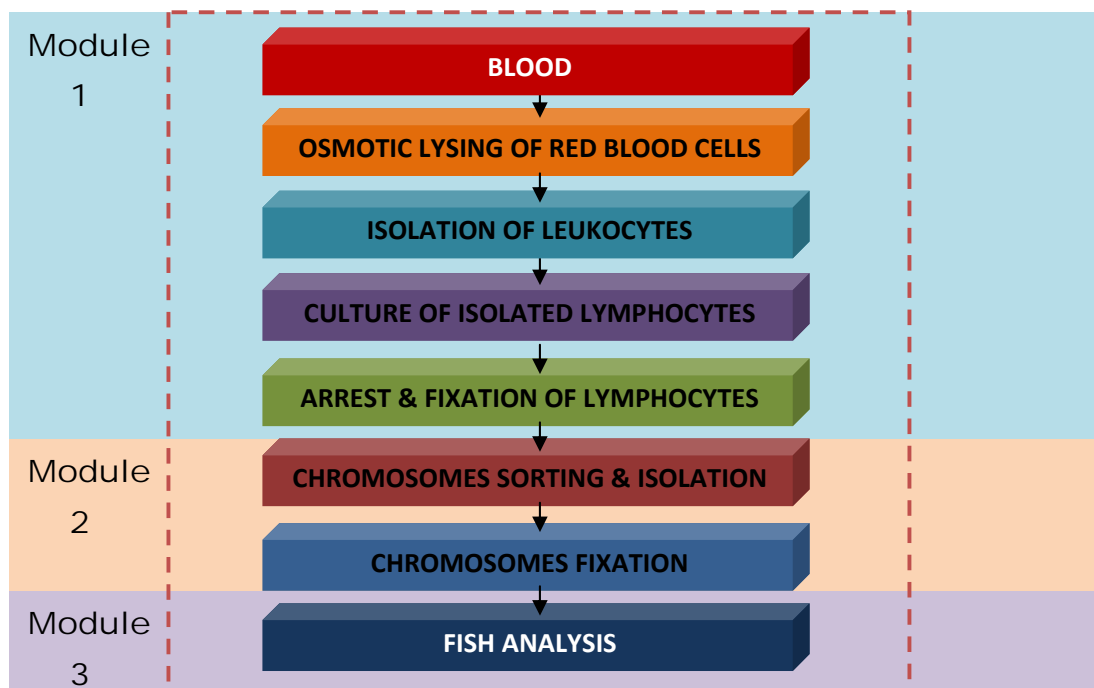


Fig. 2.1: The vision of the C-TAS system. Outer circle: Represents the steps involved in the conventional analysis protocol. Inner Block Diagram (Blue): Depicts the vision of a modular C-TAS system

## 2.2 C-TAS: The challenge

The mammoth task of realizing a C-TAS system was an exercise encompassing multiple disciplines including biology, genetics, image analysis, added with the new tasks attached to devising a miniaturized version of the protocol demanding expertise in microfluidics, micro and nanofabrication, surface chemistry, among others. The task was assigned to a group of 4 PhDs with backgrounds in multiple fields. The common understanding was to design and develop a modular plug and play based system to perform the entire chromosomal analysis protocol.

The goal of this project was to design a strategy and develop a functional motherboard allowing for rapid plug and play based assembly of the C-TAS system by means of plugging in various modules covering the entire protocol. A microfluidic integrated solution for analyzing chromosomes from whole blood will need to integrate various sub modules to achieve a total chromosome analysis protocol [C-TAS protocol]. In the other 3 PhD projects which were part of the C-TAS project, tasks for preparing modules for firstly, whole blood to chromosome preparation, secondly, chromosome sorting and isolation and finally subsequent FISH analysis were being undertaken [Fig 2.2].

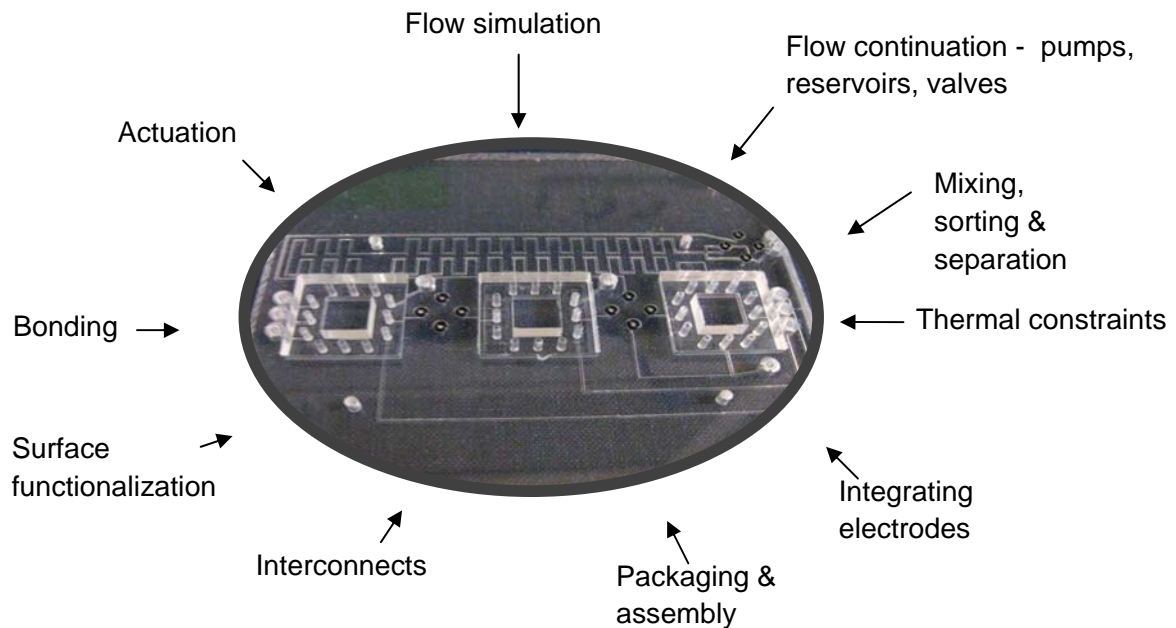


*Figure. 2.2: The C-TAS protocol and original modules*

Modular microfluidic platforms are becoming increasingly relevant for biological analysis. The focus of this work is to address the biggest vexing challenges ahead of microfluidics: fluidic packing and system level integration & compatibility and interoperability among various microfluidic components. The efforts to mainstream microfluidic based biological applications and cell handling devices can only succeed, if platforms which enable easy integration and interfacing of microfluidic devices into the existing clinical setups emerge rapidly. These modular platforms will have to be based on robust technologies which can provide accurate fluid handling operations (actuation, valving, mixing, concentration, separation, reagent storage, among others) backed by a robust, low cost and mass producible fabrication technology.

As a design problem, the motherboard approach amalgamates components belonging to two fundamental categories: fluidic components (channels, reservoirs, mixers, valves) and electrical circuits for providing electrical connections to the modules. The process of design of the motherboard was influenced by the number of needs which were used as development guidelines throughout the designing phase of the project [Fig. 2.3]. The motherboard should provide biochemical compatibility (for cell culture), fluid actuation, waste removal, channel surface passivation (non-reactive to samples), surface functionalisation, optical transparency, ease of microfabrication (no cleanroom and scalable), easy plug and play assembly strategy (taking maximum 5 s per module assembly), reusability (up to 20 times), easy cleaning protocol (cleaning by single solvent flushing), and low cost of development (under \$50).

Hence, my objective was to design a motherboard to easily integrate on an active platform all the functionalities for fluid routing, valving, mixing (for lysing red blood cells and fixing of metaphase lymphocytes), providing electrical connections, and overall providing effortless plug and play based interconnection strategy for rapid assembly of the C-TAS system from the 3 modules. While modular motherboards have been around, no demonstrations of handling complex biological protocols as this one have yet been proposed [93-96]. While most demonstrators of modular platforms are passive and do not provide fluidic routing, some are made with materials which cannot allow for the platform to be reused for biological analysis.



*Figure 2.3: Modular motherboard and the development challenge*

## 2.3 Impending decisions

At the start of the project, some technical design rules had to be set to allow for interoperability of various sub-modules and these rules were also important to achieve easy interfacing of the modules with the motherboard, at the end of the project. These design decisions had to be made keeping in mind the requirements of the biological protocols, fundamental limits of micro and nanofabrication and at the same time leaving enough room for each PhD project to function individually. The key was to design a mechanism by which while progressing individually all the projects will lead to the development of a module compatible with the common motherboard. Hence it was important to have laid down some common design rules (size, materials, fabrication protocol, etc) for the project.

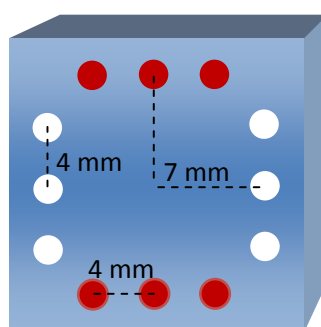
### 2.3.1 Standardization

The most important decision taken over the design phase of C-TAS project was to standardize the size of the modules. The benefits of standardizing device sizes were apparent. For the C-TAS system, the foremost benefit of standardizing modules was to allow simultaneous development of the motherboard in parallel with the modules. And finally, adopting a standardized device format allows easy application of a plug and play motherboard developed for C-TAS project to other areas. In future, we envisaged that by means of

standardizing the device sizes, the output of the C-TAS project could be leveraged for other biological protocols.

### Final Design Specifications:

The module dimensions were fixed to be 20 x 20 mm and the positions and number of fluidic inlets/outlets and electrical connections were decided as standards for all the modules to comply with based on all module requirements [Fig. 2.4]. The red dots highlight the positions of the electrical connections and the white dots depict fluidic interconnections. Arrays of 3 interconnections (fluidic as well as electrical) are placed equidistant from the centre at a distance of 7 mm. The distance between the 2 interconnections in the array is 4 mm. There are 6 fluidic and 6 electrical connections in total based on the requirements made from the C-TAS participants.



**Figure 2.4:** Design specifications & schematic drawing for motherboard socket and modules (Red dots depict electrical connections and the white dots depict positions of fluidic interconnects. Size is not to scale (2x).

This design was considered an ideal and viable solution as some of the modules were to be fabricated in the cleanroom and having a 2 x 2 cm module size was a good trade-off between having enough space on chip for structures and microfluidic handling while at the same time having sufficient number of chips per wafer to justify the fabrication costs. A maximum of 12 chips per wafer can be fabricated with a chip size of 2 x 2 cm. Also, this was a standardization attempt for the prototyping stages of the project and can be easily modified as per the requirement of the modules or end-user and when moving towards a commercial solution.

### 2.3.2 Choice of material

Biology is extremely complex and we started to realize the intricacies of the complex problem we had on our hands while picking the right material for the modules and motherboard. The choice of material is often the first consideration while designing microfluidic devices and systems; it was crucial to select material offering biocompatibility and protocol compatibility (in terms of fabrication and operation). Polymers are rapidly becoming the popular choice for development of microfluidic devices [42, 97-99]. The basic requirements from the material for this project was low cost, ability to bond to different substrates (Glass, Silicon) irreversibly, suitable for microfluidics, ease of fabrication, gas permeability, good optical properties, good chemical stability. Such a material can either be Polydimethylsiloxane (PDMS), Polymethyl methacrylate (PMMA), Polycarbonate (PC) or Cyclic Olefin Copolymer (COC).


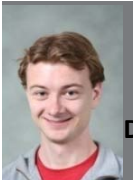

PDMS was selected as initial material of choice for the fluidic channels of the modules owing to the group's expertise and experience with PDMS. Other factors considered were its widely cited biocompatibility, ease of fabrication, low cost, optical transparency, gas permeability, good chemical stability and abundance of literature to refer to for biological and cell handling protocols on PDMS based devices [14-18, 100-102]. In case of modules needing electrodes, the electrodes were to be fabricated on Pyrex wafers, which can be bonded on PDMS channels using oxygen plasma bonding [103, 104]. But over the course of the project, the modules evolved and ended up in materials other than planned during the initial design phase of project [Table 2.1]. As the work on individual modules is part of other PhD projects, related issues and solutions will not be described in details here.

PMMA was the chosen material for preparing the motherboard due to ease of fabrication and in-house expertise with micromilling and laser-ablation on PMMA [105-107]. Using PMMA for the development was advantageous owing to PMMA being inexpensive, transparent, biocompatible and finally easy to fabricate using the methods listed above [108-111]. PMMA was used for the overall design optimization and test phase of the motherboard, but it was later discovered that PMMA cracks with ethanol treatment. Hence, to enable reusing of the motherboard, the final motherboard for testing with cells was fabricated in polycarbonate (PC), to allow for simple cleaning with ethanol.

Table 2.1 depicts the path of evolution of the C-TAS modules during the project tenure including various materials used and fabrication methods tested in order to realize the modules. The table also highlights the final material of choice for the modules at the completion of the C-TAS project.



**Table 2.1:** Evolution of C-TAS modules and their final versions

 <b>Culture and Isolation of Lymphocytes</b> <b>Dr. Jacob Lange</b>	 <b>Sorting and Isolation of chromosomes</b> <b>Dr. Casper Clausen</b>	 <b>Fish on Chip</b> <b>Ms. Indumathi Vedarethinam</b>
<b>Substrates Tested:</b> PDMS PMMA PC Silicon	<b>Substrates Tested:</b> Pyrex PDMS	<b>Substrates Tested:</b> COC PDMS PC PMMA Glass slides
<b>Bonding techniques:</b> UV Curing Thermal Bonding Solvent assisted Bonding Oxygen plasma	<b>Bonding techniques:</b> Compression holder	<b>Bonding techniques:</b> Oxygen plasma Adhesive bonding
<b>Final device:</b> PC with solvent bonding with integrated membranes	<b>Final device:</b> Pyrex and PDMS complex with electrical connections	<b>Final device:</b> PDMS with glass slides bonded using adhesive bonding.

The complexities of the biological minutiae of the C-TAS protocol governed the course of module development and to a greater extent even the choice of material. My project goal was to integrate these devices into a functional protocol. While the individual modules described in the table above did not function as intended or were discarded due to operational complexities, a plug and play motherboard was designed in order to integrate and operate modules developed in any substrate and provide them with electrical and fluidic interconnections. This motherboard was designed, fabricated and tested as described further.



## 2.4 Versatile motherboard for substrate independent plug and play microfluidics<sup>3</sup>

**Pranjul Shah,<sup>\*a</sup> Romen Rodriguez-Trujillo<sup>a</sup> , Simon Levinsen<sup>a</sup> , Maria Dimaki<sup>a</sup> and Winnie Edith Svendsen<sup>a</sup>**

*a Department of Micro and Nanotechnology, Technical University of Denmark, Kgs. Lyngby 2800, Denmark*

This article presents a versatile modular motherboard which provides users compatibility with all substrates and eases the efforts with respect to developing microfluidic and electrical interconnections. By developing a simple plug and play motherboard and related interfacing techniques enabled by means of a simple press fit socket type assembly, this work presents an effortless ‘one touch’ plug and play protocol for simultaneous formation of rapid, multiple, aligned, flexible, reliable and reusable electrical and fluidic interconnections. In an effort towards standardizing microfluidic development efforts, this motherboard restricts the size of the microfluidic devices and locks in the positions of the electrical and fluidic interconnections. In doing so, the user is granted freedom to design their devices in any material as long as they follow the size and interconnections positioning guidelines. These user-designed modules can then be interfaced with the motherboard by attaching them with a pluggable PDMS lid ‘Pluggy’ by adhesive tape based assembly. The motherboard has integrated fluidic networks and electrical connectors accessible via sockets which provide seamless connectivity between the modules and macro world. This versatile motherboard takes a step further in standardizing the device size and provides the first demonstration of a substrate independent plug and play motherboard. We have tested the fluidic and electrical connectivity of the motherboard with an impedance cytometer for counting of micro particles.

### Introduction

Despite an exponential growth in the patents and publications featuring microfluidic applications, the commercial and wide scale adoption of microfluidic based technologies has simply not come about [46, 50]. Microfluidic research in the last decade has led to successful demonstrations of applications in vast areas including but not limited to biology, genetics,

---

<sup>3</sup> Submitted to Biomicrofluidics journal

medicine, chemistry, polymers, *etc* [112-116]. But the exponential growth of microfluidic based devices has not been complemented with techniques to interface and integrate such devices into multi-functional platforms [42]. As a result, the public visibility of these devices continues to be negligible. One can easily imagine countless possibilities of various analysis protocols which could be designed, if there was an interfacing protocol which would allow for arranging any of these successfully demonstrated devices in sequential or parallel fashion. However, the lack of such a system providing reliability, ease of handling and versatile assembly of microfluidic devices is hindering the growth of commercial and clinical microfluidic devices.

The impending need to solve these practical concerns has been recognized and as a result many demonstrations of plug and play modular systems have come about as possible solutions. These modular systems should ideally provide leak-free assembly of fluidic interconnections, rapid simultaneous assembly of electrical connections, substrate independent operation allowing users the freedom to design their devices in any material as per the need of the applications and, most importantly, easy handling and assembly protocol suitable for non-technical personnel. These features should be coupled with on-board fluidic routing and valving operations and incorporate the possibility to automate the fluidic handling in the future.

Although promising, none of the published systems accommodate all of the desired features and versatility in terms of substrates. Typically, these systems have been designed in many materials including silicon and polymers [93-96, 117-120]. Most of these systems lack provisions for establishing electrical connections for sensing applications, which are rapidly emerging as one of the major applications of microfluidics [88]. It could also be of interest to integrate optical connections in to such platforms [121]. While very few systems offer the possibility of establishing electrical and fluidic connections simultaneously [122, 123], none have the ability to provide flexibility of interfacing with microfluidic devices fabricated in any substrate.

Simultaneously, the need for standardizing future development efforts has been repeatedly highlighted [51, 52]. But there is still not a single standardized technique in terms of interconnections and hence every research group has their own application specific or preferred way of fabricating these interconnects which they continue to use and progress [124-131]. In order to standardize interconnection technology for microfluidics, there is a need for a technique which can allow rapid, robust, flexible, multiple, reliable and easy fluidic and

electrical interconnections on microfluidic devices [129]. This is the key to moving microfluidic applications to market and increase the development of novel applications.

We propose a novel socket type plug and play approach enabled by means of a PDMS interfacing lid – Pluggy. By means of adding an interfacing layer (Pluggy) which can bond to any substrate as well as form rapid, multiple, aligned fluidic and electrical connections with a motherboard, we have demonstrated the first substrate independent modular plug and play motherboard. In order to test the fluidic and electrical functionality of this device, we have interfaced an impedance cytometer which required multiple electrical as well as fluidic connections.

## Materials and methods

### Materials:

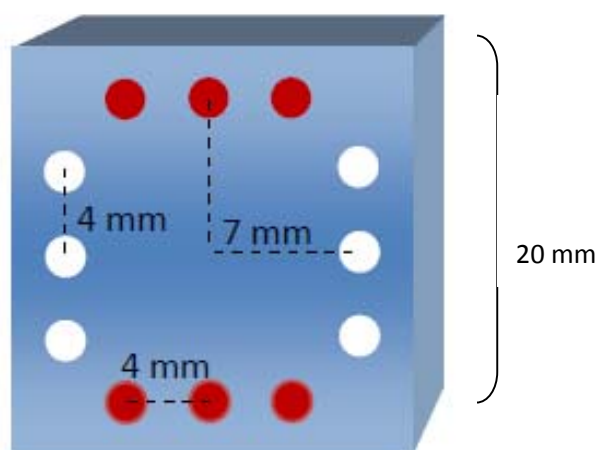
Polymethyl methacrylate (PMMA) sheets used for fabricating the motherboard were ordered from NordPlast (Denmark). Polydimethyl Siloxane (PDMS), Silicone tubing, Blue film, alignment pins, syringes and other consumables were ordered from VWR Denmark. The medical grade double-sided adhesive tape (AR100) was procured from Adhesives Research (Ireland). The O-rings were ordered from M-seals (Denmark). A milling machine from Folken Industries (USA) was used to fabricate the motherboard and rotors. A 50W CO<sub>2</sub> Laser system from Synrad Inc. (USA) was used to ablate the double sided adhesive tape. The drawings of the tape and the milling parameters for the motherboard were drawn using the commercial softwares Winmark and AutoCAD respectively. The spring contacts for the electrical connections of the motherboard were ordered from RS components (Rodium-plated Beryllium Copper pins: 261-5121). Beads were ordered from MicroBeads AS.

### Fabrication:

We have developed a novel modular motherboard providing versatile substrate-independent plug and play functionality based on a socket type press-fit multiple interconnection assembly. Such a scheme allows establishment of rapid, multiple interconnections for microfluidic devices. This interconnect technology consists of a two parts assembly: The micromilled socket fabricated on the motherboard and an interfacing PDMS lid ‘Pluggy’ which interfaces with this socket providing effortless multiple, aligned, reliable, robust, fluidic and electrical connections in a matter of seconds by means of a simple ‘One touch’ plugging protocol. In order to have a standardized socket assembly to streamline future

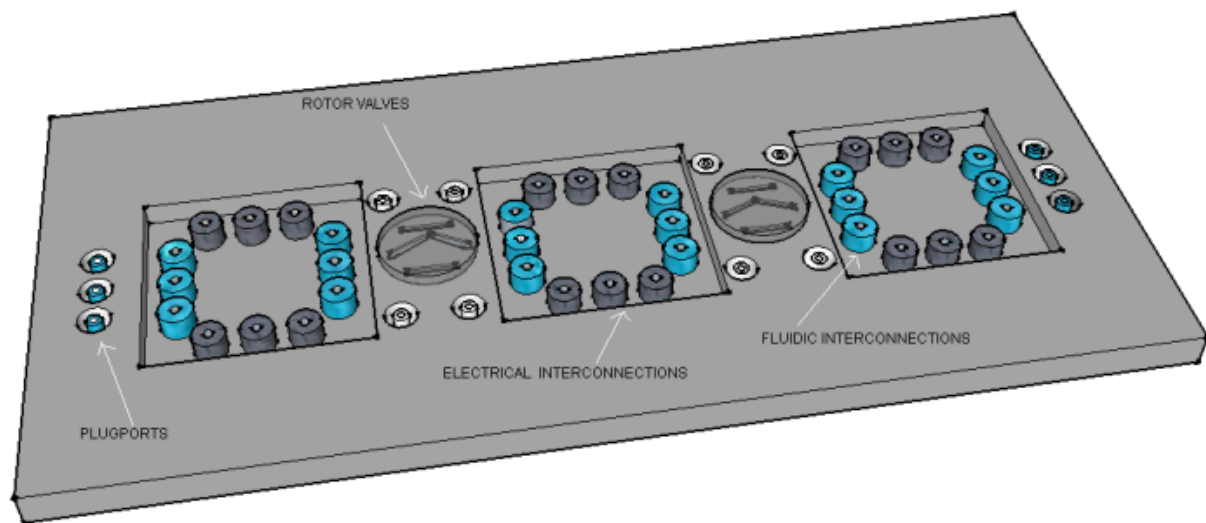
microfluidic device development, we laid some design rules for all modules to be interfaced with the motherboard. The microfluidic device dimensions were fixed at 20 x 20 mm and the position of fluidic and electrical connections have also been fixed as shown in figure 2.5.

Figure 2.6 depicts the schematic of the versatile modular motherboard with integrated press fit sockets. Each socket contains 12 interconnections (6 fluidic and 6 electrical) for interfacing with the modules based on the standard guidelines. The motherboard is fabricated using micromilling in 5 mm thick PMMA sheets [109, 132, 133]. In principle, the motherboard can be designed with multiple sockets, but in this work we only present a motherboard with 3 sockets [Fig. 2.6].



**Figure 2.5:** Designs specifications for the motherboard modules (Red dots depict 6 electrical connections and white dots depict the 6 fluidic connections). Overall dimension 20 x 20 mm.

Figure 2.7 highlights the schematic of the fabrication process of the motherboard. In step 1, the sockets with the interconnection needles are milled. The height of the interconnections needles in the sockets is 3.9 mm. For fluidic interconnections, the needles have an inner diameter of 0.5 mm and an outer diameter of 1.4 mm. In the case of the electrical connections, the inner diameter of the needles is set at 0.7 mm to match the diameter of the spring pins. The outer diameter is fixed at 1.4 mm to allow leak-free and tight coupling with the flexible PDMS lid 'Pluggy' and silicone tubing. The motherboard also contains a fluidic network for placing rotors for valving and routing of fluids by means of turning the rotors manually or with stepper motors.



*Figure 2.6: Schematic of the motherboard*

On the other side of the sockets, a concealed fluidic network is milled to provide fluidic and electrical connectivity to all the plugged modules (step 2). The fluidic channels are designed to be 500  $\mu\text{m}$  wide and 200  $\mu\text{m}$  deep. Every socket is interconnected by a rotor valve which can route fluids by means of turning the rotor to the required position.

In order to actuate fluids pumps are used and to connect the motherboard with pumps, Plugports for plugging external silicone tubings with similar dimensions as needles in the sockets are placed separately outside the sockets on the motherboard. These tubing Plugports have needles with outer diameter (OD) of 1.4 mm and inner diameter (ID) of 0.5 mm which form tight seals with the silicon tubing (OD- 3mm and ID- 1mm).

Finally, a 500  $\mu\text{m}$  PMMA sheet is bonded on to the channels side of the motherboard to seal the fluidic network (step 3). The bonding is achieved by thoroughly cleaning both surfaces with Isopropyl alcohol (IPA), followed by UV activated thermal bonding in P/O/Weber bonding press at 90° C (15 kN bonding pressure, 60 s exposure in DYMAX EC5000 UV light source).

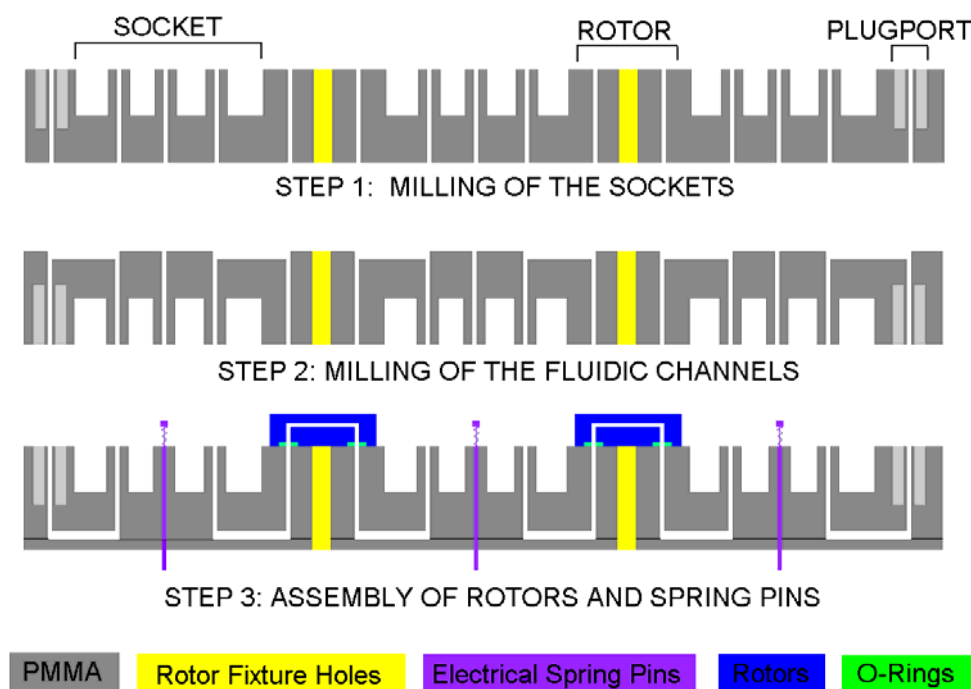
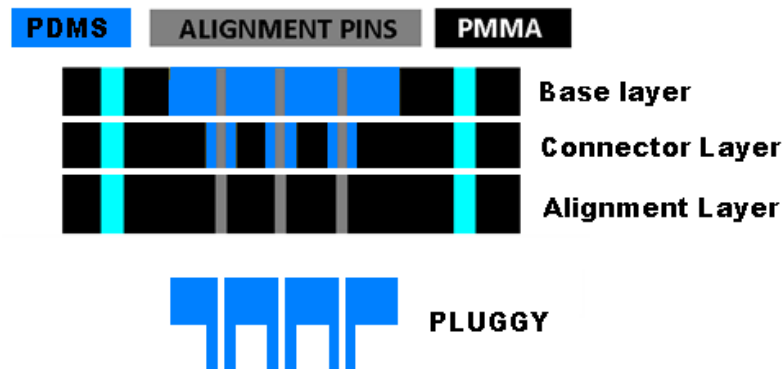


Figure 2.7: Steps of motherboard fabrication and assembly

### PDMS interfacing lid - Pluggy

Pluggy consists of two parts: On one side, the interconnection connectors are placed and, the other side is the lid base, which bonds and provides support to the microfluidic chip. The PDMS lid mould is fabricated by micromilling in 4 mm and 3 mm PMMA sheets [109, 132, 133] [Fig. 2.8]. The mould consists of 3 layers (from bottom to top): The alignment layer allows for fastening the alignment pins for forming through the holes (3 mm sheet), the connector layer for making connectors which form the tight seal with the motherboard socket (3 mm sheet) and finally the base layer, which forms the flat layer of the Pluggy lid, which bonds to the device and supports it during the plugging in procedure (4 mm sheet). The through hole is formed by passing a 1 mm alignment pin through the alignment hole and leaving it in the mould while fabricating the PDMS lids - Pluggy. Pluggy is moulded using the Sylgard 184 - PDMS kit by mixing in a 10:2 (weight: weight) ratio elastomer and curing agent using a replica moulding process [17, 18, 134]. The PDMS is cured at 60° C for 3-4 hours and then peeled from the mould using tweezers. The moulds are thoroughly cleaned after each use with detergent and air dried. This allows reusing the moulds for multiple times.



**Figure 2.8:** (Top) Schematic of the PDMS Lid mould (3 layers put together by screws in the blue slots towards the end) (Bottom) Schematic of a moulded Pluggy interfacing lid

### Adhesive Tape for assembly of modules

The double-sided adhesive tapes (AR100) for bonding the Pluggy to any module are prepared by a laser ablation process (see Section: Assembly of a plug and play device) [105, 106, 135]. The CO<sub>2</sub> laser (Synrad Inc, USA) is connected to a computer with a Winmark software based controller. The tapes are cut into 20 x 20 mm pieces as the motherboard standard and the interconnection holes are cut with a radius of 2 mm as per the positions specified by the design rules. The parameters used for ablating the tape are 25 W power, 300 mm/s velocity, 2 mark passes and resolution of 800.

### Impedance Based Counting Device

The Impedance Chip is made with electrodes fabricated on a Pyrex wafer bonded on to channels moulded in PDMS. The Pyrex wafer contains the electrodes (10 nm Ti followed by 150 nm Au) patterned using positive photolithography and then followed by metal deposition. The mould for casting the PDMS channel is fabricated by KOH wet etching in silicon. The fluidic channels were moulded in PDMS using the replica moulding technique and holes were punched into the PDMS lid using a blunted needle to form the interconnections. The positions of the fluidic and electrical interconnections of the impedance chip are based on the design specifications of the motherboard. The PDMS lid with channels and the Pyrex chip with electrodes are cleaned thoroughly with Isopropyl alcohol (IPA), followed by thorough wash with DI water. Following the washing steps, the devices are air dried and exposed to Oxygen Plasma (Power: 100 mW, O<sub>2</sub> air flow: 75 ml/min, Exposure time: 30 s). Following the exposure with oxygen plasma, the devices are aligned and brought in contact to bond them irreversibly [103, 136]. Typically, the devices are left overnight for the bonding to settle before use (or minimum 4 hrs).



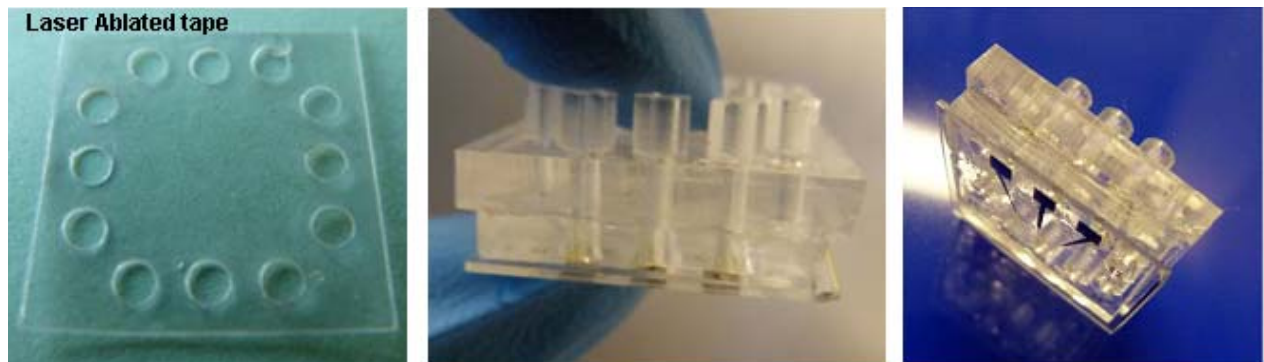
### **Assembly of the plug and play module**

In order to bond the impedance chip on to the Pluggy, to create a module which can be plugged into the motherboard socket, we need to use the laser ablated double-sided adhesive tape [Fig.2.9]. Firstly, the surface of the Pluggy and the impedance cytometer chip to be bonded are wiped with a tissue soaked in ethanol to remove any dust particles. Secondly, the double-sided tape is attached to the impedance cytometer chip aligning the holes of the chip and the tape. Finally, Pluggy is bonded onto the other side of the double-sided tape making sure of the alignment of the interconnections [Fig 2.9]. This alignment process is simple as the chip and Pluggy are of the same dimensions. The substrate and the lid can be made bigger than 20 x 20 mm because as long as the interconnections are placed as per design guidelines, the module will still interface and function with the motherboard. But for the purpose of this work, we have used devices with outer dimension of 20 x 20 mm. The bonded module is left under pressure for 10 min before use [Fig. 2.9].

### **Impedance cytometer chip testing**

In order to test the motherboard, the Impedance cytometer module was prepared by bonding of Pluggy with the impedance cytometer chip. The module was plugged into the motherboard socket to create fluidic and electrical connections. Silicone tubing was used at the connecting plugport to form the world-to-chip connections. A mixture of 5  $\mu\text{m}$  and 3  $\mu\text{m}$  beads solution was prepared in PBS solution with 5% Tween to avoid clumping of the beads. The solution was injected in a syringe and it was elevated to a particular height to create a pressure difference when connected to the motherboard which actuates the fluids. With this solution, we can easily work with flow rates ranging from 1-10 nl/min. The motherboard setup was put under a microscope to simultaneously visualize and count beads when they pass through the detection zone. Figure 2.10 depicts the schematic of the measurement setup and the principle of impedimetric counting of particles. It is based on differential impedance measurements through a Wheatstone Bridge using three consecutive electrodes [137]. The bridge is excited at 1 V amplitude and 100 kHz frequency using a function generator (Thurlby Thandar Instruments TG2000) and the output signal is further processed to extract its low-frequency modulation which provides information about the particle transitions. A stable flow reduces the noise in the signal and hence we waited for the flow to stabilize before recording the signals. The data acquisition is handled using a Labview DAQ card connected to a computer for recording the signals at 10k samples/sec. To decrease the noise, the entire setup with the microscope is placed inside a Faraday cage.

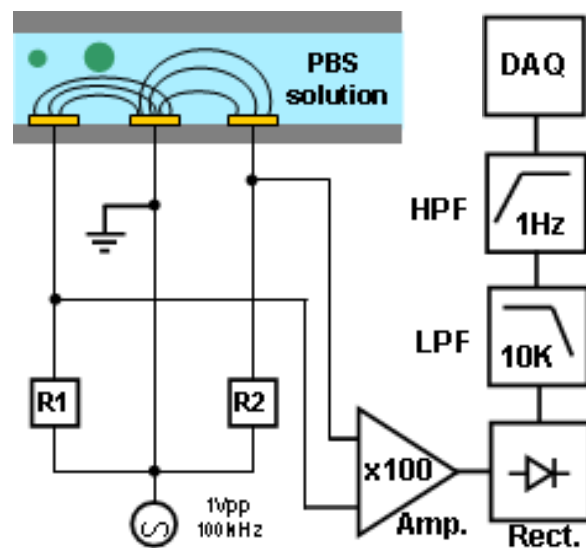




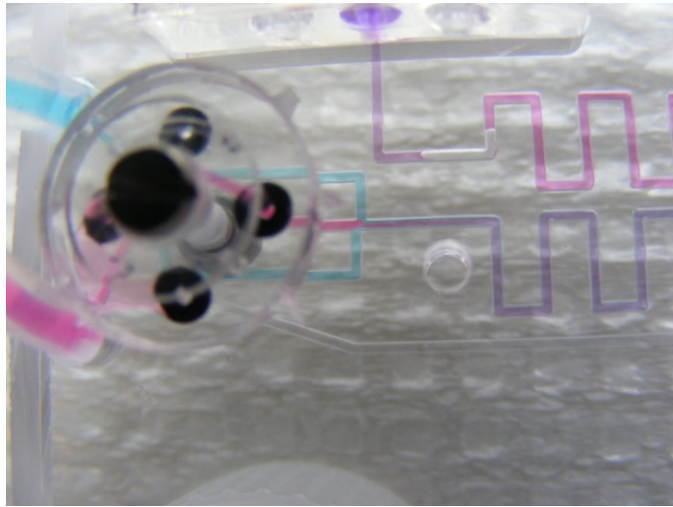
**Figure 2.9:** (Left) Laser ablated double-sided tape (Centre and Right) Pluggable module consisting of impedance chip bonded together with Pluggy by means of a double sided tape.

### Fluid Routing

The motherboard contains rotors with integrated channels for active routing of the fluids. The rotors were fabricated separately and attached to the motherboard via screws. To assemble the rotors, O-rings were placed in between rotor and motherboard connections to form leak proof interconnections. The rotors were operated manually [Fig. 2.11].



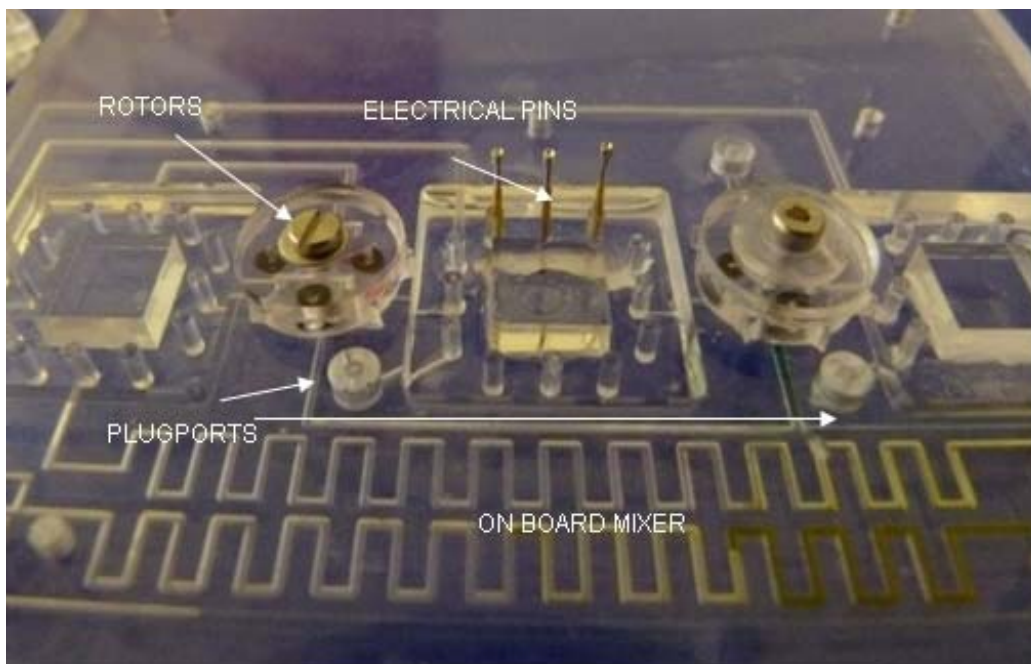
**Figure 2.10:** Schematic of the measurement setup for impedance cytometer chip.



*Figure 2.11: Rotor assembly on motherboard with integrated O-rings for leak proof interconnections*

## Results and discussion

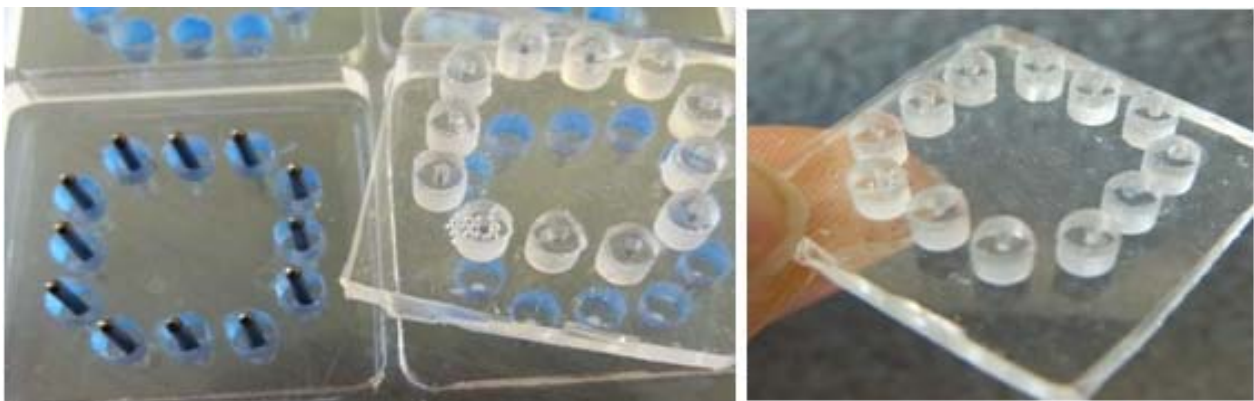
Figure 2.12 shows the fully assembled motherboard with the rotor included and 3 sockets for plugging in modules.



*Figure 2.12: Fully assembled motherboard*

## Pluggy

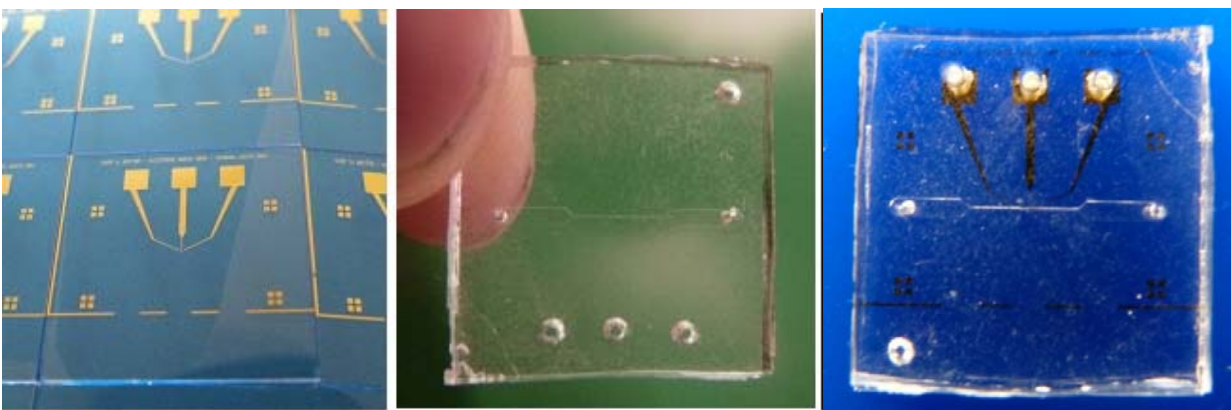
Figure 2.13 (left) shows the moulds with alignment pins inserted for moulding the PDMS interfacing lid – Pluggy. The alignment pins are removed post curing leading to through holes in the Pluggy for forming fluidic or electrical connections with the motherboard socket. The 3 layers of the Pluggy mould are then opened by unscrewing the alignment screws holding them together. Then the Pluggy is gently released by cutting the edges with a scalpel to have a cleanly cut sharp edge [Fig. 2.13 (right)].



**Figure 2.13:** (Left) Mold for curing PDMS based Pluggy with alignment pins for through holes. (Right) PDMS Moulded Lid – Pluggy

## Fabrication of the Impedance chip

Figure 2.14 shows the results of the fabrication of the electrodes as well as the PDMS lid with channels used for the impedance measurements.

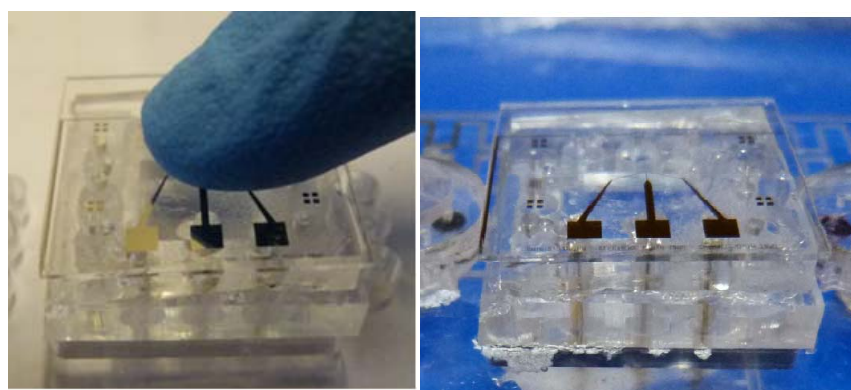


**Figure 2.14:** (Left) Electrodes on Pyrex wafer (Middle) Moulded Lid showing the PDMS channel structure and through holes for interconnections. (Right) Impedance chip after oxygen plasma bonding.

After oxygen plasma treatment, the moulded PDMS lid and Pyrex electrodes are aligned together under a microscope and bonded. The moulded impedance chip containing the Pyrex electrodes covered with a PDMS channel is depicted in fig. 2.14 (Bottom).

### **‘One touch’ Plug and play assembly**

In order to plug-in the module assembly on the socket, the Pluggy connectors are aligned on the needles on the socket and gently plugged-in by applying pressure in the centre of the module with a single finger [Fig. 2.15]. This ‘one touch’ assembly protocol takes less than 5 s and provides any module on the motherboard with instant electrical and fluidic connections. The tubing for entering fluids is connected to Plugports on the motherboard and to the syringe pumps or pressure system on the other end. If the electrical connections are to be used the electrical measurement setup is put in place. The assembly is then ready for testing [Fig. 2.15].



**Figure 2.15:** (Left) One touch plug and play assembly (Right) Impedance chip plugged on the motherboard showing 3 electrical spring pins connecting to the impedance chip. (The fluidic connections are difficult to visualize due to channel width being 10  $\mu\text{m}$ ).

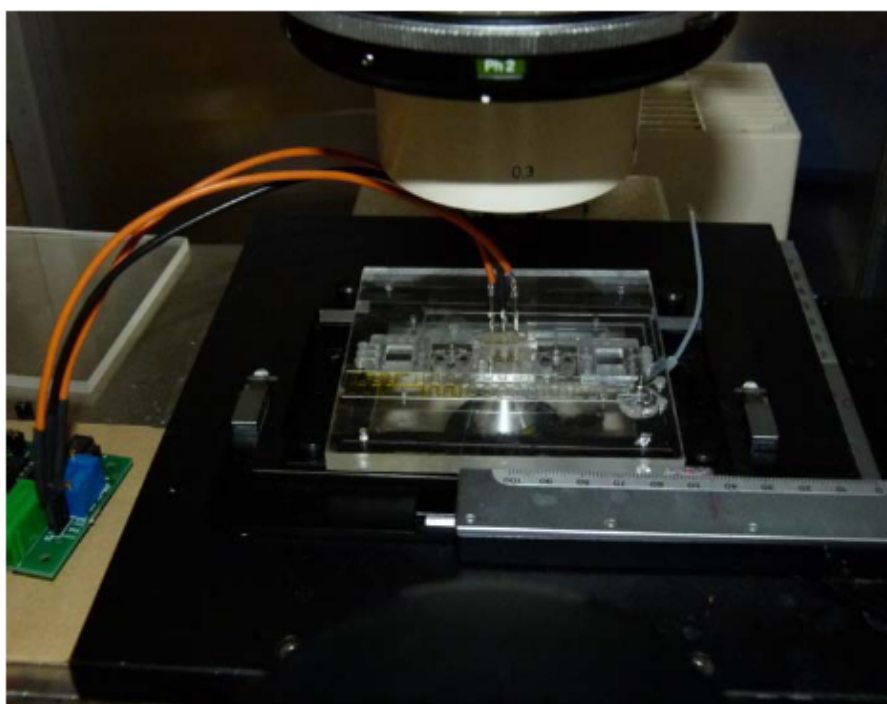
### **Impedance cytometer**

The goal of this work was to demonstrate the functionality of the motherboard by using an impedance cytometer for counting of micro-particles. The performance of this chip was previously confirmed with a specially designed holder. Therefore, proper operation of the chip on the motherboard would confirm the fluidics as well as the electrical operation of the motherboard. In order to interface the impedance chip on to the motherboard, the chip was bonded with Pluggy using an adhesive tape based bonding as mentioned in the previous section and then plugged into the motherboard [Fig. 2.15]. The plugged impedance cytometer module on to the motherboard has been depicted in Figure 11 and it clearly indicates the



spring pins forming electrical contacts with the electrodes on the Pyrex wafer through the Pluggy.

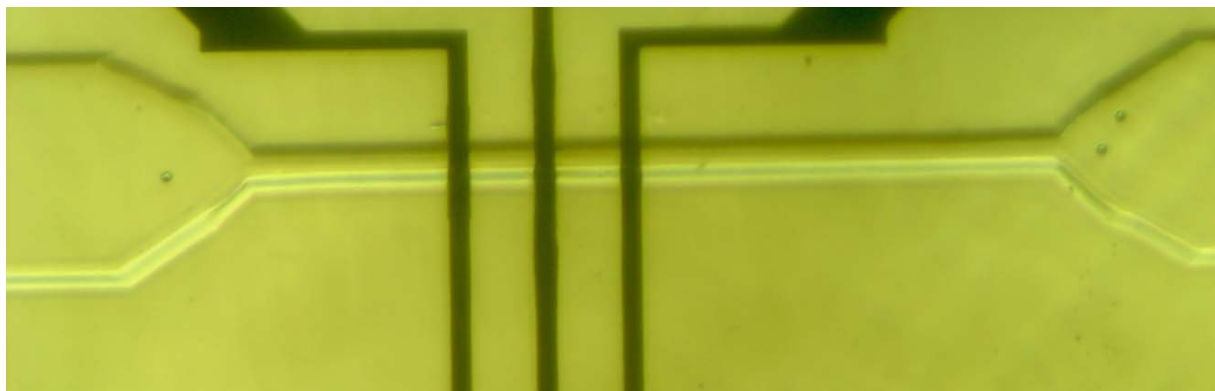
The setup for testing the impedance cytometer on the motherboard is depicted in Fig. 2.16. The motherboard is connected to a custom designed electronic board which modulates and filters the signal. The microscope provides visual confirmation of the beads in the channel, while a Labview based data acquisition program records the electronic signal. The microscope with the motherboard on it as well as the fluidic setup and the electronic board are placed in a Faraday cage [not shown in figure].



**Figure 2.16:** (Left) Motherboard with integrated electrical connections on test setup with modulation board.

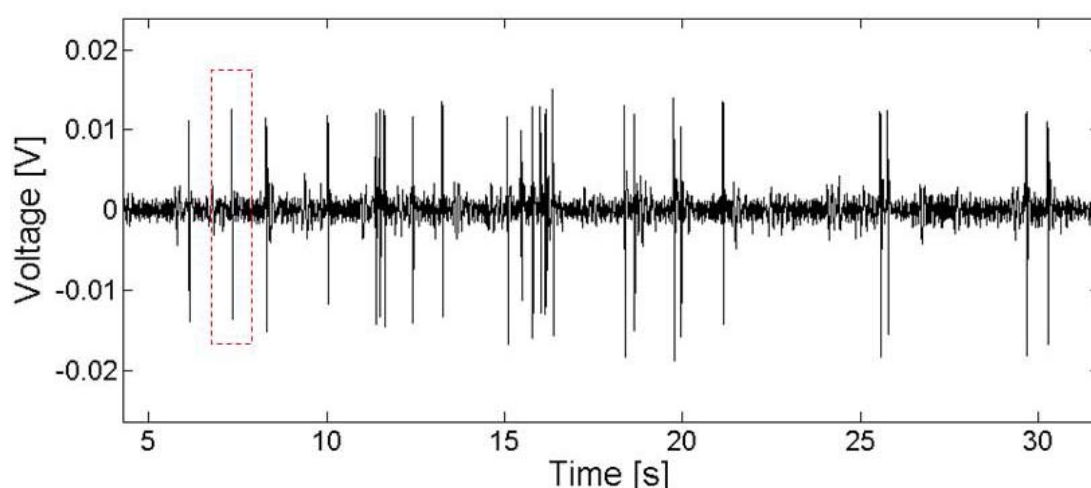
### **Fluidic and electrical operation:**

The fluidic actuation was provided based on a pressure driven system. Figure 2.17 shows the beads transiting across the detection zone. The fluidic system works immaculately even with channels size of  $10\ \mu\text{m} \times 10\ \mu\text{m}$ . The beads used in the tests were of the sizes 3 and  $5\ \mu\text{m}$ . No clogging was observed with the beads and the device was used continuously for 3 days without any leakage problems.

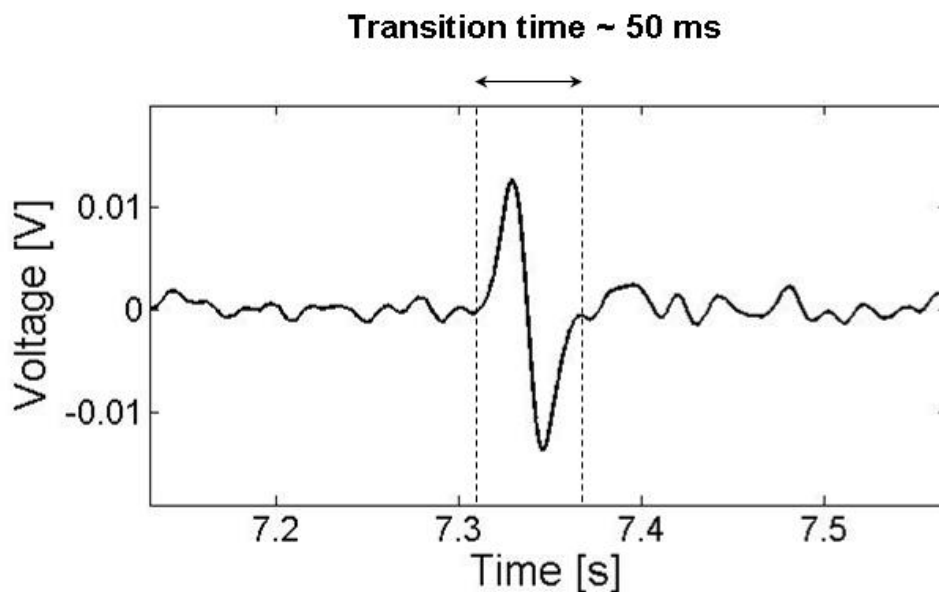


*Figure 2.17: Beads transiting through the 10  $\mu\text{m}$  channel across the detection zone*

Figure 2.18 shows the obtained signal highlighting transition of many beads passing through the system. A 100 points running average is applied to the original data once acquired in order to remove the noise. By counting the peaks recorded in the data, we can determine the number of beads that transited across the detection region. This is because the bead transition across the detection region changes the established electrical field in the channel, which can be visualised as a peak in the detected voltage signal. Looking closer into the region marked with the dotted lines in figure 2.18, one can clearly visualize the transition of one bead [Fig 2.19]. For this experiment, the transition times of the beads were found to be around 50 ms, which was also verified from the videos recorded of the beads transiting across the electrodes. These results confirm the good electrical connectivity and robust fluidic interfacing of the impedance chip with the motherboard via the Pluggy based interfacing and assembly method.



*Figure 2.18: Graph of beads transiting across the detection zone.*



*Figure 2.19: Enlarged image of one transition from the fig. 2.18.*

## Conclusion

In conclusion, the motherboard provides a very versatile and universal interfacing solution for electrical and fluidic connections to virtually any microfluidic device, fabricated in any material. A rapid, inexpensive, flexible and reliable interconnection strategy has been presented with a standardization approach, to enable faster development of microfluidic devices. In order to test the electrical connectivity and fluidic stability of the motherboard a microchip for impedance based sizing of particles was used. The results of these tests highlight the applicability of the motherboard for numerous microfluidic applications needing a simple and efficient strategy for forming fluidic and electrical connections. With this approach, we have designed a truly versatile solution for assembling microfluidic devices compatible with any substrate and providing rapid world-to-chip interconnections in a matter of seconds. This tool provides the fundamental scientists an opportunity to concentrate on development of applications without needing to focus on developing the interconnections and other building blocks of their devices. It also provides a very good application in bio, chemical and other analysis, where modular approach is required. We envisage that the easy assembly protocol and ability to combine any microfluidic devices will lead to efforts in testing complex microfluidic device combinations not possible earlier due to substrate incompatibility. Future work will be focused on integrating simpler biological protocols on the motherboard.

## 2.5 Outlook

A simple, plug and play, substrate-independent, modular motherboard was developed. Non-technical professionals were trained on how to use this motherboard and were able to operate it successfully (over 95% success rate). Finally, the motherboard was showcased to our collaborators (end-users) with the proposed modules for performing the FISH protocol during our usual strategic meetings. During this demonstration, flow through the planned C-TAS protocol [Section 2.2] was demonstrated using the modules of grooved culture chamber, dielectrophoresis based device for simultaneous lysing and extraction of chromosomes and subsequent FISH analysis using glass slide and PDMS complex device. Evaluating the modules and the motherboard, our collaborators commented on the complexities associated with the C-TAS protocol. Contrary to our expectations, the general feedback was that it would be very difficult if not impossible to implement it in genetic labs, unless it was automated.

During the development phase of the project, we had anticipated that there was a huge need for the modular C-TAS motherboard, and our logical reasoning was that, this demand was sustained due to the length and complexities of the traditional protocol. But on the other hand, collaborators found our protocol to be extremely complex and not user-friendly. This lead us to questioning our reasoning and we began a quest to figure out as to - “What were the real issues with the traditional techniques which needed microfluidic solutions?”. There was a clear consensus that it was time for us to visit the labs in person and get some better understanding of the needed solutions.

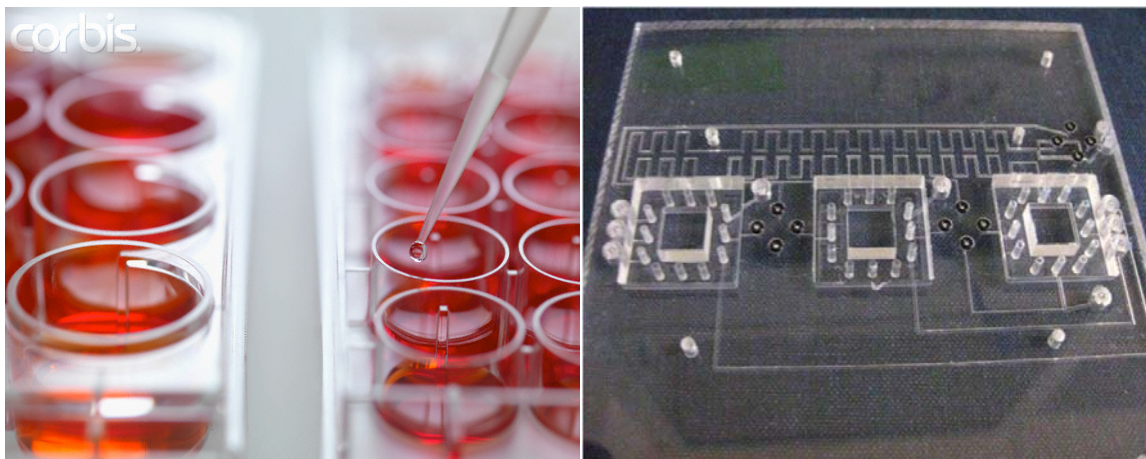
- What was the real issue with the traditional protocol?
- What modifications were needed in the C-TAS protocol to make it clinically relevant?
- But primarily - What were our collaborators expectation and vision of the C-TAS system?



### Comparison to the clinical setup:

After succeeding in prototyping a C-TAS motherboard and demonstrating its operation to the intended end-users, it occurred that the proposed solution did not provide the ease of handling and simplicity our end-users i.e. lab technicians were seeking. It was important to understand why the C-TAS protocol, based on a simple plug and play modular motherboard operated by pressing a switch on the syringe pumps, was too complex for implementation in a clinical setup.

On extensive observation and discussions with technicians at partnering cytogenetic labs revealed the real problems and the issues with respect to the complexity of C-TAS protocol. The simplicity of performing traditional protocol with culture plates and pipetting by skilled technician cannot be compared via a simple comparison of the motherboard [Fig. 2.20].



**Figure 2.20:** Comparison of traditional culture plate with pipette and the complex motherboard based protocol needing syringe pumps (not shown in image) for actuation. Apart from complexities related to extra modules, the handling on the motherboard is also much complicated compared to the pipette based traditional protocol.

Our observations and conclusions based on the interaction with our end-users is highlighted below.

- The motherboard based platform was simply too complex to handle with respect to the existing work routines and technicians skillset. Hence, **a degree of automation** needs to be developed before presenting it to the end-users.
- The technicians were well trained with using culture flasks and most operations of mixing with reagents to culturing cells took only seconds. This allowed technicians to handle multiple samples during a working day. Hence, the **time and ease of handling**

were important factor to consider when the unit operations conducted as part of the C-TAS protocol are concerned.

- We had been giving considerable attention to the pursuit of sorting, separation or trapping of lymphocytes to culture only TLs in the culture chamber [See - Chapter 4]. This concept had to be altered to **culturing whole blood** as this was the routine practice in clinics. Secondly, the red blood cells did not interfere with the FISH signals as was anticipated and also most of them were lysed during the fixation of the TLs. This made our sample preprocessing step a lot simpler and turned it into merely a basic culture and fixation protocol.
- In terms of the protocol, as the technicians need to focus on multiple samples during their daily routine, a **step by step process** is much better suited for their work process flow. This allows them to run multiple experiments simultaneously and stopping in between to work on other samples intermittently.
- **Handling of the devices needs to be more robust** as technicians are pretty much used to working quickly with one sample in flasks or plates and putting it back into the incubators or fridges and moving on to the next sample. Delicacy of the microfluidic device handling and the waiting time associated is a daunting prospect for current technicians.
- And finally, the bottom line is: Like every other product on the market, C-TAS needs to provide the end-user with an incentive to change. The incentive that technicians could care about are not low cost of device, less probe usage, better sensitivity, simpler protocol or automation providing them free time to handle more samples during a day rapidly, but **ease of existing workload, simpler work flow, automated data capture and analysis**. The cost and other factors are only marginally important.





# CHAPTER 3

## INTEGRATED C-TAS

This chapter presents the experimental work related to the development of a set of microfluidic devices for cell culture, sample pretreatment, metaphase spread preparation and leading to the development of first metaphase FISH analysis on chip. Finally, we describe the efforts towards automating the entire FISH analysis protocol.

### 3.1 Integrated C-TAS system: Needs and Approach

Our focus of development had to be shifted from modular microfluidic platforms towards developing an integrated C-TAS system for providing the end-users with a simple solution that continues to provide the traditional ‘ease of handling’ but also benefits from the advantages of a microfluidics based cell handling. Such a system should ideally also get rid of the complexities and practical challenges of interfacing with microfluidics. Additionally it should provide users with a ‘blackbox’ that looks and functions from the outside like the traditional systems but inherently packs in the advances that go hand in hand with microfluidics based miniaturized systems i.e. low cost, small sample volume, easy sample preparation and analysis, simple assembly and operation, *etc.*

While it seemed at first like going back to scratch again, we realized that we had actually learned a lot via the efforts targeted at developing the modular C-TAS system. While modular microfluidic platforms offer benefits of fluid and cell handling [Chapter 2] they generally do not provide the ease of handling unless automated, which is one advantage of integrated systems.

Integrated monolithic systems can be designed to have simpler interfacing and easy handling protocols due to the possibility of combining modules and sharing features among several modules. We had already devised a toolkit for performing C-TAS protocol [Section 2.2] on motherboard in the form of modules. Now we wanted to integrate these modules and design an integrated monolithic version of the C-TAS protocol. As a result, we could quickly zoom through the design phase of the integrated C-TAS approach and come up with a new setup of objectives which were matched with a realistic step by step approach for achieving the vision of a user friendly, simple integrated C-TAS system.

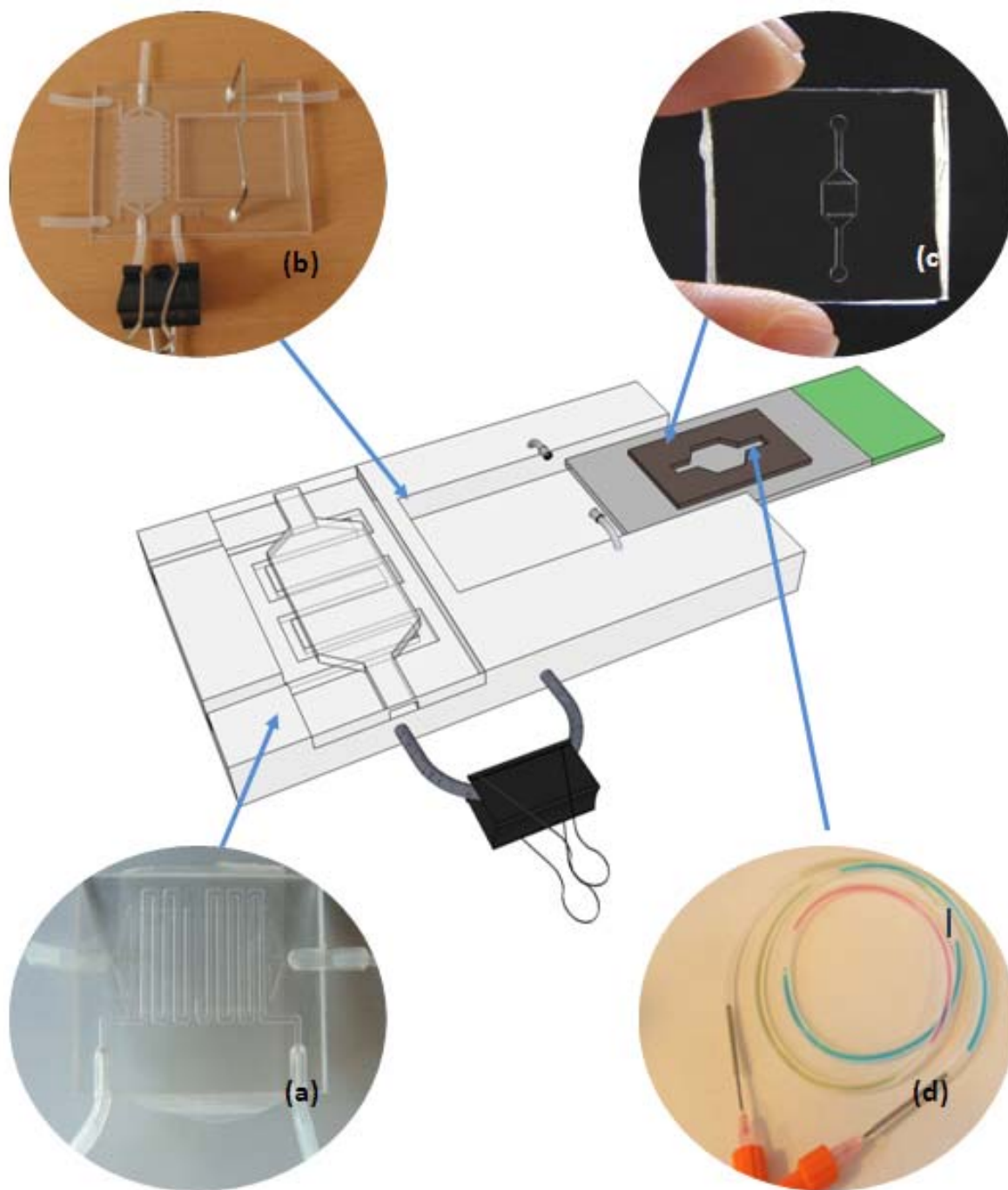
New objectives and the step by step approach:

- To design a **sample preparation module** to perform cell culture, arrest and fixation which can later be integrated with a FISH module [Paper 1: Microfluidic Bioreactors for non-adherent cell cultures].
- To realize a new reliable and integrated approach for **sample preparation** including **splashing based spreading of metaphase chromosomes** [Paper 2: FISHprep: A novel integrated device for metaphase FISH sample preparation].

- To demonstrate a novel protocol for performing **FISH on a chip**. [Paper 3: Metaphase FISH on Chip: Miniaturized microfluidic device for Fluorescence *In-Situ* Hybridization].
- Finally, the sample preparation, spreading device and the FISH chip were to be merged into a **monolithic integrated FISH device providing minimal handling and possibility to automate** [Fig. 3.1].

The following sections 3.2, 3.3 and 3.4 are papers published in peer-reviewed journals. As these papers are directed towards a specific scientific audience not all details of the procedures are described. For more information, on any methods described in this chapter, the readers of this thesis are referred to Chapter 5 Methods.

All the descriptions of cost, time, simplicity, ease of handling, reagent volumes are mentioned with respect to the standard protocols as existing currently at the Wilhelm Johannsen Centre for Functional Genome Research (WJC), The Panum Institute. All these following sections discuss the improvements in relation to the development of microtechnologies for these standard protocols. E.g. there might exist versions of standard techniques which involve less FISH probe volume usage but these minimize the scan area as well, and the process followed is not the usual standard. In the context of this thesis, the standard protocol is always considered to be the most routine FISH sample preparation and analysis protocol used for typical every day analysis at WJC [Section 1.5].



**Figure 3.1:** Schematic of the integrated C-TAS system. The schematic highlights proposed step by step approach for developing an integrated C-TAS system. The results are depicted in (a) Section 3.2: Cell culture, arrest and fixation device (b) Section 3.3: Metaphase spread preparation device and (c) Section 3.4: FISH analysis device are presented. (d) Automation of the reagents injection (AutoFISH protocol) by means of FISH reagent cartridge.



## 3.2 Microfluidic Bioreactors for culture of non-adherent cells<sup>4</sup>

Pranjul Shah<sup>1</sup>, Indumathi Vedarethinam<sup>1</sup>, Dorota Kwasny<sup>1</sup>, Lars Andresen<sup>2</sup>, Maria Dimaki<sup>1</sup>, Søren Skov<sup>2</sup> and Winnie Edith Svendsen<sup>1</sup>

1. Technical University of Denmark, DTU-Nanotech, Ørsteds Plads, Building 345 East, Denmark

2. University of Copenhagen, Department of Veterinary Disease Biology, Stigbøjlen 7, Denmark

### Abstract

Microfluidic bioreactors ( $\mu$ BR) are becoming increasingly popular for cell culture, sample preparation and analysis in case of routine genetic and clinical diagnostics. We present a novel  $\mu$ BR for non-adherent cells designed to mimic *in vivo* perfusion of cells based on diffusion of media through a sandwiched membrane. The culture chamber and perfusion chamber are separated by a sandwiched membrane and each chamber has separate inlet/outlets for easy loading/unloading of cells and perfusion of the media. The perfusion of media and exchange of nutrients occur through the sandwiched membrane, which was also verified with simulations. Finally, we present the application of this device for cytogenetic sample preparation, whereby we culture and arrest peripheral T-lymphocytes in metaphase and later fix them in the  $\mu$ BR. The expansion of T-lymphocytes from an unknown patient sample was quantified by means of CFSE staining and subsequent counting in a flow cytometer. To conclude on the applicability of  $\mu$ BR for genetic diagnostics, we prepare chromosome spreads on glass slides from the cultured samples, which is the primary step for metaphase FISH analysis.

### Key Words

Microfluidic Bioreactors ( $\mu$ BR), non-adherent cells, cytogenetics, membrane-based bioreactor, T-lymphocytes

---

<sup>4</sup> As published in journal - Sensors and Actuators B: Chemical 2011



### 3.2.1 Introduction

Despite successful demonstrations and obvious benefits of  $\mu$ BRs, traditional cultures continue to be very widely used in diagnostic labs in flasks, multi-well plates, bioreactors, etc.[138]. There are a number of outstanding issues hampering the widespread clinical adoption of the  $\mu$ BRs [139], mainly owing to lack of user friendliness, routinely occurring bubble issues [140-142], problems with interfacing with the macro-world (interconnections), cumbersome processes for depositing/seeding cells, biocompatibility [143] and finally adaptability to culturing various cell types (adherent or non-adherent cells) [144, 145]. These issues have delayed the mainstreaming of  $\mu$ BR despite the inability of traditional methods to provide to the cells controlled microenvironments resembling their *in vivo* state (short distances between cells, continuous perfusion of nutrients, waste removal, cellular structures providing adhesion) [146]. Meanwhile, traditional culture techniques (such as transwell membranes and gel based 3D cultures) continue to be laborious and expensive. Recently, it has also been noted that cells routinely alter their morphology, metabolism and growth rate in culture flasks [147]. Hence, there is clearly a need to replace the existing traditional techniques with more controlled, *in vivo* like novel cell culture techniques to enable better understanding of cell biology [148]. Microfluidic based  $\mu$ BR's can offer this by helping us benefit from specialized and microenvironment controlled cell culture systems offering possibilities of more relevant and *in-vivo* like *in vitro* studies currently not possible with traditional techniques (e.g. gradient analysis [149, 150], drugs screening [151, 152], chemotaxis [153-155], stem cell differentiation [156, 157], etc.

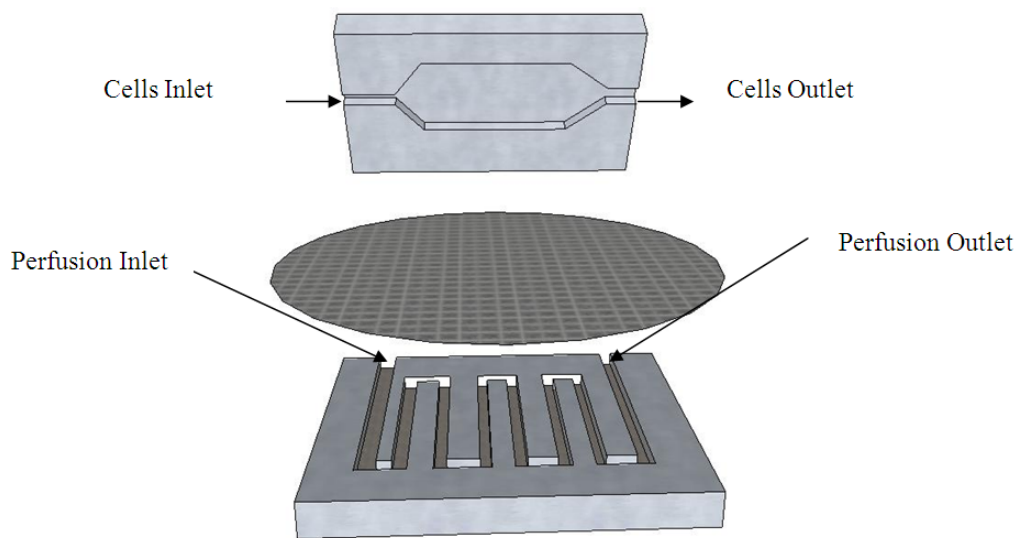
In recent years, a steady input of publications demonstrates successful culture of various cell and tissue types [158-160] and even co-cultures models [161-163], highlighting a promising future for  $\mu$ BRs in cell biology, neurobiology, genetics, proteomics, pharmacology and tissue engineering among others. While a vast amount of research has been put into solving problems like biocompatibility [142, 143], bubbles [141, 142], interconnections [129, 164]; there is still considerable lack of efforts in developing  $\mu$ BRs capable of handling non-adherent cells and providing them with a "homeostasis" microenvironment [146, 165]. This has also been influenced by the fact that the majority of analysis in cell biology and tissue engineering needs culture of adherent cells [113, 114, 125, 144, 166-168] which allows for perfusion over the cells attached to a surface unlike in the case of non-adherent cells that require a trapping mechanism.

Contrary to the popular interests, our development efforts with respect to  $\mu$ BRs have mostly focused on non-adherent cell cultures mainly due to interests in developing a lab-on-chip

device to perform fluorescence *in situ* hybridization (FISH) on a chip. In order to enable a micro total analysis system ( $\mu$ TAS) capable of performing FISH, we needed to recreate a sample pre-treatment device capable of replacing traditional culture flasks and titer plates, which can culture whole blood, arrest T-lymphocytes in metaphase, followed by subsequent inducement of a hypotonic state and ending with the fixation of the cells [84, 91]. Earlier work with non-adherent cell cultures has failed to provide a successful alternative to culture flasks due to the complexity of the devices and cell seeding procedures [169] and also due to the complexities with respect to retrieving the cells after culture for ensuing analysis [170-173].

Cytogenetists routinely perform the above mentioned sample preparation of whole blood into fixed metaphase cells for routine genetic analysis [68, 74, 174-177]. Slight variations of this sample pre-treatment methods form the initial steps of the majority of the cytogenetic diagnostic tests [178-185]. Hence, a device which can perform an automated sample preparation including expansion of T-lymphocytes (by mitogenetic stimulation with PHA), arrest of stimulated interphase cells in metaphase (by colcemid) and finally fixation of metaphase cells (using fixative – acetic acid:methanol (1:3)) can constitute a big leap in pushing  $\mu$ BRs into genetic labs for diagnostic sample preparations among many possible applications.

We have developed an innovative  $\mu$ BR enabling diffusion based perfusion to cells suspended on a sandwiched membrane separating the culture and perfusion chamber [Fig. 3.2]. Successful tests confirm that the presented  $\mu$ BR continues to provide the benefits generally associated with miniaturized microfluidic devices: low cost, portability, reduced sample and reagent volume, suitability for visual inspection, bubble free operation, chemical resistance against harsh solutions like fixative and biocompatibility. Moreover the device provides easy and effortless handling of non-adherent cell cultures on a microfluidic device. Our  $\mu$ BR there constitutes a simple and easy solution for cytogenetic sample preparation for culturing whole blood for expansion and arrest of T-lymphocytes, providing hypotonic treatment and finally fixing the cells for subsequent analysis. Moreover, by means of separation of loading/unloading of cells and perfusion channels using a two chamber approach, we have now enabled easy retrieval of cells followed by culture and/or fixation based pre-treatment. We present the results of the quantification process for the expansion of T-lymphocytes by means of CFSE staining. Finally, we validate the applicability of our  $\mu$ BR for diagnostic protocols by preparing chromosome spreads as a starting point for metaphase FISH analysis.



*Figure 3.2: Schematic of the  $\mu$ BR. (Top) culture chamber (bottom) perfusion chamber (middle) sandwiched PC membrane*

## 3.2.2. Materials and Methods

### 3.2.2.1 Reagents and Materials

Polycarbonate (PC) sheets were ordered from Nordplast. 5  $\mu$ m pore sized PC membrane (Whatman 7060-4713) was ordered from VWR Denmark. The other reagents and materials used for the experiments like Silicone tubing, Teflon tubing, RPMI (Invitrogen: SKU 72400-021), phytohemagglutinin (PHA), Fetal bovine serum (FBS) (Sigma-Aldrich:F9665), colcemid, acetic acid, methanol, DI water, ethanol, 3 way port valves, microscope slides, 4' 6-Diamidino-2-phenylindole (DAPI) and Ficoll-Paque plus were ordered from VWR Denmark and other traditional suppliers as listed. CFSE stain for cell viability assays was ordered from Invitrogen, Germany. The solvent for bonding the PC sheets was freshly prepared by mixing isopropanol: acetylacetone (1:1). The devices were milled with a micromilling machine (Folken Industries, Glendale, USA) using tools ordered from Kyocera Inc. And finally, the devices were bonded in a bonding press (P/O/Weber, Remshalden, Germany) after exposure with a UV light source (Dymax EC5000, Connecticut). A flow cytometer from Accuri C6 was used for cell proliferation assays. A Zeiss Axio Observer Z1 microscope was used for analysis of spreads.

### 3.2.2.2 $\mu$ BR Design

The  $\mu$ BR consists of two chambers: a culture chamber and a perfusion chamber separated by a sandwiched PC membrane [Fig. 3.2]. The culture chamber is designed in the form of a single monolithic chamber, while the perfusion chamber consists of a meandering channel allowing for even diffusion of media in the entire culture chamber and rapid removal of any bubbles arising in media. Both chambers have separate access inlets and outlets for easy seeding and retrieval of cells, and perfusion of media, see Fig. 1. All inlets are connected to a 3 way stopcock allowing us to avoid bubbles during changing of media and other reagents. The 3 stopcocks also allow for easy loading/unloading of cells in the culture chamber and later, for changing perfusion of various reagents in the perfusion chamber. The cells are loaded in the culture chamber through the cell inlet and retrieved for further analysis via the cell outlet. Once the cells are loaded, the cells inlet is closed and the perfusion inlet is used to perfuse the cells via diffusion through the PC membrane. The steps of the  $\mu$ BR protocol and corresponding valve states are shown in Table 1.

**Table 3.1:** Cell culture protocol for  $\mu$ BR with state of valves at each stage and inlet/outlet operation type. \*The time of culture is dependent on the cell type and length of experiment (generally ranges between 48 h and 3 weeks).

Process	Cell Inlet Valve	Cell Outlet Valve	Perfusion Inlet Valve	Perfusion Outlet Valve	Time of step
Cleaning and priming the $\mu$ BR	Open-Outlet	Open-Outlet	Open-Inlet	Open-Outlet	60 min
Loading the cells	Open- Inlet	Closed	Closed	Open-Outlet	10 min
Culture	Closed	Closed	Open-Inlet	Open-Outlet	72 hrs*
Unloading the cells	Open- Inlet	Open-Outlet	Closed	Closed	5 min

### 3.2.2.3 $\mu$ BR Simulation

We conducted an extensive simulated study of the flow through our  $\mu$ BR to validate our hypothesis of providing even diffusion based perfusion in the entire cell culture chamber. The simulations were done using Comsol Multiphysics 3.5 and combining the Convection and Diffusion and the Generalised Laminar Flow modules. There are three subdomains used: the culture chamber, the membrane and the perfusion channel. The subdomain representing the membrane has been simulated using the Darcy law for convection in porous media. Thus a term of a volume force on the liquid given by  $\vec{F} = -\alpha \cdot \vec{u}$  has been added in the flow mode, where  $\vec{u}$  is the velocity of the fluid and  $\alpha$  is a constant that can be roughly calculated using

the Darcy number. This is given by  $Da = \eta / \alpha \cdot L^2$ , where  $\eta$  is the viscosity of the fluid and  $L$  is the characteristic length scale of the system. By assuming a value for the Darcy number equal to  $10^{-4}$  and the typical length scale of our system to be  $10 \mu\text{m}$ , we can calculate that  $\alpha = 1 \cdot 10^{11} \text{ kg} / \text{m}^3 \text{ s}$ <sup>5</sup>. For diffusion through the membrane the diffusion coefficient of the diffusing species has been altered by multiplying with the porosity of the membrane, which is a good approximation.

Two main types of simulative studies were undertaken to optimize the experimental protocol for  $\mu\text{BR}$ . In the first case we would like to see how long it takes for the media to be exchanged with another, e.g. when adding KCl through the perfusion inlet for the hypotonic treatment. The flow problem was solved in steady state and the result used for the Convection and Diffusion problem, where the concentration in the perfusion inlet was set to 1. The diffusion coefficient for KCl was set to  $2 \cdot 10^{-9} \text{ m}^2 / \text{s}$ .

In the second case we would like to see how the diffusion of media through the membrane occurs during the culturing phase. In this case the concentration of the various relevant species, e.g. oxygen and glucose is already established in the entire domain, as the chamber and perfusion channels are primed. By assuming that half the chamber volume is occupied by glucose consuming leukocytes, we simulated the concentration of glucose into the culture chamber when a certain amount is being consumed by the cells (set to  $2.66 \cdot 10^{-4} \text{ mol} / \text{m}^3 \text{ s}$ ) [186]. The diffusion coefficient of glucose was set to  $6.7 \cdot 10^{-10} \text{ m}^2 / \text{s}$  [187].

### 3.2.2.4 $\mu\text{BR}$ Fabrication

The  $\mu\text{BR}$  is fabricated in two parts by micromilling in 1 mm thick PC sheets. The top [Fig. 3.2] part consists of the  $250 \mu\text{m}$  deep culture chamber with cell inlet and cell outlet. The bottom part consists of the  $300 \mu\text{m}$  deep and  $500 \mu\text{m}$  wide perfusion meander with connected perfusion inlet and outlet. The overall chip dimensions are  $26 \text{ mm} \times 30 \text{ mm}$ . The interconnections for the inlets and outlets are formed by embedding silicon tubing while bonding the two parts [188]. A PC membrane with  $5 \mu\text{m}$  pore size is sandwiched between the

---

<sup>5</sup> The characteristic length has been changed to  $10 \mu\text{m}$  (thickness of the membrane), resulting in  $\alpha = 10^{11} \text{ kg} / \text{m}^3 \text{ s}$ . This has modified the filling pattern in the bioreactor slightly [Fig. 3.4]. An erratum has been sent to the Sensors and Actuators B.

two parts during bonding providing the scaffold for the cell culture and diffusion of media and nutrients.

### **3.2.2.5 $\mu$ BR Bonding**

In order to bond the two parts, UV activated solvent bonding was used. The two parts were exposed to a UV light source for 30 s followed by 5 s exposure with solvent (isopropanol:acetylacetone(1:1)). In order to have a uniform exposure of the two parts to the solvent, the solvent is applied to a tissue and the two parts are lightly rubbed on to the wet tissue for 5 s. The two parts are allowed to rest for 15 s to allow for evaporation of the solvent. Finally, PC membrane and silicon tubings for interconnections are placed between the two parts and put in a P/O Weber bonding press at 125 °C with 10 kN pressure for 45 minutes.

It is critical to place the membrane without leaving any crease for leak-free bonding. Hence, the membrane was stretched at the edges after placing it between the two parts. The bonding protocol had to be optimized for providing leak-free bonding and to guarantee successful evaporation of the bonding solvent from the  $\mu$ BR. In order to allow for successful evaporation of the bonding solvent through the PC parts, we increased the time of the bonding from the recommended 30-45 min. Although leak proof bonding was achieved after only 20 min of bonding, we wanted to ensure with the extra bonding time that no solvent was trapped in PC which could prove toxic for the cells. The bonded device is allowed to cool under pressure down to 50°C before releasing the pressure and removing it from the bonding press to compensate for the stress induced during cooling of PC.

### **3.2.2.6 Sample Isolation**

A blood sample from a healthy donor was acquired from the blood bank. In order to purify and isolate the peripheral lymphocytes, Ficoll-Paque PLUS (GE Healthcare: 17-1440-02) was used to fractionate the several blood components by centrifuging at 2500 rpm for 15 min (as described by the manufacturer). The sample was adjusted to  $2 \times 10^6$  cells/mL using RPMI 1640 + 10% fetal bovine serum (FBS).

### **3.2.2.7 CellTrace™ CFSE Staining**

The cells were stained with CellTrace™ CFSE fluorescence stain at a concentration of 0.7  $\mu$ M in phosphate buffer saline (PBS) and incubated at 37°C for 15 min. The cells were re-pelleted and resuspended in pre-warmed cell culture medium and incubated for 30 min. The cells



were then centrifuged and resuspended in pre-warmed fresh medium and subjected to culturing.

#### **3.2.2.8 $\mu$ BR culture tests**

In order to sterilize the  $\mu$ BR, the device was entirely filled with 10% ethanol solution for 5 min and later washed with PBS for 10 min. This was done also to prime the chip and remove any trapped air in the culture and perfusion chamber. Before seeding of cells, the device was perfused with RPMI 1640 + 10% FBS for 1 h using 37.5  $\mu$ L/h flow rate (equivalent to 0.1 chamber volume/min) at 37 °C to stabilize the temperature of the device under the culture conditions. A 500  $\mu$ L buffy coat containing  $2 \times 10^6$  cells/mL was seeded into the culture chamber through the cell inlet by opening only the perfusion outlet connected to the waste collector. This ensured that all the cells were trapped on the membrane while the media solution containing the cells was filtered through the membrane to the perfusion outlet. The cells inlet was then closed and followed by perfusion of media through the perfusion inlet at 75  $\mu$ L/h (0.2 chamber volume / min) with RPMI 1640 + 10% FBS containing 10  $\mu$ L/mL PHA. After 72 hours of mitogenic stimulation, we stopped the perfusion and collected the cells through the cell outlet by flushing media from the cell inlet. As the cells are loaded through the membrane, a slower flow rate is used for loading to avoid excessive pressure on the cells which could diffuse through the 5  $\mu$ m pores. The unloading flow rate is faster compared to the loading flow rates as the unloading does not occur through the membrane. The collected cells were observed using a fluorescence cytometer to confirm the expansion of the cells. For control experiments, in parallel to the  $\mu$ BR cultures, CFSE stained cells were cultured in culture flasks and similarly observed using a fluorescence cytometer.

#### **3.2.2.9 $\mu$ BR sample pre-treatment tests**

In experiments, where we wished to perform the FISH sample pretreatment using a patient sample, we followed the  $\mu$ BR culture protocol and then we replaced the media with 75mM KCl solution at 0.4 chamber volume/min (150 $\mu$ L/h) for 25 min. This hypotonic treatment induced swelling of the cells. The  $\mu$ BR cell culture chamber is then perfused with freshly prepared cold fixative (acetic acid:methanol(3:1)) at 0.4 chamber volume/min (150  $\mu$ L/h) for 30 min. Between each change of perfusion, we removed the bubbles in the syringes using a 3 port valve. For control cultures, the traditional FISH slide preparation protocol was performed as described in section 3.2.2.10.

### 3.2.2.10 Control FISH slide preparation protocol

To prepare the control slides with chromosome spreads, we added 500  $\mu\text{L}$  of buffy coat containing  $4 \times 10^6$  cells/mL to 10 mL of RPMI 1640 + 10% FBS containing 10  $\mu\text{L}/\text{mL}$  PHA (Invitrogen: SKU 10576-015) and incubated them at  $37^\circ\text{C}$  and 5%  $\text{CO}_2$  for 68 hours. Later, the cells were arrested in their metaphase by adding 6  $\mu\text{g}/\text{mL}$  colcemid for 2 hours. The cells were centrifuged at  $190 \times g$  for 10 minutes and the supernatant was discarded. The isolated pellet was then resuspended in 10 mL 75 mM KCl (Sigma-Aldrich P9327) for 20 min before the cells were collected by centrifuging at  $190 \times g$  for 10 minutes. The supernatant was discarded leaving the pellet in about 0.5 mL of KCl solution. Slowly 10 mL of fixative (methanol:acetic acid(3:1)) was added a drop at a time all the while continuously mixing on a vortex. Finally, the fixed cells were collected at  $190 \times g$  for 10 min, and the same fixation process was repeated twice more to confirm fixation of the entire pellet.

### 3.2.2.11 Spreading of chromosomes

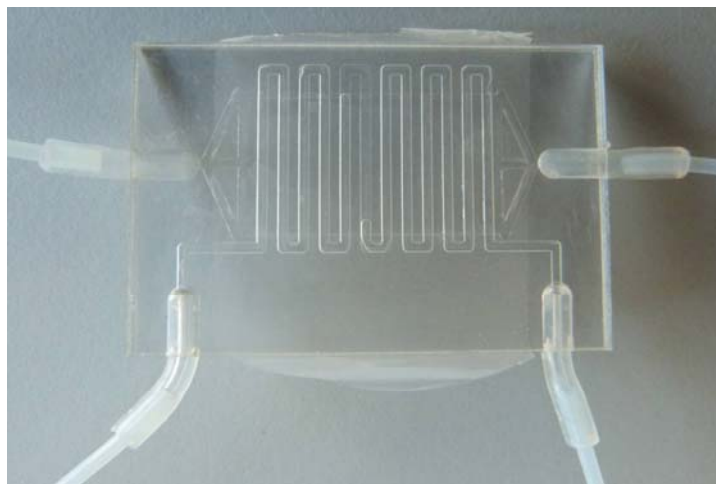
In order to test the viability of the proposed  $\mu\text{BR}$ , the retrieved fixed cells from the control and the  $\mu\text{BR}$  sample preparation tests were tested by preparing chromosome spreads on a glass slide. Acquiring good chromosome spreads forms the first and major step of successful metaphase FISH analysis [189, 190]. It also provides a confirmation of successful expansion of the lymphocytes, followed by arrest and fixation. To prepare the chromosome spreads, standard microscope glass slides were treated with a corona system for 1 min, resulting in a wetting behavior of the glass surface as described by Haubert *et al.*[191] The slides were stored in cold water at  $4^\circ\text{C}$  in a coplin jar. The slides were removed from the jar carefully leaving a thin water film on the surface of the slide. Two drops of fixed cells were applied to the wetted glass surface using a pipette in order to cover the entire glass slide. Later the glass slide was left to dry at room temperature overnight. The chromosome spreads achieved were stained with DAPI and observed with a fluorescent microscope.

## 3.2.3. Results and Discussion

### 3.2.3.1 $\mu\text{BR}$ Fabrication

The final device after bonding is shown in figure 3.3. During the bonding process, the PC membrane becomes an integral part of the PC sheets. The suspended membrane creates an optical effect of a transparent overall  $\mu\text{BR}$  and blurry cell culture and perfusion chamber.





*Figure 3.3:  $\mu$ BR with the interconnections*

### 3.2.3.2 $\mu$ BR Simulation

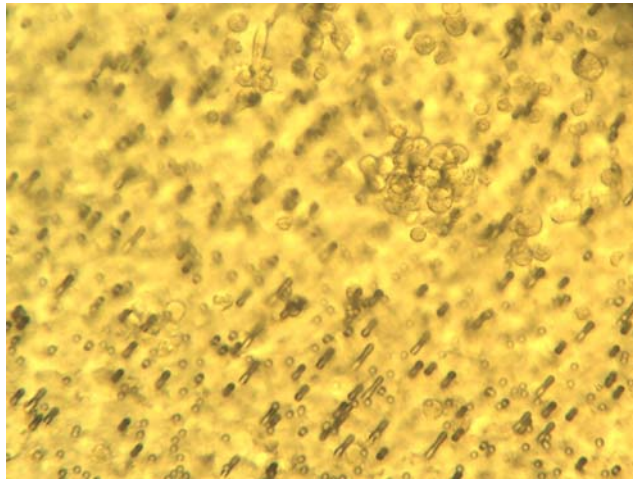
Figure 3.4 shows the diffusion of KCl into the culturing chamber when entering through the perfusion inlet 200, 1000 and 2000 s after switching the fluid from media to KCl. The simulation shows that after 2000 sec, corresponding to about 33 min, the solution in the culture chamber is almost completely replaced by KCl. In the experiments we have used 25 min of perfusion time for KCl, as it is not necessary to fully exchange the fluid to achieve cell swelling. Simulations dealing with the concentration of glucose when assuming that cells are consuming a certain amount per second per volume showed that for at least 72 hours the glucose concentration remains roughly the same as in the buffer solution. This means that the culture chamber provides the cells with adequate nutrients throughout the culture period.

### 3.2.3.3 $\mu$ BR protocol

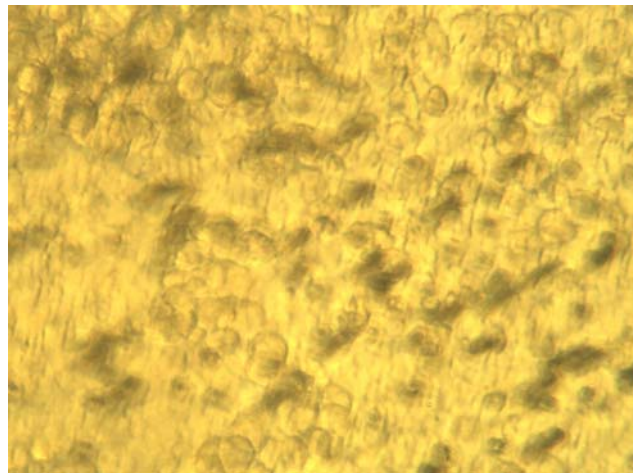
The overall culture protocol is illustrated in Table 3.1. The process starts with sterilization and priming of the chip followed by seeding of cells via cell inlet. Figure 3.5 shows the seeded lymphocytes on top of the membrane in the culture chamber. The pores in the PC membrane can be seen in the background. After 72 hours of mitogenic stimulation, there was an evident increase in the size of the cell cytoplasm [Figure 3.6]. After completion of  $\mu$ BR protocol the cells were collected and studied in a cytometer for validating the expansion of the cells by means of CFSE stain. In order to test the reusability of the  $\mu$ BR, which might be applicable for industrial batch processes, we re-cleaned the  $\mu$ BR with 10% ethanol and tested again with the  $\mu$ BR culture protocol [see- supplementary information].



67



*Figure 3.5: Cells on day 1 on the membrane*



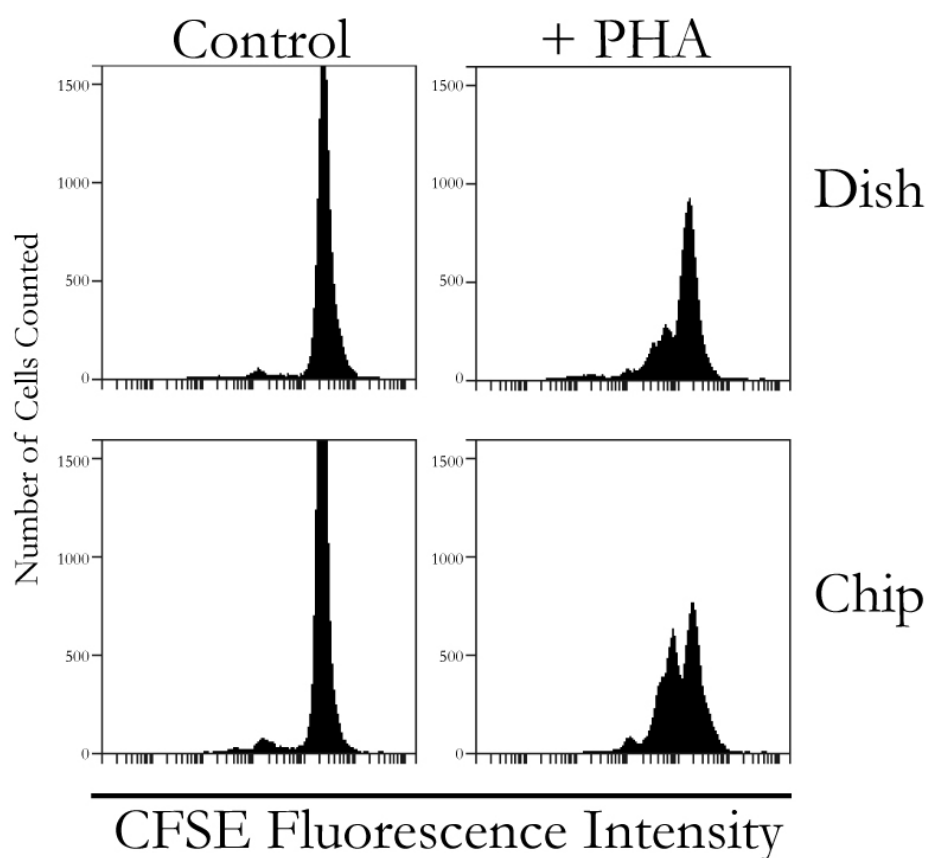
*Figure 3.6: Proliferated cells on the membrane on day 4. It was difficult to focus on the membrane on day 4 due to multiple layers of cells.*

#### **3.2.3.4 CFSE Proliferation assay:**

The collected cells were tested for proliferation in a flow cytometer by using CFSE staining of the cells. CFSE is a fluorescent stain that is retained within the cells throughout development and mitosis. The label is inherited by daughter cells after cell division but will have a lower fluorescence intensity which can be monitored on a flow cytometer. The CFSE stained cells were either left untreated or stimulated with PHA and cultured in the  $\mu$ BR device for three days and then analyzed for fluorescence intensity on a flow cytometer. In parallel, as a control, we also cultured cells with or without PHA stimulation in a normal plastic culture

dish. As seen in figure 3.7, a large fraction of PHA stimulated cells cultured in the  $\mu$ BR device started to proliferate as seen by the decrease in fluorescence intensity when compared to unstimulated cells.

On comparing the  $\mu$ BR results of the expansion of lymphocytes with the expansion on the petri dish, it is clearly evident that the  $\mu$ BR shows much better proliferation, depicted by the well defined second and emerging third peak in the CFSE fluorescence intensity from the chip sample data.

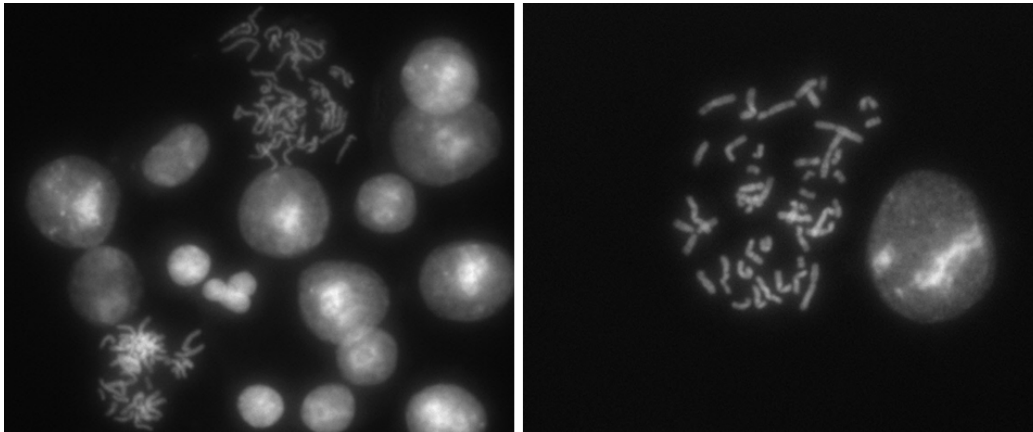


*Figure 3.7: Control and PHA stimulated growth count for 3 days culture in culture flask and on chip*

### 3.2.3.5 Spreading of the chromosomes:

The cells retrieved from the  $\mu$ BR and control cultures after the FISH sample preparation protocol i.e. expansion, hypotonic treatment and fixation of the cells were spread on glass slides. The spreads obtained were stained using DAPI and observed in an AxioVision Z1 Observer microscope. The results of the spreads received from the control and the  $\mu$ BR are presented in figure. Ample metaphase chromosome spreads were achieved on the glass slides

for  $\mu$ BR confirming successful sample pre-treatment and expansion of the peripheral lymphocytes [Fig. 3.8]. On further evaluation, we found no differences in the number and quality of the spreads from control and  $\mu$ BR samples, suggesting that the diffusion-based feeding provides a viable alternative for the expansion of peripheral T-lymphocytes and clinical cytogenetic sample preparation.



*Figure 3.8: (Left) metaphase spreads from control samples (Right) metaphase spreads from  $\mu$ BR samples*

### 3.2.4. Conclusion

A novel microfluidic bioreactor ( $\mu$ BR) was presented to enable controlled culture of non-adherent cells. The proposed device was tested with peripheral T-lymphocytes for sequential expansion as well as for cytogenetic slide preparation. The proposed  $\mu$ BR provides an easy and user-friendly solution for non-adherent cell cultures. The  $\mu$ BR tackles some of the most common challenges with respect to non-adherent cell cultures like providing diffusion based perfusion, shear stress, easy loading/unloading, removal of waste, trapping of cells, *etc.* The simple design with separate inlet/outlet for cells and perfusion chamber provides ease of handling and possibility of automating the protocol in the future. There are numerous other venues where the proposed device could prove beneficial and highly applicable such as co-cultures and adherent cell cultures. This device will soon be deployed in collaborating clinics to test its validity in clinical setups. We are also in the process of testing the presented  $\mu$ BR device for long term amniocytes culture for prenatal diagnostics.

### Acknowledgements

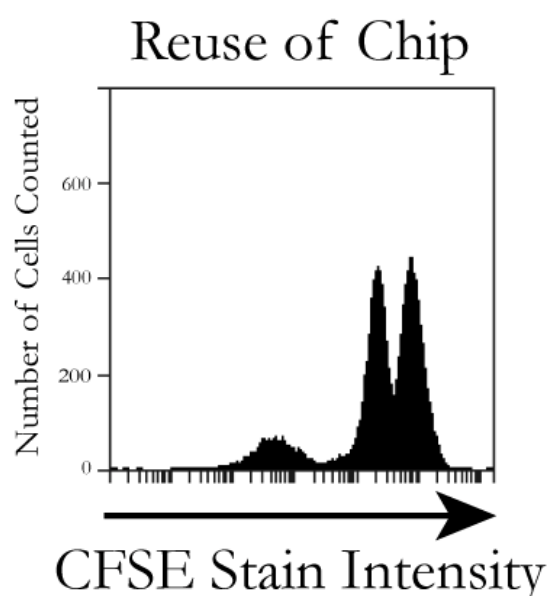
The authors would like to acknowledge the grants from The Danish Council for Independent Research and Lundbeckfonden making this research possible.



## Supplementary data

### Reusing the $\mu$ BR:

The  $\mu$ BR was reused to check the possibility of using the same device for more than one occasion. In order to clean the chip, the chip was flushed with 10% ethanol solution for 30 min. After this, the  $\mu$ BR culture protocol was performed using cells stained with CFSE. We tested the cell expansion using a flow cytometer with CFSE staining. The decrease in the intensity of the fluorescence shows successful proliferation of the T-lymphocytes on the reused chip. While not suitable for medical diagnostic applications, reusability of  $\mu$ BR can prove beneficial in industrial batch fermentation applications or in low resource settings.



*Figure 3.9: PHA stimulated growth count for 3 days T-lymphocytes culture on a reused chip.*

## 3.3 FISHprep: A novel integrated device for metaphase FISH sample preparation<sup>6</sup>

Pranjul Shah <sup>1</sup>, Indumathi Vedarethinam <sup>1</sup>, Dorota Kwasny <sup>1</sup>, Lars Andresen <sup>1,2</sup>, Søren Skov <sup>2</sup>, Asli Silahdaroglu <sup>3</sup>, Zeynep Tümer <sup>4</sup>, Maria Dimaki <sup>1</sup> and Winnie E. Svendsen <sup>1,\*</sup>

<sup>1</sup> DTU-Nanotech, Technical University of Denmark, 2800 Kgs. Lyngby, Denmark

<sup>2</sup> Dept. of Veterinary Disease Biology, Univ. of Copenhagen, Stigbøjlen 7, DK-1870, Denmark

<sup>3</sup> Wilhelm Johannsen Centre for Functional Genome Research, Uni. of Copenhagen, Denmark

<sup>4</sup> Kennedy Center, Gl. Landevej, 2600 Glostrup, Denmark

**Abstract:** We present a novel integrated device for preparing metaphase chromosomes spread slides (FISHprep). The quality of cytogenetic analysis from patient samples greatly relies on the efficiency of sample pre-treatment and/or slide preparation. In cytogenetic slide preparation, cell cultures are routinely used to process samples (for culture, arrest and fixation of cells) and/or to expand limited amount of samples (in case of prenatal diagnostics). Arguably, this expansion and other sample pretreatments form the longest part of the entire diagnostic protocols spanning over 3–4 days. We present here a novel device with an integrated expansion chamber to culture, arrest and fix metaphase cells followed by a subsequent splashing protocol leading to ample metaphase chromosome spreads on a glass slide for metaphase FISH analysis. The device provides an easy, disposable, low cost, integrated solution with minimal handling for metaphase FISH slide preparation.

**Keywords:** Fluorescence *In Situ* Hybridization (FISH); lab on chip; genetic analysis; cytogenetics; chromosome spreading; metaphase FISH; chromosomal translocations

### 3.3.1. Introduction

Fluorescence *In-Situ* Hybridization (FISH) is an indispensable molecular cytogenetic technique for diagnosis of both inherited and acquired chromosomal abnormalities at a much higher resolution than conventional karyotyping [73, 74, 85, 192-199]. Novel FISH based techniques are commonly used in diagnosis of various diseases. Recently, interphase FISH has gained much popularity, and as a result metaphase FISH has received lesser attention, which has significantly derailed the progress made in progressing metaphase FISH analysis technologies [78, 80, 90]. Interphase FISH offers numerous advantages compared to

---

<sup>6</sup> As published in journal – Micromachines 2011

metaphase FISH, such as better resolution (down to 1–15 kB) [200–203], wide range of commercial probes [204–208], shorter analysis time (for prenatal studies, dysmorphology, tumor-specific markers) [181, 195, 200, 209–213] and finally advantages of commercial imaging systems reducing data analysis time[214]. However, interphase FISH has limitations with respect to identification of unknown chromosome abnormalities and rearrangements like translocations. This is because interphase FISH relies on the availability of probes, which limits its applications only for the identification of known translocations[84, 215, 216]. As a result, metaphase FISH, still continues to be widely used for diagnosis of chromosomal aberrations in case of unknown translocations[217].

Most of these FISH-based techniques have very similar sample preparation protocols and despite such widespread use of FISH analysis, the sample preparation continues to be a manual, cumbersome and lengthy process leading to significant delays in the diagnosis as well as subsequent treatment of patients. Slide quality is one of the most important factors affecting the efficiency of FISH probe hybridization, and also the intensity and clarity of the FISH signals. Also, it is widely known that in all conventional metaphase preparations there are a large number of nuclei present suitable for interphase FISH studies[196]. Hence an automated system for FISH sample preparation can prove beneficial in multiple venues[73]. Considering the need for culturing various other cell types for FISH sample preparation (lymphocytes, amniocytes, chorionic villi and solid tumors), it would be highly beneficial to integrate the culturing protocol in such a system. This is particularly true in case of prenatal diagnosis, where the starting sample volume is not large enough to run all the necessary diagnosis tests.

Carefully evaluating the sample preparation protocol, it becomes evident that the most time consuming step is the expansion or culture of the lymphocytes (or other cell types like amniocytes, solid tumors, *etc.*) often taking from 72 h up to two weeks. Due to our interest, we only focus on metaphase FISH analysis and will not detail the steps of immobilization and preparation of interphase cells. However, every metaphase preparation includes cells in the interphase phase as well. For more information kindly refer to novel techniques for interphase FISH and related protocol for cells immobilization[80, 90, 218].

Molecular Cytogeneticists are extremely aware of the importance of preparing good metaphase chromosome spreads for getting a reliable FISH analysis[189, 190, 219]. The conventional short term protocol for preparing metaphase chromosome spreads from lymphocytes includes a 72 h cell expansion (with mitogenic stimulation) step, followed by



arrest of cells in metaphase and later fixation in Carnoy's fixative (1:3 vol:vol – acetic acid and methanol). Once fixed, the cells are splashed on a glass slide with a thin film of water on it, in order to form the chromosome spreads. While it sounds trivial and continues to be a very common protocol in cytogenetic labs, there are numerous variants of slightly modified protocols prevailing among the community with differences in time of culture, fixation, volume of stimulant, mitotic arrest and a vast number of different methods to prepare the chromosome spreads on the slides[189, 190, 219].

While many devices for controlled spreading of chromosomes exist, none of these devices have included integrated cell expansion and fixation chamber into the spreading device[190, 220, 221]. As a result, these steps (expansion, arrest and fixation) still need to be performed in traditional culture flasks. Also, the size of these existing spreading devices tend to be much larger compared to the proposed FISHprep device. This has led to reduced applicability or usage of these chromosome spreader or dropper tools, as they can be readily replaced by a pipette in the hands of a skilled technician. We have recently presented an integrated device to perform Metaphase FISH on a chip and included a splashing protocol for preparation of these metaphase spreads[84]. But we feel that lack of a complete sample pre-processing device (*i.e.*, Culture, Arrest and Fixation of cells) coupled with a mechanism to prepare chromosome slides has been the missing link for designing a fully automated sample-to-FISH analysis device. Hence, we have developed FISHprep – a novel splashing device integrated with a microfluidic cell culture chamber capable of cell expansion, arrest, fixation and finally splashing of fixed cells on a glass slide to provide metaphase chromosomes spreads for further FISH analysis. This device provides an easy to handle, low cost, disposable, integrated solution for the entire metaphase FISH slide preparation protocol.

### 3.3.2. Experimental Section

#### 3.3.2.1. Materials and Chemicals

Polycarbonate (PC) sheets procured from Nordplast (Denmark) were used to fabricate the FISHprep device. Glass slides (SuperFrost), syringes, 3 port valves, paper clips, silicone tubings, Teflon tubings and a 5  $\mu$ m pore sized PC membrane (Whatman 7060-4713) were ordered from VWR Denmark. Chemical reagents such as Phosphate Buffered Saline (PBS), phytohemagglutinin (PHA), Roswell Park Memorial Institute (RPMI) medium, Fetal bovine serum (FBS) were ordered from Sigma-Aldrich. Carboxyfluorescein succinimidyl ester (CFSE) stain used for viability studies was ordered from Invitrogen Germany. DAPI (4',6-diamidino-2-phenylindole) (Invitrogen) was used as a counter stain for coloring the chromosomes.

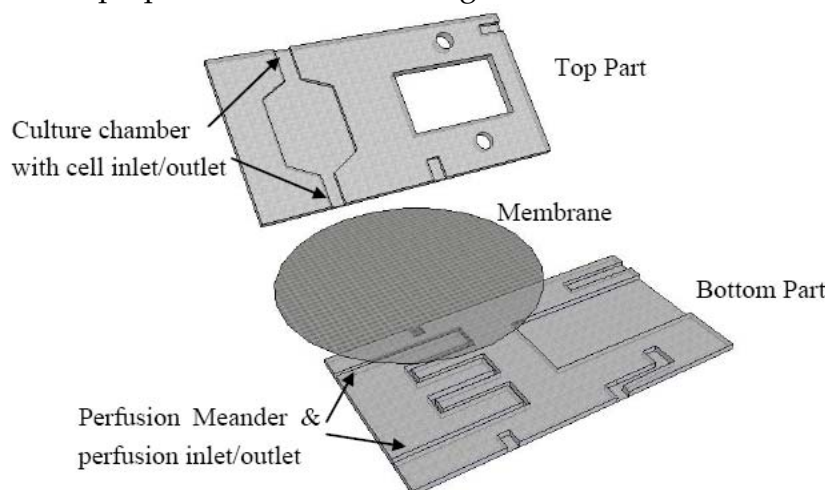
Experiments were conducted using blood samples from unknown donors received from the Blood Bank of the Rigshospitalet in Denmark.

### 3.3.2.2. Apparatus

A micromilling machine (Folken Industries, Glendale, AZ, USA) was used for milling the FISHprep device parts and a UV light source (DYMAX EC5000) was used for treating the surfaces before bonding them under pressure in a bonding press (P/O/Weber, Remshalden, Germany). Finally, a Zeiss Axio Observer Z1 Fluorescent microscope was used for analysis of the spreads and a flow cytometer (Accuri c6) was used for analysis of cell proliferation.

### 3.3.2.3. Fabrication

A schematic of the FISHprep device is shown in Figure 3.10.



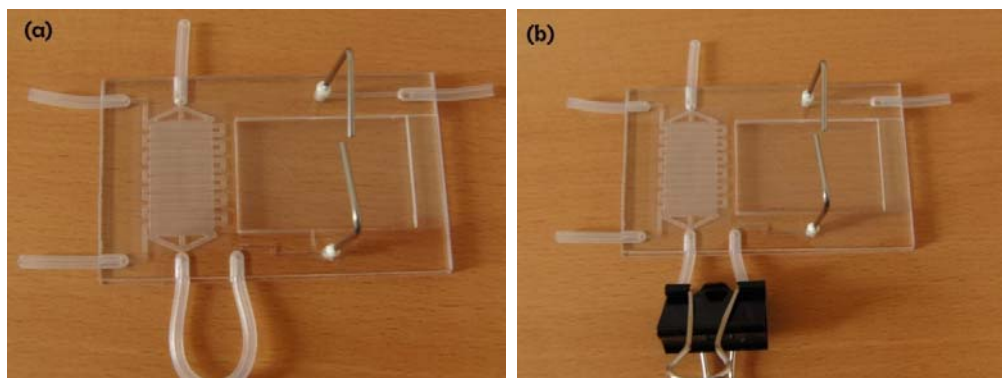
**Figure 3.10:** Exploded view of the FISHprep device top and bottom part. A polycarbonate membrane is sandwiched between the two parts to form the barrier between the culture chamber and perfusion meander.

The device is fabricated by micromilling in Polycarbonate Sheets. The bottom part contains a meander channel (1 mm wide, 300  $\mu$ m deep) for perfusion and a slot for sliding in glass slides (56  $\times$  26.2 mm). The top part contains a cell culture chamber (250  $\mu$ m deep) with a cell inlet channel and a cell outlet channel connected to the splashing chamber's fixed cells inlet. It also includes another channel to act as an inlet for splashing water on the glass slide. A polycarbonate membrane (5  $\mu$ m pore size) is sandwiched between the perfusion channel and the cell culture chamber during the bonding process of the two parts. The two parts are bonded together using UV activated bonding[188]. First the two parts are wiped clean with IPA followed by rigorous wash with a detergent soap and water. Subsequently the two parts are thoroughly air dried and exposed to UV for 45 s. Before putting the two parts together a

PC membrane and interconnection plugs (Silicon tubing: Outer Diameter (OD) 3 mm, Inner Diameter (ID) 1 mm) are placed on the lower part. A Silicon tubing U-plug is placed at the cell outlet of the culture chamber and connected to the fixed cells inlet of the splashing chamber. Finally, the top part is placed on the lower part and put in a P/O/Weber bonding press at 130 °C for 30 min.

#### 3.3.2.4. Paper Clip Valve: Leakage Test

In order to connect the culture chamber and splashing device, we have devised a simple and easy paper clip based valving strategy. This strategy was adopted in order to utilize tools commonly available in the cell labs and also to keep the protocol simple. A 3 mm OD silicone tubing is bonded from the cells outlet to the cells inlet of the splashing device [Fig. 3.11]. The tubing forms an external U-section out of the device providing enough room for putting on a paper clip to stop the flow. The paper clip valve was tested at increasing flow rates to identify the maximum permissible flow rate before leakage occurs and to validate the applicability of these valves for the cell culture protocol. The flow rate was increased gradually using a syringe pump and the flow rate at which the device leaked was recorded.



*Figure 3.11: (a) Bonded FISHprep device (b) FISHprep device depicting paper clip based valving procedure.*

#### 3.3.2.5. Culturing Protocol

The device is cleaned and primed by flushing 10% ethanol solution for 5 min and later washed with PBS for 10 min to remove any traces of ethanol from the culture chamber. This priming and sterilization helps to remove any trapped air in the culture and perfusion chamber. Before cells are seeded in the culture chamber, the device is perfused with RPMI 1640 + 10% FBS for 1 h at the flow rate of 37.5  $\mu\text{L}/\text{h}$  (the device is kept at 37 °C in a CO<sub>2</sub> incubator). A 500  $\mu\text{L}$  buffy coat with a cell count of  $2 \times 10^6$  cells/mL was seeded into the

culture chamber through the cell inlet by opening only the perfusion outlet connected to the waste collector. This protocol for seeding ensures that all the cells get trapped onto the membrane while the suspension media is filtered out from the perfusion outlet. Finally, the cells inlet is closed and a perfusion of fresh media is started through the perfusion inlet at 75  $\mu\text{L/h}$  with RPMI 1640 + 10% FBS containing 10  $\mu\text{L/mL}$  PHA. After 72 h of mitogenic stimulation, the perfusion is stopped and after wait time of 5 min, (which ensures that the flow has completely stopped) the paper clip valve is opened and the spreading protocol is initiated. Cells seeded in a well plate served as a control for the expansion experiments.

#### **3.3.2.6. CFSE Staining Protocol**

In order to confirm the expansion of lymphocytes on the culture chamber, the cells were stained with CellTrace™ CFSE fluorescence stain (Invitrogen, Germany), at a concentration of 0.7  $\mu\text{M}$  in phosphate buffer saline (PBS) and incubated at 37 °C for 15 min. The cells were later re-pelleted and resuspended in pre-warmed cell culture medium and incubated for 30 min. The cells were then centrifuged and resuspended in pre-warmed fresh medium and subjected to culturing in the FISHprep culture chamber. The CFSE stained cells were stimulated with PHA and cultured for 72 h. Finally, the cells were collected through the cell outlet. In order to collect the cells after culture to analyze their expansion, the U-plug was sliced via a scalpel and disconnected from the splashing chamber. Later, the cells were extracted from the cell outlet by flushing culture media from the cell inlet. To conclude on the expansion, the collected cells were analyzed for fluorescence intensity using a flow cytometer.

#### **3.3.2.7. Spreading Protocol**

In these experiments, the aim was to perform the FISH sample pretreatment. Therefore, after the culture protocol we replaced the media with 75 mM KCL solution at 0.4 chamber volume/min (150  $\mu\text{L/h}$ ) for 25 min. This hypotonic treatment induced swelling of the cells. Finally, in order to fix the cells, the chamber is perfused with freshly prepared fixative (acetic acid:methanol-3:1) at 0.4 chamber volume/min (150  $\mu\text{L/h}$ ) for 30 min. Between each change of perfusion, by use of 3 port stopcock, it was ensured that the bubbles were removed before starting the perfusion. For control, simultaneous cultures were conducted in culture flasks followed by the traditional FISH slide preparation protocol[196].

On completion of the sample preparation protocol, the paper clip valve was opened, which connected the spreading chamber to the cells culture chamber outlet. This allows the flushing of fixed cells from the culture chamber on the glass slide. A glass slide treated with corona for 1

min is inserted into the splashing chamber slide slot. The corona treatment helps to activate the surface and improves the wetting behavior of the slide leading to better spreads[191]. Finally, in order to create metaphase spreads on the slide, a drop of cold water is dropped on to the glass slide via the separate inlet for water. This is quickly followed by a drop of fixed cells suspension from the cell chamber by opening the paper-clip valve. The slide is allowed to dry for 2 min before removing it from the FISHprep device. This is currently done manually by use of syringe pumps, which opens the possibility of automation in future. The process is repeated onto three to four slides in order to have ample slides to have quantified FISH analysis (it is a routine process in standard FISH analysis to prepare at least three slides). For the control cultures, the traditional metaphase FISH sample preparation protocol is followed and later, the chromosome spreads are prepared using the dropping technique by an experienced technician[196].

### **3.3.2.7. Analysis**

The slides with chromosome spreads are stained with DAPI and sealed with a coverslip. Later they are analyzed using an AxioVision Z1 Observer microscope to analyze the metaphase spreads and thereby validate the applicability of the FISHprep device for metaphase FISH sample preparation. As a final step, the slides prepared with FISHprep device were analyzed using the traditional metaphase FISH protocol[196]. A centromeric probe targeting X-chromosome (Kreatech, NL) was used for the FISH analysis.

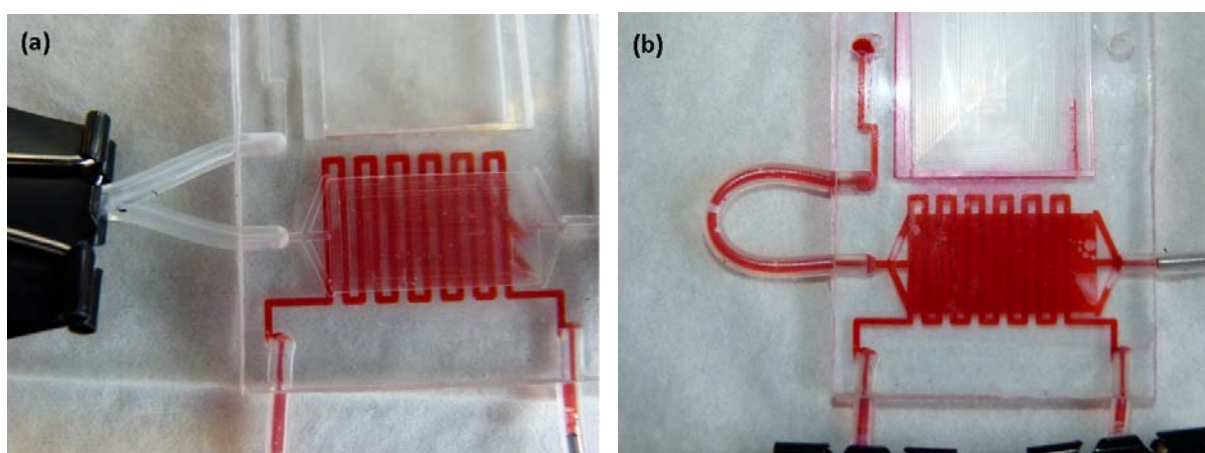
## **3.3.3. Results and Discussion**

### **3.3.3.1. Fabrication**

The fabricated FISHprep device is shown in Figure 3.11. The interconnections to the syringe pumps are made by inserting a Teflon tubing (OD 1.2 mm) in the silicon plugs (ID 1 mm) bonded between the PC sheets. At every interconnection before the syringe, a 3 way valve is attached to the Teflon tubing to allow for easy changing of reagents (sterilizing compounds, media, fixative, etc.) and removal of bubbles for bubble-free operation device operation.

### 3.3.3.2. Paper Clip Valve: Leakage Test

The paper clip based valving technique was tested for isolation between the culture chamber and the splashing chamber until the cells had been fixed in the culture chamber for 72 h. The FISHprep devices were tested for increasing flow rates starting from 150  $\mu\text{L}/\text{h}$  up to 750  $\mu\text{L}/\text{h}$ . The flow rate of 150  $\mu\text{L}/\text{h}$  represents the maximum perfusion rate for the fixation protocol used for sample preparation in the culture and fixation chamber [Fig. 3.12(a)]. The first signs of leakage in the device were visible only after 500  $\mu\text{L}/\text{min}$  flow rate due to lateral flow in the PC membrane at the bonding interface [Fig. 3.12 (b)]. Even at such high flow rates, there was no flow through the paper clip valve; the leakage only occurred through the short bonding edge in the FISHprep device. Also, it was noticed that the device was still functioning well without any leakage, when the flow rate was again reduced to 150  $\mu\text{L}/\text{h}$  [Fig. 3.12 (b)].



**Figure 3.12:** (a) Paper clip valve of the external U-section: Isolation of flow from culture chamber to splashing chamber (b) Flow through culture chamber on to the splashing chamber on opening of the paper clip valve (Leakage in the device at 500  $\mu\text{L}/\text{min}$  flow rate).

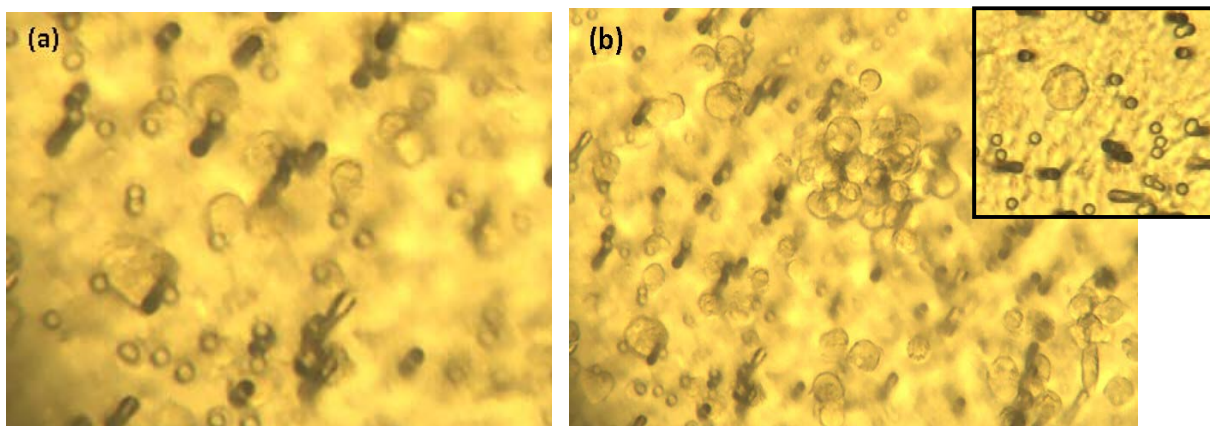
### 3.3.3.3. Expansion and Spreading Protocol

Figure 3.13(a) shows the seeded lymphocytes on top of the membrane in the culture chamber. The pores in the PC membrane can be seen in the background. After 72 h of mitogenic stimulation with PHA, we could see a significant increase in the size of the cell cytoplasm (Figure 3.13(b)).

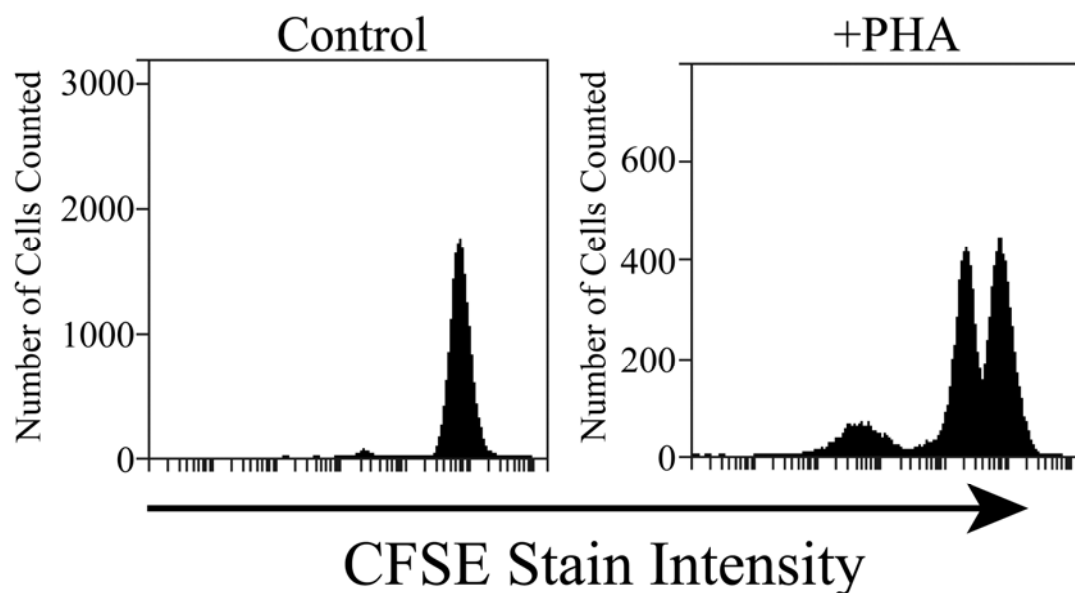


### 3.3.3.4. CFSE Proliferation Assay

The cells collected from the FISHprep culture chamber were analyzed in a flow cytometer by using CFSE staining of the cells. CFSE stain is retained within the cells throughout development and mitosis. On proliferation, the label is inherited by daughter cells but with a lower fluorescence intensity which can be monitored on a flow cytometer. Figure 3.14 shows results of fluorescence analysis of 20  $\mu$ L of FISHprep culture samples. The cells show signature peaks of proliferation as depicted by the decrease in fluorescence intensity. In contrast, the negative cultures of lymphocytes (without PHA) on the FISHprep device, hardly show any growth which confirms that the FISHprep device does not induce any activation or expansion of the lymphocytes due to microfluidic handling. As our interests were related to procuring ample FISH spreads to conduct a FISH analysis, we didn't culture the cells for longer time or quantify the culture dynamics in the FISHprep culture chamber. It might be of interest at a later point to culture cells for longer durations for characterization and comparison of the growth pattern of cells on the FISHprep device with traditional cultures. There is a possibility that cells in FISHprep culture device might follow a different expansion cycle compared to the culture flask[147].



**Figure 3.13:** FISHprep culture (a) Cells on Day 0 (b): Cells on Day 3 (background shows pores in the PC membrane). (Inset – Enlarged cytoplasm on Day 3).



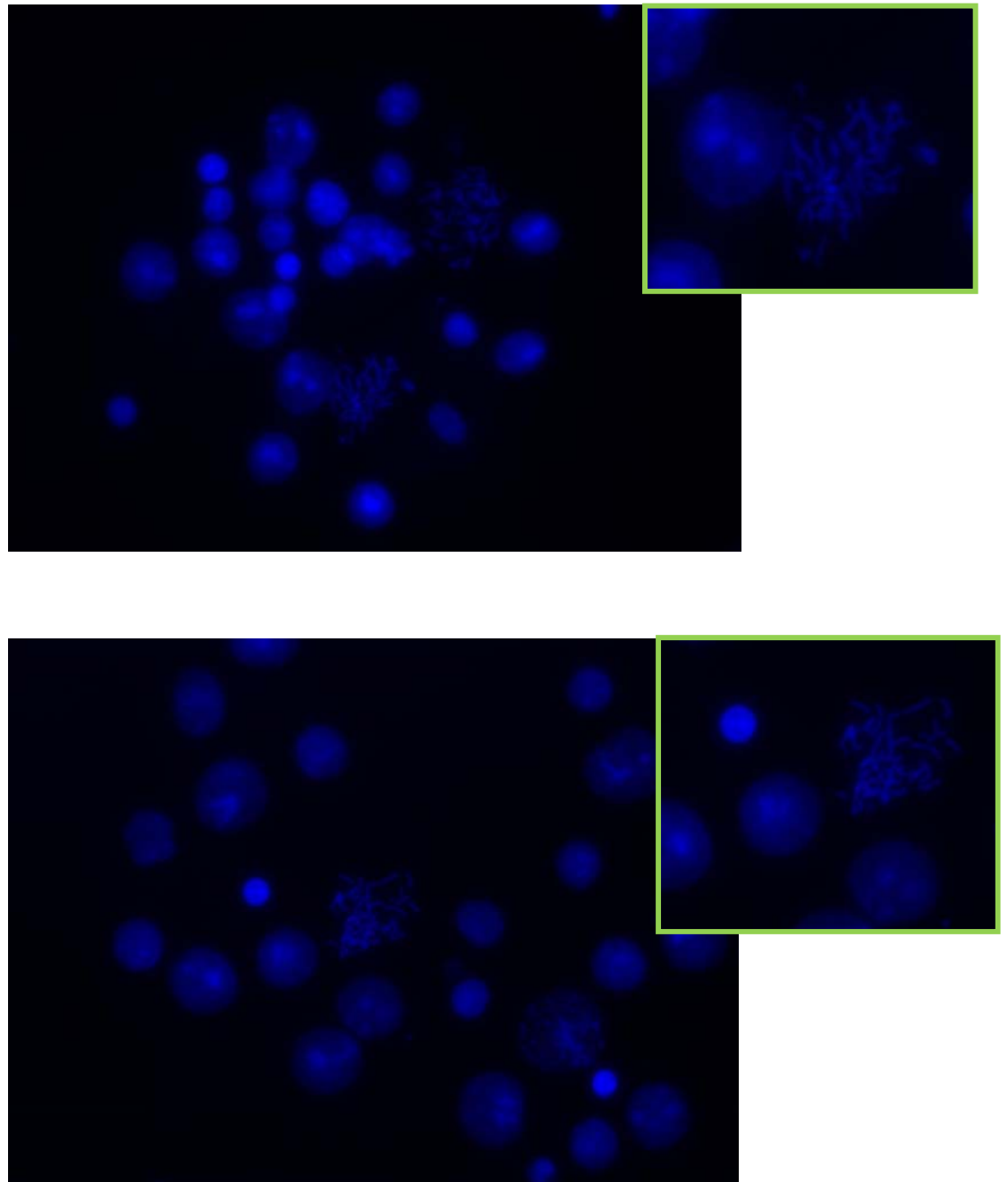
**Figure 3.14:** CFSE proliferation assay results. Count of cells vs. the fluorescence intensity of CFSE stained cells analyzed by fluorescence cytometer. (Control experiments relate to negative control of cultures on FISHprep device without PHA stimulation).

### 3.3.3.5. Analysis of the Spreads

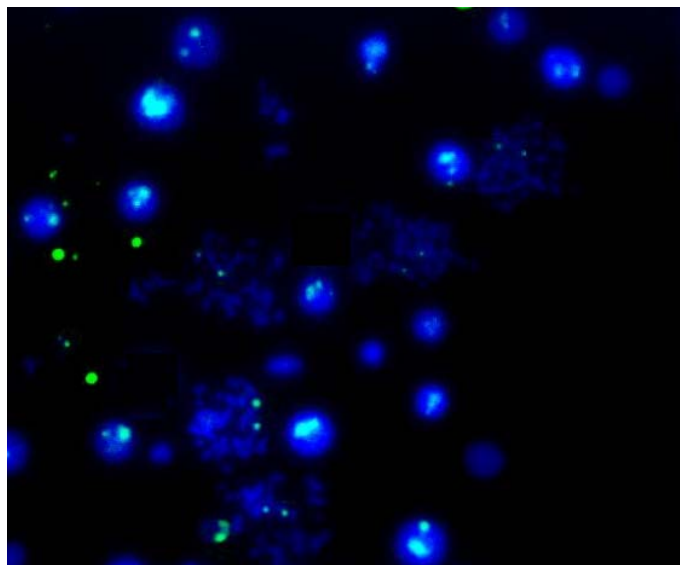
The spreads obtained from the integrated device and the control flask cultures were stained with DAPI and analyzed using an Axio Observer Z1 microscope. Figure 3.15 (a,b) presents the spreads achieved from the FISHprep device and control flask samples respectively. The mitotic index in both the slides was found to be above 75%. The spreads on the FISHprep device were comparable to the spreads received with control samples.

Finally, Figure 3.16 shows the results of the traditional metaphase FISH protocol applied to the samples prepared using the FISHprep device. The FISH signals acquired for the X-chromosomes in the spreads validate the compatibility of this proposed sample preparation technique for cytogenetic analysis. Hence, we concluded the promising applicability of FISHprep device for metaphase FISH sample preparation.





**Figure 3.15:** (a) (Top) Chromosome spreads prepared using the FISHprep device (b) (Bottom) Chromosome spreads achieved using the manual dropping technique. Offset pictures present high magnification images.



**Figure 3.16:** FISH analysis on the FISHprep samples (The FISH signals indicate the presence of two X-chromosomes in the chromosome spreads and cells).

### 3.3.4. Conclusions

A novel, simple, minimal handling, integrated device (FISHprep) was presented for processing samples and preparing slides for FISH analysis. The presented device provides a simple, low cost, disposable alternative to traditional sample preparation technique including culture, arrest, fixation and subsequent preparation of glass slides with metaphase chromosome spreads. The inclusion of a membrane based culture chamber into the FISHprep device opens possibilities for expanding the applicability of the device to other cell types like amniocytes or chorionic villus, where controlled long term expansion of cells is of great interest due to small amounts of available sample volume. In the near future, we aim to integrate the Metaphase FISH on chip protocol into the FISHprep protocol to create a chromosome total analysis system.

### Acknowledgements

The authors would like to thank the Danish Research Council for Technology and Production and the Lundbeck Foundation for their financial support to make this research possible. Finally, Peder Skafte-Pedersen for assistance with microscope for image acquisition. The Wilhelm Johannsen Centre for Functional Genome Research is established by The Danish National Research Foundation.

### 3.4 Metaphase FISH on chip: Miniaturized Microfluidic Device for Fluorescent *in situ* Hybridization<sup>7</sup>

Indumathi Vedarethinam <sup>1,†</sup>, Pranjul Shah <sup>1,†</sup>, Maria Dimaki <sup>1</sup>, Zeynep Tumer <sup>2,3</sup>,  
Niels Tommerup <sup>2</sup> and Winnie E. Svendsen <sup>1</sup>

<sup>1</sup> DTU-Nanotech, Technical University of Denmark, Denmark

<sup>2</sup> The Panum Institute, University of Copenhagen, Blegdamsvej 3, Denmark

<sup>3</sup> Kennedy Center, Gl. Landevej, 2600 Glostrup, Denmark

<sup>†</sup> Both authors contributed equally to this paper and therefore order of authorship is arbitrary.

**Abstract:** Fluorescence *in situ* Hybridization (FISH) is a major cytogenetic technique for clinical genetic diagnosis of both inherited and acquired chromosomal abnormalities. Although FISH techniques have evolved and are often used together with other cytogenetic methods like CGH, PRINS and PNA-FISH, the process continues to be a manual, labour intensive, expensive and time consuming technique, often taking over 3–5 days, even in dedicated labs. We have developed a novel microFISH device to perform metaphase FISH on a chip which overcomes many shortcomings of the current laboratory protocols. This work also introduces a novel splashing device for preparing metaphase spreads on a microscope glass slide, followed by a rapid adhesive tape-based bonding protocol leading to rapid fabrication of the microFISH device. The microFISH device allows for an optimized metaphase FISH protocol on a chip with over a 20-fold reduction in the reagent volume. This is the first demonstration of metaphase FISH on a microfluidic device and offers a possibility of automation and significant cost reduction of many routine diagnostic tests of genetic anomalies.

**Keywords:** Fluorescence *in situ* Hybridization (FISH); lab on chip; genetic analysis; cytogenetics; chromosome spreading; metaphase FISH; chromosomal translocations

#### 3.4.1. Introduction

During the last decade microfluidic techniques have evolved into a new genre of research areas targeting integration of laboratory protocols into miniaturized devices called lab on chip (LOC) or micro total analysis systems ( $\mu$ tas) [38–40, 222, 223]. The ability to control small

---

<sup>7</sup> As published in journal – Sensors 2010

sample volumes on micro-sized devices is immensely appealing for techniques involving handling of ultra small volumes of cells or other analytical samples [224]. This has spurred an exponential growth in the number of research articles published in the field of LOC systems targeting complex biological protocols to benefit from the low volume, high throughput and low cost features provided by the microfluidic devices [91, 224, 225]. We have created a novel metaphase FISH chip to benefit from the low dead volumes associated with microfluidic devices as FISH protocol reagents and commercial probes are more expensive than gold (over \$400 for 100  $\mu$ L of probe used in this work) [80, 90].

FISH is a sensitive diagnostic cytogenetic tool routinely used to visualize numerical and structural chromosomal aberrations [73, 193, 195, 197, 215, 226-229]. The traditional FISH protocol includes steps like immobilization of interphase nuclei or metaphase chromosomes, probe labeling, RNase treatment, denaturation of chromosomal and probe DNA, hybridization, post hybridization wash and image processing. FISH is routinely used by cytogeneticists in applications ranging from chromosome labeling and mapping, identification of gene expression sites, tissue analysis, mRNA synthesis tracking, tumour genetic alterations monitoring, identifying infections from viruses and other diagnostic pathological applications including cancer e.g., leukemia [71, 198].

Interphase and Metaphase FISH are two types of commonly used chromosomal FISH techniques. Each has their specific applications and advantages. Interphase FISH is used to identify numerical abnormalities as well as specific structural abnormalities. Thus, Interphase FISH depends on a specific probe, e.g., to detect known translocations, microdeletions or specific chromosomes and hence can only be used to address questions for which DNA probes are available. Lack of conformity of interphase FISH is a major disadvantage when using this technique for prenatal diagnostics [86]. On the other hand, metaphase FISH can be used to visualize the insertion, deletion or other rearrangement involving a specific region of the genome, with a resolution determined by the probe used [228]. Metaphase FISH can be performed on samples with unknown translocations by targeting all the chromosomes using multi-color FISH probes [85], derived from plasmids, cosmids, bacterial artificial chromosomes (BAC) and yeast artificial chromosomes (YAC) [229]. Recently Interphase FISH was demonstrated on a microfluidic device which highlights the obvious benefits of miniaturizing and automating the FISH protocol in a microfluidic system [78, 80, 90]. But metaphase FISH protocol has been elusive owing to the difficulty of handling chromosomes on a chip and fixing the chromosomes on a closed microfluidic device [78]. As a result, in spite of FISH being a very powerful cytogenetic tool, it continues to be an expensive and

reasonably time consuming method. There is clearly a need for replacing the traditional method with a fast and low-cost method making this technique widely available and easy to handle.

Our efforts have been directed at designing a miniaturized protocol for performing metaphase FISH in a controlled manner on a microfluidic device. It is widely known that the results of classical banding techniques, FISH analysis or Comparative Genomic Hybridization (CGH) are dependent on the quality of the metaphase spreads [190]. Hence the result of any FISH analysis depends on consistency of spreading of chromosomes [230]. During the 90s metaphase spreading techniques were widely investigated and many labs developed their own version of optimized standard methods [194, 231-235]. This led to a number of theories on what determines the quality of metaphase spreads on the glass slide, including the distance and the angle of dropping of the fixed cells onto the slide, the diameter of the pipette, the evaporation of the fixative, the temperature of the slide, the hypotonic treatment of the chromosomes, and the whole air drying process [189, 230, 236]. Renewed interest has seen a number of attempts towards making devices for preparation of chromosome spreads, which rely on controlled angle and conveyors [221], temperature gradient and humidity [190] and most recently the chromosome dropper tool which relies on dropping angle and height for fixing metaphase spreads on glass slides [220]. But none of these three devices are remotely close to the miniaturized size we are targeting or give any new insights into the mechanism of spreading compared to what was already published in the 90s. Through literature review and our own preliminary experiments we found that the basis of chromosome spreading is rooted in the optimum rate of evaporation of the fixative from the glass slide. Hliscs *et al.* suggests that the mechanism of chromosome spreading is a slow process, which leads to stretching of chromosomes via flattening [219]. Spurbeck *et al.* mentioned that in the process of spreading the fixative evaporates, leading to build up of surface tension causing the metaphase cell to flatten, which eventually leads to bursting of the cell membrane and spreading of the chromosomes [230]. Henegariu *et al.* also concluded that dropping of chromosomes from a height doesn't improve the spreading [190]. Hence, we concluded that in order to realize a micro-splashing device which produces reliable metaphase spreads on a glass slide sufficient for conducting routine FISH analysis; we need to incorporate a mechanism to allow for optimum evaporation of the fixative leading to stretching of the chromosomes and flattening of the cells. This could be aided by environmental factors like temperature of the slide and humidity but the focus has to be on maintaining an optimum rate of fixative evaporation.

In order to account for that, we devised a novel splashing device with open chamber, which allows for easy evaporation of the fixative. The device provides 11 mm dropping height with

two inlets—one for cold water and one for the fixed mitotic cells suspension. Apart from the splashing device, a novel metaphase FISH protocol was developed using a microFISH device. This microFISH device provides the possibility of replacing the traditional Coupling Jar and turning it into a miniaturized microfluidic device. We have looked into possible replacements of glass slides with various common polymers but found them unfavorable for FISH protocol on mainly three counts. Firstly, the spreading of the metaphase chromosomes on the glass slides is highly aided by the surface properties of the glass like contact angle and free surface energy. Secondly, polymers exhibit auto-fluorescent behaviour which hinders the analysis due to interference with the FISH probe signals. Finally, some polymers like PMMA couldn't withstand the fixative used for fixing the metaphase chromosomes and cracked on contact. Hence, we found it ideal to continue using the traditional microscope glass slides as substrate which also offers the benefits of easy integration into existing workplace protocols in cytogenetic labs. In order to minimize the time of fabrication of the microFISH device, an easy protocol for rapid bonding based assembly has been developed. With this the glass slide can be turned into a microFISH device in a matter of seconds by using an adhesive tape-based stencil and bonding technique (described later in Fabrication section). The ease of operation and handling in this protocol has been targeted to allow non-technical personnel to easily conduct these tests. The rapid fabrication protocol leaves room for conducting multiple tests simultaneously. In addition, the novel protocol allows for an over 20-fold reduction in reagent volume, which is significant considering the costs of commercially available probes. We hope that this first demonstration of metaphase FISH on a chip, will spur renewed efforts in automating metaphase FISH on a chip leading to wider access to low cost, reliable and fast genetic diagnostics in clinical environments. Although the presented device has been developed for metaphase FISH, we feel that the protocol could also be applied for Interphase FISH.

### **3.4.2. Experimental Section**

#### **3.4.2.1. Materials and Chemicals**

Polymethylmethacrylate (PMMA) sheets procured from Nordplast (Denmark) were used to fabricate the Splashing device; Polydimethylsiloxane (commonly known as PDMS, Sylgard 184, Dow Corning, USA) was used to fabricate the microFISH device. Glass slides (SuperFrost), syringes and silicone tubing were obtained from traditional suppliers (Sigma-Aldrich, VWR). SU8-2075 resist was ordered from Microchem (Germany). Double-sided adhesive tape AR100 (50  $\mu\text{m}$  thickness) was procured from Adhesive Research Inc. (Ireland). All the reagents used in the FISH experiment were purchased from Invitrogen (Paisley, UK). 1  $\mu\text{L}$  of RNase (10



$\mu\text{g}/\mu\text{L}$ ) stock solution was mixed with 99  $\mu\text{L}$  of  $2 \times \text{SSC}$  for removal of RNA. The probe was purchased from Kreotech Diagnostics (Amsterdam, The Netherlands) and it was used as recommended by the manufacturer.  $20 \times \text{SSC}$  (sodium citrate, sodium chloride) was purchased from G-Biosciences (USA) and further dilutions were made using Milli-Q water. The stock of absolute ethanol was used to make dilutions (50%, 60%, 90%, 99% ethanol). 4',6-diamidino-2-phenylindole (DAPI, Invitrogen) was used as a counterstain used for colouring the chromosomes. Blood sample of a female patient was received from the Wilhelm Johannsen Centre for Functional Genome Research, Department of Cellular and Molecular Medicine. Cold water used for spreading chromosomes was kept at 4 °C.

### **3.4.2.2. Apparatus**

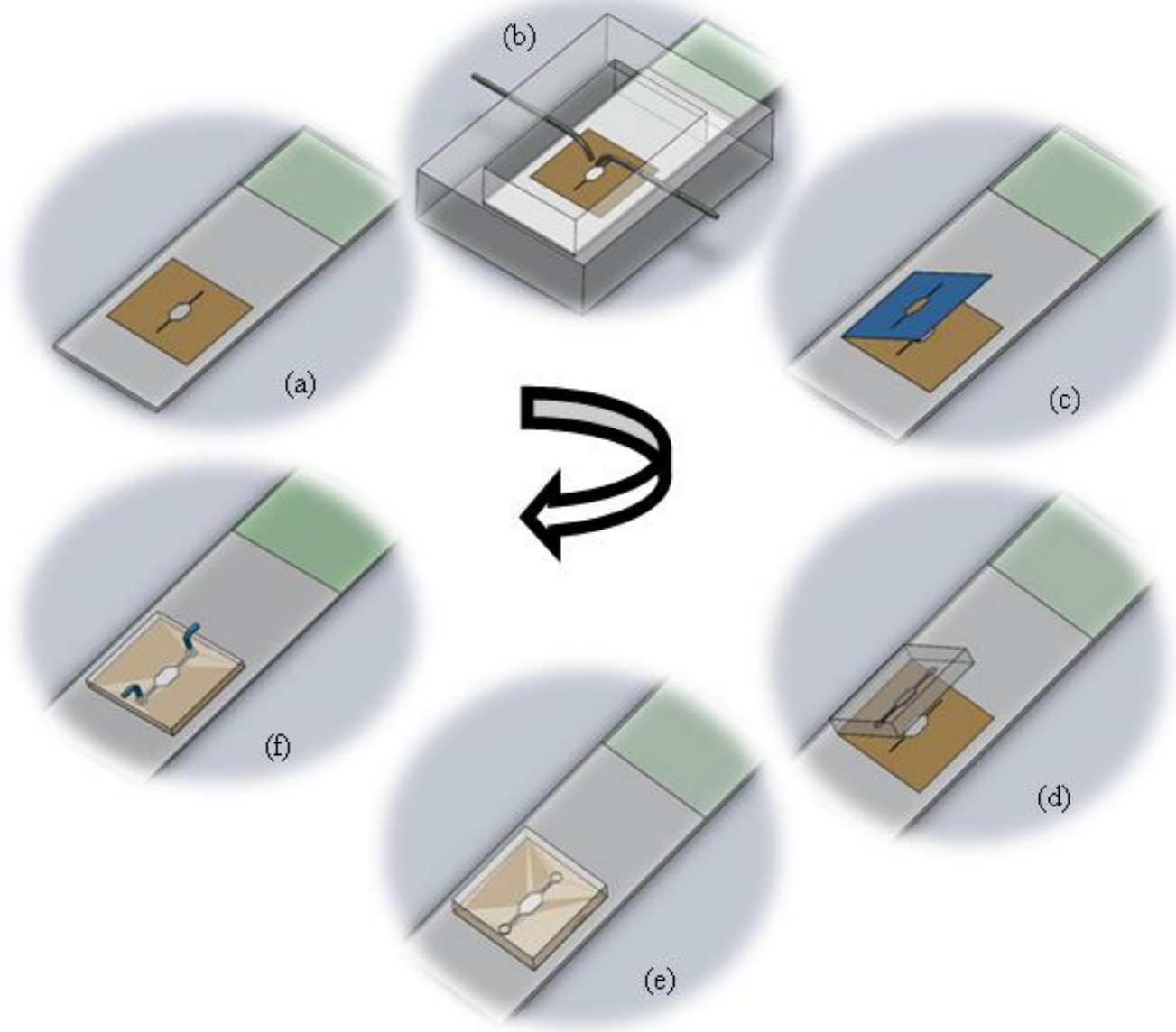
A micromilling machine (Folken Industries, Glendale, USA) was used for milling the splashing device, 50 W CO<sub>2</sub> Laser Machine (Synrad Inc., USA) was used for ablating the adhesive tapes, a photolithographic spinner and aligner from Carl-Zeiss were used for fabricating the master mould for PDMS microFISH device and a Zeiss Axio Observer Z1 Fluorescent microscope was used for analysis of the spreads and FISH signals.

### **3.4.2.3. Fabrication**

The fabrication protocol has been summarized in Figure 3.17. The figure details the protocol for splashing metaphase spreads on the glass slide using the splashing device followed by the rapid fabrication of the microFISH device to perform the metaphase FISH analysis protocol. The details of the fabrication protocol will be explained in the following subsections.

#### **3.4.2.3.1. Glass Slide with Stencil**

The stencil for localization of metaphase spreads is created using a double-sided medical grade tape. The double-sided adhesive tape is fabricated using a laser ablation process with a CO<sub>2</sub> laser [105, 106, 135]. The laser is operated at 20 W power at 250 mm/s laser velocity using resolution of 800. The operating parameters are set using the Winmark software (Synrad Inc, USA). The design of the tape corresponds to the design of the microFISH device (Figure 2). When the tape is ablated using the CO<sub>2</sub> laser, one side of the tape cover is peeled and the tape is bonded to the centre of the glass slide as shown in Figure 3.18. This tape-glass slide complex acts as a stencil when the glass slide is used in the splashing chip to create metaphase spreads. The localization of the metaphase spreads is achieved by removing the top cover of the tape which allows selective patterning on the glass slide in the centre where the tape is fully ablated using the CO<sub>2</sub> laser for creating the microFISH chamber.

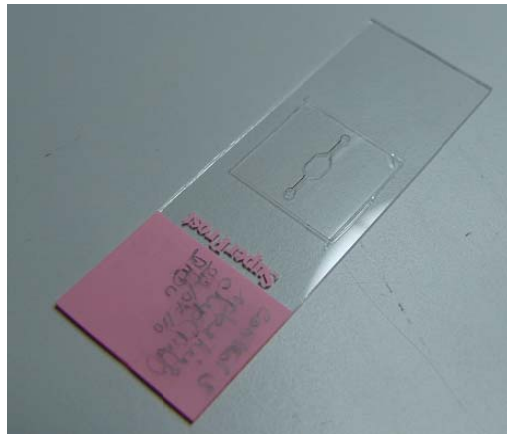


**Figure 3.17:** Schematic Protocol for splashing the metaphase spreads followed by rapid assembly of the microFISH device. (a) Bonding of the double-sided adhesive tape stencil on the glass slide; (b) Spreading of the metaphase spreads in the splashing device; (c) Peeling off the top cover of the double-sided tape stencil to leave only the spreads in the centre of the glass slide and to expose the adhesive layer to bond the PDMS microFISH lid; (d) Aligning the PDMS lid on to the adhesive tape; (e) Assembly of the microFISH by bonding the PDMS lid on to the tape using gentle pressure; (f) Making the interconnection holes and connecting the syringes for world-to-microFISH device fluidic connections.

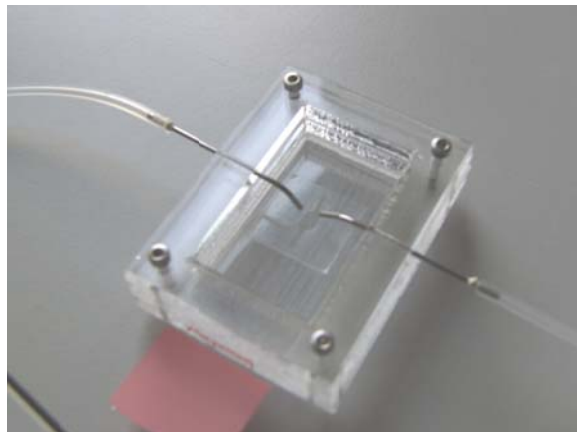


### 3.4.2.3.2. Splashing Device

The splashing device is fabricated in two PMMA layers by a micro-milling process. The bottom part contains the sliding chamber for glass slide insertion and the top lid contains the open chamber for evaporation of the fixative. It also contains the two inlet ports for fixed chromosomes and cold water [Fig. 3.19]. The syringes are slightly bent towards the end to focus the water and chromosome suspension on to the centre of the stencil which exposes the glass slide. The two PMMA layers are either bonded together using thermal bonding [106] or screwed together as shown in Figure 3.19.



*Figure 3.18: Glass slide with laser ablated tape stencil.*



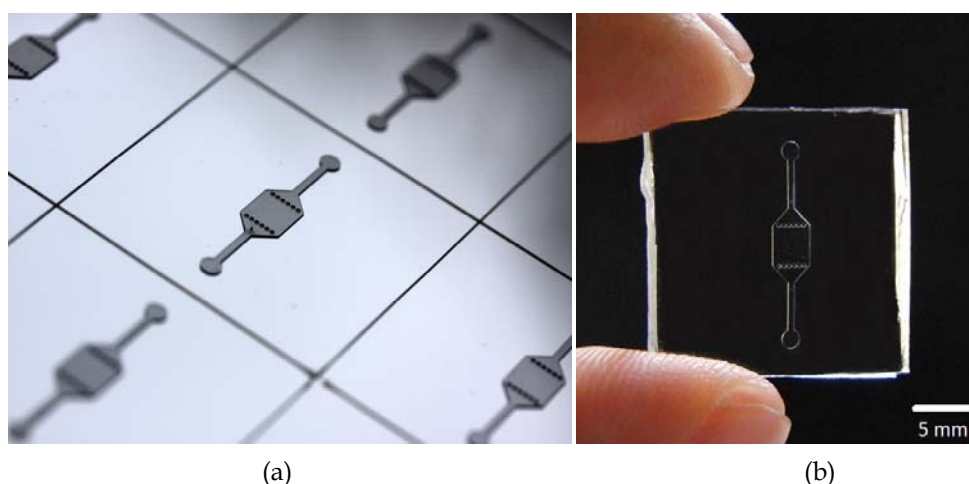
*Figure 3.19: The splashing device fabricated with two layers of PMMA. The glass slide with tape stencil is inserted into the sliding chamber in the lower PMMA and the top PMMA plate has a centre open chamber for fixative evaporation and two inlets for glacial water and fixed mitotic cell suspension.*

### 3.4.2.3.3. Master for PDMS Chip and Moulding of the PDMS MicroFISH Chip

The master for the microFISH device lid was prepared in a cleanroom using a traditional photolithography process. The structures were created on a Silicon wafer in SU-8 photoresist using negative patterning. The recipe for creating the master is shown in Table 3.2. This master can be used several times for moulding the microFISH device lid [Fig. 3.20]. The microFISH device lid is moulded in PDMS using traditional soft lithography techniques described in [18] and peeled away from the Silicon/SU-8 master. The final PDMS microFISH device lid is shown in Figure 3.20. The lid is then bonded on the glass slide with metaphase spreads for assembling the microFISH device.

**Table 3.2:** Recipe for fabrication of SU-8 mould using negative photolithography process.

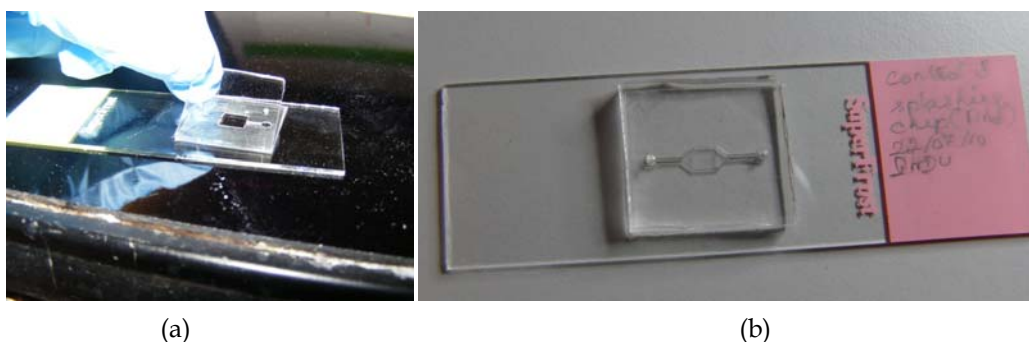
Step	Type	Parameters
1	Spin-coating of SU-8	Acceleration: 200 rpm/s, Speed: 1,000 rpm, Time 40 seconds
2	Soft Bake	Temperature: 50 °C, Time: 5 hrs, Ramp up Time: 15 mins
3	Exposure	Time: 30 seconds Type: Soft
4	Post Exposure Bake	Temperature: 50 °C, Time: 5 hrs, Ramp up Time: 15 mins
5	Development	First: 4 minute, Final: 1 minute



**Figure 3.20:** (a) Master for moulding PDMS microFISH device lid fabricated in SU-8 photoresist over silicon wafer; (b) PDMS microFISH device lid moulded using PDMS elastomer.

#### 3.4.2.3.4. Assembly of the MicroFISH Device

The double-sided adhesive tape stencil used for spreading chromosomes is now used as a bonding layer for assembling the microFISH device. Peeling the top cover off the tape provides a silicone bonding layer for the microFISH device lid (Figure 5). The PDMS lid is irreversibly attached to the glass slide using the silicone adhesive layer by gently applying pressure across the PDMS lid [Fig. 3.21]. Once the device is assembled the holes are made in the PDMS lid for access ports to create interconnections.



**Figure 3.21:** (a) Peeling off top cover of the double-sided tape stencil to expose the silicone adhesive layer (b) Assembled microFISH device by bonding the microFISH device lid on to the silicone adhesive layer.

#### 3.4.2.3.5. Interconnects

The access holes in the microFISH device lid are made on the top side in the PDMS lid. The holes are made using a 22 gauge syringe needle (0.7 mm outer diameter). The interconnects are formed by inserting an 18 gauge syringe (1.2 mm outer diameter) with a bigger outer diameter than the interconnection holes, which forms a tight seal into the microFISH device. The syringes are connected to silicone tubing with inner diameter 1 mm and outer diameter 3 mm to provide the world-to-microFISH device contacts [Fig. 3.22]. In order to test the device, silicone tubings are connected with syringe pumps (not shown in the figure) which provides the pressure needed to actuate the reagents and probes through the microFISH device.

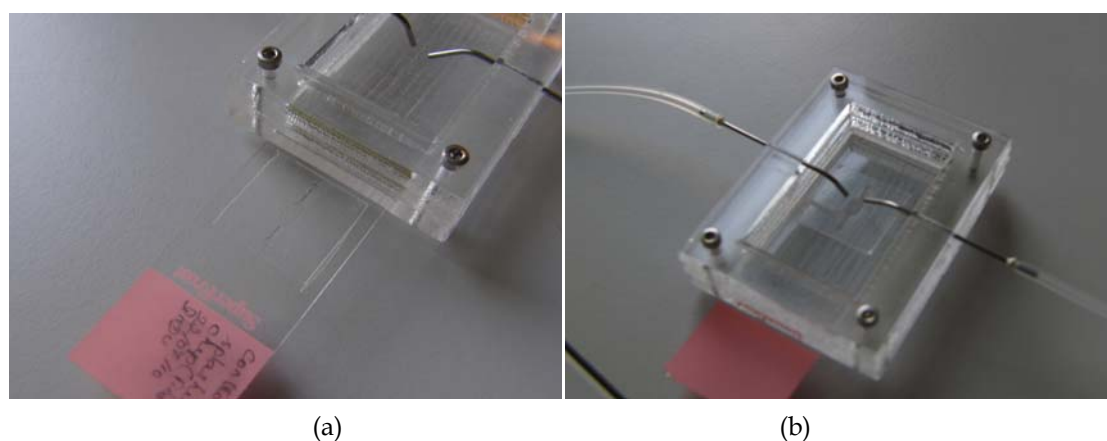


**Figure 3.22:** Fully assembled microFISH device with interconnects and tubings to connect it to the syringe pump.

### 3.4.2.4. Procedures

#### 3.4.2.4.1. Splashing Protocol

The chromosome suspensions used for creating the metaphase spreads were prepared by standard methods [22]. Peripheral blood lymphocyte cultures were prepared and treated with 75 mM KCl hypotonic solution for 5 minutes during the harvesting stage. Claussen *et al.* signified the importance of proper hypotonic treatment for achieving good quality metaphase spreads [31]. The hypotonic treatment causes the mitotic cells to swell leading to the chromosomes moving to more peripheral locations, which allows for evenly spreading of the chromosomes during fixative evaporation. After the mitotic cells are treated with the hypotonic solution they are fixed using the fixative (methanol/acetic acid, 3:1). The fixative is added drop by drop to the cells all the while mixing thoroughly on a vortex. To compare the spreads achieved using the traditional dropping method and the splashing device, control slides were prepared using the manual dropping method and test slides were prepared using the splashing device. Before dropping the cell suspension on the control slides, the slides are kept in distilled water at 4 °C. On the other hand, the test slides were prepared using the splashing device, where one drop of glacial water was dropped on to the slide followed by a drop of the fixed mitotic cell suspension through the two dedicated inlets [Fig. 3.22]. The slides were allowed to air dry in the open chamber of the splashing device. As a final step, both test and control slides were heated at 75 °C degrees for 3 min, which improves the fixation of the chromosomes to the slide.



**Figure 3.23:** (a) Sliding of the glass slide with stencil into the splashing device; (b) Splashing device with glass slide. The stencil is positioned under the syringes for splashing glacial water followed by fixed mitotic cells for spreading.

#### **3.4.2.4.2. FISH Protocol**

The FISH protocol was conducted on both the control and test slides using the microFISH device. After assembling the microFISH device using the glass slides with chromosome spreads, the optimized FISH protocol was conducted on all the slides. The inlet of the microFISH device was connected with a syringe pump for treating the metaphase spreads with the FISH reagents and probes. The specific temperatures associated with the FISH protocol were provided by a hot plate setup. Firstly, RNase (10  $\mu\text{g}/\mu\text{L}$ ) was delivered through the inlet. Following the RNase treatment, the microFISH device was kept in the humidity chamber at 37 °C for one hour. Later 2  $\times$  SSC was loaded at room temperature for washing the metaphase spreads. The microFISH device was then dehydrated with increasing percentages of ethanol (70%, 80% and 99%), and the device was heated at 75 °C to denature the chromosomal DNA for 5 minutes. Simultaneously, probe DNA was denatured at 75 °C for 5 minutes in the water bath. Then the probe was entered into the device and the inlet and outlet were closed to avoid evaporation of the probe. The microFISH device was incubated in the humidity chamber at 37 °C overnight for hybridization. Subsequently, 50% formamide was delivered as post hybridization wash at 42 °C. Final washing was performed with 0.1  $\times$  SSC at 60 °C, 4  $\times$  SSC and 1  $\times$  PBS at room temperature. The details of the conventional FISH protocol and optimized FISH protocol can be found in Table 3.3.

#### **3.4.2.4.3. Analysis**

DAPI was applied to the hybridized targets on the test slides in microFISH chamber and in case of control samples, slides were mounted with cover slips. The Zeiss AxioObserver Z1 fluorescent microscope was used to view and analyze the samples for counting the metaphase spreads and the FISH hybridization signals. The chromosomes spreads on the control and test slides were counted manually using the traditional method.

### **3.4.3. Results and Discussion**

#### **3.4.3.1. Splashing Device and Metaphase Spreads**

The motivation behind the splashing device was to create a microfluidic device which can provide reliable and sufficient number of metaphase spreads on a glass slide. After spreading the chromosomes on the slide using the traditional method and the splashing device, the slides were stained with DAPI. The metaphase spreads were counted manually in the

fluorescence microscope at 20× magnification. Figures 3.24 (a,b) show the images of the metaphase spreads obtained using the conventional method and splashing device respectively. In order to validate the splashing device protocol, we conducted tests using two different cell suspension samples. Table 3.4 shows the comparison of average spreads obtained using the two techniques.

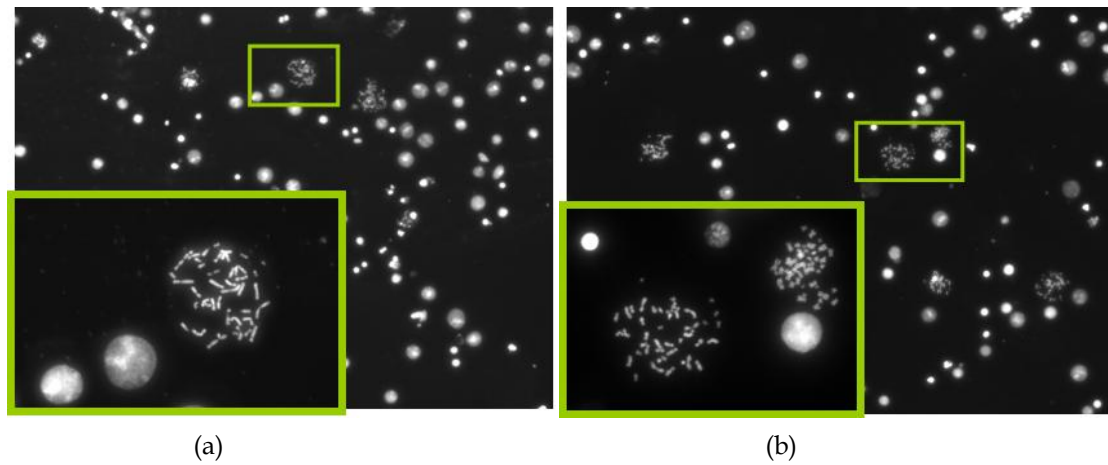
**Table 3.3:** Comparison of conventional FISH method and microFISH protocol showing over 23 fold reduction in total reagents used and a 2 fold reduction in the probe volume (highlighted in yellow) which is the most expensive reagent for conducting FISH analysis. All steps of the FISH protocol are presented and in case of the microFISH protocol the flow rates used for the FISH reagents are also presented.

Step No.:	Name of the step	Conventional protocol	microFISH protocol	
		Vol	Vol	Flow rate
1	RNAse	100 µL	25 µL	5 µL/min
2	Wait 60 mins			No flow
3	Wash 2 × SSC	75 mL	3 mL	200 µL/min
4	70% Alcohol	25 mL	1 mL	200 µL/min
5	90% Alcohol	1 mL	1 mL	200 µL/min
6	100% Alcohol	1 mL	1 mL	200 µL/min
7	Drying-Air			NA
8	70% formamide	25 mL		NA
9	90% Alcohol	25 mL		NA
10	100% Alcohol	25 mL		NA
11	Probe	10 µL	5 µL	2 µL/min
12	Hybridisation time	Overnight	Overnight	No flow
13	50% Formamide	75 mL	3 mL	200 µL/min
14	0.1 × SSC	25 mL	3 mL	200 µL/min
15	4 × SSC	25 mL	1 mL	200 µL/min
16	1 × PBS	25 mL	1 mL	100 µL/min
17	DAPI	15 µL	5 µL	2 µL/min
Total Reagent volume		327.2 mL	14.1 mL	

**Table 3.4:** Average number of metaphase spreads found in the microFISH chamber (3 × 3 mm<sup>2</sup>) using manual dripping method and our splashing device protocol.

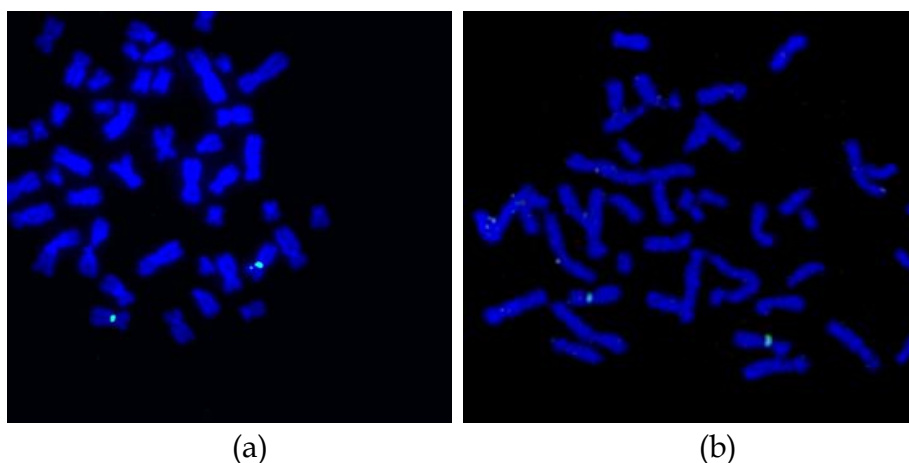
	Sample 1	Sample 2
Control Slide	41	52
Splashing device	29	34





**Figure 3.24:** (a) Metaphase spreads stained with DAPI on the control slides prepared using the traditional dropping method (Inset – 40 $\times$  resolution); (b) Metaphase spreads stained with DAPI on the test slides prepared using splashing protocol (Inset – 40 $\times$  resolution).

Even though the average numbers of spreads obtained by using the splashing device are comparatively lower, we could obtain sufficiently good chromosome spreads in order to perform the FISH analysis. The lower chromosome spread counts may be due to the splashing conditions such as height, temperature and humidity as described in the introduction. While in average the number of chromosome spreads was significantly lower in the splashing device, it must be noted that in certain samples, we found the number of chromosome spreads to be higher compared to the control slides. Considering that the splashing experiments were not studied in detail, we believe that the splashing protocol can be optimized by altering and controlling the various other factors like temperature, humidity, etc.



**Figure 3.25:** (a) FISH analysis on the control slide. The two green dots highlight the two X chromosomes in the female sample; (b) FISH analysis on the test slide. The two green dots highlight the two X chromosomes in the female sample.

Moreover, the simple fabrication protocol of the splashing device using micro milling of PMMA sheets allows us to control the height of splashing if needed by addition of more PMMA layers to increase the height of the splashing syringe. The integrated stencil and bonding layer of the adhesive tape allows for localization of the metaphase spreads on the glass slide in the splashing device. Thus, the splashing device not only provides an ability to reliably create metaphase spreads on glass slide but also provides a possibility of automating the image analysis procedure in the future due to ease of finding the metaphase spread using software and an automated stage. A number of companies (Zeiss, BioView and Vysis) and research groups are working on optimizing the data acquisition protocols as this continues to be a major issue after the FISH protocol [237, 238]. Automation of the analysis procedure is currently an on-going work where we are aiming to divide the microFISH device chamber into smaller segments to create smaller FISH microchambers corresponding to the microscope objective.

#### **3.4.3.2. FISH Protocol Results**

After the preparation of the chromosome spreads, FISH analysis was performed on the peripheral blood lymphocyte chromosomes using an X chromosome centromeric probe. A female patient sample was used in order to show the validation of the microFISH device protocol and the results obtained with XX chromosomes [Fig. 3.25(b)] confirm the successful FISH analysis result. The conventional FISH protocol was also performed on the slides to compare and evaluate the microFISH device efficiency [Fig. 3.25(a)]. As can be seen in Table 3.3, the reagent volume needed in traditional FISH analysis is 327 mL, but now has been reduced to only 14 mL, which is a major step in reducing the costs associated with FISH analysis. As mentioned earlier, the most expensive reagent in traditional FISH analysis is the probe (costing approx. \$90 per test). In the microFISH protocol the volume of this has been reduced to half (highlighted in yellow in Table 3.3). This alone cuts the cost associated with conducting the routine FISH analysis in half. Considering the cost of fabricating these microFISH devices is less than \$2, these successful FISH results will give a major push towards making genetic analysis a routine screening test.

#### **3.4.4. Conclusions**

We have successfully demonstrated the first metaphase FISH on a microfluidic device. This work also presents an alternative method for slide preparation and hybridization of FISH probes. The achievements gained in the present study will be used in further improvement of the methodology and aim to develop a completely automated system for performing



miniaturized FISH on chip. The micro splashing device designed for spreading metaphase chromosomes on a glass slide provides more reliable and easy alternative for creation of metaphase spreads. The rapid and easy assembly protocol for the microFISH device allows for quick transformation of a simple glass slide into a microFISH device, which makes it an ideal solution for integration into existing work routines at cytogenetic labs. Our current efforts are focused on further miniaturization of this device, which will offer significant benefits with respect to sample preparation and reduction in reagent costs. We are also working towards improving the chromosome spreading protocol by further miniaturization of the splashing chamber and localized micro-spotting of fixed cells, optimizing the hybridization efficiency using temperature and electro-kinetic effects, automating the protocol by incorporation of reagent reservoirs and improving the analysis by developing automated software for data acquisition and metaphase spread recognition. In the longer run, we envisage to create a chromosome total analysis system providing a more efficient and cheaper solution to the traditional protocol and enable faster diagnosis.

## **Acknowledgements**

The authors would like to thank FTP and Lundbeck for their financial support. Authors would also like to acknowledge the collaborators at Panum and Kennedy Institute and especially thank Elisabeth Larsen for technical assistance and Asli Silahtaroglu for providing samples for conventional FISH analysis and useful technical discussions, Jaya Kandi for schematic 3D diagrams and Peder Skafte-Pedersen for assistance with microscope for image acquisition. Wilhelm Johannsen Centre for Functional Genome Research is established by The Danish National Research Foundation.

### 3.5 AutoFISH: FISH Reagent cartridge for minimal handling FISH

On successful demonstration of the first miniaturized device for performing FISH (microFISH), our concentration was shifted towards developing a simple FISH protocol, which requires minimal handling from the technicians and offers a possibility to automate in the future. The major workload and stress factor in order to perform the FISH analysis (interphase and metaphase) is related to treating the slides with interphase cells or chromosome spreads with multiple reagents in a very tight time controlled sequence (Table 3.5).

**Table 3.5:** Comparison of time and reagent volume used for performing traditional FISH protocol compared to the microFISH protocol (Only the time of the protocol is indicated but the time with respect to handling can differ from person to person)

Step No.:	Process	Traditional FISH		microFISH protocol		
		Vol	Time	Vol	Flow rate	Time
1	RNase	100 $\mu$ L	1 min	25 $\mu$ L	5 $\mu$ L/min	5 min
2	Wait		60 min		No flow	45 min
3	Wash 2 $\times$ SSC	75 mL	5 min( 3x)	3 mL	200 $\mu$ L/min	15 min
4	70% Alcohol	25 mL	2 min	1 mL	200 $\mu$ L/min	5 min
5	90% Alcohol	1 mL	2 min	1 mL	200 $\mu$ L/min	5 min
6	100% Alcohol	1 mL	2 min	1 mL	200 $\mu$ L/min	5 min
7	Drying-Air		5-10 min		NA	
8	70% formamide	25 mL	5 min		NA	
9	90% Alcohol	25 mL	2 min		NA	
10	100% Alcohol	25 mL	2 min		NA	
11	Probe	10 $\mu$ L	20 min	5 $\mu$ L	2 $\mu$ L/min	
12	Hybridisation time		Overnight		No flow	12 hrs
13	50% Formamide	75 mL	5 min( 3x)	3 mL	200 $\mu$ L/min	15 min
14	0.1 $\times$ SSC	25 mL	5 min( 3x)	3 mL	200 $\mu$ L/min	15 min
15	4 $\times$ SSC	25 mL	5 min	1 mL	200 $\mu$ L/min	5 min
16	1 $\times$ PBS	25 mL	5 min	1 mL	100 $\mu$ L/min	5 min
17	DAPI	15 $\mu$ L	1 min	5 $\mu$ L	2 $\mu$ L/min	2.5 min
		327.2 mL	14 - 16 hrs	14.1 mL	13 hrs	

We carefully evaluated both the interphase and metaphase FISH protocol and both of them have a very similar sequence of reagent treatments starting with RNase exposure, followed by ethanol based drying of slides, denaturing of the DNA with temperature treatment, followed by probe hybridization and finally post hybridization washes with 50% formamide, saline-sodium citrate buffer (SSC) and phosphate buffered saline (PBS) to remove unbound probes and unspecific bindings. In between these reagent washes, there is also a need for air drying the slides and often visualizing under the microscope to check if the earlier treatment

was successful. Hence, to perform these washes on a chip, there was a need to devise a reagent storage technique to allow for sequential injection of the reagents to the interphase cells or chromosomes immobilized on the surface.

After a thorough literature search on different techniques to store and inject multiple reagents in a microfluidic device, we were left with practically two options. One for on-chip storage in reservoirs and subsequent injection by multiple actuators placed on each of these reservoirs as previously proposed by Xie et. al[239]. And the second option was to store all the reagents on single tubing in the form of reagent cartridge by means of air spacers to separate the reagents and avoid mixing presented earlier by Whitesides group [240].

We evaluated both the techniques for their advantages and mainly for their respective complexities when implementing the FISH protocol. In the end, we decided on using the technique of storing the reagents on tubing for a number of reasons. The major disadvantages with respect to using Xie's cartridge were the material of the cartridge (PDMS); and the complexity of loading and unloading the reagents which would be difficult to implement and automate in the clinical setup. Also, PDMS is known for being permeable to gases and as a result it would not be advisable to store FISH reagents on a PDMS based cartridge as they would quickly evaporate and not permit longer storage. Also, the need for multiple actuators (one per reservoir or reagent) will end up complicating the fabrication and setup. On the other hand, the cartridge system of storing reagents on a tube has number of benefits: need of only one actuator for all reagents, easy storage, simple loading procedure and comparatively easy sealing procedure. But the major advantage of using tubing cartridge compared to Xie's cartridge was the ability to use the air spacers in the cartridge for air drying the samples between different reagents, which is difficult to implement with the other options.

But the task of storing the FISH reagents on a cartridge and applying them in a sequence was not simple. Considering the current volume of reagents used for microFISH protocol [84], we would need tubing longer than 10 meter (1 mm internal diameter) in order to store all the reagents required (14.1 ml). This was not a practically feasible solution. As a result, we focused our efforts initially on optimizing the microFISH protocol and minimizing the reagent volume further to perform the FISH analysis using a cartridge.

The novel protocol (AutoFISH) developed as part of the currently on-going work for optimization of the microFISH is highlighted in Table 3.6. For optimizing the protocol, we evaluated every parameter of the microFISH protocol and tuned all the reagent volumes by performing step by step FISH and checking operation at each step. After several initial iterations, we can now perform interphase FISH using only 2  $\mu$ L probe volume with over 60%

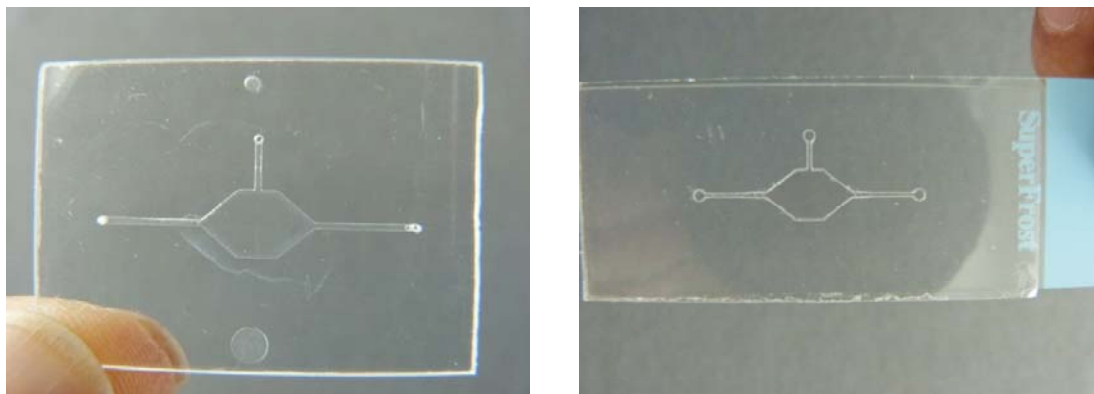
success rate. We are confident further optimizations will provide better success rates and also lead to reduction in the volumes of reagents for performing FISH analysis, but further experiments could not be conducted due to closing down of labs at DTU-Nanotech.

During the FISH reagent cartridge tests, we used only 2  $\mu\text{L}$  of probe volume as part of the optimization process, which is a huge cost reduction for the cost per FISH tests. This is because, the probes are expensive (over \$400 for 100  $\mu\text{L}$ ) and they continue to be the limiting factor for mainstreaming FISH based diagnostic tests for prenatal and hematological disorders.

**Table 3.6:** Comparison of microFISH and the current version of AutoFISH protocol.

		microFISH protocol		AutoFISH protocol		
Step No:	Name of the step	Volume	Flow rate	Volume	Flow rate	Temperature
1	RNAse	25 $\mu\text{L}$	5 $\mu\text{L}/\text{min}$	25 $\mu\text{L}$	5 $\mu\text{L}/\text{min}$	37 °C
2	Wait 60 mins		No flow		No flow	
3	Wash 2 $\times$ SSC	3 ml	200 $\mu\text{L}/\text{min}$	150 $\mu\text{L}$	15 $\mu\text{L}/\text{min}$	Room temp.
4	70% Alcohol	1 ml	200 $\mu\text{L}/\text{min}$	50 $\mu\text{L}$	15 $\mu\text{L}/\text{min}$	Room temp.
5	90% Alcohol	1 ml	200 $\mu\text{L}/\text{min}$	50 $\mu\text{L}$	15 $\mu\text{L}/\text{min}$	Room temp.
6	100% Alcohol	1 ml	200 $\mu\text{L}/\text{min}$	50 $\mu\text{L}$	15 $\mu\text{L}/\text{min}$	Room temp.
7	Probe	5 $\mu\text{L}$	2 $\mu\text{L}/\text{min}$	2 $\mu\text{L}$	1 $\mu\text{L}/\text{min}$	75 °C
8	Hybridisation time		Overnight		12 hrs	Room temp.
9	50% Formamide	3 ml	200 $\mu\text{L}/\text{min}$	150 $\mu\text{L}$	15 $\mu\text{L}/\text{min}$	42 °C
10	0.1 $\times$ SSC	3 ml	200 $\mu\text{L}/\text{min}$	150 $\mu\text{L}$	15 $\mu\text{L}/\text{min}$	60 °C
11	4 $\times$ SSC	1 ml	200 $\mu\text{L}/\text{min}$	50 $\mu\text{L}$	15 $\mu\text{L}/\text{min}$	Room temp.
12	1 $\times$ PBS	1 ml	100 $\mu\text{L}/\text{min}$	50 $\mu\text{L}$	15 $\mu\text{L}/\text{min}$	Room temp.
13	DAPI	5 $\mu\text{L}$	2 $\mu\text{L}/\text{min}$	5 $\mu\text{L}$	15 $\mu\text{L}/\text{min}$	Room temp.
Total Reagent volume		14.1 ml		732 $\mu\text{L}$		

During this optimization process, we also realized the issues with using PDMS based microFISH device. Due to permeability of PDMS, there was significant evaporation of the reagents and trapping of probes in PDMS. Hence, for the tests with the FISH reagent cartridge, we changed the material of the FISH device from PDMS to cyclic olefin copolymer (COC) in order to avoid evaporation of the reagents allowing us to use much lower volumes for FISH analysis [Fig. 3.26]. The devices were micromilled and the adhesive tapes used to assemble the AutoFISH device were laser-ablated.

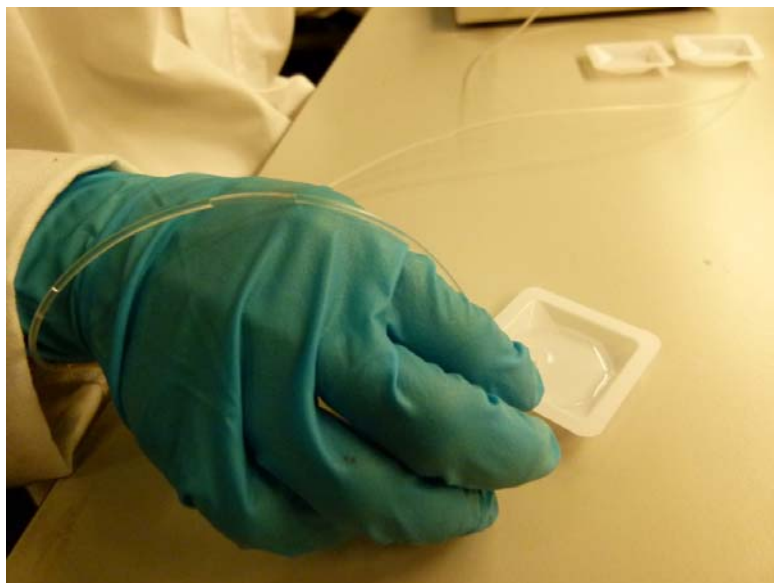


**Figure 3.26:** (Left) AutoFISH device designed in COC with 3 inlets (extra inlet for probe) (Right) Glass slide with tape stencil to spread metaphase chromosomes and bond the COC lid to create an AutoFISH device.

### 3.5.1 Fish Reagent Cartridge

#### Loading of reagents

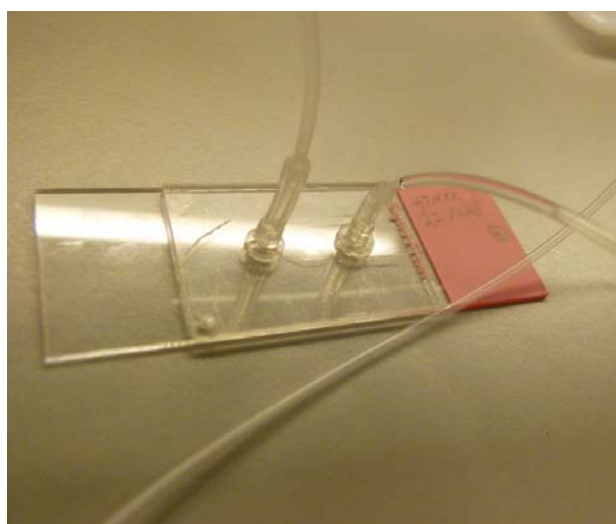
After optimization of the FISH protocol, we were interested in testing the minimal handling protocol by sequential injection of reagents from a FISH reagent cartridge [Fig. 3.27]. In order to minimize the evaporation of the reagents, we used polyethylene (PE) tubing for the FISH cartridge. A syringe pump was used to load the reagents in the cartridge (1 m of PE tubing). A 10 ml syringe was filled with 5 ml PBS solution. As a first step, a 200  $\mu$ L of 100% ethanol plug was withdrawn to rinse the tubing completely. Later, 200  $\mu$ L of PBS was injected into the cartridge to prime the cartridge and the syringe pump. After this the pump was switched to withdraw mode and all the reagents other than the FISH probe were loaded onto the cartridge with air spacers of 50  $\mu$ L. These air spacers provide timing gate and also facilitate drying of the slide by flushing the previous reagent out of the FISH chamber. Due to the viscous nature of the probe and to avoid unnecessary exposure of the probe to the residue of the other reagent's in the cartridge, we modified the microFISH device design and added a separate inlet for probe [Fig. 3.26]. This was done to avoid contamination of the probe and to make it possible to design a device offering possibility to automate easily.



*Figure 3.27: Loading of reagents on the FISH cartridge with air spacers to separate the reagents.*

### AutoFISH Testing

The fixed cells were splashed onto the glass slides using the splashing protocol and after visual confirmation of spreads on the glass slide, the adhesive tape based bonding protocol was used for assembling the AutoFISH device by means of bonding the COC lid to the glass slide [section 5.5.8]. The AutoFISH protocol was followed as described in Table 3.6. The interconnections were glued to the AutoFISH device as shown in Fig. 3.28.



*Figure 3.28: Testing of AutoFISH device with reagent cartridge (showing interconnections for rapid connection of the FISH cartridge)*

### Reagent cartridge protocol

A hot plate was used for applying temperature treatment as part of the AutoFISH protocol [Table 3.6]. The syringe pump was programmed to sequentially inject all the reagents and the air spacers until alcohol washes. This results in alternate application of the reagent washes to the spreads followed by an air drying step similar to the conventional protocol. Until the probe was to be applied, the probe inlet was kept sealed with a paper clip. The probe was loaded on another cartridge called the FISH probe cartridge (shorter PE tubing – 12-15 cm) which was later connected to the probe inlet after removing the paper clip. The probe was applied at a very low flow rate (1  $\mu$ L/min) as the probe mix is very viscous which often leads to the probe-mix plug breaking into smaller plugs. On application of the probe to the entire FISH chamber, all the inlets were sealed with parafilm and further closed with paper clips to avoid any evaporation during the hybridization process. Typically, the devices were left in the incubator overnight (shortest period tested was 12 hours) to ensure hybridization of the probe to the chromosomes.

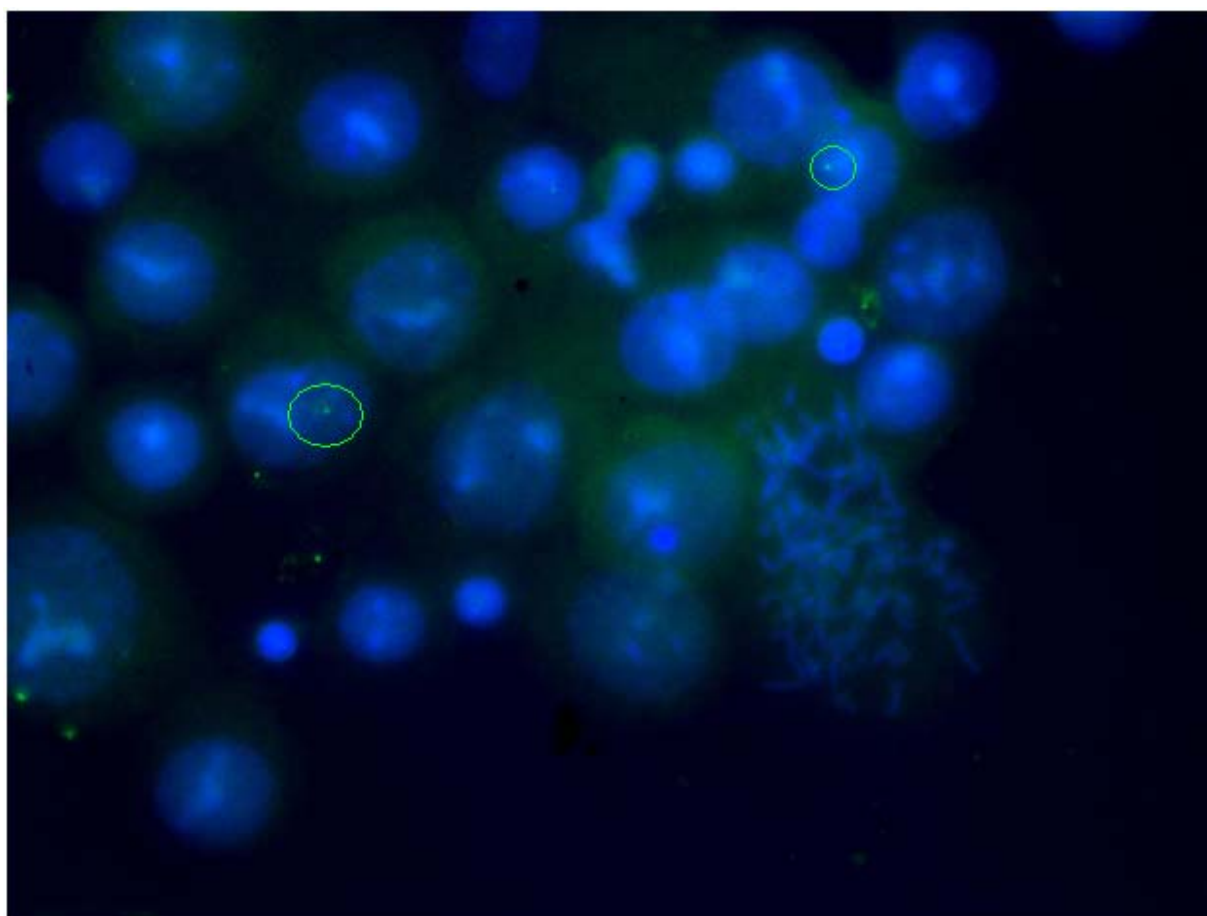
On the next day, the FISH process is started again after overnight hybridization, whereby the FISH reagent cartridge is connected again to the reagent inlet. The probe inlet remains closed and the waste outlet is opened during application of the FISH reagents. The heating cycles for formamide and SSC application are achieved using the hot plate. On completion of the AutoFISH protocol, DAPI is applied to the FISH chamber through the probe inlet and all the inlets are sealed again with parafilm and paper clips.

### 3.5.3. Results

The slides were analyzed using a Zeiss Axio Observer Z1 fluorescent microscope after 20 min of application of DAPI. While there were plenty of interphase signals, we didn't find any signals in the metaphase spreads, which could be due to a number of reasons. Firstly, as these tests were done in a makeshift lab in Copenhagen University created due to closing down of our regular labs at DTU-Nanotech, we did not have any calibration on the equipments in this new lab. Secondly, during the process of relocation we could have contaminated our reagents and finally, the probe was over a year old and therefore possibly inactive. As these experiments were the last batch of experiments done as part of the project, we did not have time to conduct proper controls to evaluate the other factors which could have gone wrong with the experiments. New tests and controls to check on the other possible factors to progress this work further will be undertaken when our labs reopen.



Nevertheless, the most promising signs of optimism came from the fact that most of these tests clearly showed FISH signals in interphase nuclei, which indicated that the reagent cartridge based AutoFISH protocol works for interphase FISH [Fig. 3.29]. The single green circles highlighting the green dots in the nuclei of interphase cells, show the presence of a single X chromosome in this donor's sample. None of the metaphase spreads showed any clear indication of hybridization. The successful results with interphase nuclei suggest possible problems with the protocol, equipment, reagents or the probe which needs to be optimized for metaphase FISH to work.



**Figure 3.29:** FISH signals on interphase cells (Green circles highlight the interphase signals)

With these promising results, we concluded that this was the way ahead in order to realize a minimal handling FISH protocol which minimizes the workload of the technicians and offers possibility to automate. In conclusion, we have shown a promise for possible automation of FISH protocol using FISH reagent cartridges. Further optimization is needed for improving the FISH signals and leading to validation of AutoFISH protocol for metaphase FISH analysis.



We clearly see application of this protocol for automating interphase FISH as well as metaphase FISH in near future.

In hindsight, the AutoFISH protocol provides a reduction in the volume of the reagents and handling time. While the AutoFISH protocol in itself is comparable to the traditional protocol, the reduction offered in the handling time improves the workflow in the clinics. In principle, the technicians could follow the same protocol and get results in couple of days, but as the technicians cannot work round the clock to complete the analysis the only effective way to improve the time to results is by automating the protocol.

### 3.5.4 Outlook

With the development of miniaturized tools for sample processing ( $\mu$ BR), slide preparation (FISHprep) and miniaturized FISH analysis (microFISH), we have provided the cytogeneticists with a new toolkit for performing routine FISH analysis. Ease of handling, simplicity and compatibility to the existing work routines and protocols in cytogenetic labs has been the key consideration in the design and development of this integrated FISH analysis platform.

Focusing on ease of use, we have moved away from the practical concerns (interconnects, complex protocols, biocompatibility), which hamper the adoption of the microfluidic devices in biological analysis. Finally, we target our efforts to automate the FISH protocol, by means of integrating the reagent handling (storage and sequential injection) on a cartridge. With successful initial results on performing FISH analysis on interphase cells, we are optimistic about further adapting the protocol for metaphase FISH analysis.

As a final step, we have developed software for controlling reagent cartridge including controlled sequential injection of reagents. In the near future, by means of adding software based hot plate control to the current software, we aim to develop fully automated miniaturized FISH analysis protocol controlling simultaneously the reagent application and thermal cycling.



# CHAPTER 4

## SIDE PROJECTS

Until now, we have described the work done towards development of the modular and integrated versions of the C-TAS protocol. In this chapter we will describe the various devices attempted to isolate lymphocytes from whole blood and to trap single cells and chromosomes.

## 4.1 The Quest of the Lymphocytes

Lab on a chip technologies are set to revolutionize diagnostics by bringing the hospitals to the patient's bedside. However, the major bottleneck towards success of these lab-on-chip systems is to integrate the pre-processing steps like cell sorting and cell isolation on the chip. This is a continuing hurdle and simultaneously there is a need for low cost, simple and efficient solutions which can handle sample pre-processing at the patient's bedside without the need for bulky centrifuges and other equipment commonly found in central labs.

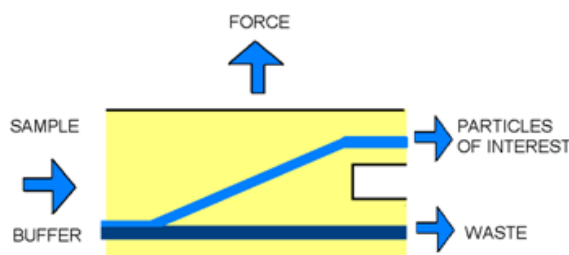
For conducting genetic analysis on blood, the first step is always to isolate the white blood cells (Leukocytes - WBCs) from the plasma and red blood cells (erythrocytes - RBCs). In human blood, the WBCs comprise only about 6-10% of blood and their proportion to RBC and platelets is roughly 1:700 and 1:30 respectively. Hence, it makes it extremely crucial that the blood cells are sorted and the WBCs are isolated before any further genetic analysis can be carried out.

In pursuit of the modular C-TAS system, we focussed initially on a number of techniques to isolate WBCs from whole blood. The main focus was to develop techniques which can be easily integrated on the C-TAS module and function seamlessly with the other C-TAS modules to complete the C-TAS protocol. The aim was to develop a sorting or separation module which can isolate the WBCs by processing the whole blood or diluted blood and deliver the isolated WBCs for further analysis to the culture and lysis modules. In relation to dilution which often occurs due to efforts related to sorting or separation of the cells, we also focussed considerably efforts concentrating the cells again for subsequent analysis.

## 4.2 Integrating Continuous Flow Separation Systems

Sorting of biochemical materials on chip is quickly becoming the biggest bottleneck for realizing  $\mu$ TAS chips. In case of clinical diagnostics systems dealing with blood, it remains the last hurdle to overcome in terms of miniaturizing the pathological diagnostic systems. While a variety of continuous flow microfluidic sorters have been proposed in the last decade, none of them provide efficient and reliable high throughput fractionation of undiluted blood cells[241].

Ideally, continuous flow separation systems are visualized as shown in the block diagram below.



**Figure 4.1:** A typical continuous flow separation procedure: sample is injected continuously together with a carrier liquid into a wide separation chamber, a force acts at an angle to the direction of flow and sample components are deflected from their flow path and thus spatially separated.

The applied force field varies according to the size and intrinsic properties of the particles to be separated and the properties of the carrier fluids. These devices are tuned to precisely handle small volumes of samples, such as proteins, DNA solutions, cell suspensions and occasionally blood.

The ease of integration provided by these systems makes continuous flow separation systems very applicable for the C-TAS system. These systems can be easily used as modules on  $\mu$ TAS systems and can function seamlessly to provide the isolated blood cells for further downstream processing and FISH analysis. We have worked towards developing modules based on 3 different techniques and used those to separate blood cells (or isolate WBCs) for further analysis with the C-TAS system.

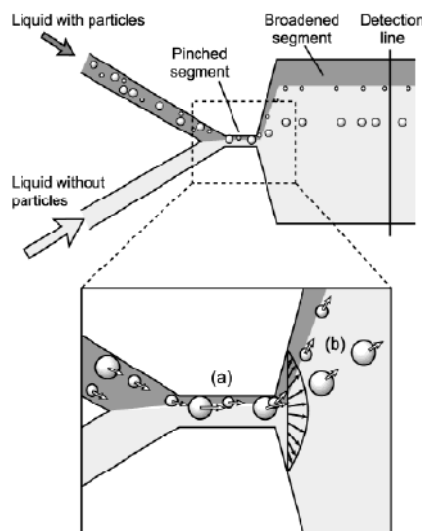
- Pinch flow fractionation system (PFF)
- Dual pinch flow fractionation system (DPFF)
- Microfluidic FACSlyser

Due to dilution of blood cells on the C-TAS modules it was important to develop strategies to either trap cells or concentrate them before they were fixed so that we have ample metaphase spreads for final FISH analysis. Two major strategies were tested in this relation, one based on trapping of cells using cell traps and the other focusing more on concentration of lymphocytes for subsequent FISH analysis. Finally, trapping of chromosomes on antibodies was targeted, which was an attempt to manipulate and localize chromosomes on a device to enable easy FISH analysis later on.

### 4.3 Pinch flow fractionation (PFF)

Pinch flow fractionation is a method used for continuous separation of particles. PFF relies on pinching of a fluid stream containing particles (such as beads or cells) by another stream flowing at typically 10-25 times faster flow rates in a narrow channel segment called the pinch segment [242] [Fig 4.2]. This method relies solely on the hydrodynamic properties of the carrier fluids to efficiently separate the particles based on their sizes. In the pinch segment [suitable width 100  $\mu\text{m}$ ], by virtue of flow ratios of the fluids at the inlet stream, the particles in the particle stream get aligned to the wall of the pinch segment. This leads to smaller particles centring on to streamlines closer to the wall and the larger particles centring to streamlines away from those on which the smaller particles centre onto [Fig 4.2]. This leads to larger particles following a different streamline compared to the smaller particles [Fig. 4.2].

Hence, on leaving the pinch segment, when the particles enter the separation chamber, they follow the flow streamlines in which their centres lie. This leads to a spatial separation of the smaller and larger particles in two different streams flowing parallel to each other in the separation chamber. As shown, the smallest particles will flow close to the channel wall and the largest closer to the centre of the separation chamber [Fig 4.2]. Ideally if you place the outlets with respect to the separate streams the different particles will be collected in different outlets.



*Figure 4.2: The model of the pinch flow fractionation system (reproduced from [242])*

While the separation of the particles occurs due to the laminar flow profile and alignment of the particles to different flow streams based on their sizes, but the sorting of these particles in the outlet streams can further be tuned by carefully designing the hydraulic resistances of the outlet streams[243, 244]. Yamada *et al.* highlights that the four parameters which needs to be tuned to achieve effective separation of the particles are flow ratios, flow rates, width of the pinch segment and microchannel geometries[242].

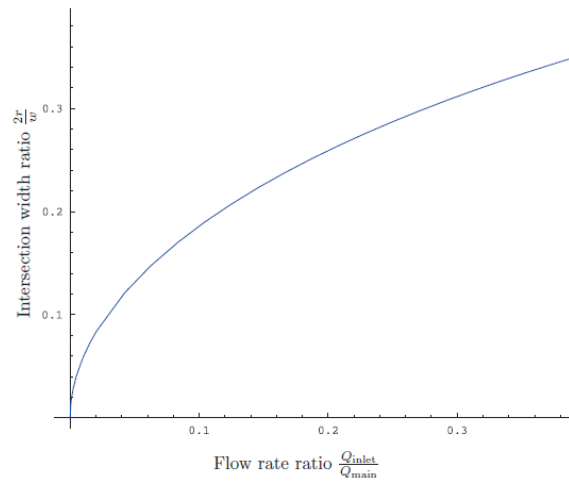
In the interest of time and in order to focus more on the project requirements, the project was divided into the theoretical project and an associated experimental project. The theoretical project was undertaken by two at the time bachelor students, Karsten Brandt Andersen and Simon Levinson under supervision of Asso. Prof. Fridolin Okkels. The results of this work, lead to novel insights which functioned as the guidelines for the design and the experimental work related to pinch flow fractionation experiments [245, 246].

### Theoretical model

An extensive theoretical study was undertaken to understand the variables involved in the designing of a pinch flow fractionation system for sorting of blood cells. We were interested in understanding, how the variations in pinch segment width, flow ratios of particles and aligning fluids, geometries of the channels, effects of the edge curvature at the end of the pinch segment, angle of inlets meeting the pinch segment and overall the tuning of the hydrodynamic resistances of the sorting channels affected the sorting of the particles[245].

Consider the schematic of the model as described in fig. 4.2. The radius of the smallest particle is  $r$  and that of the largest is  $R$ . Similarly, width of the pinch segment is  $w$  and flow rate of the particle inlet is  $Q_{\text{inlet}}$  and the flow rate of the aligning flow is depicted as  $Q_{\text{main}}$ . In brief, the flow ratios to be used depend on the width of the pinch segment and radius of the smallest particles [245]. In order to calculate the relation between the above parameters a new variable (intersection width ratio) is designed which is calculated as  $2r/w$ . Figure 4.3 shows the flow ratios to be used based on the intersection width ratio, which allows to identify the flow ratios to be used based on a particular pinch segment width and the radius of particles to be sorted.

For detailed description, please refer to the guide for designing “Pinch flow fractionation devices”[245]. This theoretical model enabled us to improve the sorting efficiency of the system by designing the hydraulic resistances of the outlet channels and by controlling the fractionation boundary in the separation chamber [245].



**Figure 4.3:** Ratio of Flow rates compared to the intersection width ratio assuring aligning of the particles to the channel walls in the pinch segment [245].

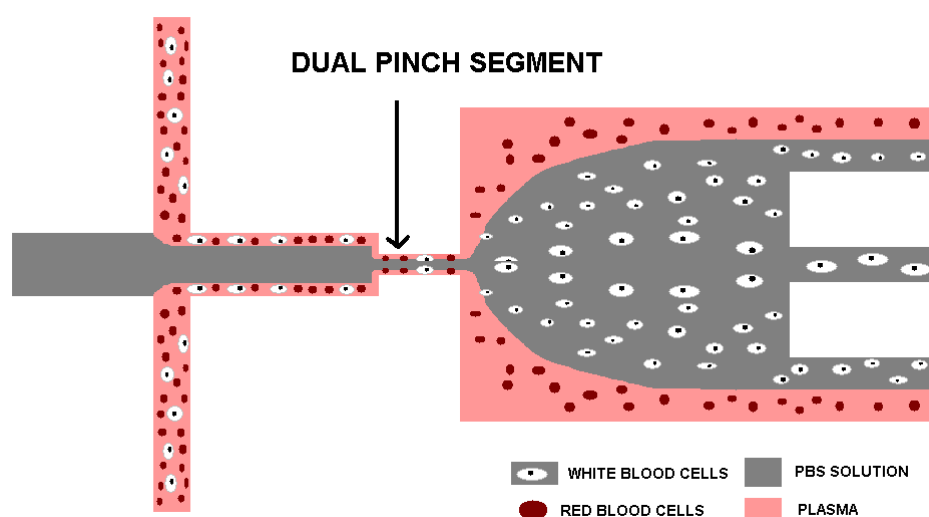
## Fabrication, testing and discussion

Based on the theoretical calculations from the theory project, Pinch Flow fractionation devices were designed and fabricated in SU-8 using traditional photolithography process [Section 5.2.1]. The SU-8 mould was used to cast the channels into PDMS [Section 5.3.3]. The inlets and outlets were created by punching holes using a blunt needle and press-fit with a larger needle into the holes leading to leak proof interconnections. The devices were tested with latex beads of 5  $\mu\text{m}$  and 9  $\mu\text{m}$ , resembling the size of the erythrocytes and lymphocytes. Other techniques like laser ablation [Section 5.3.2] and transparency based photolithography were also tested for fabricating the PFF devices[247].

While this model of PFF functions well with particles [as also simulated] which have well defined sizes and rigid boundaries (such as beads), it fails to consider and provision for the elastic nature of the cell membrane. Firstly, the theoretical models fail to take into consideration the elasticity of the cell membrane[248] and cell drifting layer (or cell free layer)[249] . Secondly, the problems with cell sizes variation from person to person make it difficult to design a universal system for sorting of white blood cells. Due to realization of these issues which highlight the non-applicability of a PFF system for sorting of blood cells, we concluded that the Pinch Flow fractionation system cannot be used for sorting of blood cells.

## 4.4 Dual pinch flow fractionation (DPFF)

In principle, for the C-TAS system to perform further downstream analysis, even few WBCs could be sufficient. A novel symmetric version of Pinch flow fractionation was conceptualized and tested with nano particles for size exclusion based filtration of particles. The idea was to create symmetry in the pinch segment whereby the smallest particles (RBCs) will continue to flow into outer collection channels, but the larger particles (WBCs) will follow streamlines closer towards the centre of the pinch segment. Now by carefully tuning the flow rates in the PBS buffer stream (aligning stream), a state could be reached where most of the RBCs and WBCs will enter the outer collection channels, but only the largest of the WBCs (about 5%) will enter the central stream and get isolated [Fig. 4.4]. This concept was devised as in principle for C-TAS system to function, we only need few WBCs which could later be cultured and used for further analysis.



*Figure 4.4: Concept of blood sorting via DPFF*

Considering the shortfalls of pinch flow fractionation system to isolate WBCs from whole blood, we have designed the novel symmetric model of Dual Pinch Flow Fractionation (DPFF). This symmetric model [Fig 4.4] utilizes enhanced hydrodynamic effects at dual interface system to selectively isolate only the largest of the WBCs from the whole blood. Also, the DPFF model incorporates the two shortcomings of the PFFF model and inherently takes into account the cell elastic behaviour and cell drifting effect [Fig. 4.5] as the system does not depend on sorting of the particles, rather than just the fact that the largest of the WBCs will follow into central streamlines.



The concept was designed to remove the uncertainties of the Pinch flow fractionation system by replacing the traditional pinch flow system where particles were aligned on only one wall of the pinch segment. Instead of the earlier version, we have realized a more symmetric system with simultaneous pinching of particles on both the walls of the pinch segment. The resultant symmetric system can function as high size based filter for particles based on tuning of the flow rates and hydrodynamic resistances of the collection channels [Fig. 4.4].

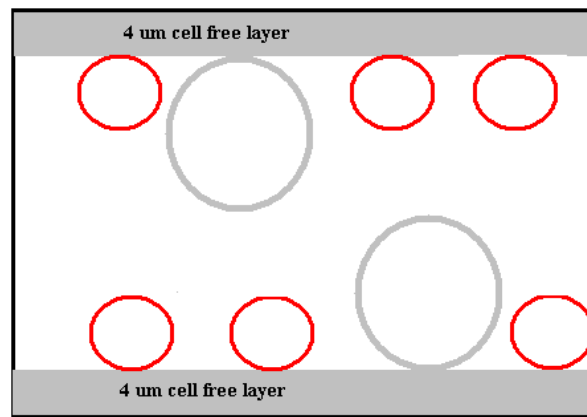


Figure 4.5: Concept of blood filtration on Dual Pinch flow fractionation device.

### Principle of the DPFF

Figure 4.6 illustrates the simulation of the principle of DPFF model. The DPFF is made of 3 inlets, 1 central aligning fluid inlet and 2 sample inlets with particles. Like the earlier PFF system, the idea is to align the particles in the sample inlet to the walls of the pinch segment, but instead of aligning them to one of the pinch segment channel walls, in the case of DPFF the particles are aligned to both the channel walls.

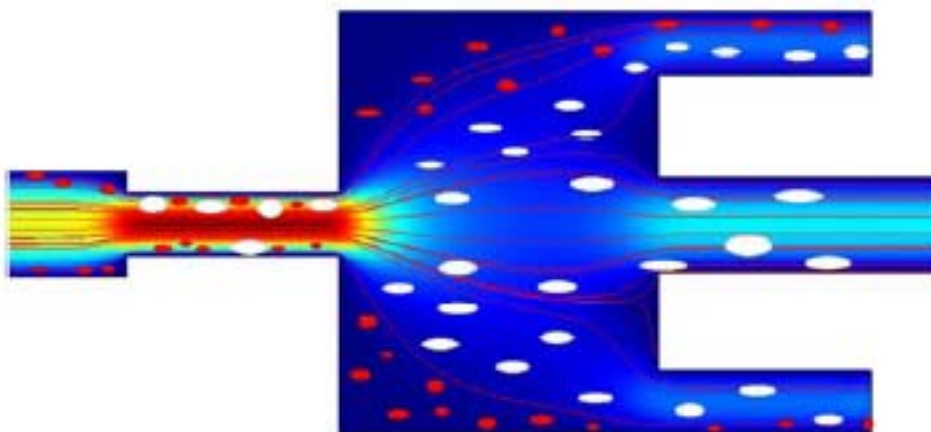


Figure 4.6: Illustration of DPFF model. The central channel collects only the WBCs, while the outer channels will collect most of the WBCs and RBCs.

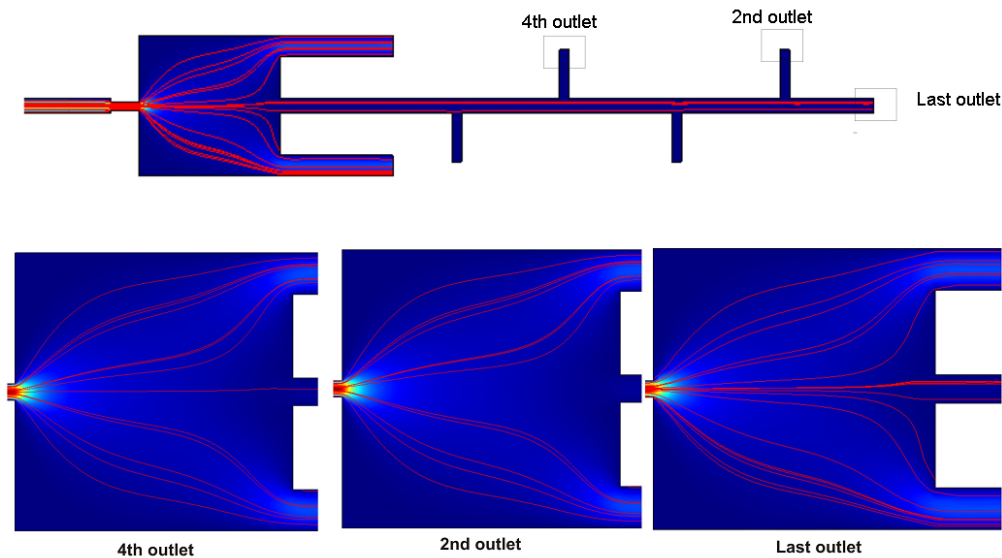
As shown in figure 4.6, this system was designed to operate in a manner that it separates the larger WBCs in the central outlet while most of the RBCs and the WBCs exit from the side channels. The requirements for optimisation of the experimental protocol are less strict with this system as we in principle only need to ensure that the central outlet does not get contaminated with smaller cell types.

The effect at the broadening or the separation section is analogous to the one in PFFF; due to the expanding laminar flow profile, the smaller particles flow through the outer outlets as their centre lies in the fluid streams closer to the pinch segment walls, which continue to flow into the outer outlets. Similarly, the largest of the particles tend to flow towards the central streams as their centre lies into central flow lines away from the streamlines closer to the pinch segment walls. In case, the outlet resistances are equal, by carefully tuning the flow rates, the separation position can be tuned in such a manner that only the largest of the particles align into the flow lines entering the central isolation outlet. Hence, in the case of blood, the largest particles being the WBCs they are collected in the central outlet stream and isolated.

## **Field programmable DPFF devices**

In another approach, apart from simulating the outlet resistances and calculating the required resistances, it is also possible to design DPFF systems with variable resistances to tune the flow entering the central outlet stream [Fig 4.7]. This concept provides the capability of programming the DPFF systems while testing as required. This capability of programming DPFF systems is essential because of the complex variations of blood cells. Blood cells sizes differ from person to person and vary accordingly to their health state and cycle of cell division[250-253]. Hence, this functionality could prove to be very important if the C-TAS system is to be commercialized.

This system could be designed with possibility to tune the hydrodynamic resistances by designing multiple outlets in the isolation channel to alter the exclusion size below which the cells or particles flow out to the outer channels. Figure 4.7 below shows the central outlet with multiple side channels providing an option to pick any one of them as required to tune the hydrodynamic resistance of the central collection outlet. The further away the outlet is moved from the separation chamber, the higher the resistance of the channel leading to the smallest fraction of the flow from the separation chamber entering the central inlet.



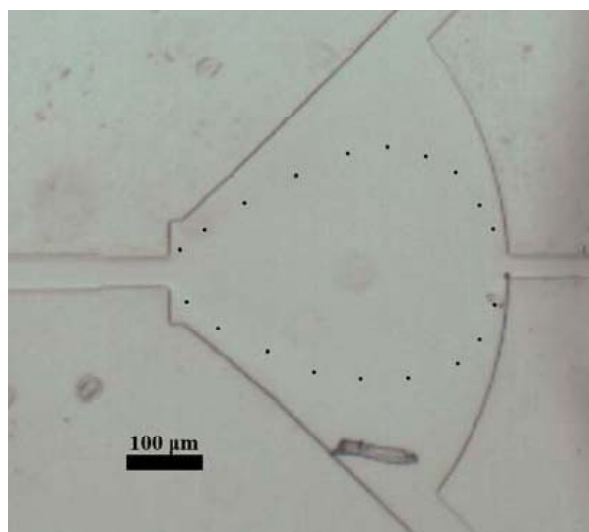
**Figure 4.7:** Tunable DPFF to tune the sorting of particles based on selection of different outlets at the time of application.

Due to interest of time and emergence of other simpler strategies, the DPFF system was never tested with cells, but we present the proof of principle of the DPFF and its application for sized based tunable filtration of particles tested with nanoparticles.

## Fabrication, testing and discussion

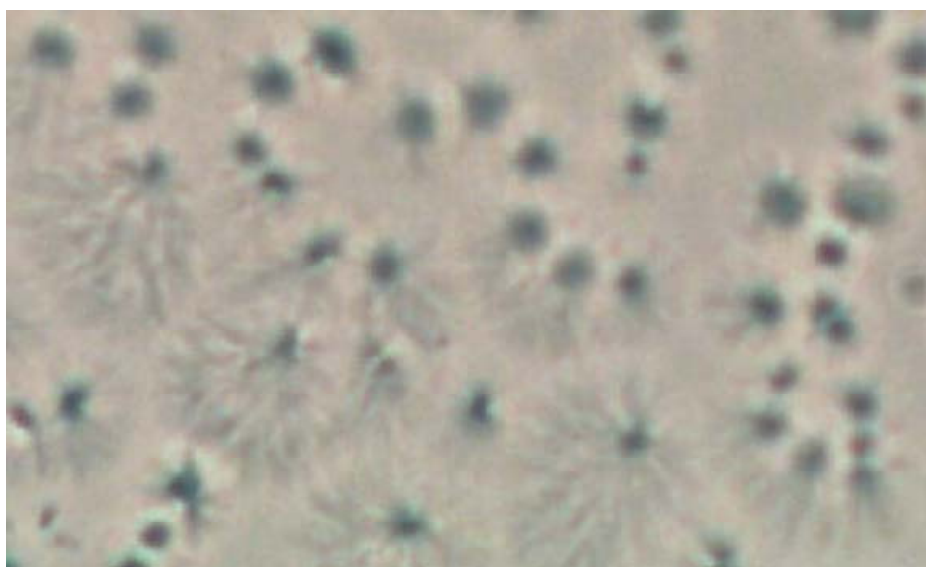
The DPFF system has not been tested with blood cells due to focus on other methods, but in order to validate the principle we tested the this system for isolation of micro and nanospheres formed by self-assembly of peptides. These particles are formed in a microfluidic channel by means of droplet emulsification process and their sizes ranged from 200 nm to 5  $\mu\text{m}$ . We were interested in separating the particles below 3  $\mu\text{m}$  in the outer channels and the larger ones in the central outlet.

The fabrication protocol similar to devices made for testing PFF systems was followed. In order to achieve the goal of isolating particles below 3  $\mu\text{m}$  into the outer channels and the higher to be isolated via the central channel, the flow rates were tuned to separate all particles smaller than 3  $\mu\text{m}$  to exit in to the outer channels [Fig. 4.8].



**Figure 4.8:** Flow profile of the separation experiment. The flow rates were 0.8  $\mu\text{l}/\text{min}$  for the particles solution and 20  $\mu\text{l}/\text{min}$  for the aligning flow. Channel height is 31  $\mu\text{m}$ . Pictures are edited by adding dots to outline the flow not clearly visible in the picture.

Based on the tests above, we could observe isolation of peptide microspheres larger than 3  $\mu\text{m}$  in the central outlet [Fig. 4.9]. Unfortunately, due to the high shear forces and dilution of the peptide stock solution by the aligning fluids these spheres disintegrated on isolation at the outlet and resulted into flakes [Fig. 4.9].



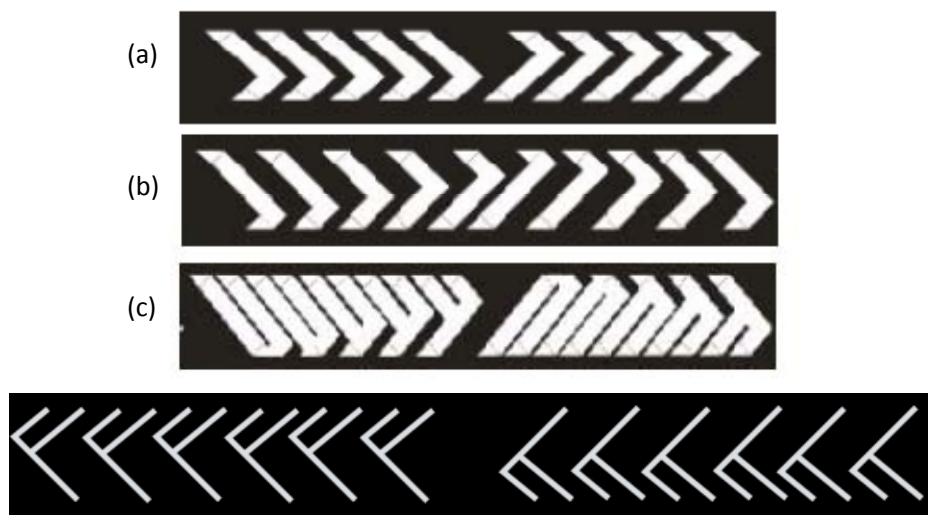
**Figure 4.9:** Microparticles extracted out of the DPFF system central outlet containing particles larger than 3  $\mu\text{m}$ .

Due to our focus on achieving the a simple C-TAS system, we decided to go away from the PFF systems and move to RBC lysing based isolation of white blood cells. In the near future, we aim to repeat the tests with beads and publish this work as a novel technique for size exclusion filtering of the largest particles of a mixed solution. We foresee numerous applications of this technique in polymer, pharmaceutical and cosmetic industry working with colloids and nanoparticles.

#### 4.5 Microfluidic FACSlyser: Lysing based isolation of lymphocytes

This work was directed towards creating an efficient, and simple microfluidic mixer capable of lysing erythrocytes selectively on chip by mixing them with water, thus enhancing separation of WBCs. In clinical diagnostics, blood cells are separated using FACSlyse protocol, whereby RBCs are lysed using lysants. Most of these lysants function on the principle of providing the RBCs with a hypotonic shock. WBCs are generally more resistant to these lysants and hypotonic treatments compared to RBCs and hence they lyse later than the RBCs. Using this window of time, the RBCs are lysed and the unlysed WBCs are collected soon after and put under isotonic conditions in phosphate buffered saline (PBS) Solution.

Recently attempts have been made to miniaturize and integrate this protocol on a miniaturized device by Sethu *et al.* by means of utilizing microfluidic mixers to mix the lysant and the whole blood[254-256].



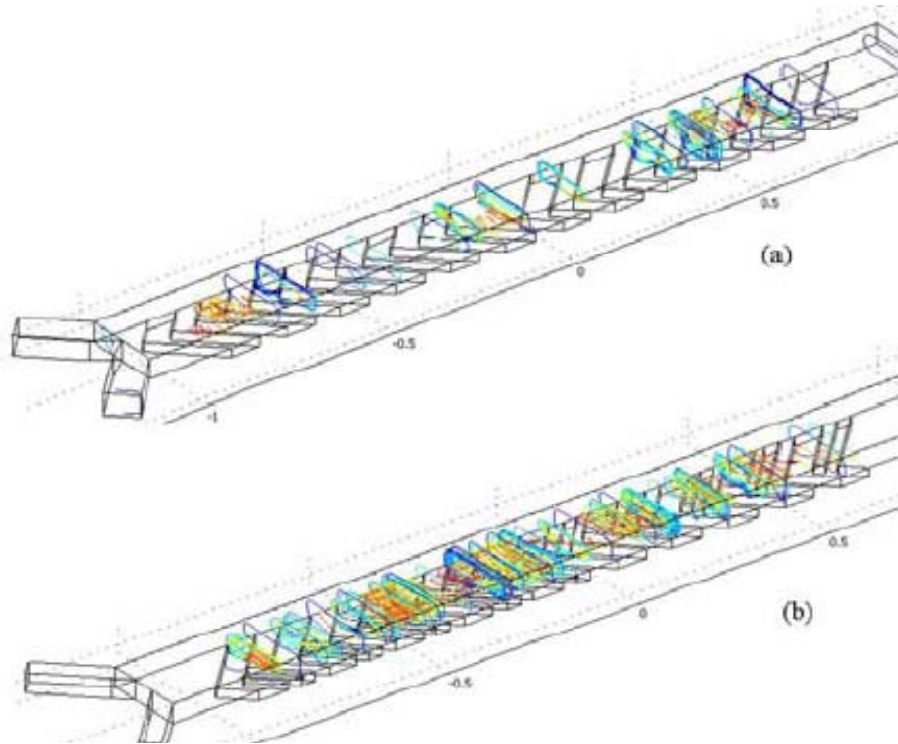
**Figure 4.10:** (a) Stroock's design (b,c) Yang's designs 1 and 2 (Bottom) Our proposed design

On simulating the mixers used by Sethu *et al.*, we found that there was significant room for improving the system by optimizing the mixer which would allow us faster lysing and subsequently rapid isotonic inducement for WBCs [256]. The earlier experiments have used the herringbone structures presented by Stroock's *et al.*[257]. We were interested in optimizing these mixers to enable rapid microscale mixing of RBCs and WBCs. As a result, we conducted an extensive study of the mixing dynamics of the Stroock's herringbone mixer and focused on the parameters which can be optimized for improving the mixing.

As it happens in research, Yang *et al.* presented their results on optimization of the Stroock's design while we were still working on our optimizations, which highlighted that Stroock's mixer can indeed be optimized and that the efficiency of herringbone mixers can be improved by up to 40%[258]. This work suggested two new designs for improving mixing based on the simple harmonic mixing principle [Fig 4.10]. The new designs were compared extensively with Stroock's design to understand the influence of the change in the design and the resultant mixing dynamics leading to better mixing. The conclusion was that Yang's design 1 did not have much improvement compared to Stroock's design and the periodic sweeping of the flow splitting boundary across the channel width did not have any justifiable optimization in the mixing rate. But in the case of design 2 there was significant improvement in the average vorticity across the length of the groove which was improving the mixing efficiency. Vorticity is the amount of fluid spin or circulation created due to the hydrodynamic mixing of the flow lines. Hence, a design providing better vorticity will induce a faster mixing of the fluids. We also found that the optimal number of herringbones per cycle is 6, after which having more herringbones per half cycle of mixer does not have any further increase in the vorticity. Hence, it was suggested to limit the number of herringbones per cycle to 6[259].

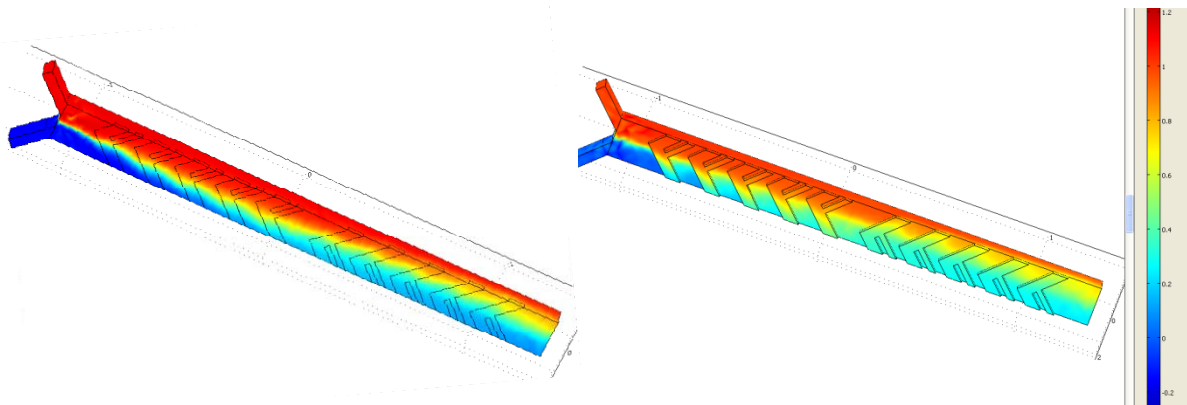
Hence, in the end we proposed a new design based on our findings, which contained periodic flow switching after every half cycle as in case of the Stroock's design but improving the vorticity of the mixer by using herringbones from Yang's design 2 [Fig. 4.11]. This was simulated by using two different concentration fluids as input parameters assigning them to one of the input channels. Figure 4.11 (b) shows more vorticities forming in our proposed device compared to the original Stroock's herringbone mixer (a). The blue and red vortices display the intensity of the mixing behavior induced by the mixers, where it can be seen clearly that Fig. 4.11 (b) has much more helical spins in the fluidic channel. This was done because we found that the asymmetry index or flow splitting boundary is optimized at  $1/3$  and  $2/3$  of the channel width as in the case of Stroock's design[260].





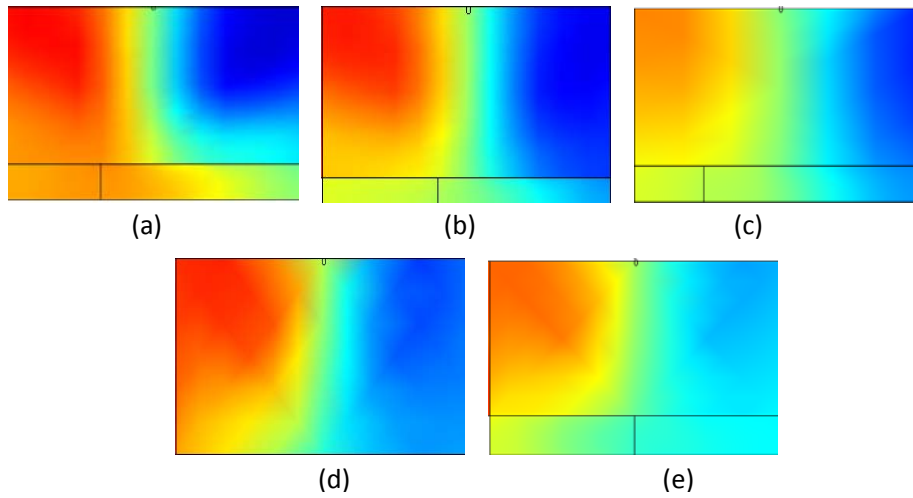
**Figure 4.11:** Improved vorticity in our design (b) compared to the Stroock's Design (a)

We were also interested in understanding the difference in mixing profile in case of having herringbones as ridges or as grooves. As a result, we also simulated our design with ridges and grooves to better our understanding of the mixing profile in both the cases.



**Figure 4.12:** (Left) Mixing in one cycle of our design with herringbone ridges (Right) Mixing in our one cycle of our design with herringbone grooves. (Red indicates concentration of 0 and blue indicates concentration of 1)

The results showed that the mixing profile with grooves and ridges was very different and in all the designs grooves were better in mixing the fluids compared to the ridges [Fig 4.12]. Finally, we compared our design with all the previous presented designs. Figure 4.13 shows the cross section at the end of one mixing cycle from all the mixers. In order to simulate mixing in one cycle of each design, we added concentrations to the fluids as depicted by red (concentration 0) and blue (concentration 1). This allowed us to use the convection-diffusion model of COMSOL, to study the effective mixing at the end of one cycle of mixing.

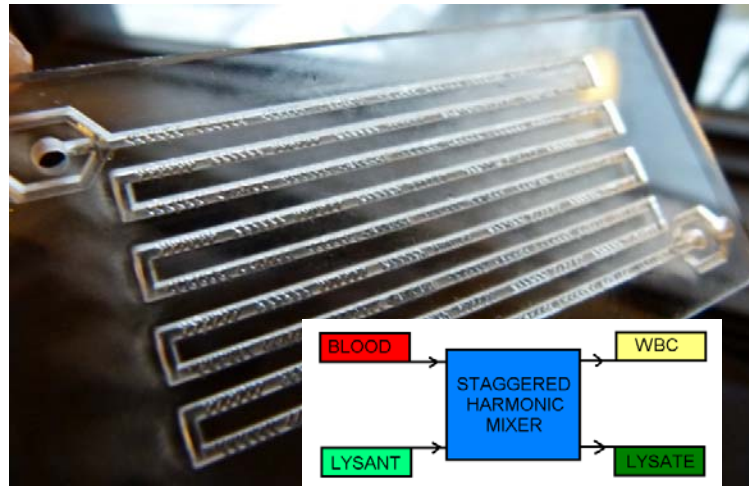


**Figure 4.13:** Figures show the simulations of concentration-diffusion profiles of the cross section after one mixing cycle. (a) Stroock's design (b) Yang's design1 (c) Yang's design 2 (d) Our design with ridges (e) Our design with grooves. (Note: (a-c,e) show the contour of the groove and (d) doesn't have a black outline of the groove as it has been simulated with a ridge to compare the difference in mixing (also shown in Fig 4.12(Left)))

Figure 4.13 (e) clearly shows a more homogeneous mixing compared to all the other herringbone mixers. There is clearly not much difference in Stroock's design and Yang's design 1. Our design with grooves clearly shows higher mixing compared to the design with ridges as is evident by blending of the red and blue colours. In conclusion, the simulations showed better mixing efficiency with the novel design and it was then time to test the lysing efficiency.

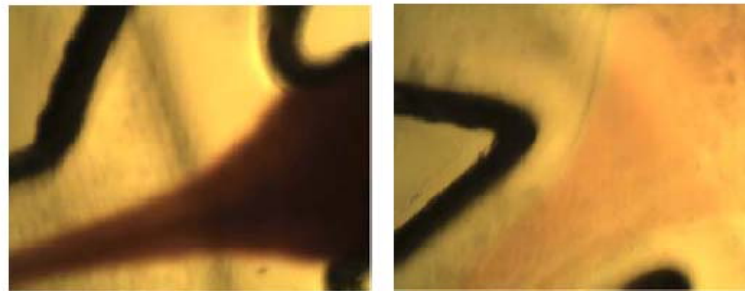


## Fabrication and Testing



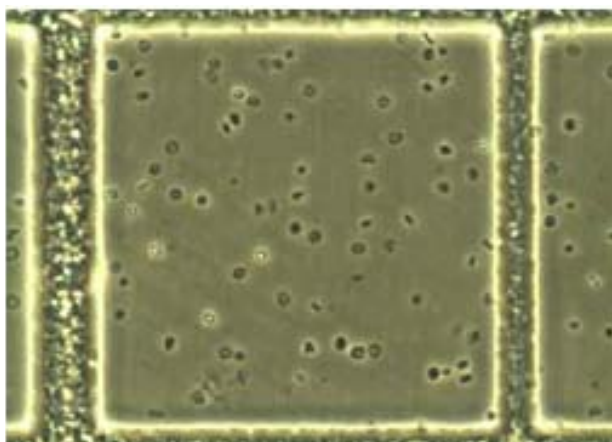
**Figure 4.14:** Schematic of the microfluidic FACSlysing principle and Laser ablated FACSlyser.

Figure 4.14 shows a schematic of the principle of the microfluidic FACSlyser for isolation of leukocytes and the laser ablated FACSlyser device. The control mixers based on Stroock's design and test mixers based on our design were fabricated using CO<sub>2</sub> laser ablation process in PMMA [Section 5.3.2] and bonded using UV activated thermal bonding [Section 5.4.2]. We used autoclaved DI water and pure blood to test the lysing of RBCs [Fig.4.15].



**Figure. 4.15:** (Left) Blood at inlet focused by DI water streams (Right) Blood at outlet focused by PBS solution.

The results showed the lysing of RBCs indicated by the decrease in red colour of the mixture at the outlet [Fig. 4.15 (right)]. But when we tried to culture the lymphocytes, after lysing with DI water there was no growth observed, despite the cells appearing viable with Trypan blue staining [Fig. 4.16]. Trypan blue is a live-dead stain providing quick assessment of the viability of cells. As cells with intact membrane exclude this dye, they appear brighter and highlight a well defined membrane compared to dead cells whose membrane is easily breached by the dye and appear dark bluish in colour.

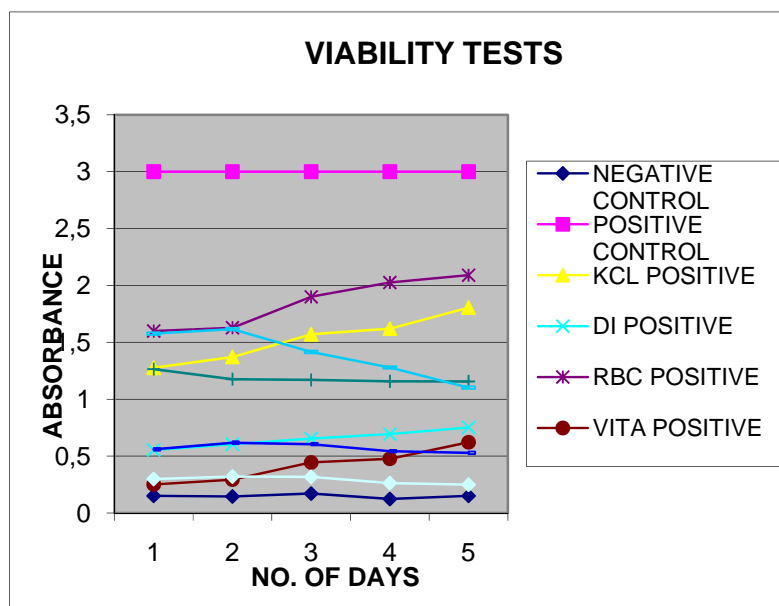


**Figure 4.16:** Trypan blue based viability testing for cells collected from FACSlyser. The background shows debris of the lysed erythrocytes.

As a result, we concluded that the DI water treatment was harsh on the lymphocytes and switched to other commercially available lysants like VitaLyse (BioE), RBC Lyser (Sigma Aldrich) and freshly prepared 0.75 mM KCL solution. But unfortunately, none of these lysants (even those which claimed 99% selectivity to erythrocytes) could isolate lymphocytes which could be cultured and used for spreading metaphase chromosomes.

Figure 4.17 shows the results of cell proliferation assay conducted with the WST-1 assay [Roche Diagnostics]. This colorimetric assay is used for studying the growth of the cells over 5 days, by means of measuring absorbance of the cell suspension treated with WST-1 assay in order to measure their proliferation, based on their metabolic consumption of assay dye. As can be seen in the figure, the cell cultures for RBC Lyser and KCL show some growth, but the growth curve didn't show the typical steep curve as expected in lymphocyte cultures. Unfortunately, none of the cells (including controls where the cells were lysed using the 4 lysants on eppendorf tubes) showed any significant proliferation, which also confirmed our hypothesis that the lysants affect the proliferation of the lymphocytes but not the viability.

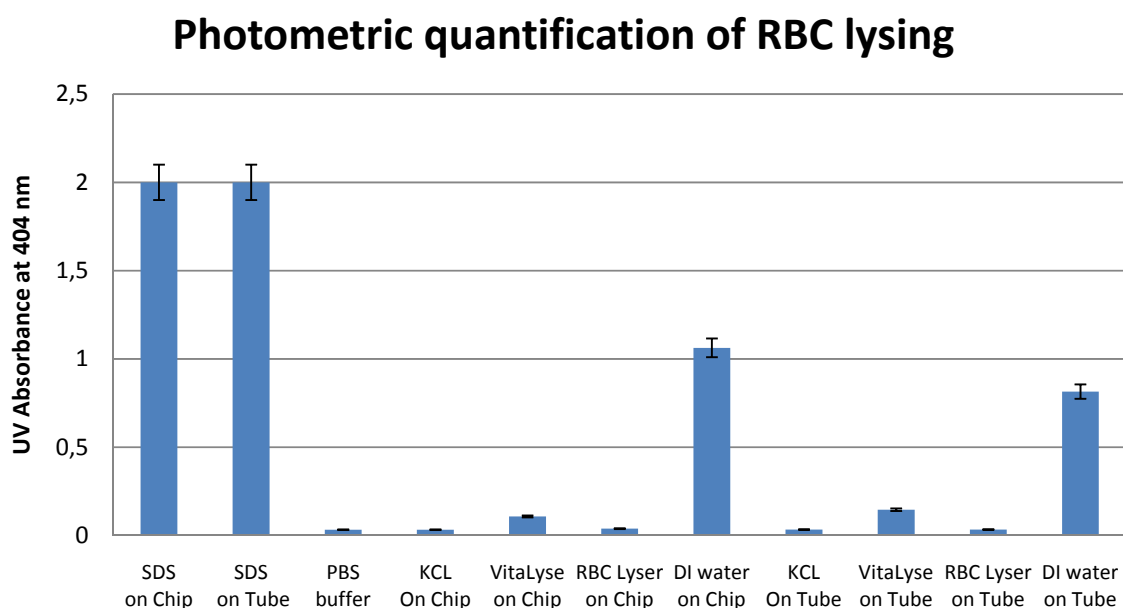
Nevertheless, we wanted to quantify the lysing based on the microfluidic FACSlyser and compare it with the lysing on the traditional eppendorf tube based vortexing using the previously mentioned RBC lysants. Hence, we adopted the photometric detection technique to compare the lysing of RBCs on chip and on tube with vortex exposed to the lysant buffer for same amount of time [261-263].



**Figure 4.17:** Colorimetric Cell Proliferation WST-1 assay for validating the viability and expansion of Leukocytes after 3 days culture [Section 5.6.11].

The photometric detection assay works on the principle of measuring absorbance of UV light by haemoglobin and other RBC components dissolved in the lysate. On comparing the results of absorbance of different lysed solutions from microfluidic FACSlyser and the traditional technique it was observed that the lysing was marginally better on the FACSlyser. The best lysing was achieved using the DI water, while the least amount of lysing was observed using 0.75mM KCL solution and Sigma Aldrich RBC lysing solution. Sodium dodecyl sulfate (SDS) buffer was used as control which lyses 100% of the cells. SDS solubilizes the cell membrane as a result releasing the entire cytoplasmic material in the lysate. On comparison, the VitaLyse solution from BioE was a better lysant for lysing RBC's from a whole blood solution.

At later stages of the project, during our visit to our collaborators we figured out that they typically prefer to culture whole blood, and arrest and fix lymphocytes instead of isolating lymphocytes prior to culturing. They also mentioned that they believe that the FACSlyse process does affect the lymphocytes. Hence despite showing viability during Trypan blue live-dead staining they might not proliferate. This reconfirmed our hypothesis that the lysants affect the proliferation capability of the cells.



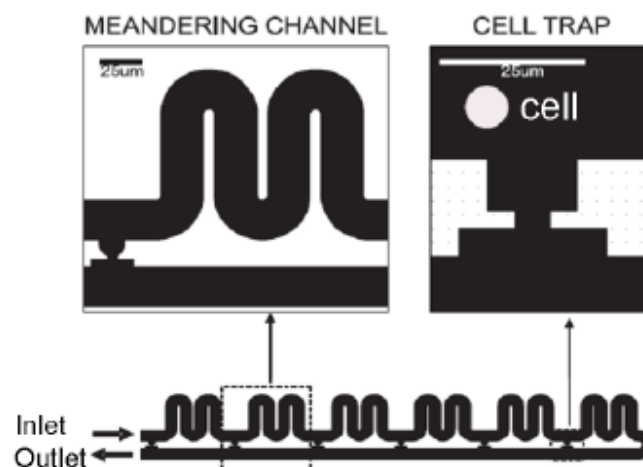
**Figure 4.18:** Quantification of lysing on chip and comparison with traditional FACSlysing technique for different lysing solutions.

We were also suggested to culture the whole blood first, followed by arrest and then apply subsequent lysing of the erythrocytes in FACSlyser with KCL. This will lead to isolation of arrested lymphocytes which don't need further culturing and could be directly splashed as they have already been treated with hypotonic solution. This was not tested as we had already started to develop the integrated FISH version, but the herringbone mixer was meanwhile tested for fixation of the cells by PhD student Indumathi Vedarethinam with good success. Hence this project was dropped and the results with improved mixing efficiency of the microfluidic herringbone based mixer were presented at the COMSOL User conference in 2008 and published in the proceedings of the conference [259].

## 4.6 Hydrodynamic cell traps

This work was conducted in collaboration with PhD student Jacob Lange and Master student Peter Paluszewski. In order to culture lymphocytes, it was important to trap them or isolate them from the rest of the blood components. In this work, cell traps were designed to trap lymphocytes in a microfluidic system. Hydrodynamic traps for sequential trapping of beads have been published before by Tan *et al*[264]. We wanted to apply the same trapping principle for sequential trapping of lymphocytes, after lysing of the red blood cells with the herringbone system. This was important for physical localization of cells and to allow for the debris to be removed from the lymphocytes, which could possibly provide background signal at a later stage.

The design of the cell trap and working principle are highlighted in Figure 4.19. The trapping mechanism is illustrated in the inset figure.

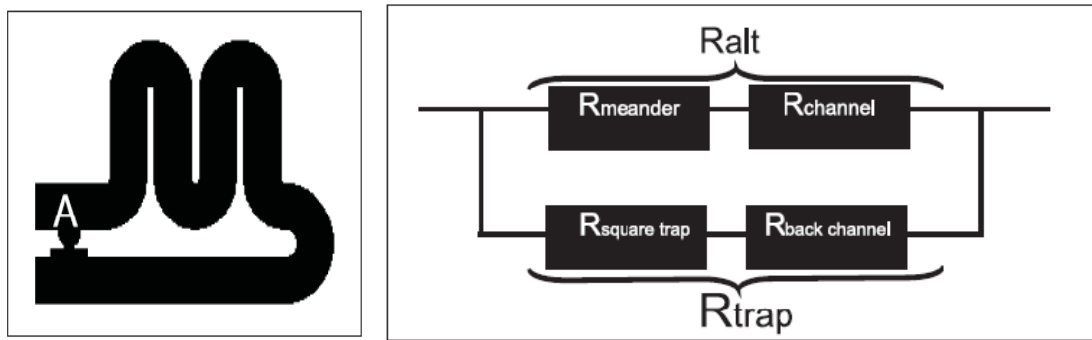


**Figure 4.19:** The schematic of the trapping system with inset pictures focussing on the positioning of cell traps before meanders and depicting the trapping mechanism of a cell in the cell trap.

The cell traps and the meanders are placed alternately in the inlet channel and finally the outlet channel is formed by connecting the last meander to the outlets of all the cell traps. The cell traps are designed to be 5  $\mu\text{m}$  wide in order to allow flow through but trap particles larger than 5  $\mu\text{m}$ . The placement of meanders after each trap ensures the cells or particles flow through the traps because at each cell trap, the cell finds the resistance of the cell trap to be lower compared to that of the meander ensuring the cell gets trapped.

The hypothesis further was that once a cell is trapped in any cell trap, its resistance will increase compared to the meander and hence the next cell will flow through the meander into the next cell trap until all the cell traps are filled after which the cells flow straight to the outlet.

Considering the height of the channel is 30  $\mu\text{m}$ , the low Reynolds number ensures the flow follows Hagen-Poiseuille principles. This allows for easy interpretation of the hydrodynamic resistance in terms of an electrical circuit, as shown in fig. 4.20.



**Figure 4.20:** (Left) one trap system (Right) Equivalent electrical circuit diagram based on hydrodynamic resistances of the one trap system

Here,  $R_{\text{meander}}$ ,  $R_{\text{channel}}$ ,  $R_{\text{square trap}}$ ,  $R_{\text{back channel}}$  resemble the hydrodynamic resistances of the meander, channel between the trap and meander, the square part of the cell trap and the channel connecting the square trap to the outlet channel respectively.

Hence, applying Ohm's law and calculating the hydrodynamic resistances of meander and the cell trap by using the dimensions of the trap and the meander, we get,

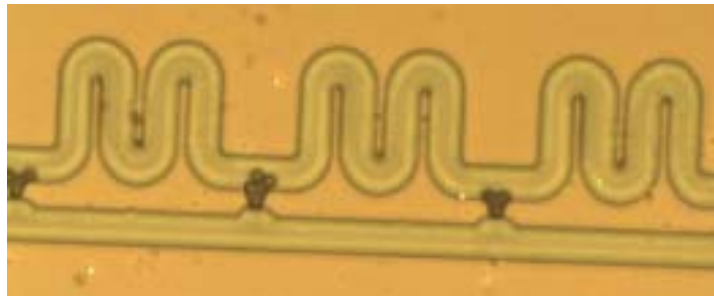
$$R_{\text{alternate}} = 3.27 \times 10^{13} \text{ Pa s m}^{-3}$$

$$R_{\text{trap}} = 1.91 \times 10^{13} \text{ Pa s m}^{-3}$$

Thus, the trap will receive majority of the flow leading to trapping of the cells. Based on theoretical evaluation, we concluded that this design will work for any number of traps as far as there are 3 or more traps connected in series. For more details on the theoretical model and the calculations please refer to Appendix A.

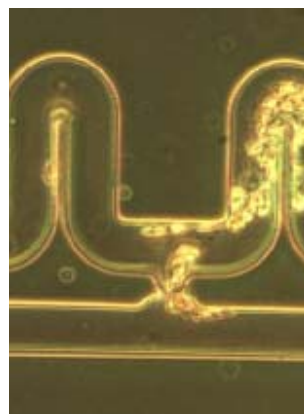
## Fabrication and testing

The devices to test the cell trapping principle were fabricated in PDMS and bonded on to another flat PDMS using oxygen plasma based bonding [Fig. 4.21] [Section 5.4.1]. The master for moulding the device was fabricated in SU-8 on a silicon wafer and later replica moulded into PDMS [Section 5.2.1, 5.3.3].



*Figure 4.21: 10  $\mu\text{m}$  polystyrene beads trapped in the cell traps (Image courtesy: Jacob Lange)*

The device was tested with beads and Jurkat cells to test the applicability of the cell traps to capture individual cells [Fig. 4.22]. The device functioned very well with polystyrene beads and several beads were trapped into each trap due to bead-bead stiction which was later minimalized using 20% Tween solution.



*Figure 4.22: Jurkat cells (15  $\mu\text{m}$ ) squeezing through a 5  $\mu\text{m}$  cell trap*

When the solution was changed to cell suspension, the problems with trapping cells started to emerge. Cells are simply too elastic to be trapped. Jurkat cells as large as 15  $\mu\text{m}$  in radius could squeeze through the 5  $\mu\text{m}$  cell traps [Fig. 4.22] and later a publication highlighted how Jurkat cells can pass through 2  $\mu\text{m}$  constrictions[169]. Hence this was the end of our efforts to take this cell trapping system further. Looking back, this system can find many applications



with beads based assays needing individual trapping and functionalisation of the beads. Later, Tan and Takeuchi presented another variation of the previous cell traps with chambers for culturing and trapping cells which look more promising[265].

## 4.7 Gravitational conditioning of cells

This work highlights development of another microfluidic technique for concentration of cells using gravity assisted sedimentation.. The concept of this device is presented in Figure. 4.23. The device consists of a loading channel and a concentration channel separated by channels which allow sedimentation of the cells without getting washed away due to the flow in the loading channel. The flow in this device works based on stop and flow principle, whereby the flow is stopped on filling of the channel with cells and the stop is initiated when the cells have sedimented into the convection free zone of the sedimentation channel. Finally, all the cells are collected into the concentration channel and extracted via the outlet of the concentration channel.

### Design 1: Validation test

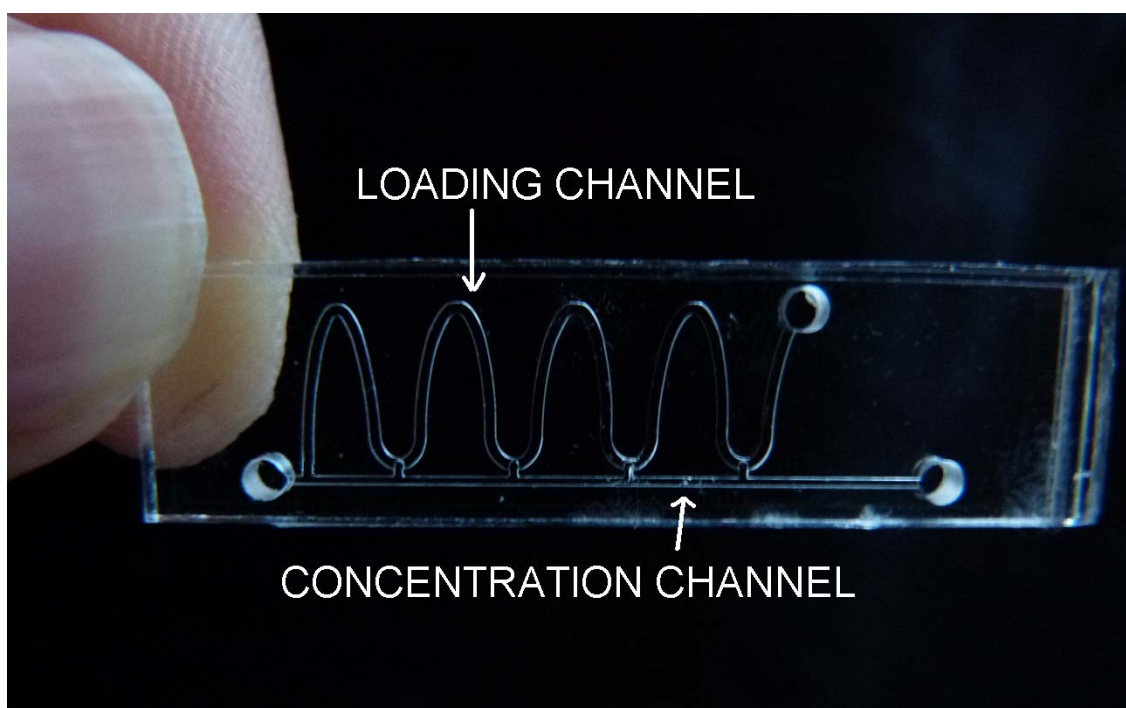
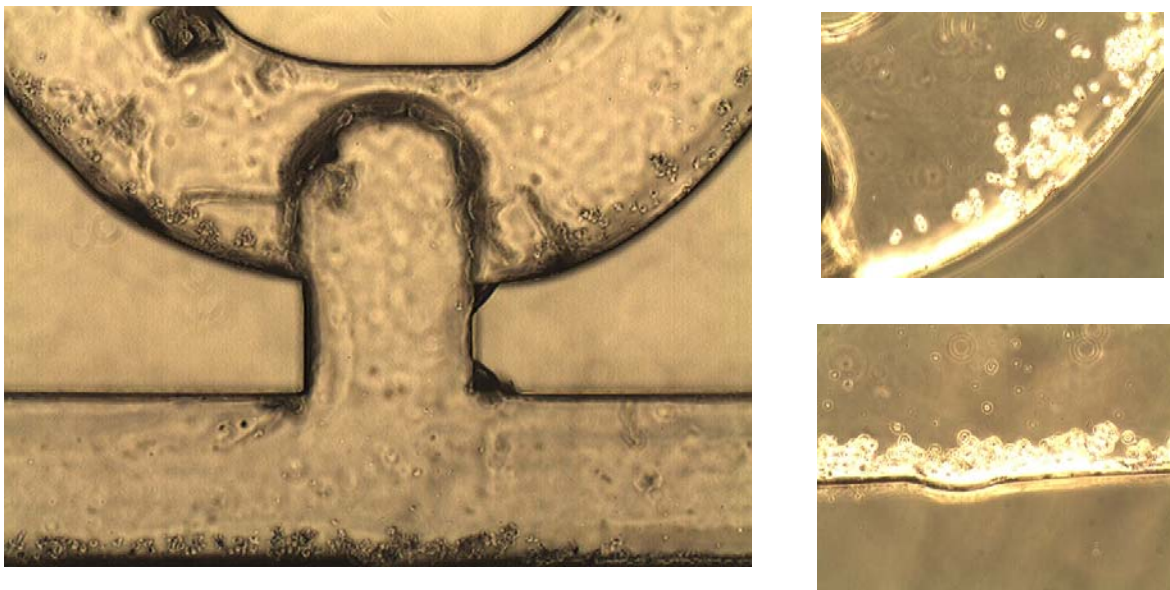


Figure 4.23: Schematic of design 1.

The figure 4.23 depicts the schematics of design 1. There is one inlet connected to two channels, the top loading channel and the bottom concentration channel [in later designs the common inlet was dropped and separate inlets/outlets were chosen for both channels]. The outlets are switched by using 3 way port valves. Initially, all outlets are kept in open state and the entire device is filled with PBS buffer. In order, to start the concentration protocol, the concentration outlet is closed and the cells are loaded via the inlet into the loading channel. Hence during loading and sedimentation of the cells the outlet for loading channel was opened and closed synchronous to the stopping of flow. The concentration channel outlet was kept closed all the time until the cells were to be extracted.

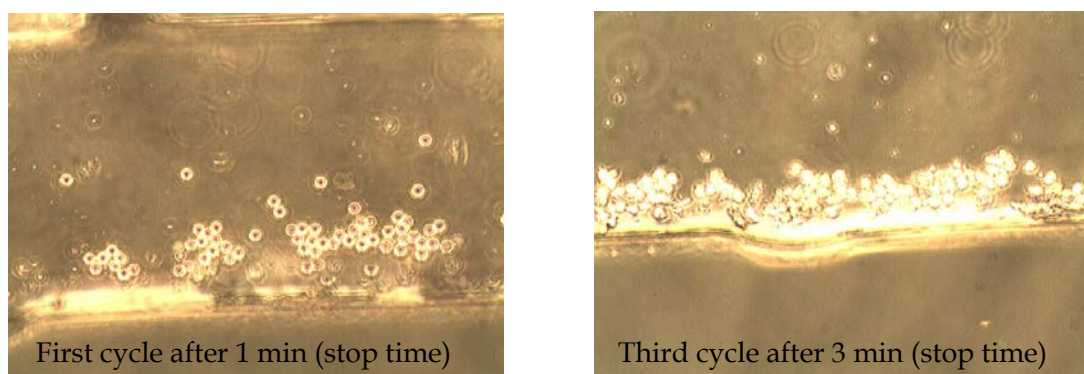
### Fabrication and testing

These devices were micro-milled into PMMA sheets and bonded using UV activated thermal bonding [Section 5.4.2]. Interconnects were formed as described earlier by embedding silicon plugs into ball end milled channels[188] . The device was tested with diluted Jurkat cells with a concentration of  $10^5$  cells /ml [Fig. 4.24].



**Figure 4.24:** *Sedimentation of cells from loading channel into concentration channel via the sedimentation channel*

The cells were concentrated upto 7 cycles and then extracted via the concentration channel outlet and counted using a cell counting slide chamber [Fig. 4.24]. In all experiments, we found a typical 5-7 times up concentration of the cells which is also presented in the Fig. 4.25.

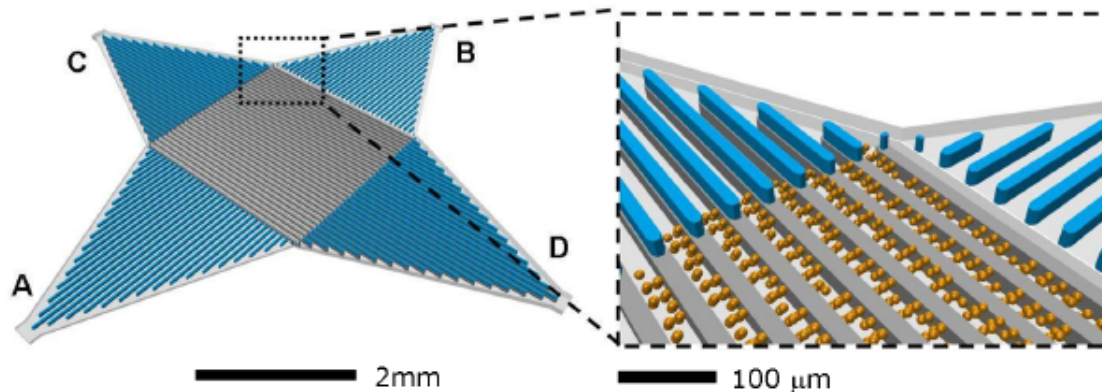


**Figure 4.25:** Cells concentrated in the concentration channel after 1 and 3 min of the concentration protocol relating to the first and third cycle of the protocols respectively.

## Design 2: Grooved chamber

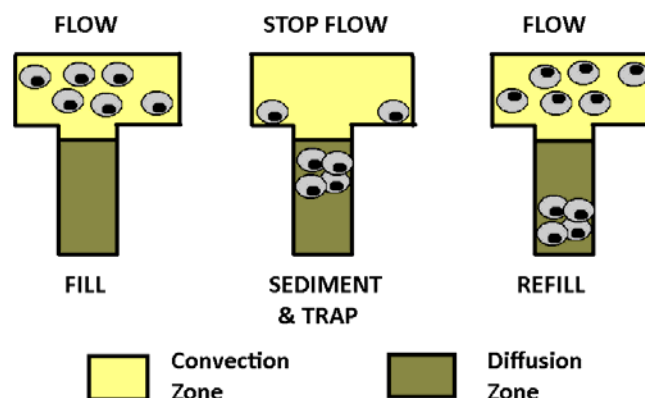
Due to sequential manipulation and handling of cells during lysing and fixation of cells on the C-TAS motherboard, there was a significant dilution of cells. This created a need for concentration of the cells before flushing them to the next module, which is traditionally done by centrifugation process in bulky centrifuges. In order to achieve concentration of cells on the motherboard, a strategy of trapping cells by gravity based sedimentation was utilized, whereby cells were concentrated in a stagnant flow in the grooves of a grooved chamber [Fig. 4.26].

The grooved chamber was designed as a culture chamber to provide diffusion based perfusion to the cells loaded at the bottom of the grooves [266]. Due to the high aspect ratio of the grooves, the perfusion in perpendicular direction above the grooves will not enter the groove which creates a convection free diffusion dominant zone in the grooves [Fig. 4.26]. While this device never functioned as a culture device as intended, it was tested on the motherboard for gravitational trapping based concentration of cells.



**Figure 4.26:** Grooved chamber for gravitational concentration of cells. The cells are perfused from A to B i.e. perpendicular to grooves leading to sedimentation of the cells in the grooves on stopping of the flow and subsequent trapping in the convection free zone on restarting of the flow.

The concept was to trap the cells in the convection free zone by sedimentation of the grooves by means of stopping the flow intermittently [Fig. 4.27]. Once the cells pass into the diffusion dominant zone in the grooves the flow is started again to refill the chamber above the grooves with new cells. During the refill process, the cells in the grooves continue to sediment as they see no convection. Lange *et al.* have demonstrated that the flow in any microgrooves with twice the height than the width of the groove, will only be diffusive and the cells in the grooves will not see any convection [266].



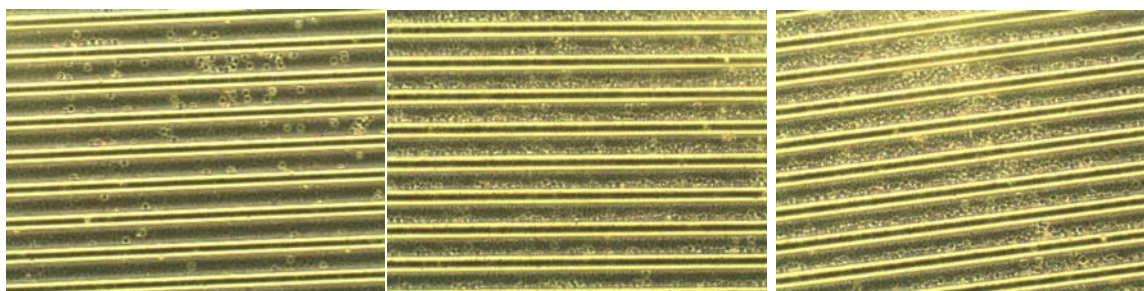
**Figure 4.27:** (Left) Simulation of flow across the grooves showing convection above the groove and diffusion in the grooves (Right) Stop and Flow based gravitational trapping of cells



## Assembly and testing

The devices used to test the motherboard were kindly provided by Jacob Lange, who was developing the C-TAS culture module. A pluggable module was assembled by adhesive bonding based assembly of the Pluggy and grooved chamber. The dilute T-Lymphocyte cell suspension was prepared with concentration of  $10^5$  cells/ml and loaded in a 1 ml syringe. A syringe pump was used to actuate the cells through the motherboard. The syringe pump was programmed to pump for 1.5 min and then stop the flow for 3.5 min. When the diluted cells were flushed into the grooved chamber filled with Phosphate Buffered Saline (PBS) buffer, the flow was stopped when the chamber was filled with cells. Once the cells had sedimented in to the grooves and left the convection zone, the flow could be restarted to enter more cells into the grooved chamber without disturbing the sedimentation of the cells which were no longer in the transverse flow lines reach. This process can be used repeatedly to up concentrate the dilute cells, which can later be collected via the unloading outlet or perfused to culture on the culture chip.

## Results of concentration

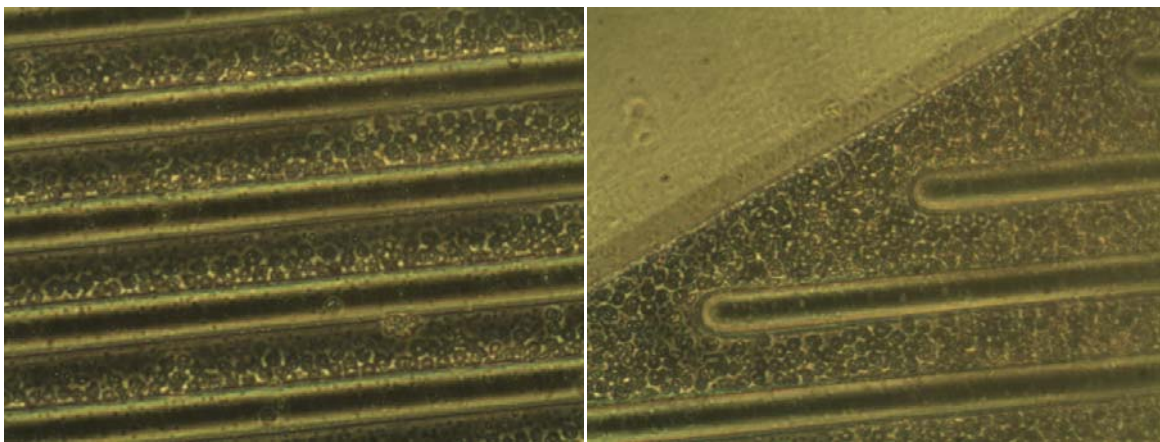


**Figure 4.28:** Time lapse of concentration of cells using gravitational sedimentation into convection free zone of the grooved chamber.

Figure 4.28 highlights the results of the gravitational concentration of cells in the grooved chamber. The cells took roughly 3 min to leave the convection zone and enter into the diffusion zone and hence the syringe pump was programmed to flush cells for 1.5 min and then stop flow for 3.5 min at  $2 \mu\text{l}/\text{min}$ . After every cycle an image was taken and the results of the cells concentrated in the grooves after 2, 8 and 15 cycles have been depicted in the Figure 4.28. The increasing concentration of cells was clearly evident after every cycle of sedimentation.

This chip was originally designed for cell culture work, but due to a fault in the design the flow was uneven in the chamber [266]. As a result, there were more cells getting collected in

the edge of the chip compared to the central grooves [Fig. 4.29]. With 15 rounds of gravitational sedimentation, we processed  $50 \pm 3 \mu\text{l}$  of cell suspension each time and concentrated cells with an average efficiency of 69%. The experiment was conducted 10 times for 3 different samples. The cells were counted before the sedimentation protocol and after as an end point result to calculate the average concentration efficiency of the device. The aim of this experiment was not to characterize the system, but to ascertain if it would be possible to load cells on the culture chip and concentrated that way. It was also important to figure out how many cycles would be needed to capture sufficient amount of cells to conduct the FISH protocol. The entire protocol took 75 min in total for the 15 rounds of sedimentation.



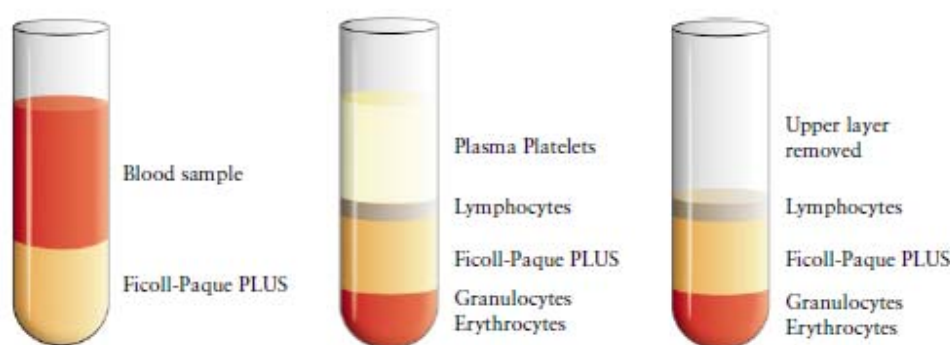
**Figure 4.29:** (Left) Magnified image of concentration showing multiple layer buildup of cells and (Right) Higher concentration of cells in the edge of the grooved chamber due to unbalanced hydrodynamic resistances due to clogging in the middle of groove.

We successfully demonstrated the concept of gravitational sedimentation of cells in the grooved chamber on a motherboard. However, due to changes in the culture device, we didn't use the grooved chamber for C-TAS protocol. Nevertheless, these results highlight the applicability of the motherboard for manipulating cells and the possibility of using the sedimentation principle for loading and concentrating cells in the culture chamber. If this device is to be used as sedimentation based device for concentrating cells then optimizing the sedimentation protocol will be the first task. But as we realized it would take over 1 h to capture sufficient amount of cells to start the cell culture protocol, we discarded this solution from the C-TAS protocol and hence no experiments were conducted to characterize the system further or optimize the stoppage and flushing times to improve the concentration efficiency.

## 4.8 Continuous gravitational fractionation of lymphocytes

In the above experiments, the sedimentation of the cells was purely based on the gravity. As a result, this was a time consuming process which would need fair amounts of time if we intended to concentrate a large volume of cell suspensions (300 nL/cycle). In order to increase the speed of the process and to improve applicability for C-TAS project, we redesigned the gravitational concentrators into various designs providing high throughput concentration of cells as well as novel approaches for utilizing the same designs for Ficoll-paque based sorting of the cells i.e. without the need for stopping the flow.

Ficoll-Paque is widely used in biological labs to extract WBCs from whole blood. The principle of operation is density driven fractionation of whole blood as the density of Ficoll-Paque medium is between the density of the red blood cells and the white blood cells leading to their separation into separate layers above and below the Ficoll medium [Fig 4.30].



*Figure 4.30: Operation of Ficoll-Paque based isolation of blood sub-types. (www.ge.com)*

The principle of continuous flow sorting of lymphocytes using a gravitational fractionation device is based on simultaneous sedimentation of erythrocytes in the Ficoll-paque and floatation or anti-sedimentation of lymphocytes. Hence if you imagine a mixture of blood cells in Ficoll-paque solution passing through a microfluidic channel, the erythrocytes are continually sedimenting in this channel, while the lymphocytes are continually rising due to the anti-sedimentation or floatation caused due to rapidly sedimenting erythrocytes [267]. Hence, in principle if you have the channel long enough you could just extract the lymphocytes from the top of the channel after a certain time.

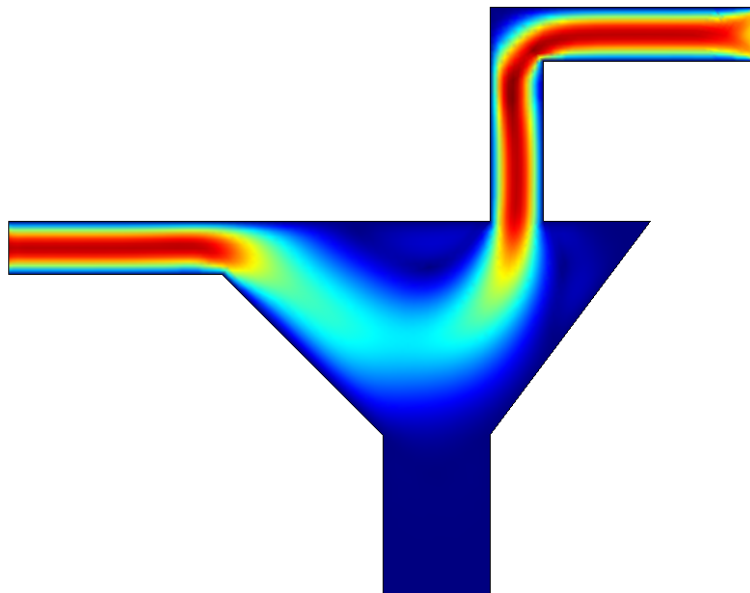
But we were interested in utilizing the high throughput system which benefited from hydrodynamic flow manipulation, leading to faster sedimentation of the cells due to their slipping into a no flow zone at each gravitational trap. We simulated this high throughput



system to calculate the number of gravitational traps required in an array for trapping 100% of the lymphocytes in the system.

### **Simulations of high throughput gravitational trapping of erythrocytes:**

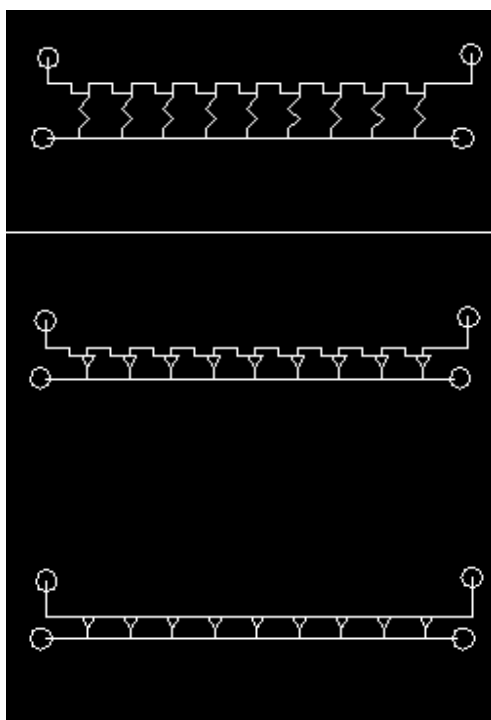
It was well known from literature that erythrocytes sediment roughly about  $0.8 \mu\text{m/s}$  and at a faster rate in Ficoll-paque due to creation of a density gradient [268]. In order to simulate the sedimentation of erythrocytes in the high throughput gravitational sedimentation system, we simulated sedimentation of particles by adding a gravitational drop of  $3 \text{ mm/hr}$  on the particles. In traditional microfluidic systems, effect of gravity is neglected as a result. The flow through such a trapping system appears as shown in Fig. 4.31



*Figure 4.31: Depicting normal flow of cells without including gravitational sedimentation*

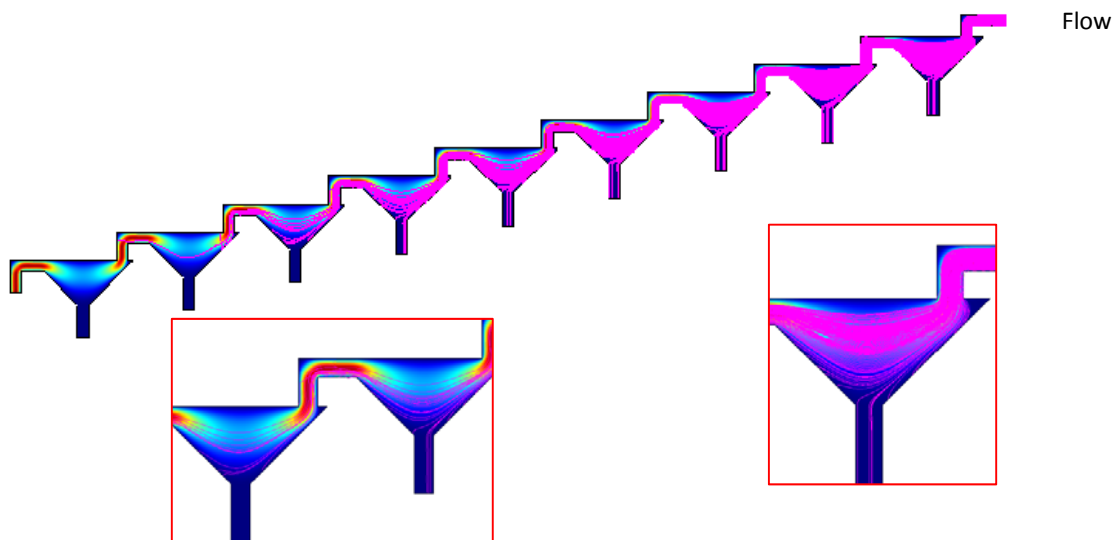
But from earlier results, we were aware of the rapid sedimentation of cells in microfluidic systems. Hence, we were interested in optimizing the earlier design into a continuous flow separation gravitational sedimentation system. We started with optimizing the 3 designs depicted in Fig. 4.32. Soon we realized the need for reducing vertical lifts in the design which disrupts the sedimentation of the erythrocytes. Hence, we avoided the top two designs in the Fig. 4.32. But on simulation of the bottom design, we observed the lack of convection-diffusion boundaries leading to rapid sedimentation of the erythrocytes. Hence, we created a new design with a novel stepped approach [Fig. 4.33], whereby the gravitational traps were arranged in a stairway-like fashion, and each trap was placed in the place of a step. In this way the output of the first trap (one at the top) will lead to the inlet of the next trap placed a step below

leading to no vertical lifts in the fluids. This also ensures that multiple convection-diffusion boundaries exist for the cells to sediment into at every trap. These systems benefit from the similar principle but have an advantage due to multiple arrays of traps being positioned in a sequence leading to faster trapping of particles without the need for stopping of flow.

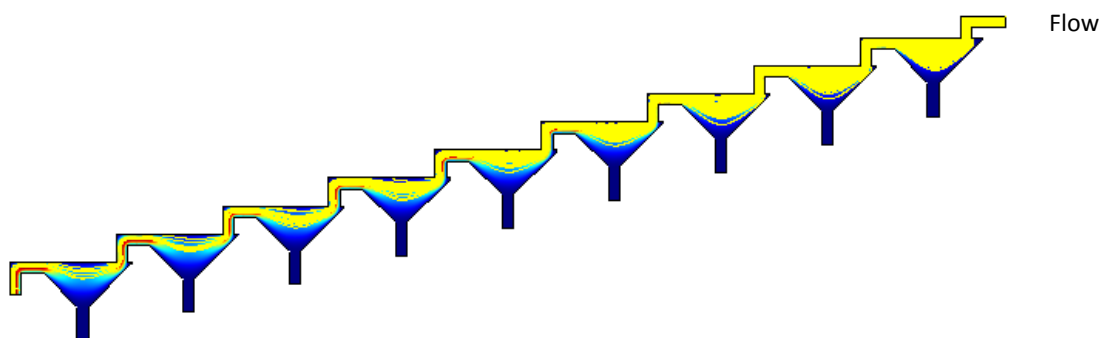


*Figure 4.32: High throughput gravitational hydrodynamic sedimentation designs*

After iterative simulations, we discovered that placing 9 gravitational traps connected in sequence, we can capture all the erythrocytes from the cell suspension [Fig. 4.33]. Also, considering that the lymphocytes feel an anti-sedimentation rate (simulated as equal to the sedimentation rate of erythrocytes i.e.  $0.8 \mu\text{m/s}$ ), they will continue to flow and rise in the convective stream towards the top of the channel and as a result can be sorted and isolated in the outlet [Fig. 4.34]. In these simulations, the erythrocytes and lymphocytes are simulated by tracing the trajectory of particles of diameter 6 and  $9 \mu\text{m}$  under the effect of gravity.



*Figure 4.33: High throughput gravitational sedimentation of erythrocytes*



*Figure 4.34: Depicting isolation of lymphocytes due to floatation in Ficoll-Paque medium.*

Unfortunately, due to time constraints and other interesting discoveries, these results only ended up only as a theoretical study. It has been spun off now into a Master's project and hopefully we will soon have results to corroborate this fascinating theoretical observation.

## 4.9 Antibody based trapping of chromosomes

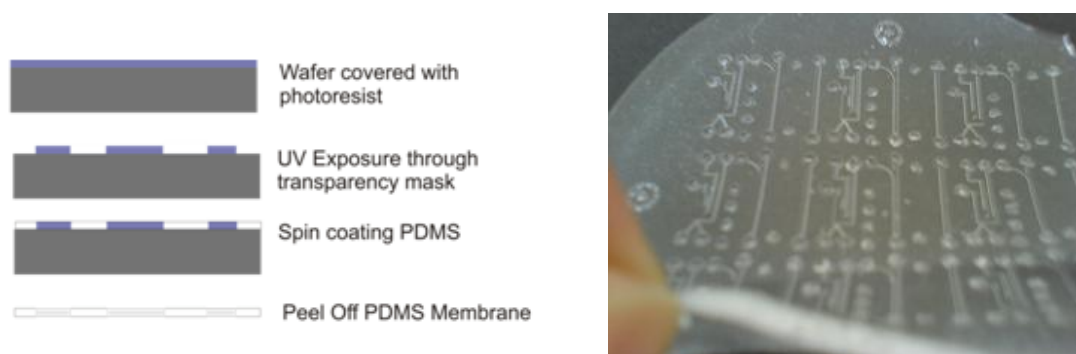
During the course of the C-TAS project, a number of surface modification techniques were tested. The major goal of these experiments was to develop a toolkit to immobilize or rather capture chromosomes on a surface functionalized with an antibody via a linker (surface binding molecule). All the surface modifications work was conducted with Jacob Lange (another PhD student also part of C-TAS project) and under the guidance of Asso. Prof. Mogens Havsteen Jakobsen. With the intention to use known chemistries for modifying the

surface, we started with triazine, 2,4,6-trichloro-1,3,5-triazine (TsT) based selective activation and Polyethylene Glycol (PEG) based passivation chemistry developed by the Surface Chemistry group.

## Anti CENP-A Immobilization

In order to test our hypothesis that we could capture chromosomes by using surface-bound antibodies having affinity to specific regions of the chromosomes, we needed to activate selective regions on the surface to bind the antibody while passivate the rest of the regions so that the chromosomes don't bind unselectively. To begin the TsT-PEG surface chemistry was tested with Biotin-Streptavidin assay to mimick the binding of antibody and histones[266]. On successful results of this test assay, we switched to immobilizing CENP-A (Centromeric Protein) which binds to histones on the centromere of chromosomes.

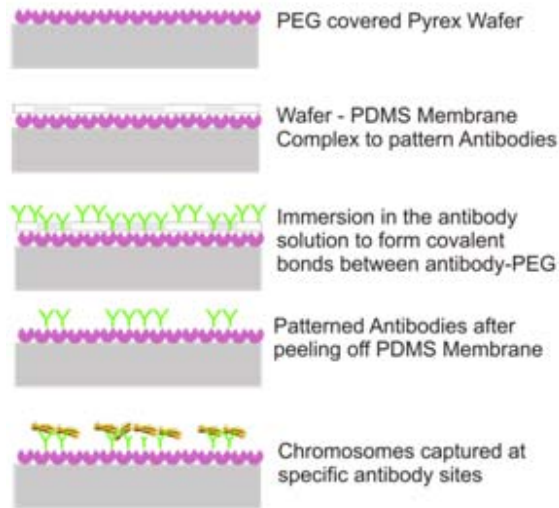
The surface was prepared with TsT-PEG chemistry and the antibody was patterned selectively on to the surface by means of selective patterning using a stenciled PDMS membrane. The membrane was fabricated as described below and applied to the surface covered with PEG [Fig. 4.35]. After selectively patterning of the activation and immersion of the wafer in antibody solution, we had localized spots containing antibodies. The chromosomes suspension was prepared in a polyamine buffer using the technique described by Wray *et al*[269]. Later, a drop of suspension was applied to the surface and left overnight to hybridize. Overnight hybridization times were preferred as chromosomes have slower diffusion.



**Figure 4.35:** Fabrication of PDMS membranes to act as stencil for selective surface activation for antibody binding.

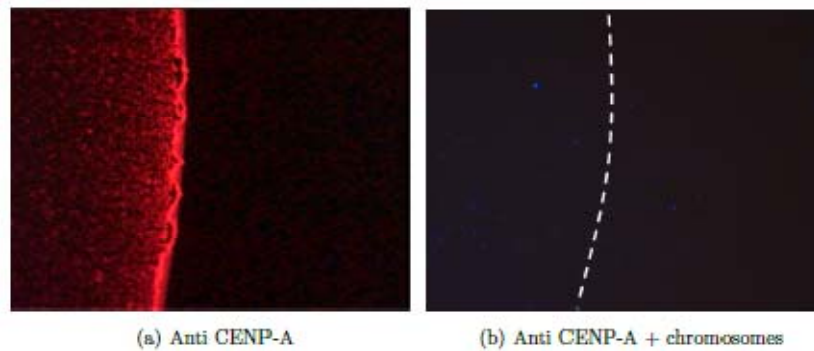
Unfortunately, the results were not as successful as with the test assay. While the antibodies could be localized using the technique shown in Figure 4.36, which was promising, the

chromosomes were nevertheless bound to the entire surface and not selectively to anti CENP-A [Fig. 4.37].



**Figure 4.36:** Process of surface passivation, selective activation and subsequent trapping of the antibodies

We tested the results with numerous other substrates like COC, PMMA and even  $\text{TiO}_2$  coated silicon wafers. But the results were the same, leading us to conclusion that the surface chemistry was not that specific.



**Figure 4.37:** (Left) Anti-CENP A patterning showing clear defined edge of coating (Right) Showing unspecific binding of chromosomes on both the sides of the dotted line demarking the edge of the CENP-A coating.

In the end, we concluded that this surface chemistry toolbox will not work for chromosomes and we had to revert back to traditional chromosome immobilization techniques as described in Paper 1. Looking back, we could have done few things differently especially to improve the hybridization. Firstly we could have treated the chromosome suspension with elevated temperature ( $75^\circ\text{C}$ ) to denature the DNA before applying them to the surface. Finally, a flow based system would be better suited to avoid unspecific binding of the chromosomes based on sedimentation.



# CHAPTER 5

## METHODS

This chapter serves as a compendium of the methods used as part of the experimental work described earlier in this thesis. All the methodologies related to the design, simulations, fabrication and further, the biological analysis protocols are explained in detail.

## 5.1 Simulations

When necessary, extensive theoretical studies have been conducted as part of optimization exercises in order to assist in the designing process, leading to fundamentally sound designs as well as to characterize the flow through microfluidic devices presented in earlier chapters. The simulations were always conducted using COMSOL Multiphysics software (versions 3, 3.4 and 3.5).

**Table 5.1:** Parameters used for theoretical analysis of various microfluidic systems

Device	Constant	Description	Value	Unit	Source
Microfluidic Bioreactor ( $\mu$ BR)	U	Inlet Velocity of perfusion	$2.083 \times 10^{-11}$	$\text{m}^3/\text{s}$	
	W	Width of perfusion meander	$5 \times 10^{-4}$	M	
	$h_{\text{culture}}$	Height of culture chamber	$2.5 \times 10^{-4}$	M	
	$H_{\text{perfusion}}$	Height of perfusion meander	$3 \times 10^{-4}$	m	
	$\rho$	Density of water	$1 \times 10^3$	$\text{kg}/\text{m}^3$	
	$\eta$	Viscosity of water	$1 \times 10^{-3}$	Pa s	
	$\Phi_{\text{membrane}}$	Membrane Porosity	0.14		Manufacturer
	$D_{\text{glucose}}$	Diffusion coefficient of Glucose	$6.7 \times 10^{-10}$	$\text{m}^2/\text{s}$	[187]
	$D_{\text{KCl}}$	Diffusion coefficient of KCl	$2 \times 10^{-9}$	$\text{m}^2/\text{s}$	[270]
		Glucose consumption	$2.66 \times 10^{-4}$	$\text{mol}/\text{m}^3\text{s}$	[186]
Continuous Gravitational Sedimenter		Concentration of glucose in media	11.11	mM	Manufacturer
		Porosity of the membrane	0.14		Manufacturer
	$R_{\text{rbc}}$	Radius of red blood cells	$5 \times 10^{-6}$	m	
	$R_{\text{wbc}}$	Radius of white blood cells	$9 \times 10^{-6}$	m	
	U	Inlet Flow velocity	$6.6 \times 10^{-4}$	m/s	
	$S_{\text{rbc}}$	Erythrocyte Sedimentation Rate	$0.8 \times 10^{-6}$	m/s	[268]
	$S_{\text{wbc}}$	Leukocyte Anti-Sedimentation Rate	$0.8 \times 10^{-6}$	m/s	[267]
	P	Density of water	$1 \times 10^3$	$\text{kg}/\text{m}^3$	
FACSLyser	H	Viscosity of water	$1 \times 10^{-3}$	Pa s	
	T	Thickness of channel	$1 \times 10^{-4}$	m	
	$D_{\text{blood}}$	Diffusion coefficient of RBC	$6.8 \times 10^{-14}$	$\text{m}^2/\text{s}$	www.nanomedicine.com
	$D_{\text{lysant}}$	Diffusion coefficient of KCL	$2 \times 10^{-9}$	$\text{m}^2/\text{s}$	[270]
	$U_{\text{lysant}}$	Inlet velocity of lysant	$1 \times 10^{-4}$	m/s	
	$U_{\text{blood}}$	Inlet velocity of blood	$1 \times 10^{-4}$	m/s	
	P	Density of water	$1 \times 10^3$	$\text{kg}/\text{m}^3$	
	H	Viscosity of water	$1 \times 10^{-3}$	Pa s	
	c0	Concentration of blood stream	1	$\text{mol}/\text{m}^3$	
	c1	Concentration of lysant stream	0	$\text{mol}/\text{m}^3$	



Integrated relevant modules of “Convection-Diffusion” and “General Laminar Flow”, part of the MEMS - Microfluidics application mode were used to match the scale and aspects of the problems being simulated. The simulations were conducted in transient or stationary modes depending on the design problem. The various constants used as part of the simulation work are listed in Table 5.1.

### **Microfluidic Bioreactor**

The entire system was simulated. Version 3.6 of COMSOL Multiphysics was used by coupling the General Laminar Flow and the Convection-Diffusion application modes. The two physics modes could however be solved independently so first the fluid flow was solved for in a steady state analysis. The solution was saved and used for solving the concentration using a transient analysis from 0 to 2000 s with the solution stored in 50 s time intervals. In the first case we looked at how KCl fills the channel and chamber in this period. The actual concentration of KCl is not important and therefore a concentration of 1 M was used at the inlet as a “normalized” concentration for the KCl. In the case of glucose consumption by the cells the transient analysis was conducted from 0 to 72 hours with a time step of 5000 s. The initial concentration in the all subdomains was set to 10 mM, as was the inlet concentration at the solution inlet. In this case the concentration values are therefore absolute. All boundaries apart from the inlet and outlet were set to “wall” for the laminar flow application mode and to “insulation/symmetry” for the convection-diffusion application mode.

### **Gravitational Sedimenter**

The entire problem was simulated with version 3.6 of COMSOL Multiphysics using the General Laminar Flow module. In this case we simulated the flow through the system and then processed the solution by adding streamlines. By modifying the solution parameters, we added tracking of 200 particles released simultaneously at the inlet. For simulation of the erythrocytes, we added a velocity component in Z direction equivalent to the free fall velocity or sedimentation velocity of cells (3  $\mu\text{m/s}$ ). Similarly for simulation of the leukocytes, we added an anti-sedimentation rate or floatation rate equivalent to the sedimentation rate of erythrocytes [267]. The particle sizes were tuned accordingly to 5 and 9  $\mu\text{m}$  during the particle tracking to match the sizes of the erythrocytes and leukocytes respectively. All boundaries apart from the inlet and outlet were set to “wall” for the laminar flow application mode.

## Microfluidics FACSlyser

The entire mixer was simulated with version 3.6 of COMSOL Multiphysics by coupling the General Laminar Flow and the Convection-Diffusion application modes using 3D geometry mode. As both the modules can be solved independently, at first we solved the fluid flow in a steady state. Later, by using this flow solution, we added concentration of 1 and 0 to the two mixing streams. In this case we looked at how quickly the fluids mixed in the mixer. The cross sectional plots of the mixers were taken after one cycle of mixing to compare the different mixer geometries. The mixers were also tested for their efficiency in mixing with respect to having the herringbone structures in the channels placed as ridges or as grooves. All boundaries apart from the inlet and outlet were set to “wall” for the laminar flow application mode and to “insulation/symmetry” for the convection-diffusion application mode.

## 5.2 Cleanroom fabrication protocols

### 5.2.1 Fabrication of SU-8 master

This section describes the process of making a SU-8 master which can be reused several times to replica mould PDMS structures. The SU-8 master is made by spinning SU-8 2075 (obtained from microchem.com) on a Si (1 0 0) wafer using a Karl Suss (KS) spinner. The spinning parameters are selected based on the required height of the channel structures. SU-8 2075 is a negative photoresist with a high viscosity. The SU-8 resist is exposed (with a Karl Suss aligner) using a dark field mask and subsequently developed with Propylene Glycol Methyl Ether Acetate (PGMEA) to create raised channels structures on the Si wafer. The overall process flow for SU-8 master fabrication is described in Table 5.2.

A syringe filled with SU-8 2075 resist is allowed to rest for 18 hr prior to use to allow for degassing of the air which could be trapped during loading of the syringe due to high viscosity of the resist. Failing to remove trapped air will result in uneven spinning of the resist over the wafer. Degassing could also be improved by heating the resist to 60 °C. Simultaneous to the degassing of SU-8, we leave Si wafers in the 250 °C oven to dehydrate them to improve adhesion of the SU-8 resist to the wafer. For spin coating SU-8 roughly 4-5 ml of SU-8 is used per wafer and the process recipe for spinning the SU-8 is run based on the desired height of the channel structures (100 µm for microFISH and 40 µm for Pinch Flow Fractionation devices).

**Table 5.2:** SU-8 master fabrication recipe

	Process Step	Equipment	Protocol	Comments
1	Degassing SU-8	Syringe and SU-8	Load Syringe and Wait 18 hrs	Leads to air bubbles getting accumulated at the top of the syringe
2	Dehydration of Si	Si (1 0 0) wafer and an oven	Temp. 250 °C for 18 hrs	Dehydrates the wafers
3	Spinning of SU-8	KS Spinner	Typically Time: 30-80 s, Acceleration: 200 rpm/s and Speed: 1000-5000 rpm	Parameters differ from design to design and described further in individual devices
4	Prebaking SU-8	Hotplate	95 °C for 5 hrs with ramp time of 30 min	Cooling period of 3 hr
5	Exposure	KS Aligner	Design dependent – typically time: 30 – 120 s with intermittent wait times of 15-30 s, Intensity of 9 mW/cm <sup>2</sup>	Parameters differ with each design based on the devices.
6	Postbaking SU-8	Hotplate	95 °C for 5 hrs with ramp time of 30 min	Cooling period of 3 hr
7	Development	PGMEA developer baths	First 4 min and later final 1 min	First is for rough development
8	Washing	Isopropanol (IPA)	Rigorous flushing of Si Wafer	
9	Drying	Air drying chamber	Air drying to remove any IPA	

A polished Al hotplate setup is used for pre and post exposure baking at 95 °C for 5 hrs to remove any stress from the SU-8 resist. The exposure time is set accordingly to the thickness of the SU-8 resist layer. This baking step leads to evaporation of the solvent from SU-8 and improves the resist film adhesion to the wafer. Post baking leads to better cross-linking of the exposed SU-8 regions and reduces appearance of cracks and bowing of certain regions due to internal stresses. For developing the structures, PGMEA baths are used. The first development is a rough development which dissolves the unexposed and uncrossed linked SU-8 followed by a final development. Finally, the wafers are thoroughly washed in IPA and air dried in the automatic dryer.

### 5.2.2 Fabrication of Silicon Master

The master mould for curing PDMS channels can also be made in Si (1 0 0) wafer by KOH based anisotropic wet etching process defining pyramidal structures for channels. The process used for fabricating the Si master using KOH wet etch is highlighted in Table 5.3.

The wet oxidation process is used to grow oxide to act as a mask for KOH etch. The HMDS treatment improves the adhesion of the resist to the wafers. Before spinning the resist on to the Si wafer, the nozzle of the Track 1 spinner is cleaned and spin coating is tested on 3 test wafers. After this step, 1.5 µm AZ5214E resist is spun on the Si wafer followed by a soft baking recipe. The KS Aligner is used for hard contact exposure of the resist for 7 s with intensity of 9 mW/cm<sup>2</sup>.

Following oxide removal with BHF, liftoff is performed by acetone rinse and finally the Si wafer is etched with KOH to define the raised channel structures. Dektak profiler is used to characterize the height of the channel structures.

### 5.2.3 Fabrication of Pyrex electrodes chip

After treating the Pyrex wafers with HMDS, 1.5 µm layer of AZ5214E resist was spun on to the wafers. Following the first exposure with an inverted mask, a reversal bake is applied which is followed by a flood exposure to define the electrodes. After development, the electrodes are created in Wordentec by deposition of 10 nm Ti and 150 nm Au. Finally, the process ends with a lift off. The detailed sequence of the process is listed in Table 5.4.

**Table 5.3:** Process flow for fabricating Silicon Master with KOH wet etch process

	Process Step	Equipment	Protocol	Comments
1	Thermal wet oxidation	Boron drive-in	Recipe: Wet 1050 H <sub>2</sub> O: 30 min N <sub>2</sub> : 20 min Thickness: 300 nm	KOH mask
2	Film inspection	Flimtek	Measure film thickness	
3	HMDS	HMDS oven	Program 4, Recipe time: 30 min T = 150°C	Improve resist adhesion
4	Spinning resist	SSI spinner	Prebake: 90°C Time = 60 s Resist: AZ5214E Recipe: 1.5 µm	BHF mask
5	Exposure	KS Aligner	Hard Contact Time: 7 s Intensity: 9 mW/cm <sup>2</sup>	
6	Development	Developer 2	Time: 70 s	
7	Oxide etch	BHF tank	Time: 4 min Rate: 80 nm/min	Protect backside with blue film
8	Rinse	Acetone Bath	Time: 15 min	Strips remaining resist
9	7up (98% sulphuric acid and ammonium sulphate)	7 up bath	Time: 10 min Temp: 80°C	Remove any residues and get a smoother etch
10	Silicon Etch	KOH 28%, Wet etch bath	Time: 7.5 min Rate: 1.28 µm/min Temp: 80 °C	Channel height of 10 µm for impedance cytometer chip.
11	Oxide Etch	HF tank	Time: 10 min Rate: 80 nm/min	Strip remaining oxide
12	Cleaning with 7 up	7 up bath	Time: 10 min Temp: 80 °C	
13	Characterization	Dektak	Measurement of channel height	Remove any residues and get a smoother etch

**Table 5.4:** Process flow for creating electrodes on a Pyrex wafer.

	Process Step	Equipment	Protocol	Comments
1	HMDS	HMDS oven	Program 4, Recipe time: 30 min T = 150°C	Improve resist adhesion
2	Spinning resist	SSI spinner	Prebake: 90°C Time = 60 s Resist: AZ5214E Recipe: 1.5 µm	
3	Exposure	KS Aligner	Hard Contact Time: 4 s Intensity: 9 mW/cm <sup>2</sup>	
4	Inversion bake	Hot plate	REV120 Temp: 120 °C Time: 2 min	
5	Flood Exposure	KS Aligner	Time: 30 s Intensity: 9 mW/cm <sup>2</sup>	
6	Development	Developer 1 or 2	Time: 70 s Wash: 3 min in water	
7	Drying	Air Dryer	Recipe	
8	Electrode Deposition	Wordentec	10 nm Ti 150 nm Au	E-beam evaporation
9	Lift-Off	Lift-Off bench	Acetone + Ultrasound Time: 30-60s	Continue until all metal is fallen off
10	Drying	Spin Dryer	Time: 2 min	

## 5.3 Polymer fabrication protocols

### 5.3.1 Micromilling:

Micromilling relies on the mechanical removal of material from substrates by use of specially designed tools [Fig. 5.1]. These tools are readily available in a variety of sizes [25 µm to 6 mm] and shapes based on the application [end mills, ball end mills, drills, *etc.*]. Milling machines consist of stationary tool holders where tools can be controlled in the Z axis and a moving X-Y stage to move the substrate with respect to the tool leading to patterning of the substrate. The tools are rotated during operation leading to either cutting or drilling in the substrate

based on the tool selected i.e. either end mills for cutting channels and drill for drilling holes for interconnections.

Structures of feature sizes down to tens of micrometers can be milled dependent on the overall accuracy of the machine and the flatness of the substrate. The desktop Mini-Mill machines used for the experimental work contain stepper motors controlling the XYZ stage micro-positioning down to a resolution of 1  $\mu\text{m}$ . The repeatability of the system with inclusion of the spindle-runout is typically found to be less than 5  $\mu\text{m}$ . As Nordplast, our substrate supplier specifies a variation of 20  $\mu\text{m}$  in a 10 x 10 cm PMMA sheet, we expect on average to have a 2  $\mu\text{m}$  difference in our channel dimensions for the typical 2 x 2 cm devices. Another source of error is the quality of the tool, and also with wear the tool dimensions change and the flute loses its features. Yet, the difficulty associated with detecting dimensional changes of tools remains a limitation.



*Figure 5.1: (Left) Micromilling process (Right) Tools used for micro milling (Courtesy: Janpo)*

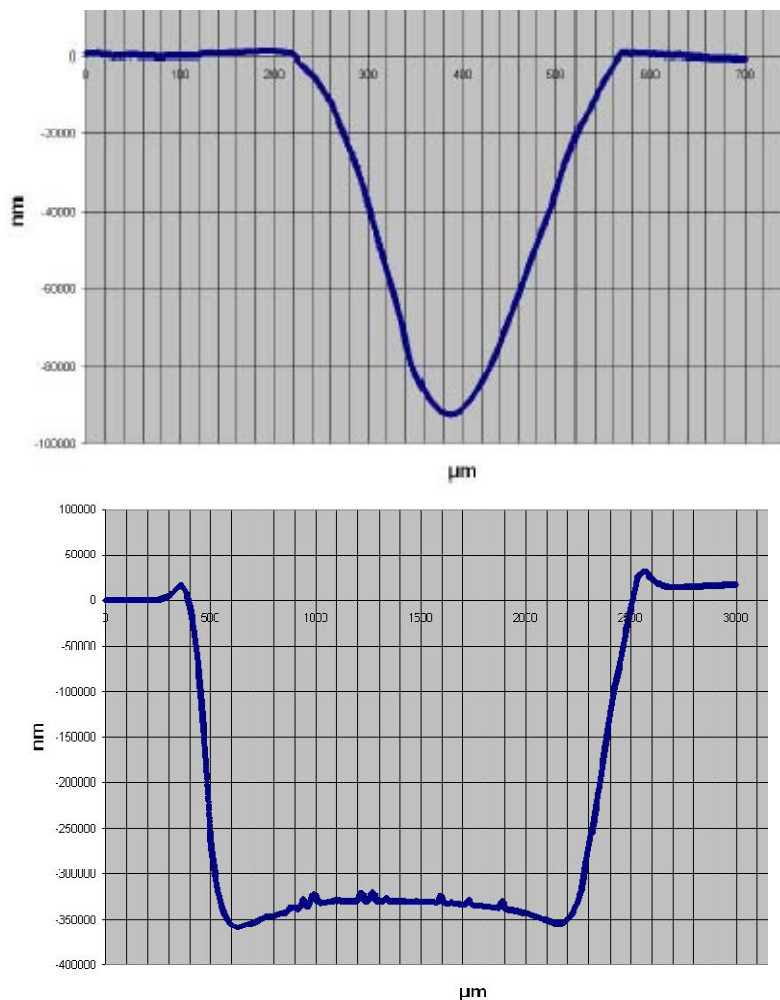
The parameters used for the milling are dependent on the tool and substrate to be milled. Typically, you vary the feed rate, Z step size and the tool rotation speed depending on the features of the device. Commercial CAD software's AutoCAD and Solidworks were used to draw the 2D and 3D versions of the devices respectively and finally converted to the machine readable G-code using Lazycam and EZcam softwares. The milling machines were controlled using Mach3 software. Due to the relatively high reproducibility (with precision of 5  $\mu\text{m}$ ) of devices fabricated with micromilling technique, this project made use of micromilling extensively for fabrication of the motherboard, microfluidic devices and moulds for PDMS lids [271]. In order to account for the melting of the polymers at high rotational speeds,



generally low rotational speeds (2000 – 14000 rpm) and cooling with Milli-Q water was preferred. All devices were cleaned using Isopropanol and later sonicated in an ultrasonic bath to remove any burrs remaining on the milled features.

### 5.3.2 Laser ablation

Laser ablation is another technique used as part of the PhD project to pattern substrates. The laser used for ablation of the polymers and adhesive tapes is a CO<sub>2</sub> laser from Synrad Inc., USA, with an output power of 50 W and a wavelength of 10.6  $\mu\text{m}$ .



**Figure 5.2:** (Top) Typical Gaussian profile of structures (under 400  $\mu\text{m}$ ) ablated in PMMA with fewer than 60% laser power (Bottom) Typical profile of a large channel structure (wider than 1 mm) made in PMMA with 50% laser power. Another typical effect observed in channel structures made with laser ablation is the edges near the channel sides on both sides (marked with dotted circles). This is believed to be mostly the result of re-solidification of ablated polymer or cold fracture at the interface [272].

A controller unit is attached to the laser which allows the user to control the path of the beam through a commercial drawing and control software: WinMarkPro (v 5.1.1.5942). In the setup, the focusing mirrors deflect the beam onto a work area of 110 mm by 110 mm positioned under the lens at a focal length of 189 mm. The parameters used for laser ablation of a substrate depend on the design and required features. The typical parameters controlled to tune the ablation of the devices are laser power (percentage of the total power), velocity (mm/s), resolution (dots per inch) and mark passes (no. of laser passes). Generally, the device designs were drawn in CorelDraw or AutoCAD and later exported to Winmark software to ablate using the laser.

Laser ablation is a relatively rapid technique for creating microfluidic structures and can be recommended for rapid prototyping and quick testing of microfluidic devices. To compare with micromilling, a 200  $\mu\text{m}$  wide and 200  $\mu\text{m}$  deep channel with length of 5 cm will only take few seconds to ablate using this technique, while with micromilling it can easily take over 30 min. Only drawbacks of laser ablation technique are the highest resolution achieved [ $\sim 100\ \mu\text{m}$ ], the Gaussian profile of laser ablated structures [Fig. 5.2] and compatibility to only few materials. For detailed description of the technique refer to Christiansen and Hansen *et al.* [106, 247].

### 5.3.3 Replica Moulding

Replica moulding is a rapid prototyping technique which belongs to the family of polymer fabrication techniques grouped as “Soft Lithography”[14-16]. Replication methods are generally suited for applications where multiple copy of a master or mould needs to be generated rapidly. This technique is often used in multiple forms like injection moulding, hot embossing and casting. These methods depend on solidification or hardening of a liquid polymer or softened polymer by means of a thermal, optical or chemical treatment, when in contact with a rigid or elastomeric master with a particular pattern which needs to be replicated. During, this PhD project, we used the PDMS casting technique to generate multiple copies of devices from Si, SU-8 or PMMA masters. The PDMS Kit (Sylgard 184) was ordered from Dow Corning. The typical ratios of PDMS and curing agent used were as per the manufacturer specifications i.e. 10:1. Only in case of the Pluggy, we used 10:2 ratio for PDMS and the curing agent to gain more mechanical strength due to substantive cross-linking leading to the harder and more rigid Pluggy.

## 5.4 Bonding

### 5.4.1 PDMS bonding protocol

Oxygen plasma based bonding of PDMS to various substrates is a well documented procedure [191, 273]. We used this technique for bonding PDMS to Pyrex wafers for sealing the channels and assembling the devices [Chapter-2]. This technique offers numerous advantages being simple, quick and providing a good irreversible bond. The protocol used for bonding PDMS lids (with channels) to Pyrex devices (with electrodes) is listed in Table 5.6.

*Table 5.5: PDMS Replica Moulding*

	Process Step	Equipment	Protocol	Comments
1	Mix Precursors	Plastic container	Mix 10:1 (wt/wt) PDMS and curing agent For Pluggy: Use 10:5	Mix thoroughly for 2 mins.
2	Degassing PDMS	Vacuum Chamber	Time: 45 min Pressure: 0.2 mbar	
3	Casting	Oven	Pour PDMS mixture over the master and heat cure.  Temperature: 60 °C (3 hrs) 85 °C (2 hrs) or Overnight at room temperature.	
4	Remove casted PDMS	Tweezers	Gently remove the casted PDMS replica from the master	

**Table 5.6:** Process flow for bonding PDMS to other substrates using Plasma oxidation

	Process Step	Equipment	Protocol
1	Cleaning surfaces	Isopropanol DI water	Clean the surfaces to be bonded thoroughly with IPA followed by DI Water
2	Drying	Compressed Nitrogen	Dry the surfaces thoroughly with N <sub>2</sub>
3	Surface activation	Oxygen Plasma Asher	O <sub>2</sub> gas flow: 100 mL/min Power = 100 W Time = 30 s
4	Bonding	Microscope	Align the devices under the microscope and put the surfaces together as fast as possible. Leave for at least 15 mins before use. Typically overnight for the bonding to settle.
5	PostBake	Oven	80 °C for 15 mins

The oxidation of PDMS changes the surface properties and turns it hydrophilic, due to creation of hydroxyl groups on the surface as part of the dehydration process. As the hydrophilic surface forms chemical bonds rapidly with other surfaces, it helps in bonding PDMS lids to Pyrex device. The hydroxyl groups will regroup and the hydrophobic properties of PDMS start to re-emerge in about 10 min. In order to slow down this reversal process, it is suggested to put the exposed PDMS in DI water until used[103, 104, 136, 274]. The post bake leads to rapid and stronger bonding of devices.

### 5.4.2 Thermal bonding

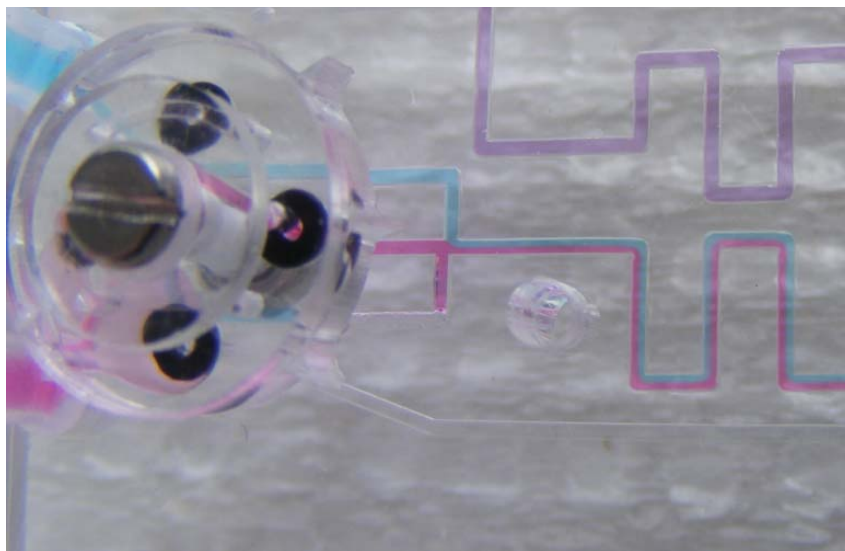
For bonding devices made in PMMA and PC, we preferred thermal bonding protocol over adhesive bonding for biocompatibility and reproducibility issues. Two different bonding techniques were used for bonding micromilled substrates: UV activated bonding[275, 276] for

PMMA, PC and solvent activated bonding for PC[266]. In order to bond the devices, they were first rigorously cleaned with detergent to remove any burrs in the channels or milled structures. This was followed by a 3 s dip in 70% ethanol which was immediately followed by a Milli-Q water washing step for 1 min. After drying the devices with compressed air, they were ready to be activated with UV exposure. Exposing PMMA and PC to UV light source (DYMAX EC5000) results in a thin layer of activated surface on the substrates, which has reduced glass transition temperature compared to the bulk substrate. This allows for rapid thermal bonding of the substrates at lower temperatures than the bulk glass transition temperature. In case of solvent bonding, the solvent was freshly prepared by mixing isopropanol: acetylacetone (1:1). In order to have a uniform exposure of the solvent to the substrates, the solvent is applied to a tissue and the two parts are lightly rubbed on to the wet tissue for 5 s. The two parts are allowed to rest for 15 s to allow for evaporation of the solvent. The substrates were always bonded in P/O/Weber bonding press at pressures typically about 0.5 kN/cm<sup>2</sup> of bonding surface area.

## 5.5 Device Recipes

### 5.5.1 Fabrication of modular motherboard

Owing to the design features of the motherboard, especially the depth of the sockets, we had only two choices for fabrication of motherboard i.e. micromilling or laser ablation. But due to the Gaussian profile of the tall features fabricated with laser ablation process, micromilling was chosen for motherboard fabrication. The motherboard sockets were milled in PMMA or PC using a 2 mm end mill while the through holes for the needles were made using a 500  $\mu$ m drill. The plug-in ports for external fluidic connections were milled using 1 mm end mill and 500  $\mu$ m drills. The electrical through holes were milled with a 700  $\mu$ m drill. The fluidic channels on the back of the sockets were milled using 500  $\mu$ m end mills and finally the motherboard channels were sealed by bonding a flat PMMA sheet to conceal the fluidic channels [Section 5.4.2].

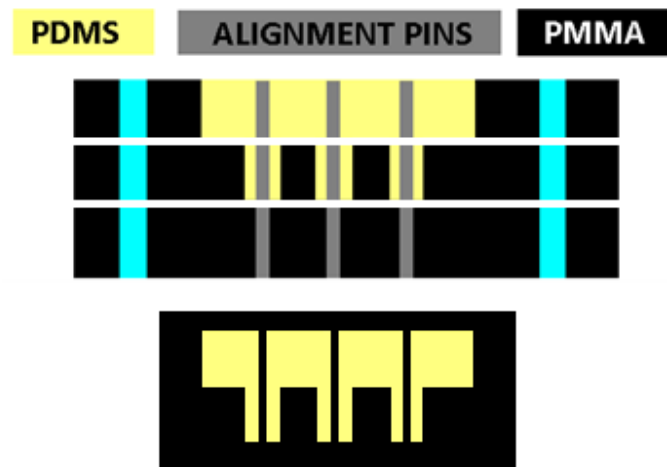


*Figure 5.3: Rotors assembly on motherboard for flow routing*

The rotors were fabricated separately and attached to the motherboard via screws. To assemble the rotors, O-rings were placed in between rotor and motherboard connections to form leak proof interconnections [Fig. 5.3]. The rotors were operated manually.

### 5.5.2 Fabrication of Pluggy mould

The mould for casting Pluggy lids is micromilled in PMMA. It consists of 3 layers as shown in the figure 5.4. From bottom to top: Alignment layer for putting through pins for forming through holes (3 mm PMMA sheet), connector layer for forming connectors which form the tight seal with the motherboard socket (3 mm PMMA sheet) and finally base layer which is a flat layer which bonds to the device and supports it during the plugging in procedure (4mm PMMA sheet). The through hole is formed by passing a 1 mm alignment pin through the alignment hole and leaving it in the mould while moulding of the PDMS lids – Pluggy.



**Figure 5.4:** (Top) Schematic of the PDMS Lid mould layers (put together by screws in the blue slots towards the edges) (Bottom) schematic of moulded Pluggy

### 5.5.3 Fabrication of Microfluidic Cell Culture Device ( $\mu$ BR)

The  $\mu$ BR devices are micromilled in PC material and bonded together using UV activated solvent bonding. The devices are exposed to UV light for 30 s followed by a 5 s exposure to the bonding solvent. Before putting the devices into bonding press, the membrane and silicone tubings are assembled in between the two parts. The irreversible leakproof bonding is achieved at 125 °C with 10 kN pressure for 45 min. Typically, the recommended bonding time for PC is 30 min but we use the extra time to ensure evaporation of the solvent from the PC. It is important that no solvent is left inside the device, which could possibly prove toxic to the cells. The interconnections to the syringe pumps are created by press fitting Teflon tubing's through the silicone interconnection tubings.

### 5.5.4 Fabrication of FISH prep device

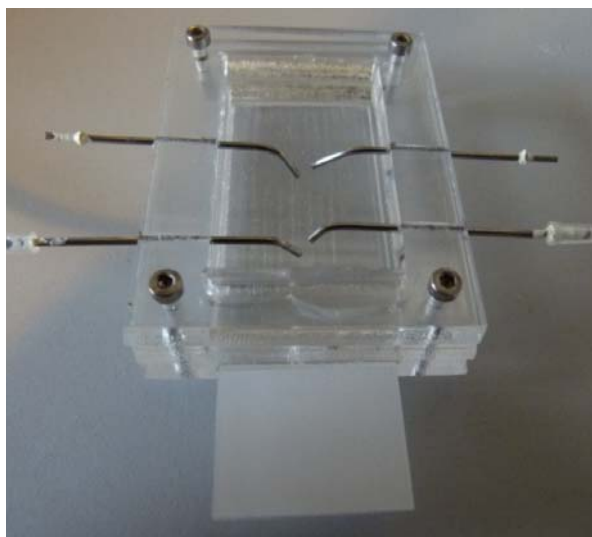
The FISHprep devices are micromilled in PC material and bonded together using UV activated thermal bonding. The devices are exposed to UV light for 30 s and bonded in the bonding press at 130 °C with 10 kN pressure for 30 min. Before the two parts are put in the bonding press, the membrane and silicone tubings for interconnections and the U-plug are assembled in between the two parts. The solvent bonding was not used for FISHprep devices because leak proof bonding was achieved by increasing the temperature to 130 °C instead of



125 °C. In this way, we could reduce the bonding time as well as minimize any chances of solvent related toxicity to the cells.

### 5.5.5 Fabrication of splashing device

The splashing device was micromilled in three 5 mm thick PMMA sheets. The top two layers have the splashing window for creating the open splashing chamber to splash the cells suspension onto the slides. The top layer has typically one set (in some cases two sets) of aligned needles (one for water and one for cell suspension) slightly bent towards the end and focused towards the splashing point. The bottom layer has a slot for inserting glass slides. The 3 layers are either screwed together or bonded using thermal bonding.



*Figure 5.5: Splashing device with two sets of inlets (typically splashing device has only one set of needles)*

### 5.5.6 Fabrication of Gravitational Sedimenter

The gravitational sedimentation device was micromilled in a 2 mm thick PMMA sheet. The loading channel was milled with a 500  $\mu\text{m}$  end mill and the concentration channel was milled using a 200  $\mu\text{m}$  end mill. The lid for sealing the channels was also made in PMMA by micromilling and contained slots for assembling silicone tubing interconnections. The devices were sealed using UV activated thermal bonding as described earlier.

### 5.5.7 Fabrication of FACSlyser

The FACSlyser was fabricated by laser ablation process in 2 mm thick PMMA sheets. Firstly, the channels with interconnections were ablated followed by the ablation of the herringbone structures in the channels. The parameters used for ablation are depicted in the table 5.7. The lids were formed by ablating through holes in the position of inlets and outlets with radius of 2.7 mm. The devices were bonded using UV activated thermal bonding described earlier. The interconnections were formed by press fitting 3 mm outer diameter silicone tubing in the 2.7 mm holes in the lid [Fig. 5.6]. A leak proof seal was obtained by pressing through a 1.2 mm outer diameter needle in the silicone tubing with inner diameter of 1 mm.

**Table 5.7:** Laser ablation parameters of FACSlyser in PMMA. Passes means number of runs per design feature. Power means % power from the total power, Resolution means dots per inch of the marking.

	Structures	Parameters
1	Channels [~400 um deep]	Passes: 2 Power: 35% Resolution: 600 Velocity: 400 mm/s
2	Herringbones [~200 um]	Passes: 2 Power: 20% Resolution: 800 Velocity: 600 mm/s
3	Lid – Interconnects	Passes: 2 Power: 80% Resolution: 400 Velocity: 300 mm/s
4	Cut-Out	Passes: 10 Power: 80% Resolution: 200 Velocity: 200 mm/s



*Figure 5.6: Interconnections of FACSlyser with press fitted silicone tubing inserts and needles*

### 5.5.8 Fabrication of adhesive tape stencil and assembly of devices

The laser ablation process was used to pattern the stencils used in the splashing device for localizing chromosome spreads on glass slides. The AR100 double-sided tape used was procured from Adhesives Research, Ireland. The tape consists of silicone glue supported by an acrylic support layer [25  $\mu\text{m}$ ]. The tape was ablated using 2 passes of 35% power at resolution of 800. The cover from one side of the tape is peeled and applied on to corona treated glass slides. This tape acts as a stencil to localize the chromosome spreads, when a drop of cold water is splashed on to the glass slide followed by a suspension of fixed cells. Finally, the cover from the second side of the tape is removed and the FISH devices are bonded onto the glass slide to create the microfluidic FISH chamber.

### 5.5.9 Fabrication of adhesive tape for Pluggy

The laser ablation process was used to pattern the adhesive tapes for bonding Pluggy with any modules. The AR100 double-sided tape used was procured from Adhesives Research, Ireland. The tape contains 12 x 2 mm holes placed in the positions of the interconnections as per the design specifications. The tape was ablated using 2 passes of 35% power at resolution of 800. The tape is cut out into squares of 2 x 2 cm<sup>2</sup> to match the dimensions of the modules.

### 5.5.10 Fabrication of the impedance cytometer chip

The impedance Cytometer chip is formed by bonding a PDMS lid with channels onto a pyrex wafer with electrodes. The master is created in Si wafer and replica molded in PDMS as described earlier. The electrodes are fabricated on Pyrex wafer and finally, the impedance

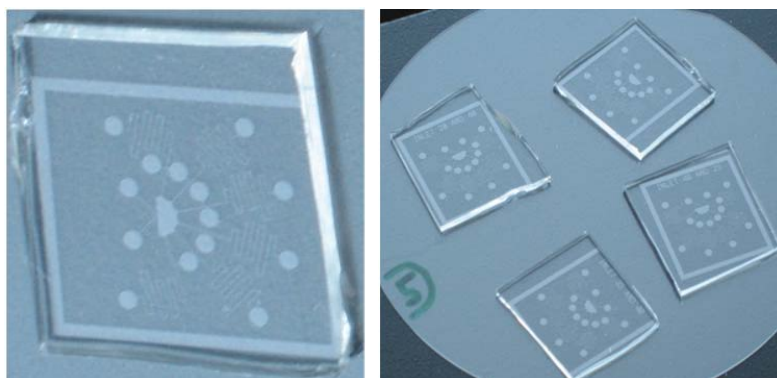
chip is put together by oxygen plasma bonding. Before bonding the PDMS lid onto the Pyrex chip, through holes are made in PDMS for fluidic connections. Finally, the impedance chip is bonded onto a Pluggy by double-sided tape and plugged onto the motherboard for forming electrical and fluidic connections.

#### 5.5.11 Fabrication of microFISH device:

The microFISH device was moulded from a SU-8 master mould fabricated on a Si wafer. The channel height was around  $100 \pm 4 \mu\text{m}$ . The parameters used for spin coating were acceleration of 200 rpm/s, Speed of 1,000 rpm and Time 40 seconds. The PDMS microFISH lid was casted by curing PDMS at  $60^\circ\text{C}$  for 4 hrs. The microFISH devices were bonded onto glass slides with chromosome spreads by means of adhesive tape based bonding. The holes for interconnections were formed by a 0.9 mm blunt needle and the fluidic connections were created by press fitting a 1.2 mm needle in the 0.9 mm hole forming a leak proof sealing.

#### 5.5.12 Fabrication of PFF & DPFF devices:

The PFF devices were molded from a SU-8 master mould fabricated on a Si wafer. The height of the channels was around  $40 \pm 2 \mu\text{m}$ . The parameters used for spin coating were acceleration of 100 rpm/s, Speed of 5,000 rpm and Time 60 seconds. The PDMS PFF devices were casted by curing PDMS at  $60^\circ\text{C}$  for 4 hrs. The devices were bonded onto Pyrex or Silicon wafers by oxygen plasma bonding to form irreversible bonding of the PFF devices. The holes for interconnections were formed by a 0.9 mm blunt needle and the fluidic connections were created by press fitting a 1.2 mm needle in the 0.9 mm hole forming a leak proof sealing. The same protocol was followed for DPFF devices for testing of sorting with peptide nanospheres.



*Figure 5.7: PFF devices bonded onto Si wafer.*

## 5.6 Biological Protocols

### 5.6.1 Conventional Jurkat culture

Jurkat cells were used to test all culture devices primarily after which the devices were tested with healthy donor samples. As a result, all through the project, Jurkat cells were maintained at 37 °C in 5% CO<sub>2</sub> with approximately  $0.5 \times 10^6$  cells/ml confluence in RPMI-1640 media containing 10% FBS, 100 units/ml penicillin and streptomycin and 2 mM Glutamax. Jurkat cells were also used for the gravitational sedimentation and concentration experiments.

### 5.6.2 Processing of the buffy coat

All blood samples used as part of the PhD project were acquired from the Blood bank of Rigshospitalet. These buffy coat samples were stored at room temperature until used (maximum of 24 hours). For longer storage, the leukocytes were purified using Ficoll-Paque medium by centrifugation at 1000 rpm for 15 min. Later, they were diluted in media and stored at 5 °C until further use. Stored leukocytes were used only for testing of flow through, counting cells and also for sedimentation of cells in microfluidic devices presented earlier.

### 5.6.3 Conventional expansion

For control experiments, in order to compare the results obtained from the microfluidic devices, conventional expansion of buffy coat was performed simultaneous to the tests on the devices. The protocol included culture of 5 µl/ml of buffy coat in RPMI 1640 media containing 10% FBS, 100 units/ml penicillin and streptomycin, 2 mM Glutamax and 10 µl/ml of phytohemagglutinin (PHA) stock solution as suggested by supplier. The cells were incubated at 37 °C in 5% CO<sub>2</sub>. For purpose of FISH sample pretreatment these cultures lasted 72 hours before the expanded cells were collected.

### 5.6.4 Priming and cleaning of the device

Before the bonding of the devices, the parts were dipped in 70% ethanol to remove any dust or other toxic particles from the surface. Immediately after bonding the device, they were stored in Ziploc bags to avoid contamination. Before seeding the cells, in order to clean and prime the culture devices, 10% ethanol solution was flushed through the system for 5 min

and later the systems were washed with PBS for 10 min. Between changing reagents, bubbles were removed using the stopcocks to ensure proper priming of the devices before seeding the cells.

#### **5.6.5 $\mu$ BR and FISHprep culture protocol**

Before seeding of cells, the device was perfused with RPMI 1640 + 10% FBS for 1 hr at 37.5  $\mu$ l/hr (equivalent to 0.1 chamber volume/min). A 500  $\mu$ L buffy coat containing  $2 \times 10^6$  cells/mL was seeded into the culture chamber through the cell inlet by opening only the perfusion outlet connected to the waste collector. This ensured that all the cells were trapped on the membrane while the media solution containing the cells was filtered through the membrane to the perfusion outlet. The cells inlet was then closed and followed by perfusion of media through the perfusion inlet at 75  $\mu$ l/hr (0.2 chamber volumes/min) with RPMI 1640 + 10% FBS containing 10  $\mu$ l/ml PHA. After 72 hours of mitogenic stimulation, we stopped the perfusion and collected the cells through the cell outlet by flushing media from the cell inlet.

#### **5.6.7 FISH sample pre-treatment tests:**

For FISH sample pretreatment experiments in  $\mu$ BR and FISHprep devices, we followed the culture protocol (5.6.6) for 72 hrs and then replaced the media with 75mM KCL solution at 0.4 chamber volume/min (150  $\mu$ l/hr) for 25 minutes. This hypotonic treatment induced swelling of the cells. The cell culture chamber is then perfused with freshly prepared cold fixative (acetic acid:methanol-3:1) at 0.4 chamber volume/min (150  $\mu$ l/hr) for 30 min. Later, the cells were arrested in their metaphase by perfusion of media containing 6  $\mu$ g/mL colcemid for 25 mins. Between each change of perfusion, we removed the bubbles in the syringes using a 3 way stopcock. In order to perform the conventional spreading protocol, the fixed cells were extracted from the cell outlet. In case of FISHprep device, slide fixation protocol, the FISHprep splashing protocol was used to prepare metaphase chromosome spreads on the glass slides.

#### **5.6.8 Conventional chromosome spread preparation**

For the spreading of chromosomes to prepare metaphase spreads, standard microscope glass slides were treated with a corona for one minute to clean the slides and improve their wetting behavior. The slides were stored in a coplin jar immersed in water at 4 °C until used. At the time of use, these slides are gently removed from the coplin jar, leaving a thin film of water

on the glass surface. The majority of the water was removed by tapping the slide into the bench a few times, leaving only a very thin film of water on the surface. Two drops of fixed cells were applied to the surface straightaway approximately 20 mm apart from each other. The preferred dropping height was roughly 10-11 mm. The slides were left aside for 15 min to dry completely and in order to observe the spreads a phase contrast microscope was used. Often to quicken the spread formation process on humid days, the slides were put on a hot plate at 40 °C.

### **5.6.9 Splashing protocol**

In order to form the spreads using the splashing device, a drop of cold water is splashed on to the glass slides pre-cleaned with corona. After the water drop is splashed on the glass side, the fixed cells are flushed through the second outlet on to the splashing chamber. In case of the FISHprep device, this includes opening the paper clip valve. Finally, a drop of fixed cells suspension is dropped on the water droplet on the glass slide. The glass slide is left in the splashing chamber until the slide is dry and then observed under the microscope for evaluating the spreads. In case of the microFISH splashing protocol, the slide is removed and following the bonding of the microFISH PDMS lid, the FISH protocol is performed on the splashing chamber. The FISHprep splashing protocol was optimized (from microFISH protocol) by studying the effect of temperature of slide storage (at 4°C in coplin jar filled with DI water), temperature of water for wetting the slides (preferably glacial water), age of fixative solution (now preferred with freshly prepared fixative) and the drying time (10 min). As a result of these optimizations, the spreads achieved with FISHprep protocol are better than earlier published microFISH splashing protocol and comparable to spreads achieved using manual splashing technique. In 85% of cases, we achieve over 50 spreads with the new protocol which is comparable to the traditional protocol and sufficient for the FISH analysis.

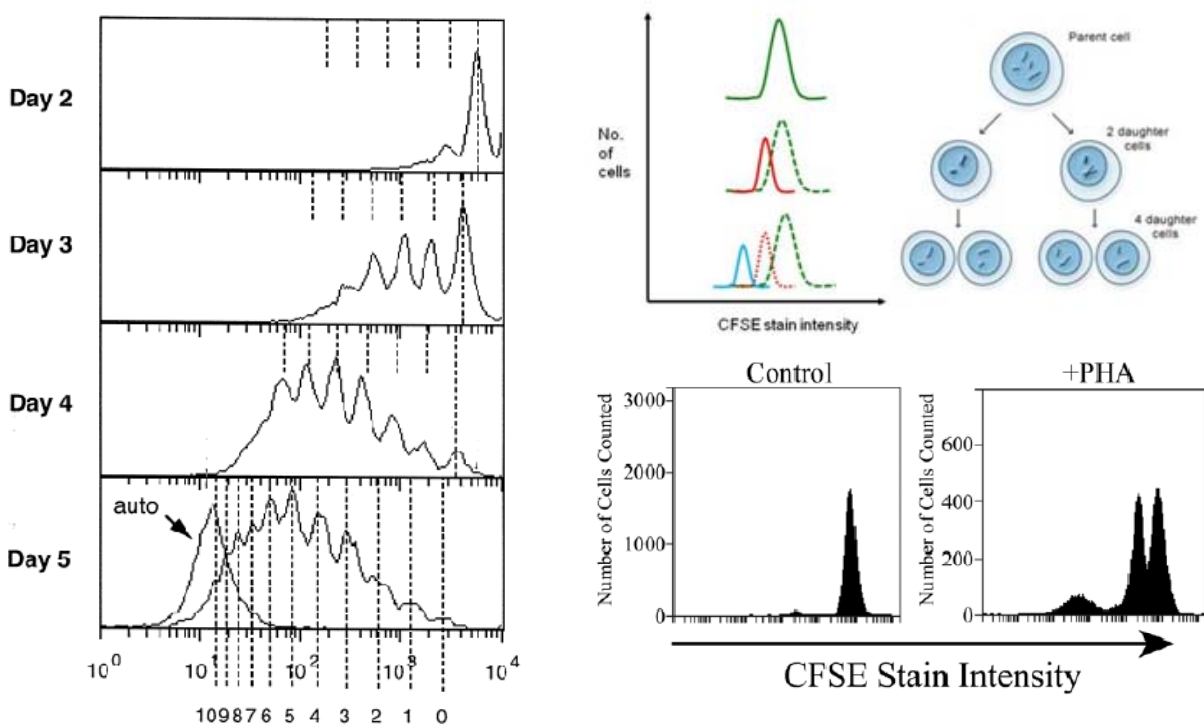
### **5.6.10 CFSE viability assay**

The size of lymphocytes varies from person to person and can range from 9-14 µm in the same sample. As a result in lymphocyte cultures, unless you track the same cell for 3 days measuring cell sizes to ascertain growth doesn't provide any reliable data. As a result, dyeing based techniques are used frequently to analyze cell proliferation and growth qualitatively as well as quantitatively. These dyes typically target cellular components which can be quantified using different analytical techniques. The CFSE fluorescence stain (Invitrogen, Germany) provides a much homogenous cellular labeling and as a result is widely used for inter-generational tracking



of cell growth and proliferation. Using this cytoplasmic dye, researchers can successively track upto 10 generations of lymphocytes [277-279] [Fig. 5.8 (Left)].

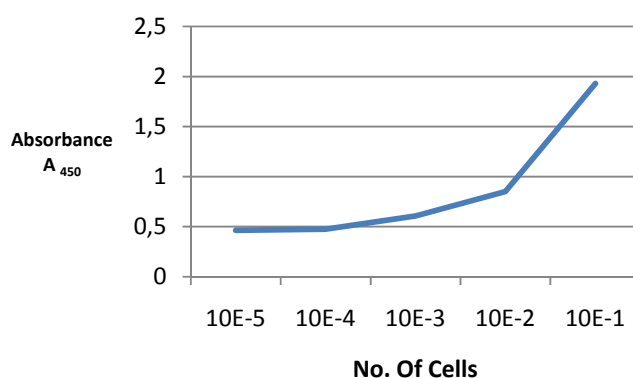
CFSE is a fluorescent stain that is retained within the cells throughout the cell division cycle i.e. development and mitosis. The label is inherited by daughter cells after cell division but due to the division in a lower fluorescence intensity which can be monitored on a flow cytometer [Fig. 5.8 (Right & Top)]. For our experiments the cells were stained with CellTrace™ CFSE fluorescence stain (Invitrogen, Germany) at a concentration of 0.7  $\mu\text{M}$  in phosphate buffer saline (PBS) and incubated at 37°C for 15 min. The cells were re-pelleted and resuspended in pre-warmed cell culture medium and incubated for 30 min. The cells were then centrifuged and resuspended in pre-warmed fresh medium and subjected to culturing. The collected cells were tested for proliferation in a flow cytometer by using CFSE staining of the cells. The CFSE stained cells were either left untreated (for control) or stimulated with PHA and cultured in the culture devices for 72 hrs. After this, they were analyzed for fluorescence intensity on a flow cytometer. In parallel, as a control, we also cultured cells with or without PHA stimulation in a normal plastic culture dish [Fig. 5.8 (Right & Bottom)].



**Figure 5.8:** (Left) Tracking 10 generations of cells using CFSE stain [279] (Right & Top) Schematic of the CFSE staining and related signals for 3 generations of a cell (Right & Bottom)  $\mu\text{BR}$  testing via CFSE staining [Paper-2].

### 5.6.11 WST-1 assay

WST-1 is a cell proliferation assay (Roche Applied Science) used extensively for its capability to perform the entire assay from culture to analysis in the same microtitre plate. The underlying principle of this assay is the cleaving of the stable tetrazolium salt WST-1 to a soluble formazan by a complex cellular mechanism that occurs primarily at the cell surface. This bioreduction depends on the glycolytic production of NAD(P)H in viable cells. Therefore, the amount of formazan dye generated in the well directly correlates to the number of metabolically active cells in the culture. Typically in our experiments, we used this assay for measuring viability of the cells extracted from the FACSlyser. As a result, we would take a 90  $\mu$ l of the cells suspension from the test cultures and add 10  $\mu$ l of the cell proliferation reagent WST-1 to the well. Typically, the measurements of the formazan production are taken using a ELISA plate reader at intervals of 0.5, 1, 2 and 4 hrs. After optimization of the assay and incubation periods, we only took measurements of future test assays at 40 min and 3 hr intervals. Before the assay was applied to the test cultures, a control assay was run with Jurkat cells to confirm the functionality of the assay. Figure 5.9 shows the proliferation curve of Jurkat cells and the measured absorbance with respect to the growth of Jurkat cells which depicts the characteristic growth curve of proliferation as expected.



*Figure 5.9: Validation of WST-1 assay with Jurkat cells test assay*





# CHAPTER 6

## PATENTS

This chapter serves as a compendium of the methods used as part of the experimental work described earlier in this thesis. All the methodologies related to the design, simulations, fabrication and further, the biological analysis protocols are explained in detail.

## 6.1 Multiplexed Analyte Concentration Measurement

[ PCT Phase, 2009, Patent Application # 09169729.2-2404]

This patent describes a technique for multiplexed protein concentrations from a patient sample. Proteins are used as indicators of different diseases. Therefore, accurate measurement of the concentration of specific proteins is a valuable tool to diagnose a wide range of potential diseases, e.g. viral-, bacterial-, parasite infections and autoimmune diseases and to determine whether the disease is in an active state. The critical point is to be able to measure the protein concentration for specific proteins (antibodies and hormones) in the bloodstream.

Currently, these tests are conducted either manually using Enzyme-Linked Immunosorbent Assays (ELISA) or high throughput automated versions based on chemiluminescence techniques. While ELISA continues to be a labor-intensive, costly and time consuming process, chemiluminescence techniques have been associated with high upfront costs (above \$200000) and false positive reports. Today's dominating technologies can only measure a single concentration at a time, taking between 4 – 6 hours before the result is available and requiring considerable manual labor and extensive use of expensive equipment. Fast and multiple protein concentration measurements is a serious issue for hospitals and laboratories which conduct thousands of these measurements on a yearly basis and they often need to measure several different protein concentrations just in order to diagnose a single disease.

Our diagnostic technology fills this gap, with a microfluidic bead-based immunoassay technique which provides cheaper, faster, automated, point-of-care, multiplexed protein concentration measurements. Removing the need for a spectral signal acquisition as in the case of ELISA and chemiluminescence techniques, this technique reduces the cost related to the initial setup as well as opens up possibilities of extending the applications to point-of-care settings.

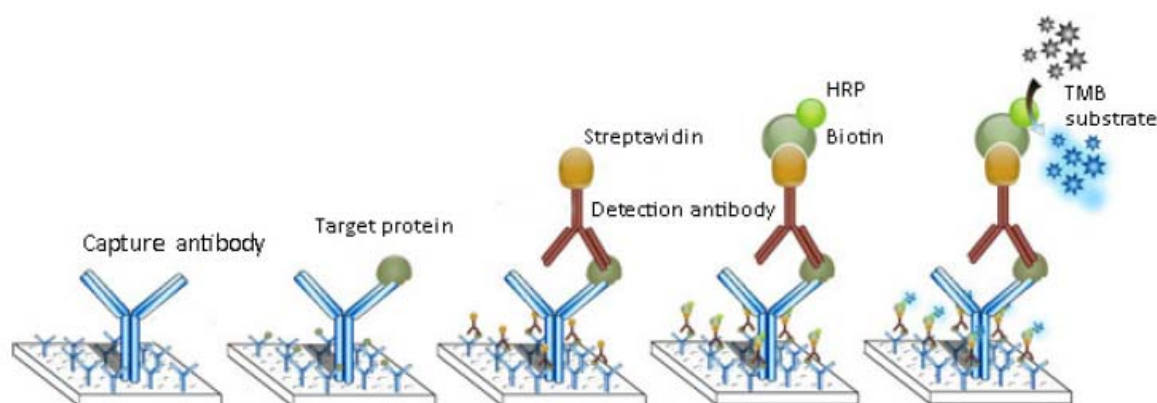
### The technology

Immunoassays represent a predominant form of analysis in the modern-day clinical analysis repertoire. Immunoassays are quantitative analyses based on utilizing the binding properties of an antibody to a specific antigen in a sample. This interaction between antibody and antigen is converted into a measureable signal that can be related to the concentration of a specific protein.

Current State of the art within Immunoassays is Enzyme Linked Immuno Sorbent Assay (ELISA). ELISA converts the concentration of a specific protein into a measurable signal by an

antibody-bound enzyme converting a non-colored substance into a colored substance. The color intensity of this substance is measured with a spectrometer and corresponds to a certain concentration of a specific protein. As shown in figure 6.1, the traditional ELISA method involves multiple reaction steps and equal number of washing steps with different reagents resulting in an overall measurement time between 4 - 6 hours. In case of ELISA, antibodies of interest are bound to the surface of a multiwell plate and target protein in the form of a patient sample is applied to this plate. This results in the antibody-antigen coupling which is of interest to detect. In order to detect, this binding in the subsequent 3 steps another antibody is bound to this protein, which is in turn bound to a fluorophore, which fluoresces when illuminated in an ELISA plate reader [Fig 6.1]. This fluorescent signal is hence directly related to the amount of protein bound to the antibodies on the surface. Unspecific binding signals are removed by multiple washing steps in between each of the steps.

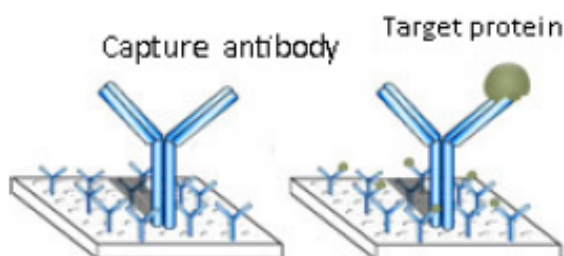
As a result of such a lengthy protocol, ELISA is considered to be both a slow and labor intensive method needing multiple reagents and a bulky spectrometer. Often ELISA testing is highly automated using expensive automated equipments which can offer possibility of lowering operational costs at the expense of huge investment costs. However the measurement time cannot be reduced because of the binding events required between each step in the process, and even though it is highly automated, it still requires a significant amount of manual work from the lab-technician both in post and pre-analysis.



*Figure 6.1: Steps of ELISA based techniques*

In contrast, while our technology is also based on detecting the antibody-antigen interaction like ELISA, we do not need multiple reactions steps to convert this binding into a measurable signal. Our technology exploits the fact that the antibody-antigen interaction can be converted into a detectable electrical signal, revealing the concentration of a specific protein in a sample [Fig. 6.2]. Furthermore, with our unique multiplexing feature, this technology makes it

possible to simultaneously measure the concentration of multiple proteins in a sample, which is not possible with ELISA. We anticipate that we will be capable of measuring 10 different protein concentrations simultaneously and deliver the result within minutes.



*Figure 6.2: Steps of our technology*

Going into the specifics, our technology depends on impedance based electrical detection of antigen-antibody binding on the surface of a bead. Using antibody bound beads instead of surface bound beads, we open up the possibility of multiplexing this assay by means of microfluidic manipulation of beads across a detection zone. We foresee numerous advantages of our technology compared to the industry standard ELISA, in terms of cost, time, sensitivity and the biggest of all the ability to multiplex the assay [Fig. 6.3].

	Our technology	ELISA
Time per measurement	5 - 10 min	4 – 6 hours
Sample size	microliter	milliliters
Able to measure protein concentrations	Yes	Yes
Able to measure Yes/No test	Yes	Yes
Able to measure multiple protein concentrations	Yes	No
Sensitivity	<20 ng/ml	20 ng/ml
Skill level required by technicians	Low	High

*Figure 6.3: Comparison of our technology with ELISA.*

In order to be able to multiplex this technology, we have moved away from binding the antibodies on to the electrode or device surface. Currently, we are working on two strategies for multiplexed protein concentration measurement.



## Strategy 1: Direct Detection

In this strategy, we are interested in directly detecting the change in the impedance of beads by addition or binding of proteins to its surface. Hence, we start by coating beads with antibodies and calibrate their impedance before applying the protein sample to the beads. Once calibrated, these beads are exposed to the sample which leads to binding of the proteins on to the beads. After exposure to the sample, these beads are rescanned for impedance change and the number of beads which show increase in impedance are counted, which relates to the concentration of the particular protein in the patient sample [Fig. 6.4].

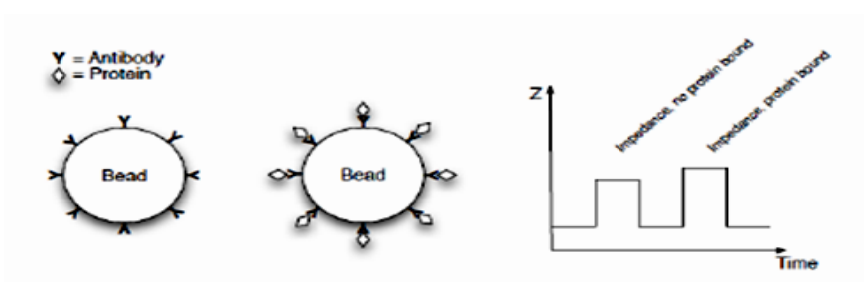


Figure 6.4: Principle of Impedance based protein concentration measurement

By means of binding several antibodies specific to different target proteins on beads of different sizes respectively, we can effectively multiplex the signals received from different beads and correlate the signals with concentrations of related proteins [Fig. 6.5].

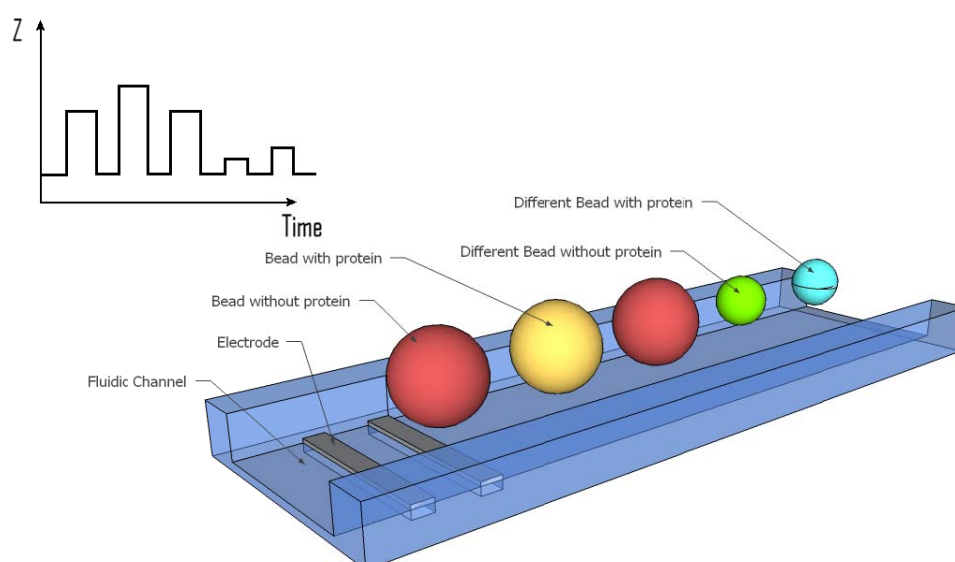


Figure 6.5: Principle of multiplexed protein concentration measurement

This multiplexed technique is based on simultaneous impedance detection of beads at low and high frequencies. At lower frequencies, the impedance signal received corresponds to the size of the beads which helps us differentiate between the beads i.e. multiplex the signals, but at higher frequencies, we scan the change in the membrane properties of the beads i.e. the amount of proteins bound on the membrane [Fig. 6.6].

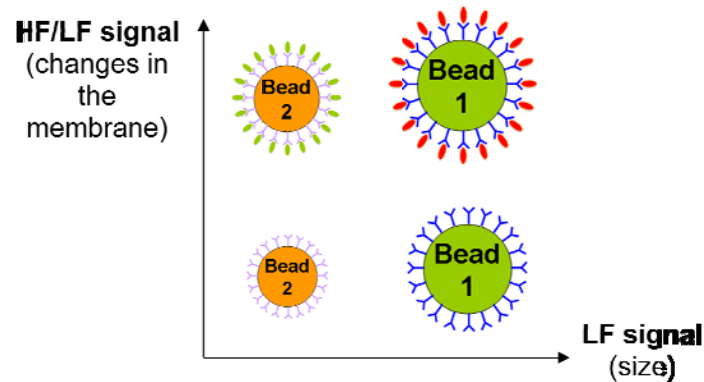


Figure 6.6: Multiplexed Impedance based simultaneous sizing and protein concentration measurement.

## Strategy 2: Indirect detection

In the indirect strategy, we are detecting the target protein by binding two beads coated with antibody to the proteins in the patient sample i.e. by detection of this dimer instead of the protein itself [Fig. 6.7].

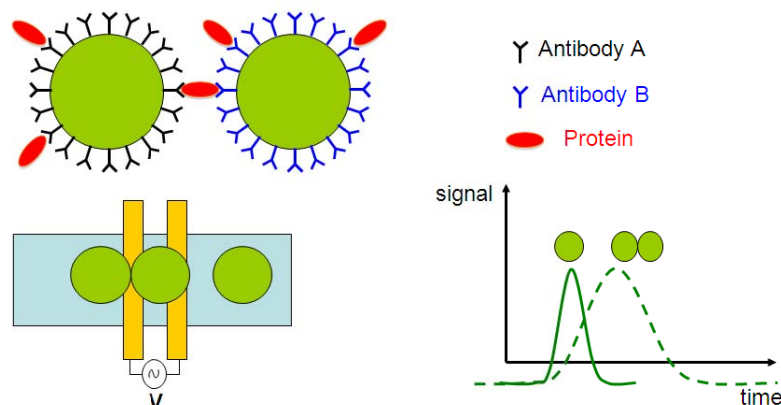
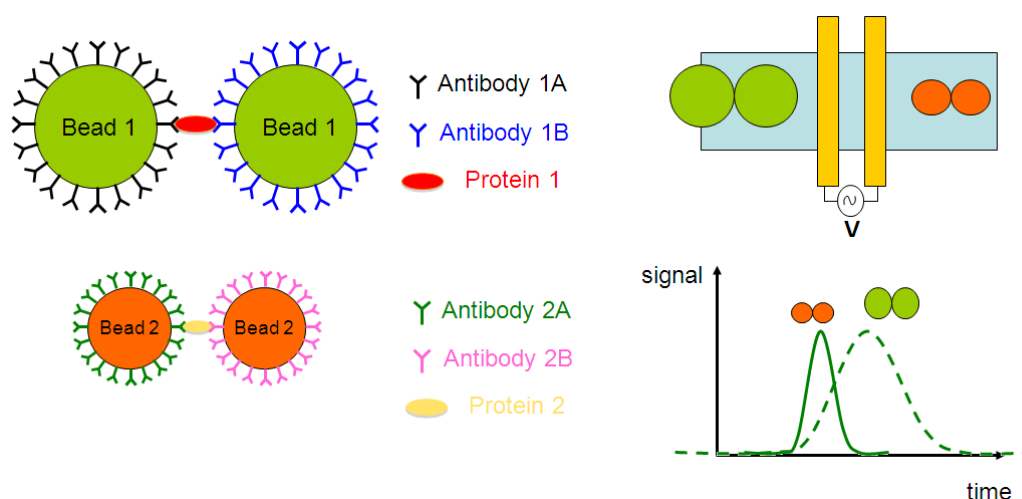


Figure 6.7 Principle of differentiation of dimers (bead-bead conjugates) from monomers (unbound beads).

As shown in the figure 6.7, two beads with different antibodies each targeting a different region on the target protein are shown. Once two these beads and the protein conjugate, it results in the creation of a dimer. In this detection technique, we rely on the time difference in the transition of dimers (bead-bead complex) and monomers (unbound beads) in the detection region to calculate the amount of protein in the sample.

In order to multiplex this technique, we rely on the time difference of transition of dimers of different sized beads and unbound beads [Fig. 6.8]. To ascertain that the transition times vary, we have devised microfluidic flow focusing strategies to align the dimers with the flow, to allow the detection system to differentiate between the dimers and single beads by increasing the transition time difference.



**Figure 6.8:** Multiplexing of bead-bead conjugates by means of differentiating the transition times.

## Project Status:

We have already demonstrated the multiplexing principles of both strategies. Using an impedance cytometer we can successfully distinguish between beads of 3 and 5  $\mu\text{m}$  [Fig. 6.9] and beads of different materials [Fig. 6.10].

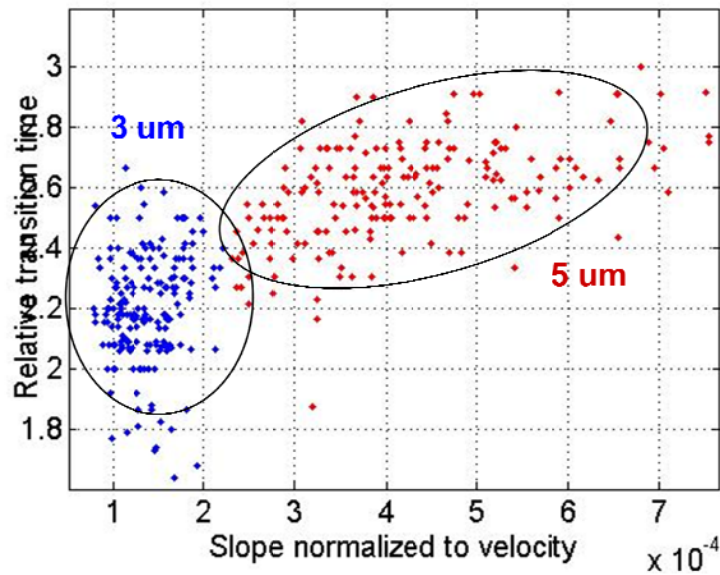


Figure 6.9: Differentiation of beads of 3 and 5  $\mu\text{m}$  sizes using an impedance cytometer.

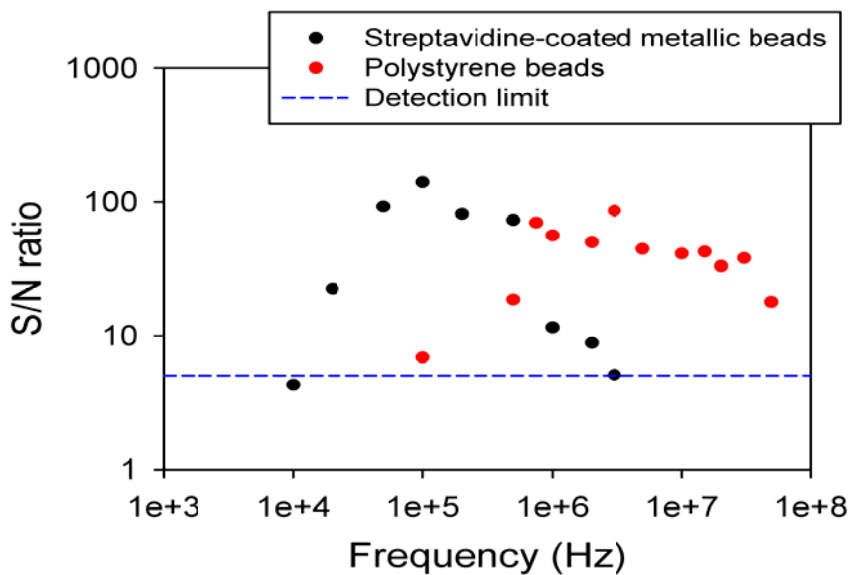
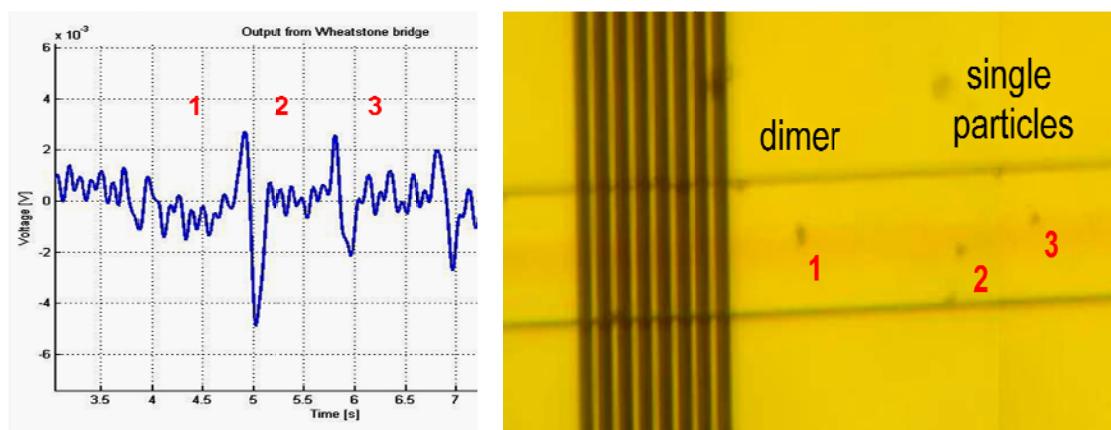


Figure 6.10: The differentiation of metallic beads and polystyrene beads using an impedance cytometer.



**Figure 6.11:** (Left) Transition times of dimer and two unbound single particles (Right) Corresponding image of a dimer and two unbound single particles across detection zone

Similarly, we have also shown that the impedance cytometer can distinguish between single particles and dimers of beads [Fig. 6.11].

The project is currently funded by a Proof of Concept Grant from the Danish Ministry of Science and Technology. The experimental work is currently undertaken by Romen Rodriguez-Trujillo, Simon Levinsen and Mohammad Akram-Ajine. Our current and future efforts are directed towards validation of these techniques with protein samples from collaborating partners. We also foresee applications of this technique in other areas like biomarker detection for cancer, infection screening, and toxicology, among others. On commercialization side, we have had successful initial meetings with Roche who have shown interest in licensing this technology when mature and validated with clinical samples.

## 6.2 Radial peristaltic pump

[2010, Patent Application # 10159495.0-2315]

This patent relates to the invention of a novel radial peristaltic pump enabling simultaneous pumping and addressing of multiple channels. Pumps are useful in a multitude of applications ranging from large-scale industrial process pumps to bed-side infusion pumps in hospitals.

Generally pumps have singular outlet capacity, but peristaltic pumps have shown capability to pump multiple channels simultaneously. This has found many applications in the infusion pumps market and recently in microfluidic high throughput applications. However, existing peristaltic pump systems have limitations in the number of channels they are able to pump simultaneously. The current miniaturized versions only pump about 8-12 channels, due to the assembly being based on rollers.

Developing on this model, a novel radial pump assembly has been designed capable of pumping at least 4 times the number of channels using the traditional single motor. This system operates on the same principle for pumping the fluids but utilizes cd-like radial structures with ridges which compress the elastomeric channels and in process actuates the fluids.

Furthermore, while various pump brands and designs are available on the market, they don't have the capability to address individual channels which is an important application when there is a need for sequential injection of fluids. Our radial peristaltic pump provides the ability to pump multiple channels (20 plus) simultaneously and to control them in multiple combinations to pump multiple fluids precisely and addressably.

### **Applications:**

This technology will reduce costs and prove highly beneficial for applications needing pumping of multiple fluids (eg. high throughput analysis, drug screening applications, infusion pumps for emergency care). The potential market for the technology was just below \$500m in 2007 and is expected to reach more than \$1 billion in 2012.

## 6.3 Multichannel infusion pump

[2010, Patent Application # 10159494.3-2320]

Infusion pumps form a key part of patient care especially in diseases like diabetes, analgesia, chemotherapy and several others. While the market is full of expensive pumps for hospital care (\$1000 plus) and personal care (\$2500-\$5000), the high costs are prohibitive of being widely applied to healthcare globally. Also in many cases, these high end pumps don't have the ability to pump multiple fluids simultaneously (hence the need for multiple pumps), which is often the need for maintaining and providing life support in Intensive Care units. Hence, a solution which is cheap to allow wider access and has ability to pump multiple channels simultaneously can prove to be a benefit for hospitals and patients worldwide.

We are simultaneously targeting two different segments of the market, with the current development focus. Our novel low cost (< \$1000) pump is designed to pump multiple channels simultaneously and can be made in multiple form factors (personal-disc player size to a personal patch pump size) to suit the requirements based on setting either at a hospital bed-side or a personal infusion pump for diabetes management or home-care. The ability to pump multiple fluids simultaneously could simplify the work routine for nurses and reduce accidents which are often caused due to wrong dosages as a consequence of the complex setups in the emergency units. Also, an ultra low power, low cost (< \$100-\$200) and self-actuated version of this pump is currently under development to suit the needs of the patients in remote locations and 3rd world countries.

The market for personal wearable pumps for diabetes management is over \$1 billion and growing. The market for hospital pumps is equally large and expanding. But the biggest opportunity with this technology is to open up new markets in the 3<sup>rd</sup> world countries with the low cost version of this pump, where patients today continue to use needles for diabetes and pain management.

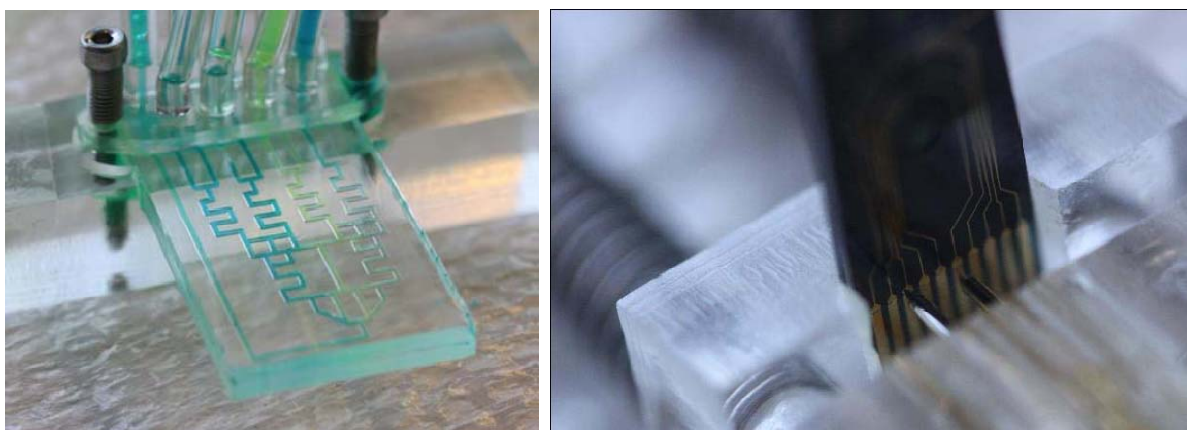


## 6.4 Spring-actuated microfluidic interconnects

[PCT Phase, 2010, Patent Application # 10164907.7-1270]

This patent depicts a novel self-actuating self-sealing interconnection technology based on integrated compression springs used to seal and actuate interconnects. Interconnections are the top practical concern regarding wide scale application of microfluidic technologies. The issues with interfacing microfluidic devices with other existing setups continue to derail the progress made by successful demonstrations of microfluidic applications.

With this technology, we provide a simple method for creating rapid, aligned, multiple, parallel, reusable, self-actuating, self-sealing fluidic and electrical interconnections [Fig. 6.12]. The need of flexible microfluidic platforms is widely recognized and with this technology we are targeting to build a simple microfluidic platform solving practical issues outstanding with microfluidic device interfaces. Taking a step further, this interconnect technology comes with integrated bubble traps minimizing the need for developing bubble trapping strategies on board microfluidic devices.



**Figure 6.12:** (Left) View of fluidic connection holder with a microfluidic chip. (Right) View of the electrical connections on a silicon nanowire chip with alignment accuracy down to 25  $\mu\text{m}$ .

Moving towards standardization of microfluidic device development, these interconnects have been developed in microscope slide sized formats in planar as well as upright settings allowing easy operation with all microscope types. The focus of current development is towards building slide-sized microfluidic devices compatible with this interconnect technology i.e. cell culture devices, high throughput migration analysis devices, mixers, gradient generators, *etc* to widen the applications of this platform.

## 6.5 Sandwiched membranes

[In process]

This technique highlights the development of novel injection molded sandwiched membranes, with integrated features allowing rapid assembly of microfluidic devices with scaffolds for cell and neuronal culture applications.

Membranes are always difficult to integrate in microfluidic devices and especially so, in cases where the devices need to be assembled and sealed after seeding or placement of biological analytes on top of integrated membranes functioning as scaffolds. This process necessitates sealing of microfluidic devices without application of temperature or adhesive based bonding, which makes it imperative to rely on good mechanical sealing for leak-proof operation.

Routinely, this is attempted with O-rings, which has provided partial success at low pressure and flow rates. But this continues to be a difficult solution which doesn't provide good success rate and gets considerably challenging when you put cells or brain slices in the equation. Some of these challenges were faced by other members of the research group, which lead to a need for an easy solution for integrating membranes in microfluidic devices after loading of biological material.

These sandwiches membranes provide the much needed ease of handling, reliable seals, rapid assembly and most importantly, a biocompatible bonding-free solution for neuronal and cell culture applications. In the preliminary tests, the flow rates in our brain slice culture devices could be increased from the routine 0.5  $\mu\text{l}/\text{min}$  up to 50  $\mu\text{l}/\text{min}$  without any leakage (100 fold improvement) which are sufficient for cell culture and neuronal applications.

We aim to further integrate novel functionality via multi-component injection molding for developing biochemical sensors based on this active scaffolds.

[Related publication pending – Novel scaffolds for microfluidic cell and neuronal cultures]

## 6.6 Adhocly attachable microfluidic interconnections

[In review – publication pending]

Microfluidic Interconnections have never been so easy to handle. Offering the simplest of all the interconnection solutions presented in this thesis, QuickFix interconnects allow for rapid one second assembly of microfluidic interconnects based on two interconnection strategies (magnetic and adhesive tape based). This technique offers reliable, reusable, flexible (single or multiple), bonding free, adhocly attachable, ultra low cost interconnection scheme for rapid assembly and testing of microfluidic devices.

The newer version of these interconnects is designed with integrated bubble traps allowing bubble free long term operations for cell culture and other biological applications. With the inclusion of an integrated circular recess for O-rings, this interconnects offer leak-free fluidic operation at relatively high flow rates (tested up to 200  $\mu\text{l}/\text{min}$ ).

Due to the optimized current design, these interconnects can easily be mass produced using injection molding technique. This interconnects have been fabricated and tested in various formats in multiples of 3 and 5 interconnections for testing the possibility to establish multiple fluidic interconnections simultaneously.

With on-going development, we aim to integrate these interconnects with the microfluidic systems presented in the earlier chapters.

[Related publication pending – Plug2Flow: Adhocly attachable microfluidic applications]



# CHAPTER 7

# CONCLUSIONS

In this chapter, we summarize the results described in the previous sections and present our new laws of microfluidic research which have led to numerous exciting discoveries and resulted in the evolution of the microfluidic toolkit available for cytogenetic analysis.

## Conclusion and Outlook

Microfluidics is an ideal tool for tackling problems in biology and medicine. The ability to provide control over the immediate microenvironment of individual cells is a fascinating science in itself. I envision that it is only a matter of time before the large amount of research based demonstrations lead to breakthroughs which pave their way into the clinical labs. While the significant contributions and achievements in the fields of diagnostics, sensors, chemical assays, genetics, *etc.* have been duly noted, there is still a long way ahead before they can address real problems leading to clinical solutions.

This thesis presented such efforts towards bridging streams of microfluidics and clinical cytogenetics. In an effort to tackle the practical concerns inherently rooted in current microfluidic toolkits, this thesis presented novel interconnection techniques to form rapid, reliable, robust, flexible, multiple, aligned, reusable fluidic as well as electrical interconnects.

The overall aim of this PhD. project was to develop a miniaturized microfluidic system for total chromosome translocation analysis on a microfluidic device. The initial goal was to develop a modular system for enabling plug and play functionality, which will effectively function with various modules related to the FISH analysis protocol and be used for analysis of translocations in traditional cytogenetic laboratories. In pursuit of this goal, we developed a novel versatile **microfluidic modular motherboard** providing **substrate independent plug and play functionality**. This motherboard was tested for fluidic and electrical connectivity with various modules and discussed as a possible solution for standardizing microfluidic development efforts.

Based on critical feedback from the end-user and collaborators, the goals for the PhD project were changed to focus more on development of an integrated system, providing ease of handling, minimal complexity, compatibility with existing setups and work routines and most importantly lead towards an automated FISH protocol. This led to a focused user-driven research effort, leading to the development of multiple devices which cumulate to entire Fluorescence *In-Situ* Hybridization protocol currently used for clinical genetic analysis.

A **microfluidic bioreactor (μBR)** which was a more suitable and better solution for culturing non-adherent cells compared to traditional culture flasks was designed and it provided cells with a controlled micro-niche mimicking their *in vivo* extra-curricular matrix.

This μBR device was modified to integrate a chromosome slide preparation protocol, which will lead to the development of a **FISHprep** device providing complete FISH sample

preprocessing to the slide preparation protocol for preparing metaphase FISH chromosome slides.

On completion of the slide preparation device, the focused was aimed towards realizing a miniaturized device for performing low cost and low reagent volume FISH analysis. These efforts lead to **microFISH**, which was the first demonstration of performing metaphase FISH analysis on a microfluidic chip.

In order to realize a minimal handling FISH protocol and provide a possibility to automate FISH analysis, the **AutoFISH** protocol was developed by means of a FISH reagent cartridge. After the positive initial results achieved with interphase FISH using a **FISH reagent cartridge**, the next step is to use FISH cartridge for metaphase FISH analysis and thereby automating the FISH protocol using an automated sequential reagent injection protocol.

Finally, not just adhering to the C-TAS project, this PhD has led to multiple patent pending inventions related to the development of novel micro pumps, interconnects, functional membranes and a new diagnostic technology for multiplexing immunoassays on a chip.

In doing so, three new laws of microfluidic research have evolved which we suggest are used by any future microfluidic researcher attempting to develop clinically relevant medical devices.

**1) Be the lead user**

Before you even start designing a microfluidic device, it's a must that you spent time familiarizing and using the traditional protocol or methods you aim to change. Only by becoming the end-user yourself, you will realize the other complexities and minor details not often listed in the printer versions of the protocols.

**2) Research and don't re-search.**

Microfluidics has a lot more to offer than just miniaturized versions of current devices. Be creative and explore the possibilities.

**3) Usability is in fact user-ability**

The often commonly used word for microfluidic devices 'Usability' fails to recognize and put into equation the end-user's ability. Hence, most common and claimed user-friendly solutions in microfluidic research labs are nightmarish for the end-users.

With the new laws and the evolved microfluidic toolkit, we aim to develop novel clinical devices, catered for the clinical end-users.







# BIBLIOGRAPHY

1. Manz A, Graber N, Widmer HM: **Miniaturized total chemical-analysis systems - A novel concept for chemical sensing.** *Sensors and Actuators B-Chemical* 1990, **1**(1-6):244-248.
2. Blom N, Fetting JC, Koch J, Ludi H, Manz A, Widmer HM: **Implementing chemical sensors in industry - Novel approaches.** *Sensors and Actuators B-Chemical* 1991, **5**(1-4):75-78.
3. Harrison DJ, Manz A, Fan ZH, Ludi H, Widmer HM: **Capillary electrophoresis and sample injection systems integrated on a planar glass chip.** *Analytical Chemistry* 1992, **64**(17):1926-1932.
4. Feynman R: **There's plenty of room at the bottom.** *Engineering and Science* 1960, **23**(5):22-36.
5. Terry SC, Jerman JH, Angell JB: **Gas-Chromatographic air analyzer fabricated on a silicon-wafer.** *IEEE Transactions on Electron Devices* 1979, **26**(12):1880-1886.
6. Bassous E, Baran E: **Fabrication of silicon nozzle arrays for ink jet printing.** *Journal of the Electrochemical Society* 1977, **124**(8):C310-C310.
7. Bassous E, Taub HH, Kuhn L: **Ink jet printing nozzle arrays etched in silicon.** *Applied Physics Letters* 1977, **31**(2):135-137.
8. Petersen KE: **Fabrication of an integrated, planar silicon ink-jet structure** *IEEE Transactions on Electron Devices* 1979, **26**(12):1918-1920.
9. Hansen EH, Ruzicka J, Krug FJ, Zagatto EAG: **Selectivity in Flow-Injection Analysis.** *Analytica Chimica Acta* 1983, **148**(APR):111-125.
10. Ruzicka J: **Flow-Injection analysis - From test tube to integrated microconduits.** *Analytical Chemistry* 1983, **55**(11):1040-&.
11. Thogersen N, Janata J, Ruzicka J: **Flow-Injection Analysis and Cyclic Voltammetry.** *Analytical Chemistry* 1983, **55**(12):1986-1988.
12. Denboef G, Schothorst RC, Appelqvist R, Beecher GR, Bergamin H, Emneus J, Fang Z, Gorton L, Hansen EH, Hare PE *et al*: **Flow-Injection Analysis (FIA) - A personal view.** *Analytica Chimica Acta* 1986, **180**:1-67.
13. Vanderlinden WE: **Flow-Injection analysis in online process-control.** *Analytica Chimica Acta* 1986, **179**:91-101.
14. Xia YN, Whitesides GM: **Soft lithography.** *Annual Review of Materials Science* 1998, **28**:153-184.
15. Xia YN, Whitesides GM: **Soft lithography.** *Angewandte Chemie-International Edition* 1998, **37**(5):551-575.
16. Xia YN, Rogers JA, Paul KE, Whitesides GM: **Unconventional methods for fabricating and patterning nanostructures.** *Chemical Reviews* 1999, **99**(7):1823-1848.
17. Duffy DC, McDonald JC, Schueller OJA, Whitesides GM: **Rapid prototyping of microfluidic systems in poly(dimethylsiloxane).** *Analytical Chemistry* 1998, **70**(23):4974-4984.
18. McDonald JC, Duffy DC, Anderson JR, Chiu DT, Wu HK, Schueller OJA, Whitesides GM: **Fabrication of microfluidic systems in poly(dimethylsiloxane).** *Electrophoresis* 2000, **21**(1):27-40.
19. **Emerging Markets for Microfluidic Applications: Market Report.** In.: Yole Developpement; 2009.
20. Wlodkowic D, Cooper JM: **Tumors on chips: oncology meets microfluidics.** *Current Opinion in Chemical Biology* 2010, **14**(5):556-567.
21. Brandenburg A, Curdt F, Nestler J, Otto T, Wunderlich K, Michel D: **Integrated point of care testing system based on low cost polymer biochips.** In: *Advanced Biomedical and Clinical Diagnostic Systems VII*. Edited by MahadevanJansen A, VoDinh T, Grundfest WS, vol. 7169; 2009.
22. Sun S, Yang MH, Kostov Y, Rasooly A: **ELISA-LOC: lab-on-a-chip for enzyme-linked immunodetection.** *Lab on a Chip* 2010, **10**(16):2093-2100.
23. Rosen Y, Gurman P: **MEMS and Microfluidics for Diagnostics Devices.** *Current Pharmaceutical Biotechnology* 2010, **11**(4):366-375.

24. Lee WG, Kim YG, Chung BG, Demirci U, Khademhosseini A: **Nano/Microfluidics for diagnosis of infectious diseases in developing countries.** *Advanced Drug Delivery Reviews* 2010, **62**(4-5):449-457.
25. Wurm M, Schopke B, Lutz D, Muller J, Zeng AP: **Microtechnology meets systems biology: The small molecules of metabolome as next big targets.** *Journal of Biotechnology* 2010, **149**(1-2):33-51.
26. McCaughan F, Dear PH: **Single-molecule genomics.** *Journal of Pathology* 2010, **220**(2):297-306.
27. Coupland P: **Microfluidics for the upstream pipeline of DNA sequencing - a worthy application?** *Lab on a Chip* 2010, **10**(5):544-547.
28. Lombardi D, Dittrich PS: **Advances in microfluidics for drug discovery.** *Expert Opinion on Drug Discovery* 2010, **5**(11):1081-1094.
29. Kool J, Lingeman H, Niessen W, Irth H: **High Throughput Screening Methodologies Classified for Major Drug Target Classes According to Target Signaling Pathways.** *Combinatorial Chemistry & High Throughput Screening* 2010, **13**(6):548-561.
30. Gupta K, Kim DH, Ellison D, Smith C, Kundu A, Tuan J, Suh KY, Levchenko A: **Lab-on-a-chip devices as an emerging platform for stem cell biology.** *Lab on a Chip* 2010, **10**(16):2019-2031.
31. Cheong R, Paliwal S, Levchenko A: **High-content screening in microfluidic devices.** *Expert Opinion on Drug Discovery* 2010, **5**(8):715-720.
32. Kim JK, Bang HW, Chung S, Chin-Yu AD, Chung C, Jo HS, Yoo JY, Chang JK: **Single-cell manipulation and fluorescence detection in benchtop flow cytometry system with disposable plastic microfluidic chip.** In: *Microfluidics, Biomems, and Medical Microsystems*. Edited by Becker H, Woias P, vol. 4982; 2003: 8-20.
33. Pilarski LM, Lauzon J, Strachan E, Adamia S, Atrazhev A, Belch AR, Backhouse CJ: **Sensitive detection using microfluidics technology of single cell PCR products from high and low abundance IgH VDJ templates in multiple myeloma.** *Journal of Immunological Methods* 2005, **305**(1):94-105.
34. Wang HY, Lu C: **High-throughput and real-time study of single cell electroporation using microfluidics: Effects of medium osmolarity.** *Biotechnology and Bioengineering* 2006, **95**(6):1116-1125.
35. Ryley J, Pereira-Smith OM: **Microfluidics device for single cell gene expression analysis in *Saccharomyces cerevisiae*.** *Yeast* 2006, **23**(14-15):1065-1073.
36. Zare RN, Kim S: **Microfluidic Platforms for Single-Cell Analysis.** In: *Annual Review of Biomedical Engineering, Vol 12*. vol. 12; 2010: 187-201.
37. Zhang CS, Xing D, Li YY: **Micropumps, microvalves, and micromixers within PCR microfluidic chips: Advances and trends.** *Biotechnology Advances* 2007, **25**(5):483-514.
38. Vilkner T, Janasek D, Manz A: **Micro total analysis systems. Recent developments.** *Analytical Chemistry* 2004, **76**(12):3373-3385.
39. West J, Becker M, Tombrink S, Manz A: **Micro total analysis systems: Latest achievements.** *Analytical Chemistry* 2008, **80**(12):4403-4419.
40. Dittrich PS, Tachikawa K, Manz A: **Micro total analysis systems. Latest advancements and trends.** *Analytical Chemistry* 2006, **78**(12):3887-3907.
41. Kamholz AE: **Proliferation of microfluidics in literature and intellectual property.** *Lab on a Chip* 2004, **4**(2):16N-20N.
42. Mark D, Haeberle S, Roth G, von Stetten F, Zengerle R: **Microfluidic lab-on-a-chip platforms: requirements, characteristics and applications.** *Chemical Society Reviews* 2010, **39**(3):1153-1182.
43. Becker H: **IP or no IP: that is the question.** *Lab on a Chip* 2009, **9**(23):3327-3329.
44. Haeberle S, Zengerle R: **Microfluidic platforms for lab-on-a-chip applications.** *Lab on a Chip* 2007, **7**(9):1094-1110.

45. Gartner C, Becker H, Anton B, Rotting O: **The microfluidic toolbox - Tools and standardization solutions for microfluidic devices for life sciences applications.** In: *Microfluidics, Biomems, and Medical Microsystems II*. Edited by Woias P, Papautsky I, vol. 5345; 2004: 159-162.
46. Becker H: **Mind the gap! Lab on a Chip** 2010, **10**(3):271-273.
47. Becker H: **Hype, hope and hubris: the quest for the killer application in microfluidics.** *Lab on a Chip* 2009, **9**(15):2119-2122.
48. Becker H: **It's the economy.** *Lab on a Chip* 2009, **9**(19):2759-2762.
49. Ouelette J: **A new wave of microfluidic devices.** In: *The Industrial Physicist*. 2003.
50. Whitesides G: **Solving problems.** *Lab on a Chip* 2010, **10**(18):2317-2318.
51. Klapperich CM: **Microfluidic diagnostics: time for industry standards.** *Expert Review of Medical Devices* 2009, **6**(3):211-213.
52. Blow N: **Microfluidics: in search of a killer application.** *Nature Methods* 2007, **4**(8):665-668.
53. Becker H: **Microfluidics: a technology coming of age.** *Medical device technology* 2008, **19**(3):21-24.
54. Standardization IOF: **Microscopes - Slides. Part I: Dimensions, Optical properties and marking.** In: *Optics and Optical Instruments*. Switzerland; 1986.
55. Jackson L: **Cytogenetics and molecular cytogenetics.** *Clinical Obstetrics and Gynecology* 2002, **45**(3):622-639.
56. Hsu L: **Prenatal diagnosis of chromosomal abnormalities through amniocentesis.** In: *Genetic Disorders and the Fetus, 4th ed.* Edited by Milunsky A. Baltimore: The Johns Hopkins University Press; 1998.
57. Kluin P, Schuurin E: **Molecular cytogenetics of lymphoma: where do we stand in 2010?** *Histopathology* 2011, **58**(1):128-144.
58. Cheung SW, Shaw CA, Yu W, Li JZ, Ou ZS, Patel A, Yatsenko SA, Cooper ML, Furman P, Stankiewicz P *et al*: **Development and validation of a CGH microarray for clinical cytogenetic diagnosis (vol 6, pg 422, 2005).** *Genetics in Medicine* 2005, **7**(7):478-478.
59. Fox JL, Hsu PH, Legator MS, Morrison LE, Seelig SA: **Fluorescence In-Situ Hybridization - powerful molecular tool for cancer prognosis.** *Clinical Chemistry* 1995, **41**(11):1554-1559.
60. Sandberg AA, Meloni-Ehrig AM: **Cytogenetics and genetics of human cancer: methods and accomplishments.** *Cancer Genetics and Cytogenetics* 2010, **203**(2):102-126.
61. Dave BJ, Sanger WG: **Role of Cytogenetics and Molecular Cytogenetics in the Diagnosis of Genetic Imbalances.** *Seminars in Pediatric Neurology* 2007, **14**:2-6.
62. Volpi EV, Bridger JM: **FISH glossary: an overview of the fluorescence in situ hybridization technique.** *Biotechniques* 2008, **45**(4):385-+.
63. Campbell LJ: **Cytogenetic and FISH techniques in myeloid malignancies.** In: *Methods in Molecular Medicine*. Edited by Iland H, Hertzberg M, Marlton P: Humana Press Inc; 2006: 13-26.
64. de Klein A, Tibboel D: **Genetics.** *Seminars in Pediatric Surgery* 2010, **19**(3):234-239.
65. Park JH, Woo JH, Shim SH, Yang SJ, Choi YM, Yang KS, Cha DH: **Application of a target array Comparative Genomic Hybridization to prenatal diagnosis.** *Bmc Medical Genetics* 2010, **11**.
66. Beatty B, Mai S, Squire J: **FISH. A Practical Approach.** Oxford: Oxford University Press; 2002.
67. Trask BJ: **Human cytogenetics: 46 chromosomes, 46 years and counting.** *Nature Reviews Genetics* 2002, **3**(10):769-778.
68. Smeets D: **Historical prospective of human cytogenetics: from microscope to microarray.** *Clinical Biochemistry* 2004, **37**(6):439-446.
69. Fauth C, Speicher MR: **Classifying by colors: FISH-based genome analysis.** *Cytogenetics and Cell Genetics* 2001, **93**(1-2):1-10.
70. Andrieux J, Sheth F: **Comparative genomic hybridization array study and its utility in detection of constitutional and acquired anomalies.** *Indian Journal of Experimental Biology* 2009, **47**(10):779-791.

71. Jain KK: **Current Status of Fluorescent In-Situ Hybridisation**. In: *Medical Device Technology*. vol. 15(4); 2004: 14-17.
72. Gambardella S, Ciabattini E, Motta F, Stoico G, Gullotta F, Biancolella M, Nardone A, Novelli A, Brunetti E, Bernardini L *et al*: **Design, Construction and Validation of Targeted BAC Array-Based CGH Test for Detecting the Most Commons Chromosomal Abnormalities**. In., vol. 3. Genetics Insights; 2010: 9-21.
73. Jiang F, Katz RL: **Use of interphase fluorescence in situ hybridization as a powerful diagnostic tool in cytology**. *Diagnostic Molecular Pathology* 2002, **11**(1):47-57.
74. Nath J, Johnson KL: **A review of fluorescence in situ hybridization (FISH): Current status and future prospects**. *Biotechnic and Histochemistry* 2000, **75**(2):54-78.
75. Trask BJ: **Fluorescence in-situ hybridization - Applications in cytogenetic and gene-mapping**. *Trends in Genetics* 1991, **7**(5):149-154.
76. Garimberti E, Tosi S: **Fluorescence in situ Hybridization (FISH), Basic Principles and Methodology**. *Fluorescence in situ Hybridization (FISH): Protocols and Applications* 2010:3-20.
77. Tonnies H: **Modern molecular cytogenetic techniques in genetic diagnostics**. *Trends in Molecular Medicine* 2002, **8**(6):246-250.
78. Zanardi A, Bandiera D, Bertolini F, Corsini C, Gregato G, Milani P, Barborini E, Carbone R: **Miniaturized FISH for screening of onco-hematological malignancies**. 2010, *BioTechniques*, **49**, 1:497-504.
79. van der Ploeg M: **Cytochemical nucleic acid research during the twentieth century**. *European Journal of Histochemistry* 2000, **44**(1):7-42.
80. Sieben VJ, Marun CSD, Pilarski PM, Kaigala GV, Pilarski LM, Backhouse CJ: **FISH and chips: chromosomal analysis on microfluidic platforms**. *IET Nanobiotechnology* 2007, **1**(3):27-35.
81. Kearney L, Horsley SW: **Molecular cytogenetics in haematological malignancy: current technology and future prospects**. *Chromosoma* 2005, **114**(4):286-294.
82. Speicher MR, Carter NP: **The new cytogenetics: Blurring the boundaries with molecular biology**. *Nature Reviews Genetics* 2005, **6**(10):782-792.
83. Levsky JM, Singer RH: **Fluorescence in situ hybridization: past, present and future**. *Journal of Cell Science* 2003, **116**(14):2833-2838.
84. Vedarethinam I, Shah P, Dimaki M, Tumer Z, Tommerup N, Svendsen WE: **Metaphase FISH on a Chip: Miniaturized Microfluidic Device for Fluorescence in situ Hybridization**. *Sensors* 2010, **10**(11):9831-9846.
85. Liehr T, Starke H, Heller A, Kosyakova N, Mrasek K, Gross M, Karst C, Steinhäuser U, Hunstig F, Fickelscher I *et al*: **Multicolor fluorescence in situ hybridization (FISH) applied to FISH-banding**. *Cytogenetic and Genome Research* 2006, **114**(3-4):240-244.
86. Lee C, Lemyre E, Miron PM, Morton CC: **Multicolor fluorescence in situ hybridization in clinical cytogenetic diagnostics**. *Current Opinion in Pediatrics* 2001, **13**(6):550-555.
87. Shah P, Vedarethinam I, Kwasny D, Andresen L, Dimaki M, Skov S, Svendsen WE: **Microfluidic bioreactors for culture of non-adherent cell**. *Sensors and Actuators B:Chemical* 2011.
88. Svendsen WE, Castillo-Leon J, Lange JM, Sasso L, Olsen MH, Abaddi M, Andresen L, Levinsen S, Shah P, Vedarethinam I *et al*: **Micro and nano-platforms for biological cell analysis**. *Sensors and Actuators A:Physical* 2011.
89. Lee DS, Lee JH, Min HC, Kim TY, Oh BR, Kim HY, Lee JY, Lee CK, Chun HG, Kim HC: **Application of high throughput cell array technology to FISH: Investigation of the role of deletion of p16 gene in leukemias**. *Journal of Biotechnology* 2007, **127**(3):355-360.
90. Sieben VJ, Debes-Marun CS, Pilarski LM, Backhouse CJ: **An integrated microfluidic chip for chromosome enumeration using fluorescence in situ hybridization**. *Lab on a Chip* 2008, **8**(12):2151-2156.



91. Dimaki M, Clausen CH, Lange J, Shah P, Jensen LB, Svendsen W: **A microfabricated platform for chromosome separation and analysis**. In: *Proceedings of the 17th International Vacuum Congress/13th International Conference on Surface Science/International Conference on Nanoscience and Technology*. Edited by Johansson LSO, Andersen JN, Gothelid M, Helmersson U, Montelius L, Rubel M, Setina J, Wernersson LE, vol. 100; 2008.
92. G.T. L: **Genetic translocations and other chromosome aberrations**: Nova Science Publishers; 2008.
93. Gonzalez C, Collins SD, Smith RL: **Fluidic interconnects for modular assembly of chemical microsystems**. *Sensors and Actuators B-Chemical* 1998, **49**(1-2):40-45.
94. Shaikh KA, Ryu KS, Goluch ED, Nam JM, Liu JW, Thaxton S, Chiesl TN, Barron AE, Lu Y, Mirkin CA *et al*: **A modular microfluidic architecture for integrated biochemical analysis**. *Proceedings of the National Academy of Sciences of the United States of America* 2005, **102**(28):9745-9750.
95. Wu A, Wang L, Jensen E, Mathies R, Boser B: **Modular integration of electronics and microfluidic systems using flexible printed circuit boards**. *Lab on a Chip* 2010, **10**(4):519-521.
96. Sun K, Wang ZX, Jiang XY: **Modular microfluidics for gradient generation**. *Lab on a Chip* 2008, **8**(9):1536-1543.
97. Ni M, Tong WH, Choudhury D, Rahim NAA, Iliescu C, Yu H: **Cell Culture on MEMS Platforms: A Review**. *International Journal of Molecular Sciences* 2009, **10**(12):5411-5441.
98. Attia UM, Marson S, Alcock JR: **Micro-injection moulding of polymer microfluidic devices**. *Microfluidics and Nanofluidics* 2009, **7**(1):1-28.
99. Becker H, Locascio LE: **Polymer microfluidic devices**. *Talanta* 2002, **56**(2):267-287.
100. Mata A, Fleischman AJ, Roy S: **Characterization of polydimethylsiloxane (PDMS) properties for biomedical micro/nanosystems**. *Biomedical Microdevices* 2005, **7**(4):281-293.
101. Qin D, Xia YN, Whitesides GM: **Soft lithography for micro- and nanoscale patterning**. *Nature Protocols* 2010, **5**(3):491-502.
102. McDonald JC, Whitesides GM: **Poly(dimethylsiloxane) as a material for fabricating microfluidic devices**. *Accounts of Chemical Research* 2002, **35**(7):491-499.
103. Zou J, Wong PY: **Thermal effects in plasma treatment of patterned PDMS for bonding stacked channels**. In: *Micro- and Nanosystems*. Edited by LaVan DA, Ayon AA, Madou MJ, McNie ME, Prasad SV, vol. 782; 2004: 125-130.
104. Jo BH, Van Lerberghe LM, Motsegood KM, Beebe DJ: **Three-dimensional micro-channel fabrication in polydimethylsiloxane (PDMS) elastomer**. *Journal of Microelectromechanical Systems* 2000, **9**(1):76-81.
105. Jensen MF, Noerholm M, Christensen LH, Geschke O: **Microstructure fabrication with a CO<sub>2</sub> laser system: characterization and fabrication of cavities produced by raster scanning of the laser beam**. *Lab on a Chip* 2003, **3**(4):302-307.
106. Klank H, Kutter JP, Geschke O: **CO<sub>2</sub>-laser micromachining and back-end processing for rapid production of PMMA-based microfluidic systems**. *Lab on a Chip* 2002, **2**(4):242-246.
107. Geschke O, Klank H, Telleman P: **Microsystem Engineering of Lab-on-a-chip Devices**: Wiley-VCH; 2004.
108. Chen Y, Zhang LY, Chen G: **Fabrication, modification, and application of department of analytical poly(methyl methacrylate) microfluidic chips**. *Electrophoresis* 2008, **29**(9):1801-1814.
109. Ogilvie IRG, Sieben VJ, Floquet CFA, Zmijan R, Mowlem MC, Morgan H: **Reduction of surface roughness for optical quality microfluidic devices in PMMA and COC**. *Journal of Micromechanics and Microengineering* 2010, **20**(6):8.
110. Stangegaard M, Petronis S, Jorgensen AM, Christensen CBV, Dufva M: **A biocompatible micro cell culture chamber (mu CCC) for the culturing and on-line monitoring of eukaryote cells**. *Lab on a Chip* 2006, **6**(8):1045-1051.

111. Stangegaard M, Wang Z, Kutter JP, Dufva M, Wolff A: **Whole genome expression profiling using DNA microarray for determining biocompatibility of polymeric surfaces.** *Molecular Biosystems* 2006, **2**(9):421-428.
112. Szantai E, Guttman A: **Genotyping with microfluidic devices.** *Electrophoresis* 2006, **27**(24):4896-4903.
113. Andersson H, van den Berg A: **Microfluidic devices for cellomics: a review.** *Sensors and Actuators B: Chemical* 2003, **92**(3):315-325.
114. El-Ali J, Sorger PK, Jensen KF: **Cells on chips.** *Nature* 2006, **442**(7101):403-411.
115. Srivastava Y, Marquez M, Thorsen T: **Microfluidic electrospinning of biphasic nanofibers with Janus morphology.** *Biomicrofluidics* 2009, **3**(1):6.
116. Vanapalli SA, Duits MHG, Mugele F: **Microfluidics as a functional tool for cell mechanics.** *Biomicrofluidics* 2009, **3**(1).
117. Frische N, Datta P, Goettert J: **Development of a biological detection platform utilizing a modular microfluidic stack.** *Microsystem Technologies-Micro-and Nanosystems-Information Storage and Processing Systems* 2010, **16**(8-9):1553-1561.
118. You BH, Chen PC, Park DS, Park S, Nikitopoulos DE, Soper SA, Murphy MC: **Passive micro-assembly of modular, hot embossed, polymer microfluidic devices using exact constraint design.** *Journal of Micromechanics and Microengineering* 2009, **19**(12):11.
119. Yuen PK: **SmartBuild - A truly plug-n-play modular microfluidic system.** *Lab on a Chip* 2008, **8**(8):1374-1378.
120. Yuen PK, Bliss JT, Thompson CC, Peterson RC: **Multidimensional modular microfluidic system.** *Lab on a Chip* 2009, **9**(22):3303-3305.
121. Perozziello G, Simone G, Candeloro P, Gentile F, Malara N, Larocca R, Coluccio M, Pullano S, Tirinato L, Geschke O et al: **A Fluidic Motherboard for Multiplexed Simultaneous and Modular Detection in Microfluidic Systems for Biological Application** *Micro and Nanosystems* 2010, **2**:227-238.
122. Yang Z, Maeda R: **A world-to-chip socket for microfluidic prototype development.** *Electrophoresis* 2002, **23**(20):3474-3478.
123. Benavides GL, Okandan M, Jenkins MW, Hetherington D, Galambos P: **Precision alignment packaging for microsystems with multiple fluid connections.** *ASME International Mechanical Engineering Congress and Exposition, Proceedings* 2001, **2**:3295-3302.
124. Unger MA, Chou HP, Thorsen T, Scherer A, Quake SR: **Monolithic microfabricated valves and pumps by multilayer soft lithography.** *Science* 2000, **288**(5463):113-116.
125. Gomez-Sjoberg R, Leyrat AA, Pirone DM, Chen CS, Quake SR: **Versatile, fully automated, microfluidic cell culture system.** *Analytical Chemistry* 2007, **79**(22):8557-8563.
126. Gomez-Sjoberg R, Leyrat AA, Quake SR: **ANYL 350-Highly automated microfluidic system for cell biology.** *Abstracts of Papers of the American Chemical Society* 2008, **236**:350-ANYL.
127. Liu J, Hansen C, Quake SR: **Solving the "world-to-chip" interface problem with a microfluidic matrix.** *Analytical Chemistry* 2003, **75**(18):4718-4723.
128. Thorsen T, Maerkl SJ, Quake SR: **Microfluidic large-scale integration.** *Science* 2002, **298**(5593):580-584.
129. Fredrickson CK, Fan ZH: **Macro-to-micro interfaces for microfluidic devices.** *Lab on a Chip* 2004, **4**(6):526-533.
130. Christensen AM, Chang-Yen DA, Gale BK: **Characterization of interconnects used in PDMS microfluidic systems.** *Journal of Micromechanics and Microengineering* 2005, **15**(5):928-934.
131. Chen H, Acharya D, Gajraj A, Meiners JC: **Robust interconnects and packaging for microfluidic elastomeric chips.** *Analytical Chemistry* 2003, **75**(19):5287-5291.
132. Rodrigues E, Lapa RAS: **Development of Flow Systems by Direct-milling on Poly(methyl methacrylate) Substrates Using UV-Photopolymerization as Sealing Process.** *Analytical Sciences* 2009, **25**(3):443-448.



133. Rodrigues E, Lapa RAS: **Development of micro-flow devices by direct-milling on poly(methyl methacrylate) substrates with integrated optical detection.** *Microchimica Acta* 2009, **166**(3-4):189-195.
134. Anderson JR, Chiu DT, Jackman RJ, Cherniavskaya O, McDonald JC, Wu HK, Whitesides SH, Whitesides GM: **Fabrication of topologically complex three-dimensional microfluidic systems in PDMS by rapid prototyping.** *Analytical Chemistry* 2000, **72**(14):3158-3164.
135. Bowden M, Geschke O, Kutter JP, Diamond D: **CO<sub>2</sub> laser microfabrication of an integrated polymer microfluidic manifold for the determination of phosphorus.** *Lab on a Chip* 2003, **3**(4):221-223.
136. McMahon JJ, Kwon Y, Lu JQ, Cale TS, Gutmann RJ: **Bonding characterization of oxidized PDMS thin films.** In: *Thin Films-Stresses and Mechanical Properties X*. Edited by Corcoran SG, Joo YC, Moody NR, Suo Z, vol. 795; 2004: 99-104.
137. Rodriguez-Trujillo R, Castillo-Fernandez O, Garrido M, Arundell M, Valencia A, Gomila G: **High-speed particle detection in a micro-Coulter counter with two-dimensional adjustable aperture.** *Biosensors & Bioelectronics* 2008, **24**(2):290-296.
138. Freshney I: **Culture of Animal Cells: A Manual of Basic Technique**, 5th edn. NJ,USA: Wiley-Liss; 2005.
139. Young EWK, Simmons CA: **Macro- and microscale fluid flow systems for endothelial cell biology.** *Lab on a Chip* 2010, **10**(2):143-160.
140. Kang E, Lee DH, Kim CB, Yoo SJ, Lee SH: **A hemispherical microfluidic channel for the trapping and passive dissipation of microbubbles.** *Journal of Micromechanics and Microengineering* 2010, **20**(4):9.
141. Zheng WF, Wang Z, Zhang W, Jiang XY: **A simple PDMS-based microfluidic channel design that removes bubbles for long-term on-chip culture of mammalian cells.** *Lab on a Chip* 2010, **10**(21):2906-2910.
142. Sung JH, Shuler ML: **Prevention of air bubble formation in a microfluidic perfusion cell culture system using a microscale bubble trap.** *Biomedical Microdevices* 2009, **11**(4):731-738.
143. Regehr KJ, Domenech M, Koepsel JT, Carver KC, Ellison-Zelski SJ, Murphy WL, Schuler LA, Alarid ET, Beebe DJ: **Biological implications of polydimethylsiloxane-based microfluidic cell culture.** *Lab on a Chip* 2009, **9**(15):2132-2139.
144. Kim L, Toh YC, Voldman J, Yu H: **A practical guide to microfluidic perfusion culture of adherent mammalian cells.** *Lab on a Chip* 2007, **7**(6):681-694.
145. Young EWK, Beebe DJ: **Fundamentals of microfluidic cell culture in controlled microenvironments.** *Chemical Society Reviews* 2010, **39**(3):1036-1048.
146. Walker GM, Zeringue HC, Beebe DJ: **Microenvironment design considerations for cellular scale studies.** *Lab on a Chip* 2004, **4**(2):91-97.
147. Yeon JH, Park JK: **Microfluidic cell culture systems for cellular analysis.** *Biochip Journal* 2007, **1**(1):17-27.
148. Meyvantsson I, Beebe DJ: **Cell Culture Models in Microfluidic Systems.** *Annual Review of Analytical Chemistry* 2008, **1**:423-449.
149. Takayama S, Ostuni E, LeDuc P, Naruse K, Ingber DE, Whitesides GM: **Selective chemical treatment of cellular microdomains using multiple laminar streams.** *Chemistry and Biology* 2003, **10**(2):123-130.
150. Walker GM, Sai JQ, Richmond A, Stremmer M, Chung CY, Wikswo JP: **Effects of flow and diffusion on chemotaxis studies in a microfabricated gradient generator.** *Lab on a Chip* 2005, **5**(6):611-618.
151. Fujii S, Uematsu M, Yabuki S, Abo M, Yoshimura E, Sato K: **Microbioassay system for an anti-cancer agent test using animal cells on a microfluidic gradient mixer.** *Analytical Sciences* 2006, **22**(1):87-90.
152. Shaughnessy L, Chamblin B, McMahon L, Nair A, Thomas MB, Wakefield J, Koentgen F, Ramabhadran R: **Novel approaches to models of Alzheimer's disease pathology for drug screening and development.** *Journal of Molecular Neuroscience* 2004, **24**(1):23-32.

153. Diao JP, Young L, Kim S, Fogarty EA, Heilman SM, Zhou P, Shuler ML, Wu MM, DeLisa MP: **A three-channel microfluidic device for generating static linear gradients and its application to the quantitative analysis of bacterial chemotaxis.** *Lab on a Chip* 2006, **6**(3):381-388.
154. Saadi W, Wang SJ, Lin F, Jeon NL: **A parallel-gradient microfluidic chamber for quantitative analysis of breast cancer cell chemotaxis.** *Biomedical Microdevices* 2006, **8**(2):109-118.
155. Koyama S, Amarie D, Soini HA, Novotny MV, Jacobson SC: **Chemotaxis assays of mouse sperm on microfluidic devices.** *Analytical Chemistry* 2006, **78**(10):3354-3359.
156. Chung BG, Flanagan LA, Rhee SW, Schwartz PH, Lee AP, Monuki ES, Jeon NL: **Human neural stem cell growth and differentiation in a gradient-generating microfluidic device.** *Lab on a Chip* 2005, **5**(4):401-406.
157. Tourovskaia A, Figueroa-Masot X, Folch A: **Differentiation-on-a-chip: A microfluidic platform for long-term cell culture studies.** *Lab on a Chip* 2005, **5**(1):14-19.
158. Lam RHW, Kim MC, Thorsen T: **Culturing Aerobic and Anaerobic Bacteria and Mammalian Cells with a Microfluidic Differential Oxygenator.** *Analytical Chemistry* 2009, **81**(14):5918-5924.
159. Gobbels K, Thiebes AL, van Ooyen A, Schnakenberg U, Braunig P: **Low density cell culture of locust neurons in closed-channel microfluidic devices.** *Journal of Insect Physiology* 2010, **56**(8):1003-1009.
160. Giridharan GA, Nguyen MD, Estrada R, Parichehreh V, Hamid T, Ismahil MA, Prabhu SD, Sethu P: **Microfluidic Cardiac Cell Culture Model (mu CCCM).** *Analytical Chemistry* 2010, **82**(18):7581-7587.
161. Barbulovic-Nad I, Au SH, Wheeler AR: **A microfluidic platform for complete mammalian cell culture.** *Lab on a Chip* 2010, **10**(12):1536-1542.
162. Hui EE, Bhatia SN: **Micromechanical control of cell-cell interactions.** *Proceedings of the National Academy of Sciences of the United States of America* 2007, **104**(14):5722-5726.
163. Kane BJ, Zinner MJ, Yarmush ML, Toner M: **Liver-specific functional studies in a microfluidic array of primary mammalian hepatocytes.** *Analytical Chemistry* 2006, **78**(13):4291-4298.
164. Weibel DB, DiLuzio WR, Whitesides GM: **Microfabrication meets microbiology.** *Nature Reviews Microbiology* 2007, **5**(3):209-218.
165. Yu HM, Meyvantsson I, Shkel IA, Beebe DJ: **Diffusion dependent cell behavior in microenvironments.** *Lab on a Chip* 2005, **5**(10):1089-1095.
166. Zhang BY, Kim MC, Thorsen T, Wang ZH: **A self-contained microfluidic cell culture system.** *Biomedical Microdevices* 2009, **11**(6):1233-1237.
167. Kimura H, Sakai H, Yamamoto T, Sakai Y, Fujii T: **Development of Micro Perfusion Cell Culture Device to Create In Vivo-Like Environments for Long-Period and Real-Time Monitoring of Cells Activities.** In: *Micro-NanoMechatronics and Human Science, 2006 International Symposium on: 5-8 Nov. 2006* 2006; 2006: 1-6.
168. Kimura H, Yamamoto T, Sakai H, Sakai Y, Fujii T: **An integrated microfluidic system for long-term perfusion culture and on-line monitoring of intestinal tissue models.** *Lab on a Chip* 2008, **8**(5):741-746.
169. Nevill JT, Cooper R, Dueck M, Breslauer DN, Lee LP: **Integrated microfluidic cell culture and lysis on a chip.** *Lab on a Chip* 2007, **7**(12):1689-1695.
170. Liu K, Pitchimani R, Dang D, Bayer K, Harrington T, Pappas D: **Cell culture chip using low-shear mass transport.** *Langmuir* 2008, **24**(11):5955-5960.
171. Korin N, Bransky A, Khoury M, Dinnar U, Levenberg S: **Design of Well and Groove Microchannel Bioreactors for Cell Culture.** *Biotechnology and Bioengineering* 2009, **102**(4):1222-1230.
172. McAdams TA, Sandstrom CE, Miller WM, Bender JG, Papoutsakis ET: **Ex vivo expansion of primitive hematopoietic cells for cellular therapies: An overview.** *Cytotechnology* 1995, **18**(1-2):133-146.

173. Sandstrom CE, Bender JG, Miller WM, Papoutsakis ET: **Development of novel perfusion chamber to retain nonadherent cells and its use for comparison of human "mobilized" peripheral blood mononuclear cell cultures with and without irradiated bone marrow stroma.** *Biotechnology and Bioengineering* 1996, **50**(5):493-504.
174. Jacobs PA, Baikie AG, Brown WMC, Strong JA: **The somatic chromosomes in mongolism.** *Lancet* 1959, **1**(APR4):710-710.
175. Ford CE, Jones KW, Miller OJ, Mittwoch U, Penrose LS, Ridler M, Shapiro A: **The chromosomes in a patient showing both Mongolism and the Klinefelter syndrome.** *Lancet* 1959, **1**(APR4):709-710.
176. Ford CE, Jones KW, Polani PE, Dealmeida JC, Briggs JH: **A sex-chromosome anomaly in a case of gonadal dysgenesis (Turners syndrome).** *Lancet* 1959, **1**(APR4):711-713.
177. Rowley JD: **New consistent chromosomal abnormality in chronic myelogenous leukemia identified by quinacrine fluorescence and giemsa staining.** *Nature* 1973, **243**(5405):290-293.
178. Manning M, Hudgins L: **Professional Practice Guidelines C. Array-based technology and recommendations for utilization in medical genetics practice for detection of chromosomal abnormalities.** *Genetics in Medicine* 2010, **12**(11):742-745.
179. Bystricka D, Zemanova Z, Brezinova J, Gancarcikova M, Grosova L, Sarova I, Izakova S, Berkova A, Michalova K: **The Assessment of Array Comparative Genomic Hybridization in Complex Karyotype Analyses.** *Folia Biologica* 2010, **56**(5):223-230.
180. Krabchi K, Lavoie J, Coullin P, Bronsard M, Pellestor F, Yan J, Drouin R: **From the conception of the PRINS to its coronation.** *MS: Medecine Sciences* 2004, **20**(4):465-473.
181. Xu J, Chen Z: **Advances in molecular cytogenetics for the evaluation of mental retardation.** *American Journal of Medical Genetics Part C: Seminars in Medical Genetics* 2003, **117C**(1):15-24.
182. Mennicke K, Yang J, Hinrichs F, Muller A, Diercks P, Schwinger E: **Validation of primed in situ labeling for interphase analysis of chromosomes 18, X, and Y in uncultured amniocytes.** *Fetal Diagnosis and Therapy* 2003, **18**(2):114-121.
183. Velagelati GVN, Shulman LP, Phillips OP, Tharapel SA, Tharapel AT: **Primed in situ labeling for rapid prenatal diagnosis.** *American Journal of Obstetrics and Gynecology* 1998, **178**(6):1313-1317.
184. Phillips OP, Velagelati GVN, Shulman LP, Tharapel SA, Martens PR, Wachtel SS, Tharapel AT: **Rapid prenatal diagnosis by primed in situ labeling (PRINS).** *American Journal of Human Genetics* 1997, **61**(4):918.
185. Li F, Fang WG, Wu BQ, Wang JJ, Zhong HH, Heng WJ: **Molecular cytogenetic detection of trisomy 21 in interphase nuclei and metaphase chromosomes.** *Chinese Medical Journal* 1999, **112**(9):840-844.
186. Baierlei.JI, Foster JM: **Studies on Energy Metabolism of Human Leukocytes. 2. Mechanism of Pasteur effect in Human Leukocytes.** *Blood* 1968, **32**(3):412-&.
187. Marucci M, Pettersson SG, Ragnarsson G, Axelsson A: **Determination of a diffusion coefficient in a membrane by electronic speckle pattern interferometry: a new method and a temperature sensitivity study.** *Journal of Physics D: Applied Physics* 2007, **40**(9):2870-2880.
188. Sabourin D, Dufva M, Jensen T, Kutter J, Snakenborg D: **One-step fabrication of microfluidic chips with in-plane, adhesive-free interconnections.** *Journal of Micromechanics and Microengineering* 2010, **20**(3).
189. Claussen U, Michel S, Muhlig P, Westermann M, Grummt UW, Kromeyer-Hauschild K, Liehr T: **Demystifying chromosome preparation and the implications for the concept of chromosome condensation during mitosis.** *Cytogenetic and Genome Research* 2002, **98**(2-3):136-146.
190. Henegariu O, Heerema NA, Wright LL, Bray-Ward P, Ward DC, Vance GH: **Improvements in cytogenetic slide preparation: Controlled chromosome spreading, chemical aging and gradual denaturing.** *Cytometry* 2001, **43**(2):101-109.

191. Haubert K, Drier T, Beebe D: **PDMS bonding by means of a portable, low-cost corona system.** *Lab on a Chip* 2006, **6**(12):1548-1549.
192. Liehr T: **Fluorescence In-Situ Hybridization (FISH) : Application guide**, 1st edn. Berlin Heidelberg: Springer-Verlag; 2009.
193. Ward BE, Gersen SL, Carelli MP, McGuire NM, Dackowski WR, Weinstein M, Sandlin C, Warren R, Klinger KW: **Rapid prenatal diagnosis of chromosomal aneuploidies by fluorescence in situ hybridization: clinical experience with 4,500 specimens.** *American Journal of Human Genetics* 1993, **52**(5):854-865.
194. Sasai K, Tanaka R, Kawamura M, Honjo K, Matsunaga N, Nakada T, Homma K, Fujimura H: **Chromosome spreading techniques for primary gastrointestinal tumors.** *Journal of Gastroenterology* 1996, **31**(4):505-511.
195. Tepperberg J, Pettenati MJ, Rao PN, Lese CM, Rita D, Wyandt H, Gersen S, White B, Schoonmaker MM: **Prenatal diagnosis using interphase fluorescence in situ hybridization (FISH): 2-year multi-center retrospective study and review of the literature.** *Prenatal Diagnosis* 2001, **21**(4):293-301.
196. Squire J, Marrano P, Kolomeitz E: **FISH in clinical cytogenetics**, First edition edn. Oxford New York: Oxford Publishers, USA; 2002.
197. Weise A, Liehr T: **Fluorescence in situ hybridization for prenatal screening of chromosomal aneuploidies.** *Expert Review of Molecular Diagnostics* 2008, **8**(4):355-357.
198. Tanas MR, Goldblum JR: **Fluorescence In Situ Hybridization in the Diagnosis of Soft Tissue Neoplasms: A Review.** *Advances in Anatomic Pathology* 2009, **16**(6):383-391.
199. Braselmann H, Kulka U, Baumgartner A, Eder C, Muller I, Figel M, Zitzelsberger H: **SKY and FISH analysis of radiation-induced chromosome aberrations: A comparison of whole and partial genome analysis.** *Mutation Research-Fundamental and Molecular Mechanisms of Mutagenesis* 2005, **578**(1-2):124-133.
200. Jobanputra V, Sobrino A, Kinney A, Kline J, Warburton D: **Multiplex interphase FISH as a screen for common aneuploidies in spontaneous abortions.** *Human Reproduction* 2002, **17**(5):1166-1170.
201. Pergament E, Chen PX, Thangavelu M, Fiddler M: **The clinical application of interphase FISH in prenatal diagnosis.** *Prenatal Diagnosis* 2000, **20**(3):215-220.
202. Garson JA, Vandenberghe JA, Kemshead JT: **High-resolution in situ hybridization technique using biotinylated NMYC oncogene probe reveals periodic structure of HSRs in human neuroblastoma.** *Cytogenetics and Cell Genetics* 1987, **45**(1):10-15.
203. Garson JA, Vandenberghe JA, Kemshead JT: **Novel non-isotopic in situ hybridization technique detects small (1 Kb) unique sequences in routinely G-banded human chromosomes: fine mapping of N-myc and beta-NGF genes.** *Nucleic Acids Research* 1987, **15**(12):4761-4770.
204. Cremer T, Lichter P, Borden J, Ward DC, Manuelidis L: **Detection of chromosome aberrations in metaphase and interphase tumor cells by in situ hybridization using chromosome-specific library probes.** *Human Genetics* 1988, **80**(3):235-246.
205. Julien C, Bazin A, Guyot B, Forestier F, Daffos F: **Rapid prenatal diagnosis of Down's syndrome with in-situ hybridisation of fluorescent DNA probes.** *Lancet* 1986, **2**(8511):863-864.
206. Guyot B, Bazin A, Sole Y, Julien C, Daffos F, Forestier F: **Prenatal diagnosis with biotinylated chromosome specific probes.** *Prenatal Diagnosis* 1988, **8**(7):485-493.
207. Stumm M, Wegner RD, Bloechle M, Eckel H: **Interphase M-FISH applications using commercial probes in prenatal and PGD diagnostics.** *Cytogenetic and Genome Research* 2006, **114**(3-4):296-301.
208. Dziubinski JM, Sarosdy MF, Kahn PR, Ziffer MD, Love WR, Zadra JA, Schellhammer PF, Bokinsky GB, Stenzel TT: **Multiple fluorescence in situ hybridization (FISH) probes increase sensitivity for detection of bladder cancer.** *Journal of Urology* 2006, **175**(4):890.

209. Brown J, Saracoglu K, Uhrig S, Knight SJL, Lucas SJA, Speicher MR, Eils R, Kearney L: **Development of a multicolour FISH assay for subtelomeric chromosome rearrangements in leukaemia.** *Cytogenetics and Cell Genetics* 1999, **85**(1-2):O018.
210. Kearney L: **The impact of the new fish technologies on the cytogenetics of haematological malignancies.** *British Journal of Haematology* 1999, **104**(4):648-658.
211. Kearney L: **Multiplex-FISH (M-FISH): technique, developments and applications.** *Cytogenetic and Genome Research* 2006, **114**(3-4):189-198.
212. Insabato L, Bernasconi B, Glatz K, Dirnhofer S, Krugman J, Fend F, Capella C, Tibiletti MG, Di Vizio D, Pettinato G *et al*: **High-throughput tissue microarray FISH analysis in 226 surgically resected gastric B-cell lymphomas. Frequencies of trisomy 1, 3,12 and gains of X chromosome.** *Laboratory Investigation* 2002, **82**(1):541.
213. Tibiletti MG: **Interphase FISH as a new tool in tumor pathology.** *Cytogenetic and Genome Research* 2007, **118**(2-4):229-236.
214. Denice S, Matt R, Kim O, S BJ: **Integrating a FISH imaging system into the cytology laboratory.** *CytoJournal* 2010, **7**(3).
215. Genetics ACoM: **Prenatal interphase fluorescence in situ hybridization (FISH) policy statement.** *American Journal of Human Genetics* 1993, **53**(2):526-527.
216. Schwartz S: **Efficacy and applicability of interphase fluorescence in situ hybridization for prenatal diagnosis.** *American Journal of Human Genetics* 1993, **52**(5):851-853.
217. Christel E-S, Stefan G, Inga N, Andrea H, Susanne B, Simone H, Monika K, Christian T, Reiner S, Almuth C: **Conflicting results of prenatal FISH with different probes for Down's Syndrome critical regions associated with mosaicism for a de novo del(21)(q22) characterised by molecular karyotyping: Case report.** *Molecular Cytogenetics* 2010, **3**(16).
218. Zanardi A, Bandiera D, Bertolini F, Corsini CA, Gregato G, Milani P, Barborini E, R. C: **Miniaturized FISH for screening of onco-hematological malignancies.** *Biotechniques* 2010, **49**(1):497-504.
219. Hliscs R, Muhlig P, Claussen U: **The spreading of metaphases is a slow process which leads to a stretching of chromosomes.** *Cytogenetics and Cell Genetics* 1997, **76**(3-4):167-171.
220. Qu YY, Xing LY, Hughes ED, Saunders TL: **Chromosome Dropper Tool: Effect of slide angles on chromosome spread quality for murine embryonic stem cells.** *Journal of Histotechnology* 2008, **31**(2):75-79.
221. Yamada K, Kakinuma K, Tateya H, Miyasaka C: **Development of an instrument for chromosome slide preparation.** *Journal of Radiation Research* 1992, **33**:242-249.
222. Reyes DR, Iossifidis D, Auroux PA, Manz A: **Micro total analysis systems. 1. Introduction, theory, and technology.** *Analytical Chemistry* 2002, **74**(12):2623-2636.
223. Auroux PA, Iossifidis D, Reyes DR, Manz A: **Micro total analysis systems. 2. Analytical standard operations and applications.** *Analytical Chemistry* 2002, **74**(12):2637-2652.
224. Castillo J, Tanzi S, Dimaki M, Svendsen W: **Manipulation of self-assembly amyloid peptide nanotubes by dielectrophoresis.** *Electrophoresis* 2008, **29**(24):5026-5032.
225. Crane MM, Chung K, Stirman J, Lu H: **Microfluidics-enabled phenotyping, imaging, and screening of multicellular organisms.** *Lab on a Chip* 2010, **10**(12):1509-1517.
226. Leung WC, Waters JJ, Chitty L: **Prenatal diagnosis by rapid aneuploidy detection and karyotyping: a prospective study of the role of ultrasound in 1589 second-trimester amniocenteses.** *Prenatal Diagnosis* 2004, **24**(10):790-795.
227. Evans MI, Henry GP, Miller WA, Bui TH, Snidgers RJ, Wapner RJ, Miny P, Johnson MP, Peakman D, Johnson A *et al*: **International, collaborative assessment of 146 000 prenatal karyotypes: expected**



- limitations if only chromosome-specific probes and fluorescent in-situ hybridization are used. *Human Reproduction* 1999, **14**(5):1213-1216.
228. Laan M, Kallioniemi OP, Hellsten E, Alitalo K, Peltonen L, Palotie A: **Mechanically stretched chromosomes as targets for high-resolution fish mapping.** *Genome Research* 1995, **5**(1):13-20.
  229. Korenberg JR, Yangfeng T, Schreck R, Chen XN: **Using fluorescence in situ hybridization (FISH) in genome mapping.** *Trends in Biotechnology* 1992, **10**(1-2):27-32.
  230. Spurbeck JL, Zinsmeister AR, Meyer KJ, Jalal SM: **Dynamics of chromosome spreading.** *American Journal of Medical Genetics* 1996, **61**(4):387-393.
  231. Barch MJ, Lawce HJ, Arsham MS: **Peripheral Blood Culture**, 2nd edn. New York, NY, USA: Raven Press; 1991.
  232. Chattopadhyay S, Marindue B, Gilbert F: **Ovarian cancer protocol for the preparation of banded metaphases from tumor-tissue.** *Cancer Genetics and Cytogenetics* 1992, **59**(2):210-212.
  233. Gibas LM, Grujic S, Barr MA, Jackson LG: **A simple technique for obtaining high-quality chromosome preparations from chorionic villus samples using FDU synchronization.** *Prenatal Diagnosis* 1987, **7**(5):323-327.
  234. Miron PM: **Preparation, Culture and Analysis of Amniotic Fluid Samples.** New York, NY, USA: John Wiley & Sons; 1995.
  235. Warburton D: **Preparation and Culture of Products of Conception and Other Tissue for Chromosome Analysis.** New York, NY, USA: John Wiley & Sons; 1995.
  236. Deng W, Tsao SW, Lucas JN, Leung CS, Cheung ALM: **A new method for improving metaphase chromosome spreading.** *Cytometry Part A* 2003, **51A**(1):46-51.
  237. Netten H, Young IT, vanVliet LJ, Tanke HJ, Vrolijk H, Sloos WCR: **FISH and chips: Automation of fluorescent dot counting in interphase cell nuclei.** *Cytometry* 1997, **28**(1):1-10.
  238. Theodosiou Z, Kasampalidis LN, Livanos G, Zervakis M, Pitas L, Lyroutdia K: **Automated analysis of FISH and immunohistochemistry images: A review.** *Cytometry Part A* 2007, **71A**(7):439-450.
  239. Ling X, Premachandran CS, Chew M, Ser Choong C: **Development of a Disposable Bio-Microfluidic Package With Reagents Self-Contained Reservoirs and Micro-Valves for a DNA Lab-on-a-Chip (LOC) Application.** *IEEE Transactions on Advanced Packaging* 2009, **32**(2):528-535.
  240. Linder V, Sia SK, Whitesides GM: **Reagent-loaded cartridges for valveless and automated fluid delivery in microfluidic devices.** *Analytical Chemistry* 2005, **77**(1):64-71.
  241. Pamme N: **Continuous flow separations in microfluidic devices.** *Lab on a Chip* 2007, **7**(12):1644-1659.
  242. Yamada M, Nakashima M, Seki M: **Pinched flow fractionation: Continuous size separation of particles utilizing a laminar flow profile in a pinched microchannel.** *Analytical Chemistry* 2004, **76**(18):5465-5471.
  243. Takagi J, Yamada M, Yasuda M, Seki M: **Continuous particle separation in a microchannel having asymmetrically arranged multiple branches.** *Lab on a Chip* 2005, **5**(7):778-784.
  244. Sai Y, Yamada M, Yasuda M, Seki M: **Continuous separation of particles using a microfluidic device equipped with flow rate control valves.** *Journal of Chromatography A* 2006, **1127**(1-2):214-220.
  245. Andersen K, Levinsen S: **Design and simulation of pinchflow fractionation for blood cell separation.** Bachelor Thesis. Technical University of Denmark; 2007.
  246. Andersen KB, Levinsen S, Svendsen WE, Okkels F: **A generalized theoretical model for "continuous particle separation in a microchannel having asymmetrically arranged multiple branches".** *Lab on a Chip* 2009, **9**(11):1638-1639.
  247. Christiansen N, Hansen M: **Pinch Flow Fractionation for Blood Cell Separation.** Bachelor Thesis. Technical University of Denmark; 2007.

248. Seki M: **Continuous Particle classification in microfluidic system**. In: *μTAS 2007 - Eleventh International Conference on Miniaturized Systems for Life Sciences and Chemistry: 2007; Paris; 2007*.
249. Faivre M, Abkarian M, Bickraj K, Stone HA: **Geometrical focusing of cells in a microfluidic device: An approach to separate blood plasma**. *Biorheology* 2006, **43**(2):147-159.
250. Adler SM, Denton RL: **Erythrocyte sedimentation-rate in newborn period**. *Journal of Pediatrics* 1975, **86**(6):942-948.
251. Cantini F, Salvarani C, Olivieri I: **Erythrocyte sedimentation rate and C-reactive protein in the diagnosis of polymyalgia rheumatica**. *Annals of Internal Medicine* 1998, **128**(10):873-874.
252. Erkhov VS, Ageenko AI: **Detecting blood group antigen on human cells|is based on erythrocyte sedimentation rates**. In.; 1997.
253. Wetteland P, Roger M, Solberg HE, Iversen OH: **Population-based erythrocyte sedimentation rates in 3910 subjectively healthy Norwegian adults. A statistical study based on men and women from the Oslo area**. *Journal of Internal Medicine* 1996, **240**(3):125-131.
254. Russom A, Sethu P, Irimia D, Mindrinos MN, Calvan SE, Iris GA, Finnerty C, Tannahill C, Abouhamze A, Wilhelmy J *et al*: **Inflammation and Host Response to Injury Large Scale Collaborative Research Program. Microfluidic leukocyte isolation for gene expression analysis in critically ill hospitalized patients**. *Clinical Chemistry* 2008, **54**(5):891-900.
255. Sethu P, Anahtar M, Moldawer LL, Tompkins RG, Toner M: **Continuous row microfluidic device for rapid erythrocyte lysis**. *Analytical Chemistry* 2004, **76**(21):6247-6253.
256. Sethu P, Moldawer LL, Mindrinos MN, Scumpia PO, Tannahill CL, Wilhelmy J, Efron PA, Brownstein BH, Tompkins RG, Toner M: **Microfluidic isolation of leukocytes from whole blood for phenotype and gene expression analysis**. *Analytical Chemistry* 2006, **78**(15):5453-5461.
257. Stroock AD, Dertinger SKW, Ajdari A, Mezic I, Stone HA, Whitesides GM: **Chaotic mixer for microchannels**. *Science* 2002, **295**(5555):647-651.
258. Yang YJ, Liao HH, Huang KH, Huang YY, Lin CW, Yang LJ, Jaw FS, Chang PZ, Lee CK: **Novel designs of herringbone chaotic mixers**. In: *1st IEEE International Conference on Nano/Micro Engineered and Molecular Systems, Vols 1-3: 2006; 2006*: 1307-1310.
259. Dimaki M, Lange JM, Vazquez P, Shah PJ, Okkels F, Svendsen WE: **Comsol Multiphysics Simulations of Microfluidic Systems for Biomedical Applications**. In: *Proceedings of the COMSOL User Conference 2008, Hannover, Germany. 2008*.
260. Yang JT, Huang KJ, Lin YC: **Geometric effects on fluid mixing in passive grooved micromixers**. *Lab on a Chip* 2005, **5**(10):1140-1147.
261. Liu CC, Young JDE: **A semi-automated microassay for complement activity**. *Journal of Immunological Methods* 1988, **114**(1-2):33-39.
262. Rummage JA, Leu RW: **Photometric microassay for quantitation of macrophage FC and C3B receptor function**. *Journal of Immunological Methods* 1985, **77**(1):155-163.
263. Williams AR, Miller DL: **Photometric detection of ATP release from human-erythrocyte exposed to ultrasonically activated gas-filled pores**. *Ultrasound in Medicine and Biology* 1980, **6**(3):251-256.
264. Tan WH, Takeuchi S: **A trap-and-release integrated microfluidic system for dynamic microarray applications**. *Proceedings of the National Academy of Sciences of the United States of America* 2007, **104**(4):1146-1151.
265. Tan WH, Takeuchi S: **Dynamic microarray system with gentle retrieval mechanism for cell-encapsulating hydrogel beads**. *Lab on a Chip* 2008, **8**(2):259-266.
266. Lange J: **Growth of peripheral T-lymphocytes on chip**. PhD Thesis, Technical University of Denmark; 2010.



267. Bogar L, Tekeres M: **Leukocyte flotation during gravity sedimentation of the whole blood.** *Clinical Hemorheology and Microcirculation* 2000, **22**(1):29-33.
268. Langehanenberg P, Ivanova L, Bernhardt I, Ketelhut S, Vollmer A, Dirksen D, Georgiev G, von Bally G, Kemper B: **Automated three-dimensional tracking of living cells by digital holographic microscopy.** *Journal of Biomedical Optics* 2009, **14**(1).
269. Wray W, Stubblefield E: **A new method for rapid isolation of chromosomes, mitotic apparatus, or nuclei from mammalian fibroblasts at near neutral pH.** *Experimental Cell Research* 1970, **59**(3):469-8.
270. Harned HS, Nuttall RL: **The Differential Diffusion Coefficient of Potassium Chloride in aqueous solutions.** *Journal of the American Chemical Society* 1949, **71**(4):1460-1463.
271. Bundgaard F: **Prototyping of Microfluidic Systems with Integrated Waveguides in Cyclic Olefin Copolymer (COC).** PhD thesis. Technical University of Denmark; 2006.
272. Baudach S, Bonse J, Kruger J, Kautek W: **Ultrashort pulse laser ablation of polycarbonate and polymethylmethacrylate.** *Applied Surface Science* 2000, **154**:555-560.
273. Eddings MA, Johnson MA, Gale BK: **Determining the optimal PDMS-PDMS bonding technique for microfluidic devices.** *Journal of Micromechanics and Microengineering* 2008, **18**(6).
274. Satyanarayana S, Karnik RN, Majumdar A: **Stamp-and-stick room-temperature bonding technique for microdevices.** *Journal of Microelectromechanical Systems* 2005, **14**(2):392-399.
275. Truckenmuller R, Henzi P, Herrmann D, Saile V, Schomburg WK: **A new bonding process for polymer micro- and nanostructures based on near-surface degradation.** *Mems 2004: 17th IEEE International Conference on Micro Electro Mechanical Systems, Technical Digest* 2004:761-764.
276. Truckenmuller R, Henzi P, Herrmann D, Saile V, Schomburg WK: **Bonding of polymer microstructures by UV irradiation and subsequent welding at low temperatures.** *Microsystem Technologies-Micro-and Nanosystems-Information Storage and Processing Systems* 2004, **10**(5):372-374.
277. Lyons AB: **Divided we stand: Tracking cell proliferation with carboxyfluorescein diacetate succinimidyl ester.** *Immunology and Cell Biology* 1999, **77**(6):509-515.
278. Lyons AB: **Analysing cell division in vivo and in vitro using flow cytometric measurement of CFSE dye dilution.** *Journal of Immunological Methods* 2000, **243**(1-2):147-154.
279. Lyons AB, Hasbold J, Hodgkin PD: **Flow cytometric analysis of cell division history using dilution of carboxyfluorescein diacetate succinimidyl ester, a stably integrated fluorescent probe.** *Methods in Cell Biology*, Vol 63 2001, **63**:375-398.

# APPENDIX A

# A microfluidic system to capture single cells

Pranjul Shah\* and Jacob Moresco Lange†

MIC – Department of Micro and Nanotechnology, DTU bldg. 345 east  
Technical University of Denmark, DK-2800 Kongens Lyngby, Denmark

(Dated: 21 June, 2007)

The present paper is written for PhD course 33641, *Topics in theoretical microfluidics*. We here present a microfluidic system capable of capturing single cells using hydrodynamic confinement. The system has been designed for downstream processing of cellular contents. We present a theoretical study of the system which shows that the system should perform best with four or more traps connected in series.

PACS numbers: 47.65.+a, 47.32.-y, 47.70.-n, 85.90.+h

## I. INTRODUCTION

Chromosomal rearrangements, known as translocation, may result in diseases such as retardation and cancer but the analysis of chromosomes from one single patient easily takes weeks or months. Thus, it is desirable to automate the process, which may indeed be realized by "on chip" analysis. One of the challenges, however, is the dynamic nature of chromosomal architecture meaning that the volume of e.g. chromosome 1 in one cell may be different from another cell (although the contained information is identical). Therefore, single cell analysis is desirable if facilitating a robust capture of single cells of various sizes (e.g diameter of 8-15  $\mu\text{m}$ ) followed by their lysis and subsequent trafficking of the chromosomes (structures of approximately 1-6  $\mu\text{m}$ ) to the "analysis area". Many approaches have indeed been made; Deutsch *et al*[1] fabricated a chamber with small reservoirs with the size of a cell facilitating the isolation of single cells, and Carlo *et al*[2] succeeded in arraying cells using simple structural traps. Although facilitating the isolation of a single cell, they do not facilitate the subsequent trafficking of single cell material with the size of condensed chromosomes. Tan *et al*[3] developed a design for arraying particles using flow dynamics combined with structural traps and we used a similar principle in our approach while keeping an eye on downstream processing of single cell material.

## II. DESIGN

An overview of the trap is given in figure 1.

This system consists of two main features. Firstly, the long meandering channel with  $n$  number of repeats which finally joins the outlet channel. Secondly, the  $n$  number of traps which lie parallel to the meandering channel and connect the inlet channel to the outlet channel.

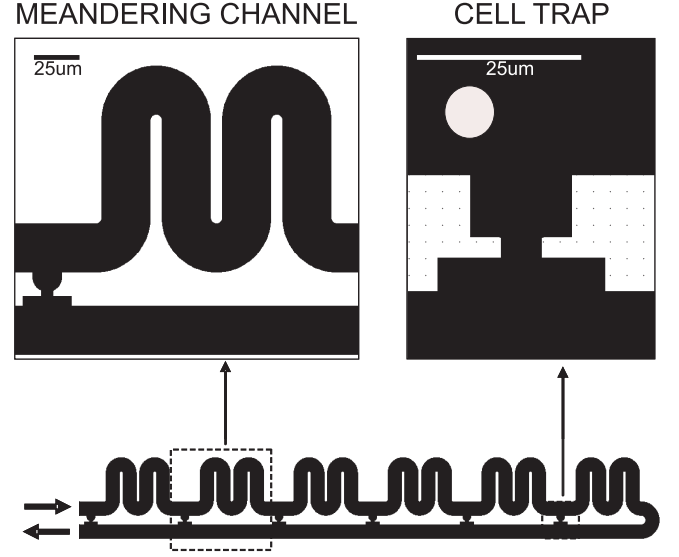


FIG. 1: Design of the system cell trap system

## III. MATHEMATICAL DESCRIPTION

### A. Validity of Hagen-Poiseuille law

The nonlinear term in the Navier-Stokes equation may often be neglected in microfluidics because of translational invariance. In the design presented here the traps introduces potential contribution from the non-linear term, but at small Reynolds numbers this contribution may be neglected. Ideally Reynolds number should be found numerically through the whole system but we restrict our analysis to three positions in the system, namely the main channel and the two parts of the trap (see below). Reynolds number ( $Re$ ) can be calculated using:

$$Re = \frac{\rho V_0 h}{\eta} \quad (1)$$

where  $\rho$  is the density,  $V_0$  is the average velocity,  $h$  is the smallest length-scale and  $\eta$  is the viscosity of the liquid.

\*pjs@mic.dtu.dk

†jml@mic.dtu.dk

Using an average velocity of  $10 \text{ mm s}^{-1}$  and the viscosity of water,  $Re$  becomes 0.25, 0.15 and 0.06 respectively. Thus we consider the nonlinear term in Navier-Stokes as negligible and the Hagen-Poiseuille law should be valid since we expect to work with much lower velocities. The following analysis will therefore originate from an equivalent circuit diagram found in the following sections.

## B. Equivalent Circuit

### 1. Case: One trap

Imagine, a system where we have just a single cell trap in the microfluidic circuit (Fig.2a). Considering that a cell is present at the point A, a cell in the fluid will have choice of two pathways. Either travel the shorter distance through trap or take the longer path through the meander and back to the outlet channel. The particle at this point will consider the hydraulic resistances ( $R_{hyd}$ ) of both the paths to decide on the pathway (Fig.2b).

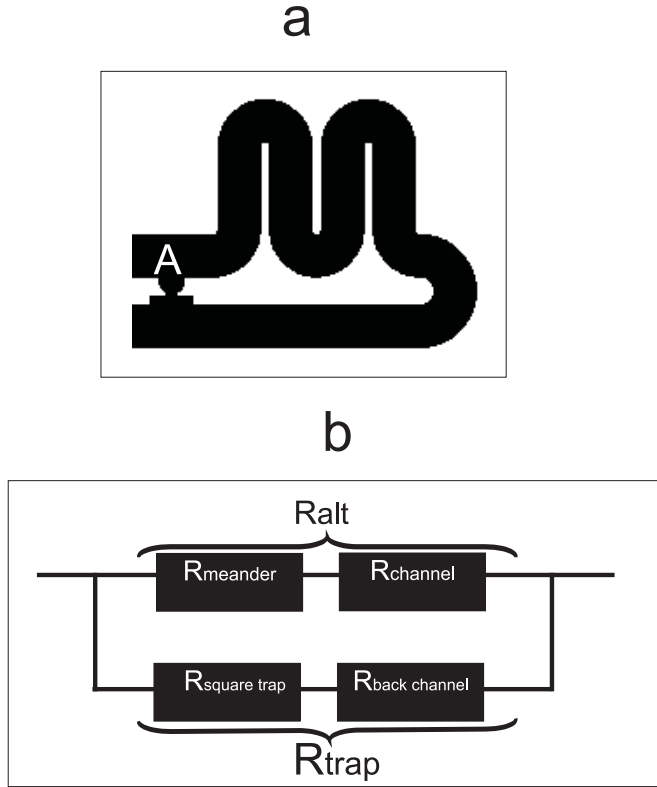


FIG. 2: (a) Design of the system (b)Equivalent electrical resistance circuit

Considering the  $R_{hyd}$  of the trap as  $R_{trap}$  and of the alternate route with the meander and the straight outlet channel as  $R_{alt}$  then we know that the majority of the flow (and thereby the majority of cells) will follow the trap-path only if:  $\frac{R_{trap}}{R_{alt}} < 1$  or  $R_{trap} < R_{alt}$ . For this

case, as

$$R_{alt} = R_{meander} + R_{channel} \quad (2)$$

We know that the  $R_{hyd}$ 's of meander( $R_{meander}$ ) and following outlet channel ( $R_{channel}$ ) can be calculated as below [4].

$$R_{hyd} = \frac{12 \cdot \eta \cdot L}{1 - (0.913) \cdot (0.63)) \cdot (25 \cdot 10^{-6}m)^4} \quad (3)$$

where  $L_{meander} = 300 \cdot 10^{-6}m$  and  $L_{channel} = 150 \cdot 10^{-6}m$ .

The hydraulic resistance of the trap,  $R_{trap}$ , is calculated as the sum of hydraulic resistances of the cell trap itself,  $R_{sq}$ , ( $15 \mu m$  cell trap square) plus the hydraulic resistance of the  $6 \mu m$  connection to the outlet channel,  $R_{connection}$ .

$$R_{trap} = R_{sq} + R_{connection} \quad (4)$$

Placing all the values for our design, we can calculate that:

$$R_{meander} = 2.18 \cdot 10^{13} \text{ Pa s m}^{-3} \quad (5)$$

$$R_{channel} = 1.09 \cdot 10^{13} \text{ Pa s m}^{-3} \quad (6)$$

$$\therefore R_{alt} = 3.27 \cdot 10^{13} \text{ Pa s m}^{-3} \quad (7)$$

In a similar manner we find the hydraulic resistance of the trap,  $R_{trap}$ .

$$R_{trap} = 1.91 \cdot 10^{13} \text{ Pa s m}^{-3} \quad (8)$$

Thus,

$$\frac{R_{trap}}{R_{alt}} = 0.58 \quad (9)$$

Therefore, at the first trap as  $R_{trap} < R_{alt}$  the majority of the cells will tend to flow into the trap. While  $\approx 63\%$  of the flow will flow through the trap  $\approx 37\%$  of the flow will go through the alternate route through meander providing a higher chance that a cell will get trapped in the trap.

### 2. Case: Two traps

Considering that we add one more cell trap to the previously described single cell trap system, we have an array of two cell traps in series as shown in fig.3a.

When we draw the equivalent electrical circuit, we realize it can be considered as in fig 3b. Here again, the particle flowing into the microfluidic channel will face two choices at junction A. It will be faced with the hydraulic resistances of the trap  $R_{trap}$  and series of meander and the single trap system as considered in case A.

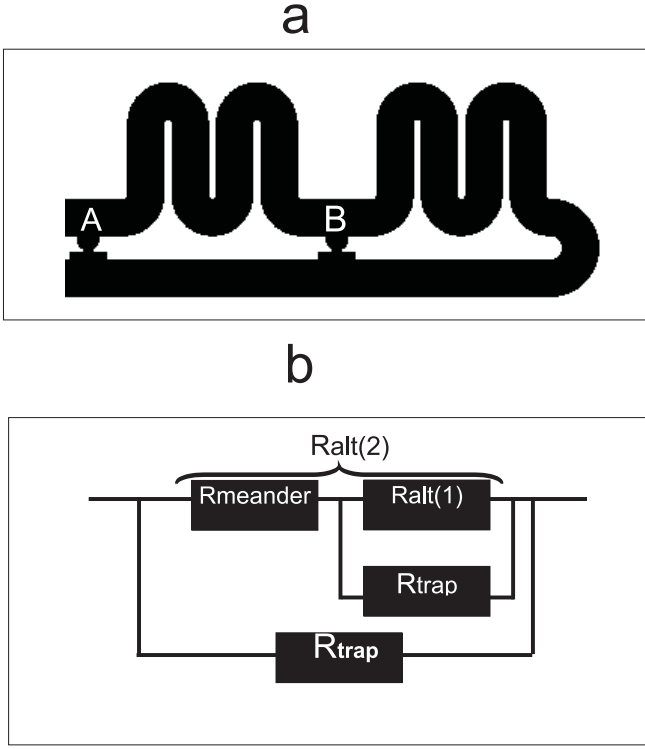


FIG. 3: (a) Design of the system with two cell traps (b)Equivalent electrical resistance circuit

i.e.  $R_{trap}/R_{alt}(1)$ , where  $R_{alt(i)}$  is the hydraulic resistance of the alternate route with  $i$  number of cell traps. Hence we get:

$$R_{alt}(2) = R_{alt}(1) + R_{trap}/R_{alt}(1) \quad (10)$$

$$R_{alt}(2) = 4.47 \cdot 10^{13} \text{ Pa s m}^{-3} \quad (11)$$

In this case, the particle will flow towards the trap considering  $R_{trap} < R_{alt}(2)$ . Now the resistance ratio is

$$\frac{R_{trap}}{R_{alt}} = 0.43 \quad (12)$$

meaning that  $\approx 70\%$  of flow will go through the trap and the rest will continue through the meander.

Once, we have a cell trapped in the trap, we would like to see if the flow will then be diverted towards the next available trap. To calculate, the new  $R_{hyd}$ ,  $R_{trap,cell}$ , in this case (figure 4a), we consider the cell to be a cube of height  $10 \mu\text{m}$  and in this case as shown in (figure 4b) the height of the trap will reduce to  $15 \mu\text{m}$ , which will increase the hydraulic resistance of the trap as  $R_{hyd} \propto \frac{1}{h^4}$ .

Hence we get,  $R_{trap,cell} = 1.12 \cdot 10^{14} \text{ Pa s m}^{-3}$ .

Thus,  $R_{trap,cell} > R_{alt}(2)$ , and so most of the fluid will choose to flow through the meander and ignore the

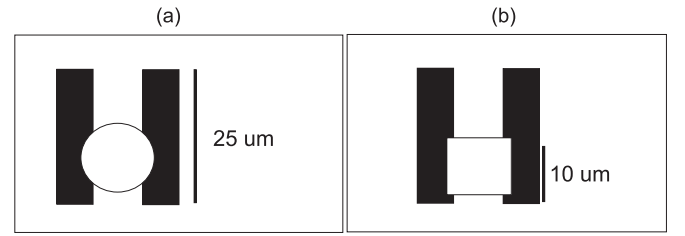


FIG. 4: (a) Cross section of a cell trap with a spherical cell (b) Cross section of a cell trap with an assumed cubic cell trapped

trap.

Also the flow division factor can be calculated as,

$$\frac{R_{alt}(2)}{R_{trap,cell}} = 0.40$$

Hence,  $\approx 70\%$  of the flow will travel through meander, while only  $\approx 30\%$  will choose to go through the reduced trap channel.

For the next cell reaching the point B, the cell will consider the system as a single trap system as discussed before and the cells will try to flow through the trap and once a cell is trapped the rest of the cells will exit through the meander to the outlet channel.

### 3. Case: Three traps

In this case, we place three traps in series in a microfluidic chip as shown in fig. Continuing the argument for a cell at junction A in fig.5a like before, the cell will choose its path based on  $R_{alt(3)}$  and  $R_{trap}$ .

$$\text{Here, } R_{alt(3)} = R_{alt}(1) + R_{trap} // R_{alt}(2)$$

$$R_{alt(3)} = 4.61 \cdot 10^{13} \text{ Pa s m}^{-3}$$

Thus,  $R_{alt(3)} \gg R_{trap}$ , hence the cells will tend to flow towards the trap and later the rest of the cells will continue to travel through the meanders as  $R_{trap,cell} \gg R_{alt(3)}$ .

### 4. General

Finally, considering the above three cases, we can now generalize this system and conclude the behavior for a system with  $n$  cell traps in series (fig.6),

$$R_{alt(n)} = R_{alt}(1) + R_{trap} // R_{alt}(n-1) \quad (13)$$

which implies that as we pass through such a system, the hydraulic resistance of the alternate route will continue to decrease with respect to  $n$ .

The graph of  $R_{alt(n)}$  for  $n = 10$ , is represented in fig 7.

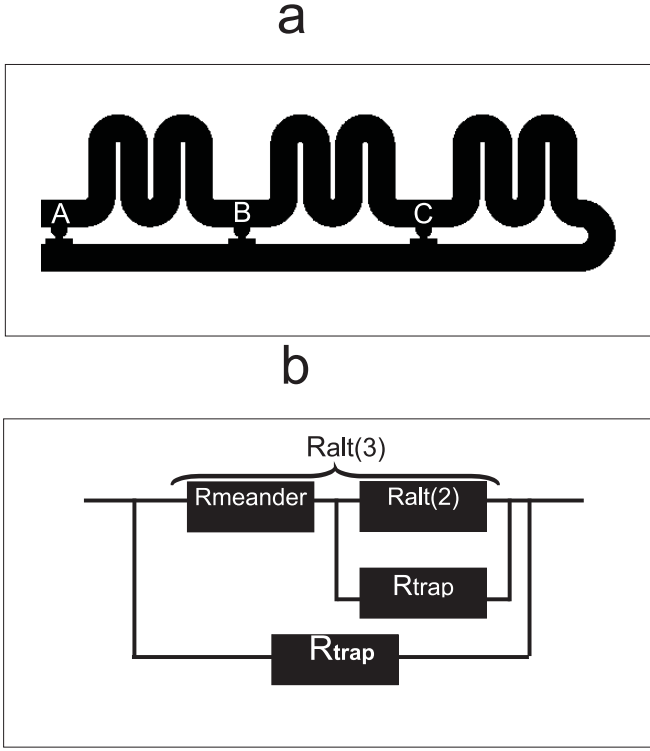


FIG. 5: (a) Design of the system with three cell traps (b)Equivalent electrical resistance circuit

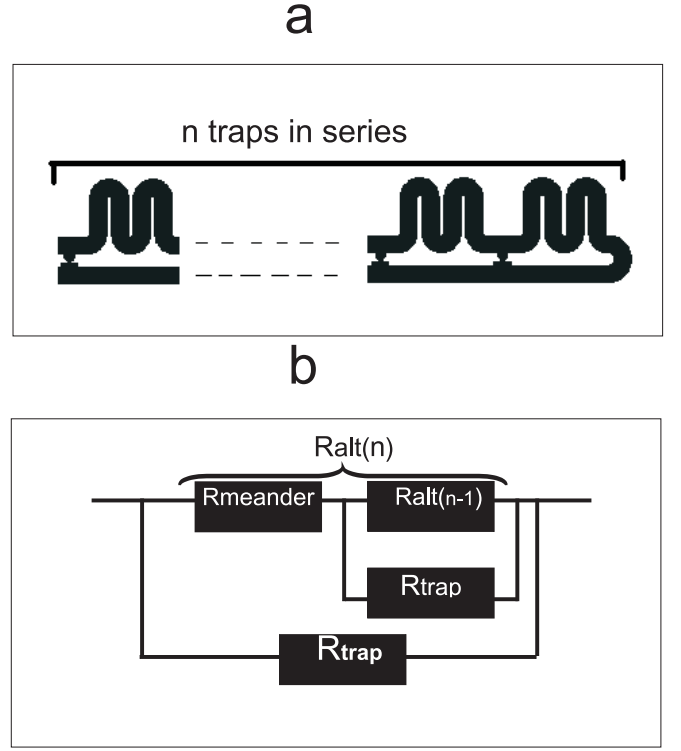


FIG. 6: (a) Design of the system with n cell traps (b)Equivalent electrical resistance circuit

This graph implies that for a system with  $n$  greater than 4, the hydraulic resistance of the alternate route will always be almost constant. Thus, the change in resistance for the alternative route becomes almost zero for  $n = [4, \infty]$ .

Hence, the system will be able to function for a series of large number of arrays because at each trap the ratio

$$\frac{R_{trap}}{R_{alt(n)}} \approx 0.4 < 1, \text{ for } n = [4, \infty] \quad (14)$$

Hence, the cells will be trapped at each trap along the system. Also as the ratio

$$\frac{R_{trap, cell}}{R_{alt(n)}} \approx \text{constant} > 1, \text{ for } n = [4, \infty] \quad (15)$$

Once a trap captures on cell, the remainder of cells will move through the meander or alternate route until they find the next cell trap.

#### IV. CONCLUSION

Our goal for this system was to facilitate the capture of single cells using the hydrodynamic resistance of traps.

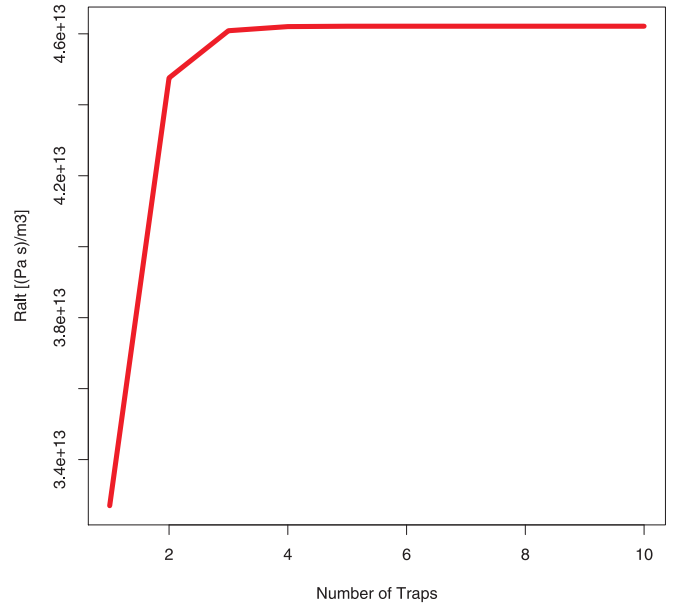


FIG. 7: Graph of  $R_{alt(n)}$  for  $n = 10$

We here presented a theoretical study into the performance of the system, which concludes that the system should function the best for  $n$  number of traps where  $n$  is greater than four. We foresee that this system could be used for the release of chromosomes from single cells

to develop single cell analysis systems.

### Acknowledgement

We are very thankful for the help from Maria Dimaki for helping us visualize the system.

- 
- [1] M. Deutsch, A. Deutsch, O. Shirihai, I. Hurevich, E. Afrimzon, Y. Shafran, and N. Zurgil, *Lab Chip* **6**, 995 (2006).
  - [2] D. Di Carlo, L. Y. Wu, and L. P. Lee, *Lab Chip* **6**, 1445 (2006).
  - [3] W.-H. Tan and S. Takeuchi, *A trap-and-release integrated microfluidic system for dynamic microarray applications* (2007).
  - [4] H. Bruus, *Theoretical microfluidics* (2006).



# APPENDIX B

# Advanced microtechnologies for detection of chromosome abnormalities

**Dorota Kwasny, Indumathi Vedarethinam, Pranjul Shah, Maria Dimaki, Asli Silahtaroglu, Zeynep Tumer, Winnie E. Svendsen**

The overall goal of cytogenetic analysis is to detect chromosome abnormalities in patient samples. This analysis is a standard procedure for prenatal as well as postnatal diagnosis and cancer detection. Cytogenetic techniques such as karyotyping by banding have been for the last years complemented by molecular cytogenetic techniques such as fluorescent *in situ* hybridization (FISH). FISH is recently evolving towards on chip detection of chromosome abnormalities with the development of microsystems for FISH analysis. The challenges addressed by the developed microsystems are mainly the automation of the assay performance, reduction in probe volume, as well as reduction of assay time. The recent focus on the development of automated systems for performing FISH on chip is summarized in this review.

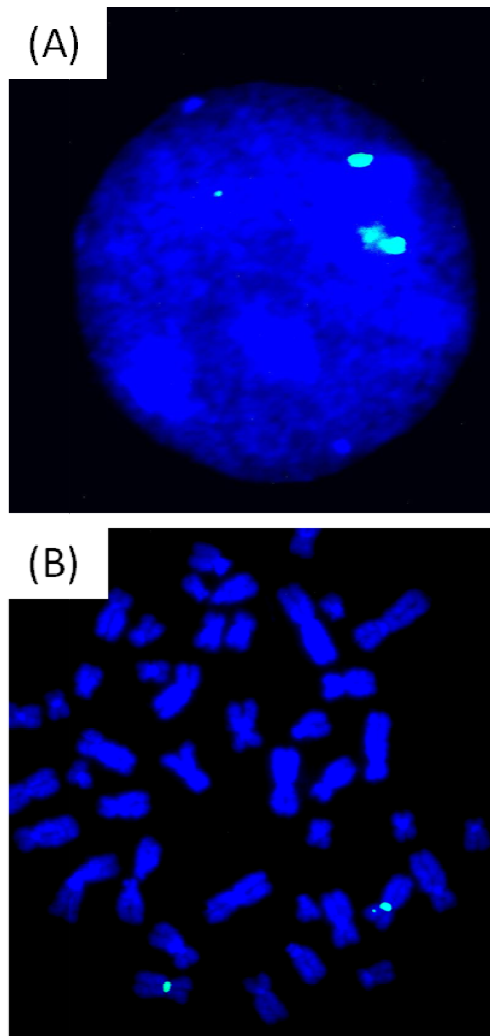
**Keywords:** Fluorescent in situ hybridization, FISH on chip, microsystems, cytogenetic analysis

## Introduction

Conventional methods for disease diagnosis are based on analysis of cells, biochemical pathways, and infectious agents. Chromosome studies provide cytogenetists with valuable information as chromosome disorders are a major category of genetic disease [1]. The incidence of chromosome abnormalities in live births is around 0.7 % [2]. Specific chromosome abnormalities are responsible for more than 100 identifiable syndromes, thus an understanding of cytogenetics and chromosome disorders is important [1]. The rapidly growing field of biomedicine focuses on detecting the genetic causes of diseases by means of molecular diagnostics. This involves studying of DNA and RNA as diagnostic targets. Cytogenetics is a study that concentrates on cell analysis with special focus on chromosomes. The conventional cytogenetic analysis known as chromosome analysis or karyotyping is based on the analysis of metaphase chromosomes through banding techniques and microscopy. The typical resolution is in the range of 5 – 10 megabases and depends on the compaction of the chromosome and number of bands. Karyotyping is still a gold standard for cytogenetics; however, new technologies have been developed to improve the resolution power of chromosome abnormalities detection. One of the mostly used techniques in molecular cytogenetics is fluorescence *in situ* hybridization, which has been a bridge between cytogenetics and molecular genetics. Even though preparation of FISH analysis is laborious it has grown in popularity in cytogenetic laboratories all over the world. However, to make the analysis a more standard procedure in genetic diagnostics some efforts need to be done to automate the protocol. Nowadays researchers focus on the development of integrated, miniaturized systems for more sensitive and rapid analysis of biological samples at low cost. Recently some efforts have been made towards fabrication of systems for analysis of chromosome abnormalities with the goal being a reduction of costs, sample volume, and hybridization time related to FISH analysis, and automation of assay. In this paper, we review the current state of the art of the microsystems developed for abnormalities detection.

## Chromosome abnormalities

Chromosomes are nuclear structures composed of DNA and proteins. Their structure and number are highly preserved in different organisms with a typical human cell containing 46 chromosomes. Conventional and molecular cytogenetic techniques are used to study the structure and number of chromosomes and to detect chromosome abnormalities [3]. A chromosome abnormality may be numerical or structural. Numerical abnormalities such as Down syndrome (three copies of chromosome 21), Turner syndrome (X chromosome monosomy) occur when an atypical chromosome number is present in the cell. Structural abnormalities can be balanced rearrangements, such as inversions or translocations; or unbalanced, such as deletions and duplications. Depending on the nature and size of the chromosome abnormality, different cytogenetic and molecular cytogenetic techniques are employed. Chromosome abnormalities are often associated with congenital anomalies, dysmorphic features, growth retardation and learning disabilities [4].



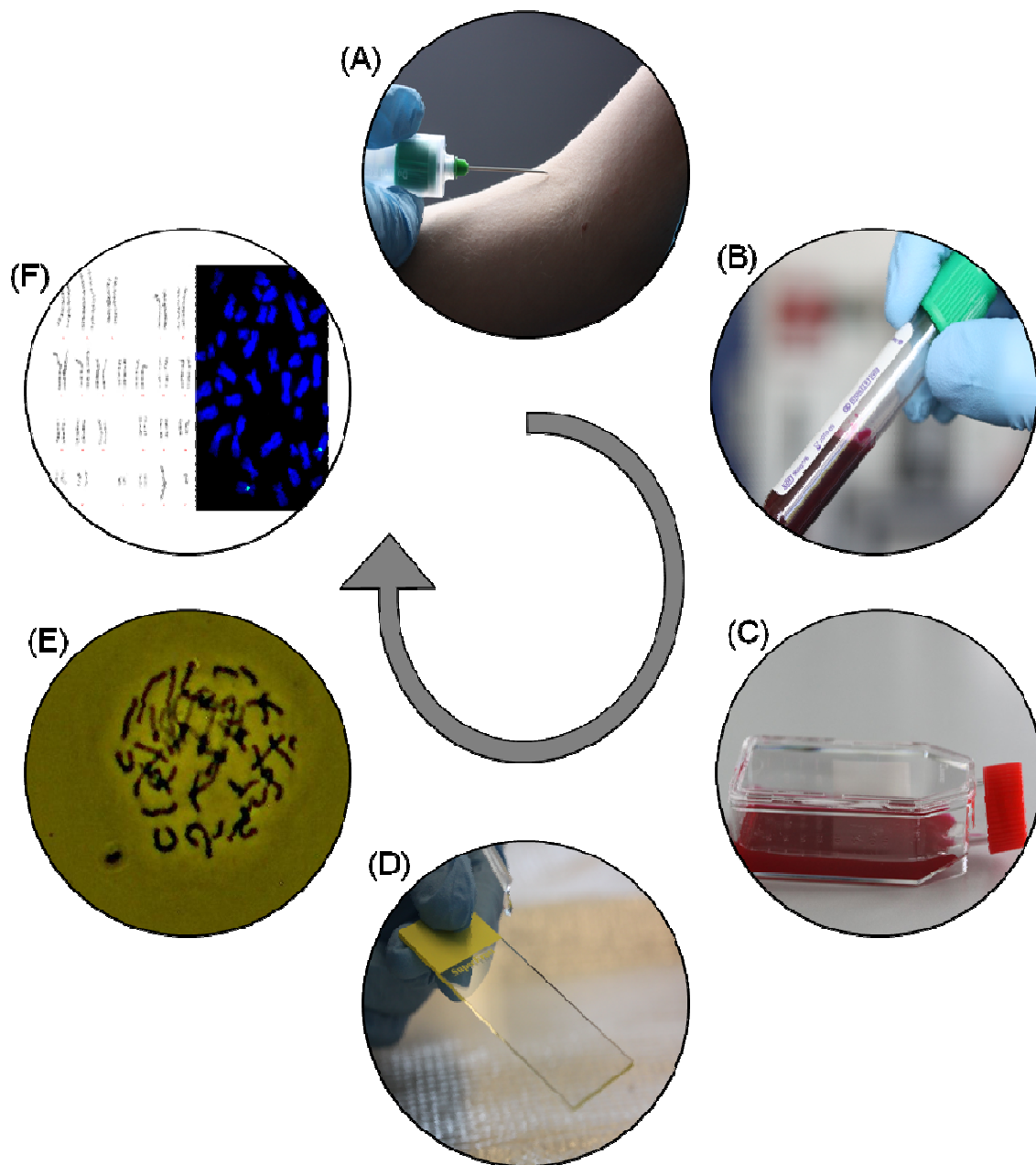
**Figure 1** An interphase nucleus (blue) (A) and metaphase spreads (B) with X centromeric FISH probes (green dots).

Furthermore, numerical chromosome abnormalities, deletions and translocations are also associated with cancer [5, 6]. Over the years cytogenetic analysis has become an integral part of genetic disorders and myeloid malignancies diagnosis. Genetic material is available in cell nucleus in different forms depending on the cell cycle phase. During interphase cells do not divide, the DNA in the form of chromatin is enclosed in a nuclear membrane with the chromosomes visible but not detectable as single entities (Fig.1A). The most condensed and highly

coiled form of DNA – metaphase chromosomes - is visible during a metaphase, with the chromosomes still enclosed in a nuclear membrane (Fig.1B).

## **Classical and molecular cytogenetics**

Any cytogenetic analysis starts with obtaining the cells as a chromosome source. The most commonly used cells for cytogenetic analysis are peripheral T-lymphocytes, because they can be obtained from peripheric blood samples (Fig.2A, B). To perform analysis on metaphase chromosome the cell culture is required to increase the amount of cells in metaphase (Fig.2C), which is not necessary for interphase analysis. Phytohemagglutinin is a typically used chemical to stimulate cell division during a 72 hours T-lymphocytes culture. A minimum of 20 cells needs to be fully analyzed to obtain reliable results [7]. A mitogenic stimulation with colchicine is further performed to arrest the cells in metaphase and thus increase the number of metaphase spreads for the analysis. After treatment with hypotonic solution, the cells are splashed on the glass slide with ice-cold water (Fig.2D) to obtain the metaphase spreads (Fig.2E). The karyotyping by banding relies on staining such chromosomes fixed on a surface and then further analyzing these under a microscope, while FISH requires a use of fluorescently labeled probes (Fig.2F). FISH is based on the hybridization between two DNA sequences, a fluorescently labeled probe and its complementary sequence on a chromosome. The fluorescent microscopy visualization of a hybrid between a probe and genetic material reveals the presence, number and distinct location of targeted sequences [8, 9].



**Figure 2** The cytogenetics analysis protocol. Blood sample is collected from the patient (A). The collected blood (B) is cultured in a medium for 3 days at 37 °C (C). Colchicine is added at the end of the culture period to arrest the cells in metaphase. Followed by hypotonic treatment, the cells are splashed on a glass slide (D) to obtain metaphase chromosome spreads (E). At this point the chromosome spreads can either be analyzed by banding or FISH.

Over many years cytogenetic techniques have been evolving enabling more accurate and faster detection of chromosome abnormalities. Nevertheless, the conventional karyotyping by banding technique is still a standard procedure in cytogenetic laboratories over the world despite the need for trained technical staff [10-12]. Such a simple, but time-consuming analysis, allows for inexpensive diagnosis of numerical and structural chromosome aberrations at a limited resolution [13-15]. The main advantage of karyotyping by banding is that it is a whole genome screening technique, where the entire genome can be visualized at once [3]. The requirement for high quality metaphase chromosome spreads for karyotyping is challenging as some cells, such as solid tumor cells, cannot produce good spreads [12]. To overcome issues with the limited resolution of karyotyping, the requirement for dividing cell population and good quality metaphase spreads; a FISH technique is often used. The conventional banding analysis can only be carried out on metaphase chromosomes, while FISH may be

performed both on metaphase and interphase chromosomes. Introduced over 30 years ago, the FISH technique commenced a new era in the cytogenetic studies providing greater resolution than was possible with the karyotyping by banding technique [4, 10, 16, 17]. The typical resolution obtained with FISH is in the range of 10-100 kilo bases sequences while karyotyping by banding has a resolution of 5-10 mega bases [10, 13, 17, 18]. FISH provides a simple, fast and reliable means to assess genetic instability in cancer [5, 6, 19, 20]. Despite many advantages of performing FISH, it is not an alternative to karyotyping but a complementary technique.

## **FISH analysis**

For the cases involving chromosome abnormalities that need a higher resolution or analysis on non-dividing cells FISH is often applied. After fixing metaphase chromosomes or interphase nuclei to the glass slide FISH analysis starts. Firstly, chromosomes are washed, dehydrated through a series of alcohol washes and air-dried. A probe solution is then prepared by mixing it with a hybridization buffer containing formamide, salt and dextran sulfate [21]. After that both, the chromosomes on a glass slide and the probe solution are heat denatured. The probe in solution is placed immediately on ice and then applied directly to the slides. They are incubated overnight at 37°C in a moist chamber. After several washing steps to remove the unbound or nonspecifically adsorbed probe the slides are incubated in a dye solution (e.g. DAPI) to label the chromosomes. Stained chromosomes are visualized under an epifluorescent microscope with an appropriate set of filters to observe the probe signal and the chromosomes [22].

FISH complements karyotyping by banding, thus is often prepared as a second step to enhance diagnostic efficiency [7, 9, 23, 24]. Moreover, FISH enables identification of numerous microdeletions and microduplications syndromes that are not generally detectable by classical cytogenetics. Thus, it is often applied for cases with a visibly affected phenotype and apparently normal karyotype to identify otherwise undetectable chromosome abnormalities. Although, one of major limitations of FISH is that it can only be used to detect known abnormalities. It depends on a probe targeting a specific DNA sequence, e.g., to detect known translocations, microdeletions or specific chromosomes and hence can only be used to address questions for which DNA probes are available.

## **FISH techniques**

One of the attractive features of FISH is that it can be performed both on metaphase spreads but also on interphase nuclei fixed on a glass slide providing valuable information about chromosome abnormalities [13, 20]. Interphase FISH has a great potential for screening large number of cells, as well as for examining archival samples. Interphase FISH is applicable for testing solid tumors as it eliminates the need for dividing cell population. It can also be performed very rapidly within 24 hours, as no cell culturing is required. Tumor cells often show numerical or structural changes in chromosomes that may provide information about the changes that initiated tumor formation. The analysis of metaphase chromosomes in solid tumors is hampered, as extensive culturing is necessary to obtain sufficient number of mitotic cells, which in few cases may induce additional chromosomal changes. Furthermore, the metaphase spreads obtained from solid tumors have poor quality that makes their proper analysis troublesome [17, 25, 26]. Interphase FISH is used to identify numerical abnormalities as well as specific structural abnormalities, by targeting them with a specific DNA probe.

On the other hand, metaphase chromosomes are widely used in cytogenetic analysis for standard karyotyping and FISH analysis. FISH can be used in metaphase cells to detect specific microdeletions at high resolution. It is also applicable in cases where it is troublesome to determine whether a chromosome has a simple deletion or is involved in some more complex rearrangement. Using metaphase spreads for analysis is beneficial as one can visualize the entire genome at once. Applying whole chromosome FISH probes, a complex mixture of sequences from the entire length of specific chromosomes available for all human chromosomes, enables detecting abnormalities at the genome level [27]. Simultaneous visualization of spectrally distinct fluorophores enabled the

As submitted to BioEssays

representation of different chromosomes with a unique fluorescent signature with a potential application to reveal complex structural abnormalities [3, 11, 13, 15, 20, 28, 29]. By performing such analysis we can obtain information about the unknown translocations between chromosomes at higher resolution than achievable by karyotyping by banding [20, 30-32]. However, such method requires specialized computer software, expensive equipment, and complex analysis by skilled technicians that can interpret the obtained data [3]. Moreover, limited use of FISH is also attributed to the high cost of FISH probes necessary to detect the chromosome abnormalities.

Generally speaking, FISH techniques are utterly useful for the confirmation of chromosome abnormalities suspected based on previous findings, with the use of specific DNA probes. Its main advantage lies in the analysis that can be performed on both interphase and metaphase chromosomes depending on the specific disorder to be detected. Interphase FISH can be performed very fast, but metaphase FISH offers observation of the entire genome that may enable identification of complex rearrangements at a genome level. These techniques present many opportunities; however, their major disadvantage is the cost of reagents (mainly probes) and the requirement for an expensive high-resolution microscope. Development of novel micro assays could significantly increase the usage of these assays broadening our knowledge on chromosome abnormalities.

## **FISH techniques worldwide application**

For the FISH techniques to be used routinely in the laboratories all over the world certain challenges need to be addressed. As stated above the FISH techniques are continuously evolving, however their use is still limited due to high cost and long experimental time. Their use is sometimes advantageous as they are capable of detecting chromosome abnormalities at a higher resolution than karyotyping by banding.

The major drawback of FISH analysis is the cost of the reagents used for the assays, mainly the fluorescent probes. In standard lab protocols 10-15  $\mu$ l of probe are used per slide containing metaphase spreads or interphase nuclei [19]. Such analysis is normally performed on a single patient's sample, thus the cost of a single analysis is extremely high. The development of a high throughput device for metaphase or interphase FISH analysis would reduce the volume of the probe used per single sample, at the same time reducing the cost of an experiment. Also, addressing the need for reduction in probe volume for single analysis would greatly increase the application of FISH in routine analysis.

Another bottleneck of the analysis is the long experiment time. To perform a complete FISH analysis, even well trained technicians spend several hours in sample preparation as well as the waiting time in between each pre- and post- hybridization washes. There are at least 12-15 different washes in a standard routine test that in total takes about 45 minutes. Apart from the cell culture work, the hybridization time is a very long process. At minimum, performing a FISH analysis with centromeric probes (repetitive sequences), will take 2 to 4 hours. Furthermore, in some FISH experiments the hybridization of a probe requires overnight incubation. The automation of sample preparation, probe delivery, imaging and analysis would result in molecular cytogenetic analysis to be performed routinely at the doctor's office as a point-of-care diagnosis.

For metaphase FISH analysis it is necessary to culture cells for three days. The disadvantage of such a culture method is the large volume of medium used and the fact that handling of suspension cells is tedious. This issue was currently addressed by developing a membrane based microfluidic bioreactor for suspension cell cultures, which makes preparation of chromosome spreads much easier [33, 34]. The proposed diffusion based microreactor facilitates culturing of lymphocytes but also expansion, hypotonic treatment, and fixation of cells with the possibility to avoid several tedious centrifugation steps [33]. Svendsen *et al.* developed a bioreactor for a suspension cells culture on the membrane with a microfluidic channel for media perfusion. The continuous flow ensures all the necessary nutrients to be delivered from the medium to the cells by diffusion. It enables fast solution changes for expansion and cell fixation to obtain high quality metaphase spreads. Separation of culture

As submitted to BioEssays



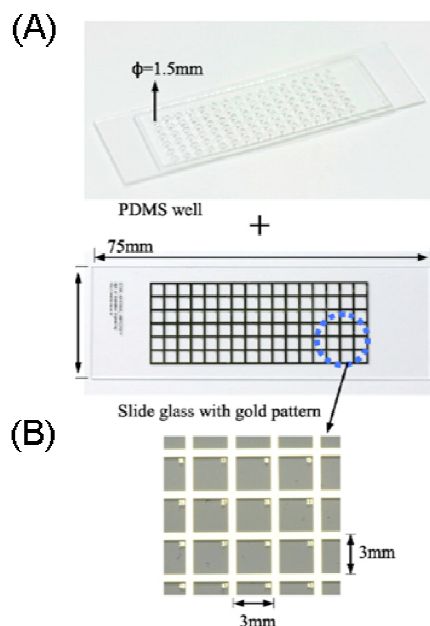
chamber by a membrane from the channel is beneficial as it protects the cells from air bubbles formed in the flowing medium and allows the perfusion to be started even before the cells settle on the membrane. Shah *et al.* modified the media perfusion channel to ensure more thorough transport of nutrients across the membrane to the resting cells [33]. Moreover, by performing CellTrace™ CFSE cell staining protocol it was demonstrated that cell proliferation on chip is better than in control experiment in a well plate culture.

One of the many advantages of microdevices for complete chromosome analysis is the possibility to perform high throughput analysis. In cytogenetic laboratories chromosome analysis is performed several times a day on different patient samples. High throughput automatic devices for cell culturing, preparation of chromosome spreads or interphase nuclei, followed by detail FISH analysis would drastically speed up the process and provide fast results.

## **Microsystems developed for FISH analysis**

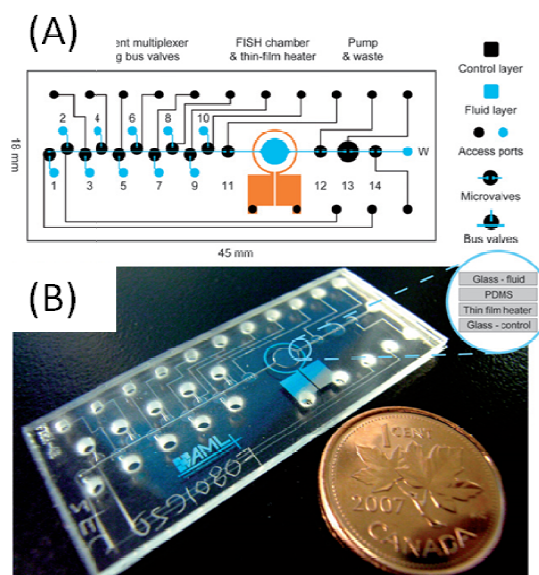
In recent years the integration and automation of cytogenetic techniques has gained more attention. Most reports in this field focus on the development of an integrated microfluidic chip for interphase FISH analysis. To our knowledge there has been only one report on a microfluidic platform for metaphase FISH on chip. This article reviews the recent developments in the field of microcytogenetics that address the need for automation, time and cost reduction in chromosome analysis.

In 2007, Lee *et al.*, presented one of the first examples of miniaturized devices for performing FISH analysis [35]. The presented work allows for high throughput FISH analysis on a cell array. The typically performed analysis lacks the possibility of conducting high throughput analysis as there is limited amount of samples available. To address this problem, the authors showed the possibility to array cells by spotting the small amounts of cell specimens onto a supporting matrix, which enables high throughput analysis. For the preparation of the chip, a glass slide was used as a supporting matrix. 1 mm thick perforated PDMS was bonded to a glass slide to form 96 cavities of 1.5 mm in diameter for spotting cells (Fig.3). To enable microscopic cell identification a matrix corresponding to the 96 PDMS wells was microfabricated by photolithography on a glass slide. They have showed that 1 µl samples were spotted onto each PDMS well followed by air drying, removal of PDMS cover and performing conventional FISH protocol. In this way, only 10 µl of probe were used to analyse 96 specimens. The device is very useful in mass sample analysis for the same kind of samples, in which the probe reduction is relevant. The authors have mentioned the probe volume reduction, but other major issues such as manual intervention and time consumption were not stated.



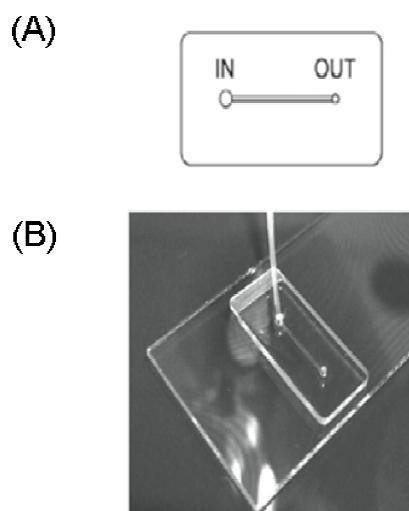
**Figure 3** Fabricated bio-cell chip slide. (A) A PDMS layer with 96 wells for multiple cell analysis. (B) A glass slide with a gold pattern for sample numbering (used with permission from Lee et al, 2007)

The first implementation of FISH on chip was showed in 2007 by Sieben, *et al.* [26]. They have adapted the conventional FISH except the cell immobilization step, where cell immobilization was achieved using temperature. They also investigated a method to reduce hybridization time by probe recirculation with on-chip peristaltic pumps, and electro-kinetic transport of probes by introducing the electrodes into the end-wells. By these two methods, they found out that electro-kinetic transport of the probes was slightly better than recirculation method. In addition, the electro-kinetic chip design is simpler than the recirculating micropump, which involves valves and complex micro fabrication. Nevertheless, by performing the analysis at microfluidic volumes, they were able to achieve a tenfold reduction in DNA probe reduction per test, with equivalent the cost reduction from \$90 for 10  $\mu\text{L}$  of probe, to \$9 for 1  $\mu\text{L}$ .



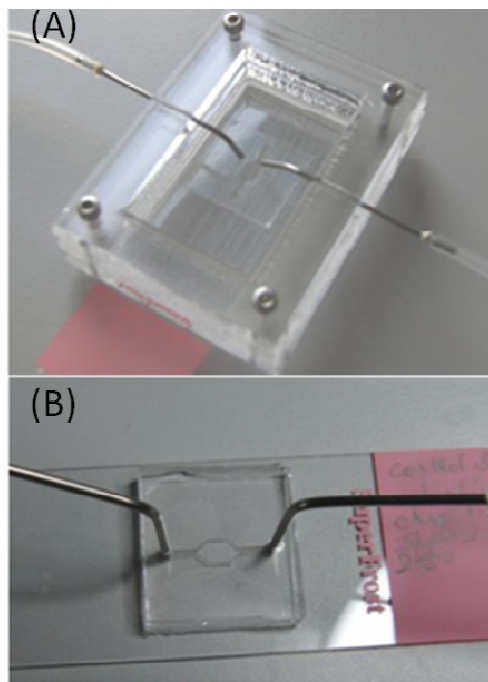
**Figure 4** (A) The mask layouts and dimensions of an integrated FISH microchip. The microchip includes a reagent multiplexer, a cell chamber with an integrated thin-film heater, and a peristaltic pump. (B) Image of a complete integrated FISH chip (used with permission from Sieben *et al*, 2008)

In 2008, Sieben, *et al.*, published another paper in which all previously performed steps with microfluidic FISH were integrated onto one chip and automated [36]. Similar to the recirculating design, the new chip consisted of a PDMS layer sandwiched between two glass layers, one of which carried fluids, while the other transmitted air pressure for valve control, e.g. for peristaltic pumping, which is a very complex fabricated system. With the valves operated by computer, preloaded reagents could be multiplexed through the hybridization chamber at appropriate intervals for each step of FISH. A copper thin-film heater was built into the design as well, for the cell-immobilization and denaturation steps (Fig.4). Unlike the previous designs, this new device did not focus on the reduction in hybridization time, but instead focused mainly on minimizing the labor time and automation of the microfluidics FISH chip. One of the issue with the conventional FISH, which takes more than an hour of on-and-off attention of a skilled technician, using their time inefficiently, whereas the automated microfluidic FISH device would reduce human intervention and only involve the technicians work during reagent preparation, and image analysis .



**Figure 5** Microfluidic device for miniaturized FISH. (A) Diagram of the microfluidic PDMS pad with inlet and outlet connected by a straight channel. (B) Complete structure of the FISH device with the PDMS pad assembled with a TiO<sub>2</sub> functionalized glass slide (used with permission from Zanardi *et al*, 2010)

The most recent advances in integrated interphase FISH analysis were presented in 2010 by Zanardi, *et al* [24]. They focused on the development of an analytical tool for performing interphase FISH on both living and fixed cells. The application of microfluidic technologies might reduce costs and improve assay performance by development of microchannels for easy reagent loading and cell immobilization. However, the fluid flowing in the microchannels causes intense shear stress on cells; this may result in their disruption or detachment from the surface. In this paper the authors' addressed this particular problem in the application of microfluidics for FISH. By changing the surface chemistry they enhanced the cell immobilization on the surface that significantly reduced the cells detachment due to shear stress. In this article, the entire glass slide is coated with nano structured TiO<sub>2</sub> using cluster beam technology which adds significant costs to the device owing to the need for access to cleanroom and costs of additional metal deposited. Moreover, routine genetic labs do not necessarily have access to cleanroom facilities, which makes the method very difficult to implement on a larger scale. The top cover bonded to the modified glass slide contains a microfluidic channel that is used for loading cells and other reagents in FISH protocol (Fig.5). Such a simple design facilitates handling of the fluids without generating bubbles that could affect assay performance.



**Figure 6** (A) The PMMA splashing device with two inlets for glacial water and cell suspension. (B) Fully assembled microFISH device with a PDMS chamber on a glass slide with chromosome spreads (from Vedarethinam *et al*, 2010).

In 2010, Vedarethinam *et al.* developed the first metaphase FISH device, which can be used to detect the microdeletion or specific translocation of unknown origin with high resolution [30]. Unlike interphase FISH, metaphase FISH is difficult to adapt to a closed microfluidic system. The chromosome immobilization needs preparation of chromosome spreads, which rely on certain factors, such as controlled angle of spotting [37], temperature gradient and humidity [38]. Recently, Qu *et al.* devised a chromosome dropper tool, which demonstrates that the dropping angle and height are the important factors getting good metaphase spreads on glass slides [37, 39].

Based on all these factors Vedarethinam *et al.* made a novel splashing device with open chamber, which allows for easy evaporation of the fixative (Fig.6A). The device provides 11 mm dropping height with two inlets—one for cold water and one for the fixed mitotic cells suspension. The rapid and easy assembly protocol for the microFISH device allows for quick transformation of a simple glass slide into a microFISH device, which makes it a solution for integration into existing work routines at cytogenetic labs (Fig.6B). Nevertheless, they have mainly focused on adapting the conventional metaphase FISH to lab-on-a-chip method. The average numbers of spreads obtained using the splashing device are comparatively lower and the splashing chip device does not improve the chromosome spreading. However, the micro-splashing device produces reliable metaphase spreads on a glass slide, which is sufficient for conducting routine FISH analysis. Even though the microFISH device allows for an optimized metaphase FISH protocol on a chip with over a 20-fold reduction in the reagent volume, the reduction of probe volume, which is the most expensive part of the process, is not very large. Considering the complete automation of the microFISH device, reduction in probe volume and hybridization time, could improve the metaphase FISH as widespread genetic testing of unknown translocations more accessible in a clinical setting [40].

For the complete FISH on chip a membrane based cell culture chamber was combined with a spreading device described above [41]. Shah *et al.* describes the FISHprep device for metaphase FISH slides preparation, which was validated by performing standard FISH protocol. The fabricated device consists of a diffusion based cell culture reactor [33] separated from the splashing device by a clip valve [30]. The culture of T-lymphocytes was performed for 72 hours with a CFSE staining to determine the proliferation rate. Further, by opening the clip

As submitted to BioEssays

valve the cultured and fixed lymphocytes were splashed on the glass slide. The quality of spreads obtained from the FISHprep was comparable to traditionally obtained spreads. The integration of all the steps required for successful metaphase FISH slide preparation in one FISHprep offers a possibility for an automation of the molecular cytogenetics in future by combining it with the described earlier metaphase FISH on chip protocol [41].

## Future prospects

The miniaturization of the integrated platforms for molecular cytogenetics will progress in the nearest future. Most of the work done in the field has addressed the probe volume used and further development will be directed towards automation of systems. The interphase FISH has been almost completely automated by means of microsystems, but some work still needs to be done in order to reduce the assay time. Moreover, the work on preparation of metaphase spreads in microdevices should be thoroughly studied. The advantages of making analysis on metaphase chromosomes are enormous and the development of such a system is of utmost importance. Further chemical modifications of the substrate surface could lead to obtaining high quality metaphase spreads even in the confined channels. Furthermore, some work needs to be done to develop systems amenable for simple and reliable detection of unknown translocations.

## Conclusion

Cytogenetic analysis is an important tool commonly used in clinical diagnosis and treatment monitoring. FISH has a numerous applications in molecular biology, including gene mapping, diagnosis of chromosome abnormalities, and cancer detection. In clinical research, FISH can be used for prenatal diagnosis of inherited chromosomal aberrations, postnatal diagnosis of carriers of genetic disease, diagnosis of infectious disease, viral and bacterial disease, tumor cytogenetic diagnosis, and detection of aberrant gene expression. Technical complexity of conventional FISH protocol has slowed down the usage of the technique in clinical settings. Significant effort has been put into enabling fast, reliable and high throughput analysis of samples. The assays and devices presented in this review can be easily incorporated in cytogenetic laboratories to improve the quality of analysis and reduce the time necessary to obtain significant results. The presented membrane based bioreactors for cell cultures offer the automation of the preparation of metaphase spreads on glass slides without the need for centrifugation steps. Most of the mentioned work was done to improve the interphase FISH analysis with just one work presenting metaphase FISH analysis. These platforms offer great advantages over conventional methods in regards to reduction of probe volume per analysis used as well as the possibility to automate the protocol. Nevertheless, there is still a gap between developing the technology and usage of these systems as a routine diagnostic tool in cytogenetic laboratories. And also, there is a great need for rapid and inexpensive detection of unknown translocations.

## References

1. **Jackson L.** 2002. Cytogenetics and molecular cytogenetics. *Clinical Obstetrics and Gynecology* **45**:622-39.
2. **Hsu L.** 1998. Prenatal diagnosis of chromosomal abnormalities through amniocentesis. In Milunsky A, ed. *Genetic Disorders and the Fetus*, 4th ed. Baltimore: The Johns Hopkins University Press.
3. **Kluin P, Schuurin E.** 2011. Molecular cytogenetics of lymphoma: where do we stand in 2010? *Histopathology* **58**:128-44.
4. **Cheung SW, Shaw CA, Yu W, Li JZ, et al.** 2005. Development and validation of a CGH microarray for clinical cytogenetic diagnosis (vol 6, pg 422, 2005). *Genetics in Medicine* **7**:478-.
5. **Fox JL, Hsu PH, Legator MS, Morrison LE, et al.** 1995. Fluorescence in-situ hybridization - powerful molecular tool for cancer prognosis. *Clinical Chemistry* **41**:1554-9.
6. **Sandberg AA, Meloni-Ehrig AM.** 2010. Cytogenetics and genetics of human cancer: methods and accomplishments. *Cancer Genetics and Cytogenetics* **203**:102-26.

7. **Dave BJ, Sanger WG.** 2007. Role of Cytogenetics and Molecular Cytogenetics in the Diagnosis of Genetic Imbalances. *Seminars in Pediatric Neurology* **14**:2-6.
8. **Volpi EV, Bridger JM.** 2008. FISH glossary: an overview of the fluorescence in situ hybridization technique. *Biotechniques* **45**:385-+.
9. **Campbell LJ.** 2006. Cytogenetic and FISH techniques in myeloid malignancies. In Iland H, Hertzberg M, Marlton P, eds. *Methods in Molecular Medicine*: Humana Press Inc. p 13-26.
10. **de Klein A, Tibboel D.** 2010. Genetics. *Seminars in Pediatric Surgery* **19**:234-9.
11. **Park JH, Woo JH, Shim SH, Yang SJ, et al.** 2010. Application of a target array Comparative Genomic Hybridization to prenatal diagnosis. *Bmc Medical Genetics* **11**.
12. **Beatty B, Mai S, Squire J.** 2002. FISH. A Practical Approach Oxford: Oxford University Press.
13. **Trask BJ.** 2002. Human cytogenetics: 46 chromosomes, 46 years and counting. *Nature Reviews Genetics* **3**:769-78.
14. **Smeets D.** 2004. Historical prospective of human cytogenetics: from microscope to microarray. *Clinical Biochemistry* **37**:439-46.
15. **Fauth C, Speicher MR.** 2001. Classifying by colors: FISH-based genome analysis. *Cytogenetics and Cell Genetics* **93**:1-10.
16. **Andrieux J, Sheth F.** 2009. Comparative genomic hybridization array study and its utility in detection of constitutional and acquired anomalies. *Indian Journal of Experimental Biology* **47**:779-91.
17. **Jain KK.** 2004. Current Status of Fluorescent In-Situ Hybridisation. *Medical Device Technology*. p 14-7.
18. **Gambardella S, Ciabattoni E, Motta F, Stoico G, et al.** 2010. Design, Construction and Validation of Targeted BAC Array-Based CGH Test for Detecting the Most Commons Chromosomal Abnormalities. *Genetics Insights*. p 9-21.
19. **Jiang F, Katz RL.** 2002. Use of interphase fluorescence in situ hybridization as a powerful diagnostic tool in cytology. *Diagnostic Molecular Pathology* **11**:47-57.
20. **Nath J, Johnson KL.** 2000. A review of fluorescence in situ hybridization (FISH): Current status and future prospects. *Biotechnic & Histochemistry* **75**:54-78.
21. **Trask BJ.** 1991. Fluorescencen in situ hybridization - applications in cytogenetics and gene-mapping. *Trends in Genetics* **7**:149-54.
22. **Garimberti E, Tosi S.** 2010. Fluorescence in situ Hybridization (FISH), Basic Principles and Methodology. *Fluorescence in situ Hybridization (FISH): Protocols and Applications*:3-20.
23. **Tonnies H.** 2002. Modern molecular cytogenetic techniques in genetic diagnostics. *Trends in Molecular Medicine* **8**:246-50.
24. **Zanardi A, Bandiero D, Bertolini F, Corsini CA, et al.** 2010. Miniaturized FISH for screening of onco-hematological malignancies. p 497-504.
25. **van der Ploeg M.** 2000. Cytochemical nucleic acid research during the twentieth century. *European Journal of Histochemistry* **44**:7-42.
26. **Sieben VJ, Marun CSD, Pilarski PM, Kaigala GV, et al.** 2007. FISH and chips: chromosomal analysis on microfluidic platforms. *Iet Nanobiotechnology* **1**:27-35.
27. **Kearney L, Horsley SW.** 2005. Molecular cytogenetics in haematological malignancy: current technology and future prospects. *Chromosoma* **114**:286-94.
28. **Speicher MR, Carter NP.** 2005. The new cytogenetics: Blurring the boundaries with molecular biology. *Nature Reviews Genetics* **6**:782-92.
29. **Levsky JM, Singer RH.** 2003. Fluorescence in situ hybridization: past, present and future. *Journal of Cell Science* **116**:2833-8.
30. **Vedarethinam I, Shah P, Dimaki M, Tumer Z, et al.** 2010. Metaphase FISH on a Chip: Miniaturized Microfluidic Device for Fluorescence in situ Hybridization. *Sensors* **10**:9831-46.
31. **Liehr T, Starke H, Heller A, Kosyakova N, et al.** 2006. Multicolor fluorescence in situ hybridization (FISH) applied to FISH-banding. *Cytogenetic and Genome Research* **114**:240-4.
32. **Lee C, Lemyre E, Miron PM, Morton CC.** 2001. Multicolor fluorescence in situ hybridization in clinical cytogenetic diagnostics. *Current Opinion in Pediatrics* **13**:550-5.
33. **Shah P, Vedarethinam I, Kwasny D, Andresen L, et al.** 2011. Microfluidic bioreactors for culture of non-adherent cell. *Sensors and Actuators B:Chemical*.
34. **Svendsen WE, Castillo-Leon J, Lange JM, Sasso L, et al.** 2011. Micro and nano-platforms for biological cell analysis. *Sensors and Actuators A:Physical*.

35. **Lee DS, Lee JH, Min HC, Kim TY, et al.** 2007. Application of high throughput cell array technology to FISH: Investigation of the role of deletion of p16 gene in leukemias. *Journal of Biotechnology* **127**:355-60.
36. **Sieben VJ, Debes-Marun CS, Pilarski LM, Backhouse CJ.** 2008. An integrated microfluidic chip for chromosome enumeration using fluorescence in situ hybridization. *Lab on a Chip* **8**:2151-6.
37. **Deng W, Tsao SW, Lucas JN, Leung CS, et al.** 2003. A new method for improving metaphase chromosome spreading. *Cytometry Part A* **51A**:46-51.
38. **Henegariu O, Heerema NA, Wright LL, Bray-Ward P, et al.** 2001. Improvements in cytogenetic slide preparation: Controlled chromosome spreading, chemical aging and gradual denaturing. *Cytometry* **43**:101-9.
39. **Qu YY, Xing LY, Hughes ED, Saunders TL.** 2008. Chromosome Dropper Tool: Effect of slide angles on chromosome spread quality for murine embryonic stem cells. *Journal of Histotechnology* **31**:75-9.
40. **Theodosiou Z, Kasampalidis LN, Livanos G, Zervakis M, et al.** 2007. Automated analysis of FISH and immunohistochemistry images: A review. *Cytometry Part A* **71A**:439-50.
41. **Shah P, Vedarethinam I, Kwasny D, Andresen L, et al.** 2011. FISHprep: A novel Integrated Device for Metaphase FISH Sample Preparation. *Micromachines* **2**:116-28.





Contents lists available at ScienceDirect

## Sensors and Actuators A: Physical

journal homepage: [www.elsevier.com/locate/sna](http://www.elsevier.com/locate/sna)



### Micro and nano-platforms for biological cell analysis

W.E. Svendsen\*, J. Castillo-León, J.M. Lange, L. Sasso, M.H. Olsen, M. Abaddi, L. Andresen, S. Levinsen, P. Shah, I. Vedarethinam, M. Dimaki

DTU Nanotech, Technical University of Denmark, Building 345 East, 2800 Kgs. Lyngby, Denmark

#### ARTICLE INFO

Article history:  
Available online xxx

Keywords:  
Cell culturing  
Cell sorting  
Nanoelectrodes  
Peptide nanotubes

#### ABSTRACT

In this paper some technological platforms developed for biological cell analysis will be presented and compared to existing systems. In brief, we present a novel micro cell culture chamber based on diffusion feeding of cells, into which cells can be introduced and extracted after culturing using normal pipettes, thus making it readily usable for clinical laboratories. To enhance the functionality of such a chamber we have been investigating the use of active or passive 3D surface modifications. Active modifications involve miniature electrodes able to record electrical or electrochemical signals from the cells, while passive modifications involve the presence of a peptide nanotube based scaffold for the cell culturing that mimics the *in vivo* environment. Two applications involving fluorescent in situ hybridization (FISH) analysis and cancer cell sorting are presented, as examples of further analysis that can be done after cell culturing. A platform able to automate the entire process from cell culturing to cell analysis by means of simple plug and play of various self-contained, individually fabricated modules is finally described.

© 2011 Elsevier B.V. All rights reserved.

#### 1. Introduction

*In vitro* cellular analysis has paved the way to major breakthroughs in the history of biology and drug discovery. However, no matter how good *in vitro* experiments are, they will never be able to represent the *in vivo* situation fully. But since *in vivo* experiments are expensive and sometimes unethical, researchers strive towards developing modifications of lab-on-a-chip systems so that they better mimic the environment experienced by cells inside the body. Micro- and nanotechnology are two very promising technologies for achieving *in vivo* like conditions. A recent example is the mimicking of the human kidney using microfluidic chambers [1]. In this paper we will illustrate the advantage of microfluidic handling of cells in combination with nano- and microsensing platforms.

For cellular analysis it is often necessary to culture the cells. The standard methods used for this, e.g. culture flasks, do not in any way represent the *in vivo* situation. Here we will demonstrate a microfluidic culturing system for adherent and non adherent cells, with controlled environment and diffusion based feeding, but without flushing away important signalling chemicals. Then a discussion of the surface of the culturing system is given, where a novel 3D nanopattern method is investigated to mimic *in vivo* conditions, where no smooth glass or plastic surfaces exist.

Probing intercellular dynamics and intercellular signalling is at the research frontiers for understanding cellular function. There-

fore, new technologies to address these issues are developing fast. It has been demonstrated that cells can survive penetration by nanoscale structures [2]. The obvious next step is to utilize this fact for probing the dynamics of the interior of living cells. Novel methods for fabricating 3D micro- and nanoelectrodes for this purpose will be presented.

Sorting of different types of cells is also an interesting research area and one that has received a fair amount of attention. Several methods have been used, both physical, based on cell dimensions alone, e.g. bumper arrays [3], biological, based on functionalizing substrates with proper markers binding on specific cell types [4], and electrical, based on differences in the dielectric properties of cells, e.g. dielectrophoresis [5] or electrorotation [6]. We here present the use of dielectrophoresis in order to sort cells expressing stress markers on their surfaces from cells without stress markers.

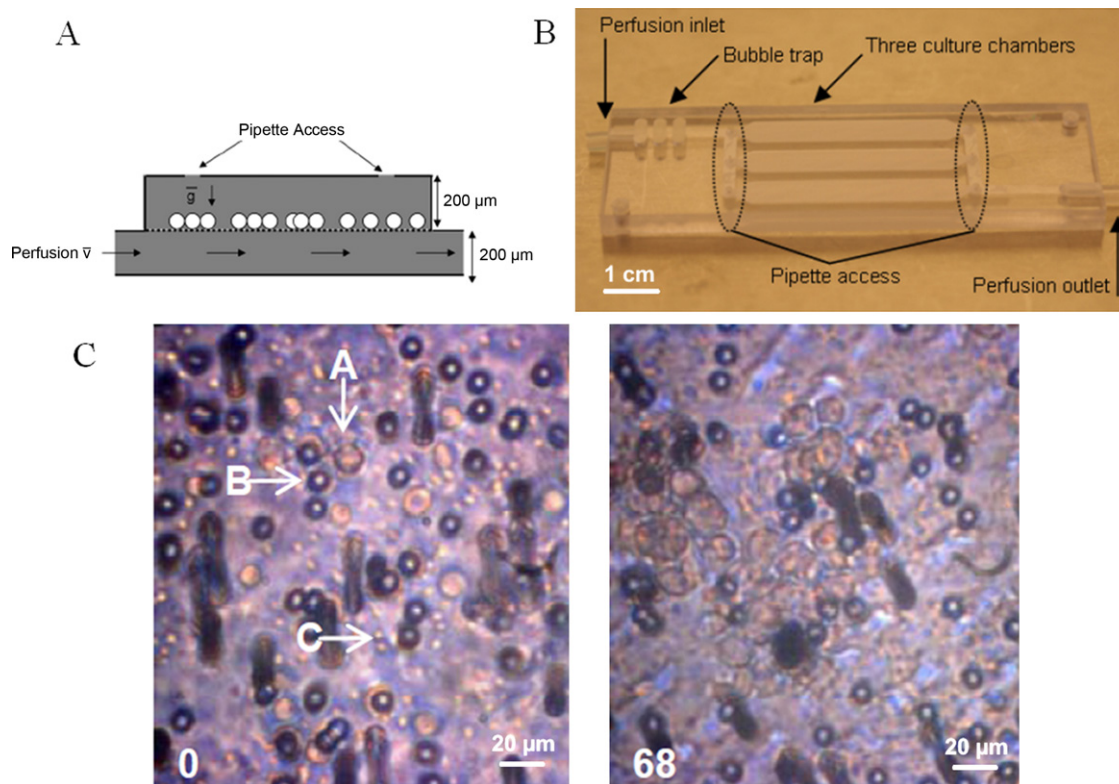
As a final point, the concept of a microfluidic motherboard, equipped with valves, simple microfluidic devices, e.g. mixers, and sockets for accepting microfluidic chips for specific applications will be presented. This motherboard can by plug-and-play integrate any chip that fits a standard general specification, irrespective of material and fabrication process.

#### 2. Cell culture microfluidic bioreactor for adherent and non-adherent cells

Microfluidics enables cell culturing mimicking *in vivo* conditions [7,8], i.e. physical, biochemical and physicochemical properties such as pH, gas concentration and temperature, unlike the conventional culturing methods. Chemical gradients represent a very

\* Corresponding author.

E-mail address: [winnie.svendsen@nanotech.dtu.dk](mailto:winnie.svendsen@nanotech.dtu.dk) (W.E. Svendsen).



**Fig. 1.** (A) A schematic of the membrane reactor with pipetting access holes. (B) The membrane reactor with three chambers and microfluidic inlets and outlets. (C) The lymphocytes resting on the membrane at start, i.e. 0 h (left) and after 68 h of post activation with phytohemagglutinin (right). Just after loading into the chamber, the lymphocytes indicated by arrow A are small with minimum cytoplasm, only slightly larger than the pores shown at arrow B. A number of platelets can also be observed at arrow C. After 68 h the platelets have disappeared and the lymphocytes have expanded their cytoplasm and are now growing into aggregates.

important factor that regulates the cell's function [9]. These gradients are obtained in the cell microenvironment by diffusion. This can easily be adapted in a microfluidic setup by adjusting the geometrical conditions of the chamber, which also helps to stabilize the gradients in the microenvironment [10,11]. A microfluidic system featuring continuous perfusion helps provide fresh media as culturing progresses and the components are metabolized. By performing cell culture in the laminar flow regime offered in microfluidic systems, precise control of pH, oxygen, nutrition and temperature can be obtained [12].

The majority of micro cell culture reactors are designed for adherent cells [13–17], as these are the dominant cell types used in biological studies. The handling and perfusion of fresh media for culturing of such cell types is much easier. Here a cell culturing microfluidic reactor is presented, where both adherent and non adherent cells can be cultured, maintaining precise control of pH, oxygen, nutrition and temperature, and sustaining the biochemical microenvironment of the cells, while supplying nutrients to the cells by diffusion controlled processes.

The membrane cell culturing bioreactor is illustrated in Fig. 1A and B. It is composed of two chambers: an upper cell culturing chamber and a lower perfusion chamber. Both are fabricated using micromilling and are bonded together, with a 7 μm thick polycarbonate membrane with a porosity of 0.14 and pore size of 5 μm sandwiched between them. The cells are loaded and kept in the upper chamber by pipetting or microfluidic inlet. The medium is perfused in the bottom chamber and the cells are fed by diffusion through a micromembrane. In Fig. 1C the culturing of lymphocytes is illustrated. In this fashion it is possible to monitor the effects of drugs on cells continuously.

There are several advantages of the membrane based cell culture chamber. Firstly, perfusion can immediately be started without

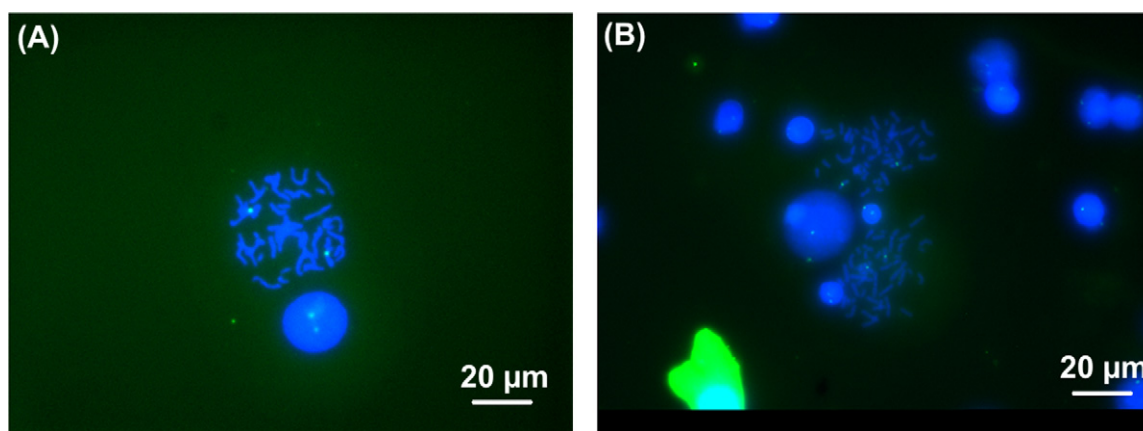
waiting for the loaded cells to settle. Secondly, the cells can be protected from air bubbles that will inevitably arise in the microfluidic channels, as the flow is not directly in contact with the cells. Thirdly, the cells can be protected from any kind of agitation, as the perfusion chamber and culture chamber are separately controlled.

To illustrate the usefulness of the chamber, a full protocol for fluorescent in situ hybridization (FISH) was carried out, mapping chromosomes translocations. The results were compared with those achieved by applying the standard protocol on microscope slides, as is the case for a routine FISH analysis, as shown in Fig. 2. No striking differences between the fluorescent images in the two cases were observed.

### 3. Self-assembled 3D nanowire structure pattern for cellular growth and sensing applications

Cell and tissue cultures have traditionally been done in 2D flat plastic or glass surfaces which are far from the topological representations of the more complex 3D environment found in the extracellular matrix. The suggestion that 3D porous nanotopographies that mimic physiological conditions represent a more accurate approximation for the growth of cells and tissue used in a long list of studies (e.g. cell migration and adherence, signal transduction) and biomedical applications (e.g. drug assays, regenerative medicine) has been supported by recent studies [18,19].

Epitaxial gallium phosphide nanowire arrays were used in cellular force and cell survival investigations [2,20–23]. These studies demonstrated that cell adhesion and survival was better on nanowire arrays than on planar substrates. However, the toxic nature of the substrate material used for the fabrication of the nanowires is a big limitation for the use of these nanostructures in biomedical applications or in *in vivo* studies [24,25].



**Fig. 2.** Comparison of the FISH results based on the spreads prepared (A) by conventional methods and (B) by the fixed cells from the reactor. X-chromosome centromere specific probes labelled with FITC are hybridized to chromosomes stained with DAPI.

Cell attachment on silicon pillars was previously studied showing the advantages of using these structures to direct the attachment, growth and morphology of cells [26,27]. Recently, Qi et al. studied cell adhesion and spreading behaviour on vertically aligned silicon nanowire (SiNW) arrays [28]. Their study showed that the SiNW arrays exhibited good biocompatibility with HepG2 and LX-2 cells and could support and favour cell adhesion. Additionally their study demonstrated that SiNW arrays enhanced the cell-substrate focal adhesion force and restricted cell spreading.

In another study using SiNW arrays, Jiang et al. investigated the use of these nanostructures as candidates for orthopaedic processes to promote bone regeneration within the body [29]. In their study they modified the SiNW surface and performed proliferation assays of mouse stromal cells in order to evaluate the biocompatibility of the modified NWs. In 2006, Patolsky et al. integrated SiNW arrays with the individual axons and dendrites of live mammalian neurons enabling simultaneous measurement of signals propagating along individual axons and dendrites [30]. However the fabrication of these arrays requires several steps and cleanroom conditions making the fabrication process tedious and expensive.

In a different work, platinum nanopillar arrays were used to study cell migration in a cultured neuronal network [31]. Using the nanopillar arrays it was possible to pin the position of neurons in a non-invasive manner.

Cohen-Karni et al. explored the combination of graphene with SiNW-FETs interfaced to electrogenic cells to record extracellu-

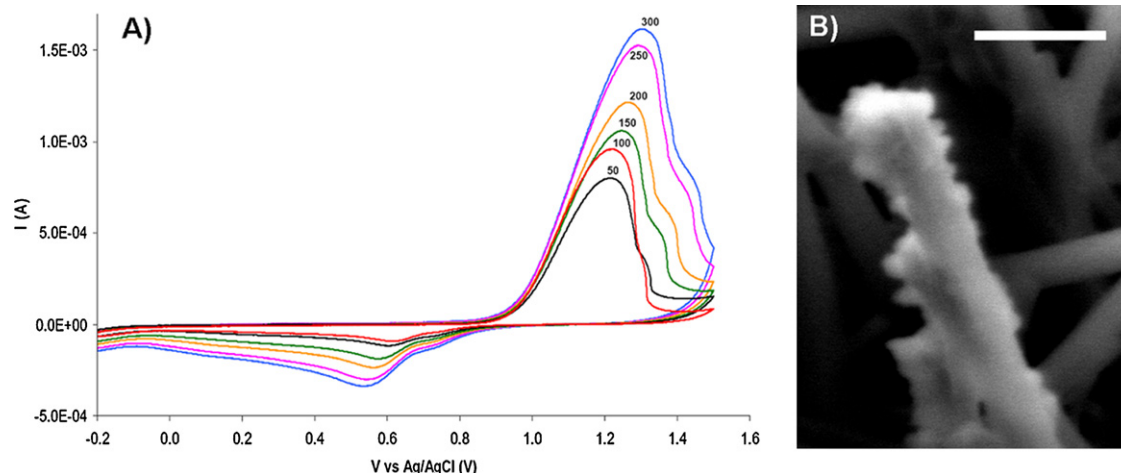
lar signals [32]. This combination demonstrated better results on simultaneous recordings of beating cellular signals compared to planar recording devices. However, this study did not explore the use of the combined design as cell culture platform and graphene biocompatibility studies were not performed.

In our work a 3D nanostructure surface formed by vertically self-assembled diphenylalanine peptide nanowires was fabricated on top of a gold electrode as described in [33].

First the 3D nanopattern was functionalized with a conductive polymer, illustrated in Fig. 3B, and its ability to electrochemically detect dopamine was evaluated. The electrochemical behaviour of a gold electrode modified with peptide/polypyrrole nanowires is shown in Fig. 3A. The voltammograms exhibit peak behaviour typical to polypyrrole on gold. The anodic and cathodic peaks reflect the redox behaviour of the polypyrrole, and the increase in current peak response with increasing potential sweep rate suggests pseudo-reversibility.

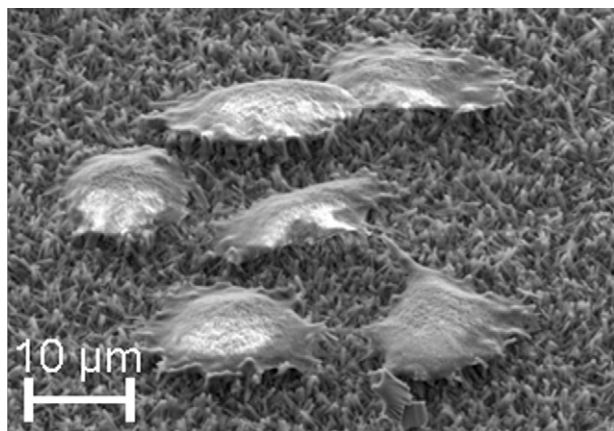
This peptide nanowires/polypyrrole modification of Au electrodes was utilized for electrochemical dopamine sensing. Chronoamperometric experiments were carried out, where the modified electrodes were exposed to small injections of 10  $\mu$ L aliquots of dopamine. This system exhibited a minimum detection value of 3.1  $\mu$ M, a value in the range of the physiological dopamine concentration.

Secondly the 3D structures were examined with respect to culturing adherent cells; here HeLa cells were used. HeLa cells were



**Fig. 3.** (A) Cyclic voltammograms of peptide/polypyrrole nanowires modified gold disk electrodes in 0.1 M KCl vs. a Ag/AgCl (3 M KCl) reference electrode at potential scan rates of 50, 100, 150, 200, 250 and 300 mV/s; (B) SEM image of a peptide nanowire coated with a polypyrrole film, scale bar correspond to 1  $\mu$ m.





**Fig. 4.** SEM image of HeLa cells grown on top of the 3D self-assembled nanowire structure after 36 h of culturing.

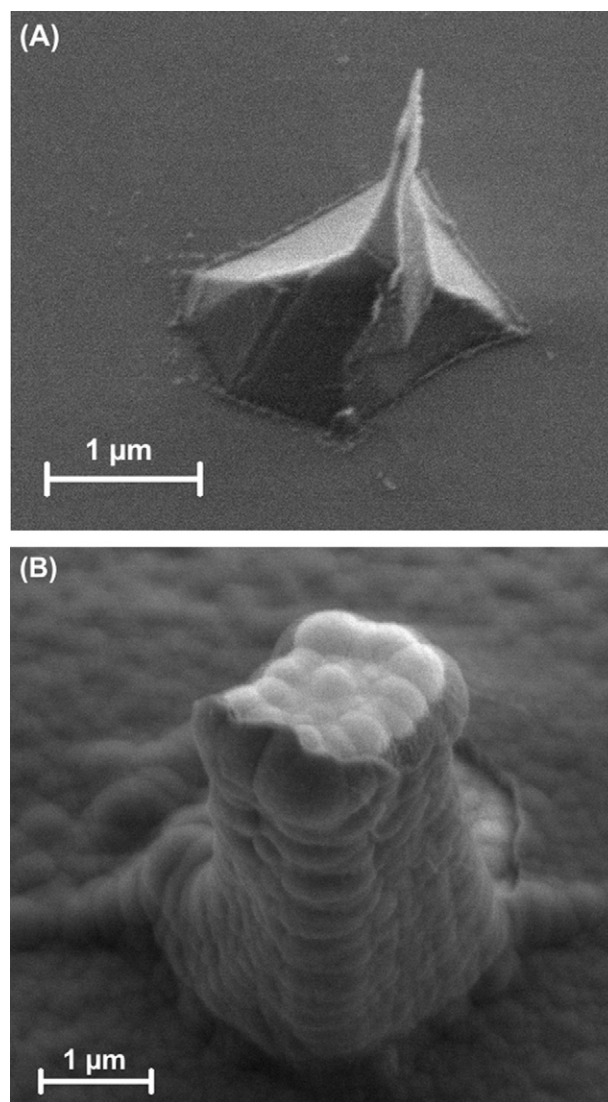
able to grow on top of the peptide nanowires for several days, as observed in Fig. 4. The obtained results indicated that the synthesized 3D nanostructure is a good platform for the growth of cells and the detection of compounds of biomedical relevance released from them. The chronoamperometric measurements performed with the functionalized peptide nanowires showed the ability of the 3D nanostructure to detect dopamine at concentrations present in *in vivo* systems. This nanoplatform offers the advantage of having a favourable environment for the growth of cells and an electrochemical sensor for the detection of compounds released from cells in the same system.

#### 4. 3D electrodes for single cell intracellular measurements

Electrical signals originating from cells are very small and therefore very prone to noise. Therefore, electrodes developed to investigate cellular dynamics need special consideration. Increasing the surface area of such electrodes reduces their impedance and thus increases the signal-to-noise ratio [34]. This can be done by increasing the planar dimensions of the recording sites; however, this would reduce the spatial resolution of the arrays. The solution is the fabrication of 3D electrodes. Many examples of such structures can be found in the literature [35,36]. However, (1) their dimensions are very large and thus unsuitable for single cell measurements and (2) the fabrication process for the small electrodes is complicated, serial in nature and involves the use of expensive equipment.

We have developed a fabrication process based entirely on standard microfabrication techniques, which allows us to create up to 10 μm tall silicon pillars with sub 200 nm tip diameter. These are then electrically isolated from each other, metalised with a standard lift-off process and passivated leaving only the tip electrically active for cell measurements. The pillars are made with a combination of wet etch in a KOH solution and a short maskless dry isotropic etch in an Advanced Silicon Etcher. Fig. 5A shows an example of a pillar fabricated in this way, but before the isolation, metallization and passivation steps. A finished pillar is shown in Fig. 5B.

The electrodes have been tested both in terms of impedance and in terms of electrochemical performance. Though their impedance is high, electrical measurements done in DI water and varying concentrations of NaCl show the expected differences [37]. Moreover, we have electrodeposited polyaniline on these electrodes and recorded the related redox reaction. The result shows that the electrodes are electrochemically active, though exhibiting an irreversible behaviour [37]. Moreover, larger electrodes covered with polymers on top of the metal layers show increased electrochemical

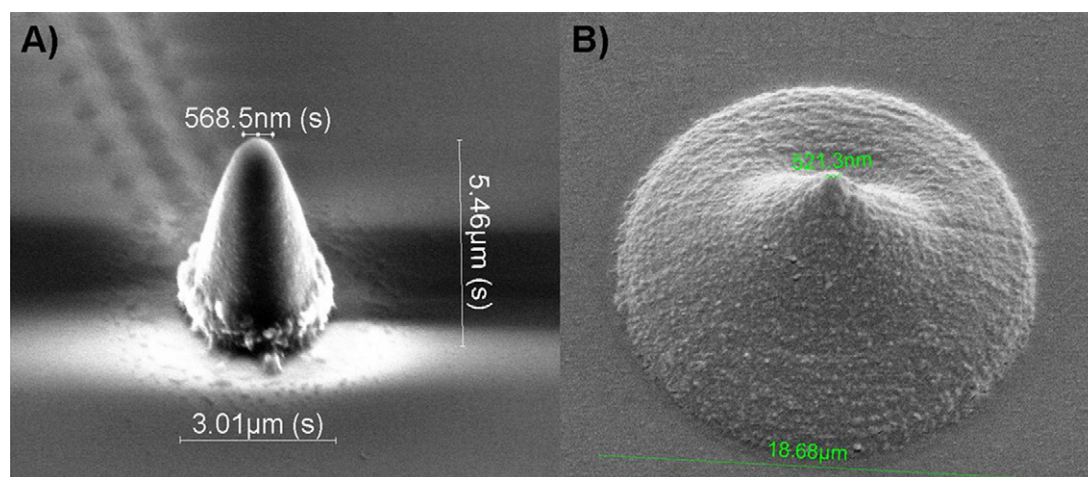


**Fig. 5.** (A) A sharp silicon pillar after etching. The pillar height is around 3 μm while the tip diameter is under 200 nm. (B) A finished pillar with 500 nm PECVD oxide for isolation, 100 nm Pt layer for metallization and 200 nm nitride layer for passivation. The nitride layer has been opened at the top of the pillar for establishing electrical contact with the cells.

activity than electrodes only covered with metal [38]. This opens up the possibility to create sensitive and selective metabolic sensors by trapping enzymes inside the electrodeposited polymer. Future work is concentrating on the fabrication and testing of these sensors as well as on the modification of the surfaces to enhance the surface area and better isolation of the arrays to reduce the parasitic capacitances.

Another approach to produce 3D electrodes is by applying two-photon lithography. This method takes advantage of the two-photon absorption process initiated when exposing a photopolymer to femto-second laser with certain power. Chemical and physical changes within a small size of the photopolymer occur to form 3D polymerized structures [39]. 3D electrodes of photopolymer (IP.L [40]) with different dimensions from 3 to 10 μm in height with sub 500 nm tip diameter have been fabricated, as presented in Fig. 6.

The fabricated structures are not easily susceptible to mechanical strain and they have good rigidity, due to an increased number of exposed points in the contour of the structures. The fabricated electrode structures are not showing any deformation or collapse



**Fig. 6.** (A) SEM image of single 3D electrode of polymerized IP-L with dimensions of 5  $\mu\text{m}$  height and sub-micron tip diameter fabricated by two photon polymerization. (B) SEM image of a 3D electrode 10  $\mu\text{m}$  in height with sub-micron tip diameter, coated with a 50 nm thick layer of silver.

as demonstrated in Fig. 6A. The finished structures can be covered with a thin metal layer by e-beam evaporation to ensure conductivity, as seen in Fig. 6B.

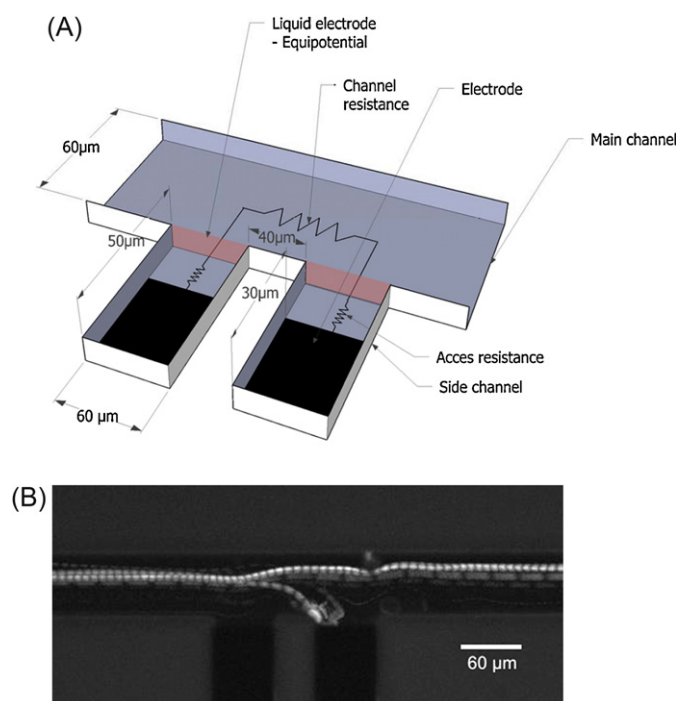
## 5. Cell sorting using dielectrophoresis

Early detection of cancer in patients is a field of research attracting a lot of attention, as cancer is becoming more common in the aging population. During transformation from a normal cell to a cancerous cell, proteins known as stress markers will be expressed on the cell surface. Their function is to activate the immune system to kill the cells that are expressing them. Occasionally the cancerous cell find a way to terminate the expression of stress markers and the cell can develop into a mature cancer cell without being recognized by the immune system [41]. Detection of cells expressing stress markers in the blood would therefore indicate that a cancer is under development and treatment can be initiated at this very early stage.

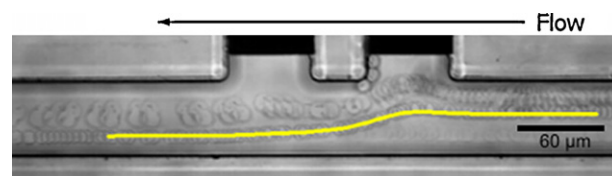
Dielectrophoresis was chosen as the sorting method and sorting between normal Jurkat cells (referred to as cancer(–) cells) and Jurkat cells transfected to express a stress marker known as MICA on their membrane [42] (referred to as cancer(+) cells) was carried out. The objective was to see if the expression of the MICA protein would also change the dielectric properties of the Jurkat cells in a way that sorting would be possible.

The chip design used for the purpose was adapted from Demierre et al. [43] and is shown in Fig. 7A. Upon application of an alternating potential on the electrodes cells would either move towards the electrodes or away from them, depending on their dielectric properties and the applied frequency. The objective was to find a frequency region, where cancer(–) cells would move one way and cancer(+) cells the other way. This is shown in Fig. 7B, where the cancer(–) cells experience positive DEP and are attracted towards the electrodes, while the cancer(+) cells experience negative DEP and are repelled from the electrodes at a frequency of 700 kHz.

Simulating particle trajectories and fitting them to the experimental results can give more information on the dielectrophoretic properties of the cells. The Comsol Multiphysics Finite Element Analysis Software is used in order to simulate the flow profile and the electric field in the channel. The results are exported into Matlab, where the trajectory simulation is done by applying Newton's 2nd law. We assume that the cell is a sphere and simulate the movement of its centre of mass. An example of one simulation can be seen in Fig. 8. By fitting the simulated trajectory to the cells flow path

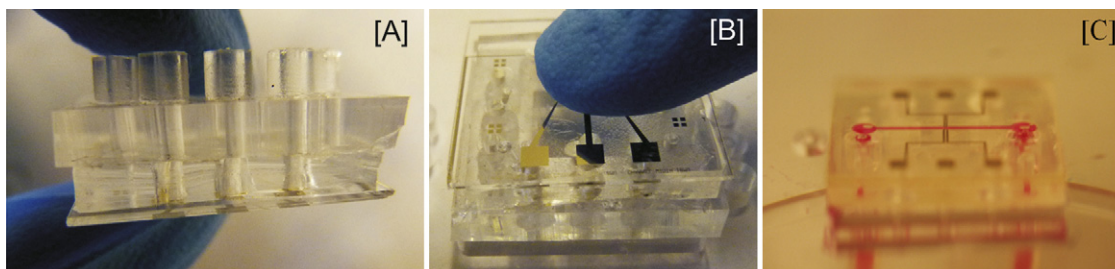


**Fig. 7.** (A) A schematic of the setup used for the dielectrophoretic manipulation of cells. The cells flow in the main channel and the field is applied by the electrodes in the side channels. (B) Fluorescence images of cancer(–) and cancer(+) cells in the channel. At 700 kHz the cancer(–) cells move towards the electrodes, while the cancer(+) cells move away from them. The image is created by stacking all the video frames.



**Fig. 8.** Simulation of trajectory for a cancer+ cell in a PBS 1:50 solution. The CM factor was adjusted to 0.07 in order for the simulation to follow the cells flow path. 20V was applied across the electrodes the flow rate was 0.01  $\mu\text{L}/\text{min}$ .





**Fig. 9.** (A) Sideview of the assembled modules with extended elastomeric tubules. (B) Attachment of the modules with the lab board. (C) Flow through the module (channel width: 100  $\mu\text{m}$ , module dimension 20  $\times$  20 mm).

it was possible to estimate the real part of the Clausius-Mossotti (CM) factor which is a key parameter for the DEP force.

## 6. Integrating of the bioanalytical devices into total analysis platforms

Integration of microfluidic and sensors systems into total analysis systems is of great interest to handle the fluidics and electronics more efficiently [44]. This can be done in two principle ways, integration or modularization. We have moved towards the latter. While integration provides the advantages of having smaller footprint devices, modularity provides easy and rapid adaptation of current manual biological protocols into various individual modules for miniaturizing these lengthy sequential protocols [45].

We have developed a novel lab-board which allows the rapid handling of different biological and analytical devices like cell culture, DEP, concentrators. The devices are assembled into modules with extended hollow elastomeric tubules providing connections with the board (Fig. 9A). The assemblies form tight seals with the board by expansion of the elastomeric tubules by the connectors on the board (Fig. 9B). This board provides an easy way of forming fluidic and electrical interconnections by means of integrated fluidic networks (Fig. 9C) and electrical spring pins. It is fabricated using micromilling on a polymethyl-methacrylate (PMMA) substrate, chosen for its high optical transparency. The board constitutes an excellent solution for microfluidic applications requiring optical analysis. The modular device, shown in Fig. 9C, can be fabricated in any material, and plugged into the major lab board with fluidic and electronic connections, thereby enabling chips fabricated in different materials to be tested sequentially.

All the devices presented earlier in this article are currently being redesigned towards a more standard format to fit with this board. Moreover, this board highlights our efforts towards standardization of our future device development efforts.

## 7. Conclusion

We have presented a selection of micro- and nanoplatforms for biological cell analysis. The presented systems cover a variety of processes. We have demonstrated a simple *in vivo* like microfluidic system for culturing adherent and most importantly non-adherent cells in contrast to other previously described micro cell culture reactors. The system was tested on the full protocol for FISH, i.e. culturing lymphocytes, arresting them in the metaphase state of the cell cycle and conducting FISH analysis, finally identifying the centromere of the X-chromosome. We went on to show that a simple peptide based 3D nanostructured surface in the system could be used to grow adherent cells (HeLa) and that it could also be used for electrochemical studies. Although this idea is not novel, the presented method creates such nanostructures in a very simple, cleanroom free – and therefore also cheap – way. The novelty of using 3D nanoelectrodes in the culture chamber to potentially investigate intercellular processes was introduced and the simple

fabrication of these nanostructures was presented as an alternative to expensive and serial nanofabrication techniques. Moreover, new novel biocompatible materials for 3D nanoelectrodes were discussed. An example of further analysis by using a microfluidic system combined with dielectrophoresis to sort non-adherent cells transfected with cancer markers from non-transfected cells was presented and discussed. These preliminary results open up the possibility of being able to identify early cancer signs and thus treat patients at an early stage of the disease. Finally, a microfluidic platform for the integration of the different modules into one single device for rapid testing was presented as an attempt to easily create electrical and fluidic connections to and interconnections between multiple chips of different materials and functionality.

## Acknowledgements

The authors would like to thank all the members of the Nano Bio Integrated Systems (NaBIS) group at the Department of Micro- and Nanotechnology at the Technical University of Denmark for their contribution to the work described in this paper. Funding from the Danish Research Council for Technology and Production (FTP) and the European Committee through the projects Excell, CellCheck and BeNatural is also gratefully acknowledged.

## References

- [1] P.M. van Midwoud, G.M.M. Groothuis, M.T. Merema, E. Verpoorte, Microfluidic biochip for the perfusion of precision-cut rat liver slices for metabolism and toxicology studies, *Biotechnology and Bioengineering* 105 (2010) 184–194.
- [2] W. Hallstrom, T. Martensson, C. Prinz, P. Gustavsson, L. Montelius, L. Samuelson, M. Kanje, Gallium phosphide nanowires as a substrate for cultured neurons, *Nano Letters* 7 (2007) 2960–2965.
- [3] Z. Siyang, R. Yung, T. Yu-Chong, H. Kasdan, Deterministic lateral displacement MEMS device for continuous blood cell separation, in: *Proceedings, IEEE Micro Electro Mechanical Systems*, 2005, pp. 851–854.
- [4] A. Sin, S.K. Murthy, A. Revzin, R.G. Tompkins, M. Toner, Enrichment using antibody-coated microfluidic chambers in shear flow: model mixtures of human lymphocytes, *Biotechnology and Bioengineering* 91 (2005) 816–826.
- [5] J. Yang, Y. Huang, X.B. Wang, F.F. Becker, P.R.C. Gascoyne, Cell separation on microfabricated electrodes using dielectrophoretic/gravitational field flow fractionation, *Analytical Chemistry* 71 (1999) 911–918.
- [6] J. Yang, Y. Huang, X.J. Wang, X.B. Wang, F.F. Becker, P.R.C. Gascoyne, Dielectric properties of human leukocyte subpopulations determined by electrorotation as a cell separation criterion, *Biophysical Journal* 76 (1999) 3307–3314.
- [7] J. Voldman, M.L. Gray, M.A. Schmidt, Microfabrication in biology and medicine, *Annual Review of Biomedical Engineering* 1 (1999) 401–425.
- [8] U.Y. Schaff, M.M.Q. Xing, K.K. Lin, N. Pan, N.L. Jeon, S.I. Simon, Vascular mimetics based on microfluidics for imaging the leukocyte-endothelial inflammatory response, *Lab on a Chip* 7 (2007) 448–456.
- [9] D.Q. Wu, Signaling mechanisms for regulation of chemotaxis, *Cell Research* 15 (2005) 52–56.
- [10] E.W.K. Young, D.J. Beebe, Fundamentals of microfluidic cell culture in controlled microenvironments, *Chemical Society Reviews* 39 (2010) 1036–1048.
- [11] L. Kim, Y.C. Toh, J. Voldman, H. Yu, A practical guide to microfluidic perfusion culture of adherent mammalian cells, *Lab on a Chip* 7 (2007) 681–694.
- [12] M.S. Kim, J.H. Yeon, J.K. Park, A microfluidic platform for 3-dimensional cell culture and cell-based assays, *Biomedical Microdevices* 9 (2007) 25–34.
- [13] A. Rosenthal, A. Macdonald, J. Voldman, Cell patterning chip for controlling the stem cell microenvironment, *Biomaterials* 28 (2007) 3208–3216.
- [14] F. Zhao, T. Ma, Perfusion bioreactor system for human mesenchymal stem cell tissue engineering: dynamic cell seeding and

- construct development, *Biotechnology and Bioengineering* 91 (2005) 482–493.
- [15] M.C. Liu, Y.C. Tai, A 3-D microfluidic combinatorial cell culture array, in: *Proceedings, IEEE Micro Electro Mechanical Systems*, 2009, pp. 427–430.
  - [16] D. Gao, H.B. Wei, G.S. Guo, J.M. Lin, Microfluidic cell culture and metabolism detection with electrospray ionization quadrupole time-of-flight mass spectrometer, *Analytical Chemistry* 82 (2010) 5679–5685.
  - [17] P. Godara, C.D. McFarland, R.E. Nordon, Design of bioreactors for mesenchymal stem cell tissue engineering, *Journal of Chemical Technology and Biotechnology* 83 (2008) 408–420.
  - [18] M. Schindler, A. Nur-E-Kamal, I. Ahmed, J. Kamal, H.Y. Liu, N. Amor, A.S. Ponery, D.P. Crockett, T.H. Grafe, H.Y. Chung, T. Weik, E. Jones, S. Meiners, Living in three dimensions – 3D nanostructured environments for cell culture and regenerative medicine, *Cell Biochemistry and Biophysics* 45 (2006) 215–227.
  - [19] C. Dionigi, M. Bianchi, P. D'Angelo, B. Chelli, P. Greco, A. Shehu, I. Tonazzini, A.N. Lazar, F. Biscarini, Control of neuronal cell adhesion on single-walled carbon nanotube 3D patterns, *Journal of Materials Chemistry* 20 (2010) 2213–2218.
  - [20] F. Johansson, W. Hallstrom, P. Gustavsson, L. Wallman, C. Prinz, L. Montelius, M. Kanje, Nanomodified surfaces and guidance of nerve cell processes, *Journal of Vacuum Science and Technology B* 26 (2008) 2558–2561.
  - [21] C. Prinz, W. Hallstrom, T. Martensson, L. Samuelson, L. Montelius, M. Kanje, Axonal guidance on patterned free-standing nanowire surfaces, *Nanotechnology* (2008) 19.
  - [22] D.B. Suyatin, W. Hallstrom, L. Samuelson, L. Montelius, C.N. Prinz, M. Kanje, Gallium phosphide nanowire arrays and their possible application in cellular force investigations, *Journal of Vacuum Science and Technology B* 27 (2009) 3092–3094.
  - [23] W. Hallstrom, M. Lexholm, D.B. Suyatin, G. Hammarin, D. Hessman, L. Samuelson, L. Montelius, M. Kanje, C.N. Prinz, Fifteen-picoNewton force detection from neural growth cones using nanowire arrays, *Nano Letters* 10 (2010) 782–787.
  - [24] C.E. Linsmeier, L. Wallman, L. Faxius, J. Schouenborg, L.M. Bjursten, N. Danielsen, Soft tissue reactions evoked by implanted gallium phosphide, *Biomaterials* 29 (2008) 4598–4604.
  - [25] C.E. Linsmeier, C.N. Prinz, L.M.E. Pettersson, P. Caroff, L. Samuelson, J. Schouenborg, L. Montelius, N. Danielsen, Nanowire biocompatibility in the brain – looking for a needle in a 3D stack, *Nano Letters* 9 (2009) 4184–4190.
  - [26] S. Turner, L. Kam, M. Isaacson, H.G. Craighead, W. Shain, J. Turner, Cell attachment on silicon nanostructures, *Journal of Vacuum Science and Technology B* 15 (1997) 2848–2854.
  - [27] S. Turner, L. Kam, M. Isaacson, H.G. Craighead, D. Szarowski, J.N. Turner, W. Shain, Cell attachment on microscopically textured silicon surfaces, in: P.L. Gourley, A. Katzir (Eds.), *Proceedings of Micro- and Nanofabricated Electro-optical Mechanical Systems for Biomedical and Environmental Applications*, 1997, pp. 41–52.
  - [28] S.J. Qi, C.Q. Yi, S.L. Ji, C.C. Fong, M.S. Yang, Cell adhesion and spreading behavior on vertically aligned silicon nanowire arrays, *ACS Applied Materials and Interfaces* 1 (2009) 30–34.
  - [29] K. Jiang, D. Fan, Y. Belabassi, G. Akkaraju, J.-L. Montchamp, J.L. Coffer, Medicinal surface modification of silicon nanowires: impact on calcification and stromal cell proliferation, *ACS Applied Materials and Interfaces* 1 (2008) 266–269.
  - [30] F. Patolsky, B.P. Timko, G.H. Yu, Y. Fang, A.B. Greytak, G.F. Zheng, C.M. Lieber, Detection, stimulation, and inhibition of neuronal signals with high-density nanowire transistor arrays, *Science* 313 (2006) 1100–1104.
  - [31] C. Xie, L. Hanson, W. Xie, Z. Lin, B. Cui, Y. Cui, Noninvasive neuron pinning with nanopillar arrays, *Nano Letters* 10 (2010) 4020–4024.
  - [32] T. Cohen-Karni, Q. Qing, Q. Li, Y. Fang, C.M. Lieber, Graphene and nanowire transistors for cellular interfaces and electrical recording, *Nano Letters* 10 (2010) 1098–1102.
  - [33] J. Ryu, C.B. Park, High-temperature self-assembly of peptides into vertically well-aligned nanowires by aniline vapor, *Advanced Materials* 20 (2008) 3754.
  - [34] M.O. Heuschkel, M. Fejt, M. Raggenbass, D. Bertrand, P. Renaud, A three-dimensional multi-electrode array for multi-site stimulation and recording in acute brain slices, *Journal of Neuroscience Methods* 114 (2002) 135–148.
  - [35] G. Barillaro, A. Diligenti, L.M. Strambini, Silicon dioxide microneedles for transdermal drug delivery, in: *Proceedings of IEEE Sensors*, 2008, pp. 1104–1107.
  - [36] Y.Z. Huang, D.J.H. Cockayne, J. Ana-Vanessa, R.P. Cowburn, S.G. Wang, R.C.C. Ward, Rapid fabrication of nanoneedle arrays by ion sputtering, *Nanotechnology* (2008) 19.
  - [37] M. Dimaki, P. Vazquez, M.H. Olsen, L. Sasso, R. Rodriguez-Trujillo, I. Vedarethinam, W.E. Svendsen, Fabrication and characterization of 3D micro- and nanoelectrodes for neuron recordings, *Sensors* 10 (2010) 10339–10355.
  - [38] L. Sasso, P. Vazquez, I. Vedarethinam, J. Castillo-Leon, J. Emneus, W.E. Svendsen, Conducting polymer 3D microelectrodes, *Sensors* 10 (2010) 10986–11000.
  - [39] S. Maruo, O. Nakamura, S. Kawata, Three-dimensional microfabrication with two-photon-absorbed photopolymerization, *Optics Letters* 22 (1997) 132–134.
  - [40] Nanoscribe GmbH, available at: <http://www.nanoscribe.de/en/products/ip-photoresists> (accessed).
  - [41] N. Nausch, A. Cerwenka, NKG2D ligands in tumor immunity, *Oncogene* 27 (2008) 5944–5958.
  - [42] L. Andresen, K.A. Hansen, H. Jensen, S.F. Pedersen, P. Stougaard, H.R. Hansen, J. Jurlander, S. Skov, Propionic acid secreted from propionibacteria induces NKG2D ligand expression on human-activated T lymphocytes and cancer cells, *Journal of Immunology* 183 (2009) 897–906.
  - [43] N. Demierre, T. Braschler, P. Linderholm, U. Seger, H. van Lintel, P. Renaud, Characterization and optimization of liquid electrodes for lateral dielectrophoresis, *Lab on a Chip* 7 (2007) 355–365.
  - [44] Y. Po, SmartBuild: a truly plug-n-play modular microfluidic system, *Lab on a Chip* 8 (2008) 1374–1378.
  - [45] M. Dimaki, C.H. Clausen, J. Lange, P. Shah, L.B. Jensen, W. Svendsen, A microfabricated platform for chromosome separation and analysis, in: *Proceedings of the 17th International Vacuum Congress/13th International Conference on Surface Science/International Conference on Nanoscience and Technology*, 2008, p. 100.

## Biographies

**Winnie E. Svendsen** received her M.Sc. degree in physics in 1993 from the University College Dublin, Ireland. She received her Ph.D. in 1996 from Copenhagen University. In 2006 she established her own research group *Nano Bio Integrated Systems (NaBIS)* at DTU-Nanotech, Denmark. The Nano-Bio Integrated System group develops integrated systems for bio-analysis with focus on medical application and point of care delivery. The major research areas are cell handling and analysis in micro fluidic device and the fabrication and development of biosensors using both 2D and 3D structures (i.e. nanowires and pillar electrodes). The current projects can be viewed on her webpage [www.nanotech.dtu.dk/NaBIS](http://www.nanotech.dtu.dk/NaBIS).

**Jaime Castillo** graduated from the Industrial University of Santander (Bucaramanga, Colombia) with a B.Sc. in chemistry. He received his Ph.D. degree in 2005 at the Department of Biotechnology, Lund University, Sweden. In 2006 he worked as post-doc at the Analytical Chemistry Department at Bochum University (Germany). He currently holds a position as assistant professor at the Department of Micro and Nanotechnology, DTU Nanotech, Denmark. His research focuses on the manipulation, characterization and integration of biological self-assembled nanostructures with micro and nano devices for the development of bioelectronic sensing platforms and drug delivery systems.

**Jacob Moresco Lange** received a M.Sc. degree at DTU at Department of System Biology and later a Ph.D. degree from the NaBIS group at DTU-Nanotech. His research interests are focused on biological applications of microtechnology as well as surface modifications of microsystems.

**Luigi Sasso** is currently a Ph.D. student in the NaBIS group at the Department of Micro and Nanotechnology at the Technical University of Denmark. His research is focused in developing 3D nanoelectrodes from novel materials such as peptide nanotubes for use as electrochemical sensors for cell measurements. Luigi has an M.Sc. degree in Physics and Nanotechnology from the Technical University of Denmark.

**Mark Holm Olsen** received a bachelor degree in nanotechnology and a master degree in nanoscience from the University of Copenhagen. In his Master Thesis, under Prof. Winnie E. Svendsen at the Technical University of Denmark, he developed microfabrication techniques for fabricating electrodes for electrophysiological measurements on neurons. He is currently a Ph.D. student at the Technical University of Denmark, where he is developing hydrogel scaffolds for immune cells with multiphoton polymerization.

**Mohammed Al Abaddi** finished his masters degree at the Department of Micro and Nanotechnology at the Technical University of Denmark. He is working on the development of novel 3D nanoelectrodes by 2 photon polymerization for use as electrical or electrochemical sensors.

**Lars Andresen** received his M.Sc. in biochemistry in 1998 and a Ph.D. in molecular immunology in 2004 at the University of Copenhagen. He joined the NaBIS group in 2009 as a post doc with the aim to integrate immunological techniques and knowledge into new micro – and nanotechnological devices.

**Simon Levinsen** is currently a research assistant at the Department of Micro and Nanotechnology at the Technical University of Denmark. His research is focused on developing lab-on-a-chips devices for multi-protein detection and manipulation of biological cells with dielectrophoresis. He received a M.Sc. degree in physics and nanotechnology in 2010 from the Technical University of Denmark.

**Pranjul Shah** is currently a Ph.D. student at the Department of Micro and Nanotechnology at Technical University of Denmark. His research interests are focused on microfluidics, cell culture, lab-on-a-chip devices, medical devices, infusion pumps, diagnostics assays, among others. He also has an M.Sc. in electronics and electrical engineering from University of Glasgow, UK and his undergraduate bachelor of engineering in computer engineering from Gujarat University, India.

**Indumathi Vedarethinam** is a Ph.D. student at the Department of Micro and Nanotechnology at the Technical University of Denmark. Her research interests include fluorescence in-situ hybridization, microfluidic cell culture devices and lab on chip systems for neuronal cultures. She has received a masters in biomedical engineering from the University of Glasgow, UK.

**Maria Dimaki** received an M.Eng. from the Department of Electrical and Computer Engineering at the National Technical University of Athens, Greece, in 2000 and an M.Sc. in engineering and physical science in medicine in 2001 from the Department of Bioengineering at Imperial College London, England. She received her Ph.D. in 2005 from the Technical University of Denmark. She is currently an associate professor with the Nano-Bio Integrated Systems group (NaBIS) at DTU Nanotech. Her research interests involve the development of micro- and nanoelectrodes in microfluidic systems for electrophysiological and electrochemical measurements on neuron cultures. She is also interested in theoretical simulations of dielectrophoresis of biological particles using COMSOL Multiphysics and Matlab.



# A microfabricated platform for chromosome separation and analysis

**Maria Dimaki, Casper Hyttel Clausen, Jacob Lange, Pranjul Shah, Linda Boye Jensen and Winnie Svendsen**

MIC – Department of Micro- and Nanotechnology, Technical University of Denmark, Bldg. 345E, 2800 Kgs. Lyngby, Denmark

mid@mic.dtu.dk

**Abstract.** More and more diseases find their cause in malfunctioning genes. There is therefore still need for rapid, low-cost and direct methods to accurately perform genetic analysis. Currently the process takes a long time to complete and is very expensive. We are proposing a system that will be able to isolate white blood cells from blood, lyse them in order to extract the chromosomes and then perform chromosome sorting on chip. As the physical properties of the chromosomes, such as size and dielectric properties, are needed for designing the chip, we have measured them using an AFM microscope.

## 1. Introduction

The identification and function of the genes in the human genome is an area where lot of research is being carried out. Of particular interest are malfunctioning genes that more and more seem to be the causes of various serious diseases, whose origin was previously unknown. Genes are particular DNA strands that can be transcribed and subsequently translated into proteins. In a malfunctioning gene, some of the DNA bases are deleted, added or exchanged with other ones. This can happen during cell division, when the chromosomes in the nucleus are copied and condense into compact structures that then separate into two different cells. During this process whole parts of a certain chromosome can be cut off and attached to a different chromosome. This particular mutation is called a translocation and is responsible for the well-known Down's syndrome.

For translocated chromosomes it is important to find the exact location of the breakpoint. A number of steps have to be carried out before this can occur. First, the white blood cells (WBCs) have to be isolated from a patient's blood and cultured, so that enough material can be available for further processing. This is currently done by blood centrifugation and incubation for a few days. Then the division of the WBCs has to be stopped in the so-called metaphase, a point in the cell-cycle when the chromosomes are condensed but before they separate into two cells. Then the cells are lysed and a drop of material is placed on a microscope slide along with a fixative chemical in order for the chromosomes to stick on the substrate. A karyotype is made of the chromosomes and a trained lab technician can then identify translocated chromosomes from the banding patterns that are formed. When a pair of translocated chromosomes is found, the samples are sent to a dedicated laboratory where chromosome sorting by flow cytometry [1] is carried out. This process relies on fluorescence signals and can sort two chromosomes at a time. When the sorted chromosomes are returned to the

lab, lab technicians use FISH (Fluorescence In Situ Hybridization) and sequencing in order to find the exact breakpoint.

This entire process usually takes more than a few months to complete, involves at least two different locations and highly trained personnel and is rather expensive. Therefore any system that can reduce the cost and time for each analysis will be of great interest both for genetic scientists and for medical doctors. In this paper we will describe such a system, which will be able to complete chromosome isolation and sorting in a small chip within a few minutes. We take advantage of the physical properties of cells and chromosomes for the purpose, therefore an investigation of these will also be presented.

## 2. Materials and methods

In order to study the physical properties of the chromosomes such as size and dielectric constant, an Atomic Force Microscope (CP-II SPM system from Veeco) working in tapping mode was used. For the dielectric constant measurements a conducting cantilever with a platinum coating from Budgetsensors (model BS-*ElectriMulti*75) [2] was used. The principle of the measurement method has been described in [3-5]. The chromosome suspension was prepared from human lymphocytes by the method described in [6]. This ensures a stable stock of chromosomes in hexylene glycol buffer from which the chromosomes can be resuspended in fixative (methanol and acetic acid, 3:1) and deposited on a substrate. Further treatment with pepsin ensured that a minimum of cell debris was present on the surface of the chromosomes.

For the isolation of WBCs from blood a method called pinched flow fractionation, first described in [7] has been used. In short the method takes advantage of the fact that small particles exiting a small channel into a large chamber will follow the streamlines passing through their center of mass. Separation can be achieved by making sure that particles of different sizes follow different streamlines that end up in different outlets. A device for the sorting of WBCs of a particular dimension corresponding to human lymphocytes from other WBCs and from smaller blood constituents such as platelets and red blood cells (RBCs) has been designed, simulated (using Comsol Multiphysics [8]) and fabricated. The fabrication process is very simple: A mould of the channel is made in SU8 2075 obtained from Microchem [9] and PDMS (polydimethylsiloxane) obtained from Dow Corning [10] is poured on the mould and cured at 65 °C for 3 hours. The PDMS cast is then removed from the SU8 mould and bonded to a pyrex wafer using a plasma asher treatment with an oxygen flow of 100 ml/min for 30 s with a power of 100 W. Inlet and outlet holes are then made on the PDMS part of the bonded chip.

After the WBCs are isolated they need to be trapped and lysed in order to extract the chromosomes. A structure inspired from [11] has been designed and fabricated for the purpose. Design considerations and results from our simulations will be presented in section 3.

## 3. Results

The first step towards a total analysis system for chromosomes (C-TAS) is to make sure that the biological matter does not stick to the surfaces of the microfluidic channels. For this purpose all surfaces have been covered with one or more layers of PEG (Polyethylene glycol) molecules. This makes the surfaces more hydrophobic, as can be seen in figure 1, where the increased hydrophobicity is visualised by a droplet of water on a pure pyrex and on a PEG surface.

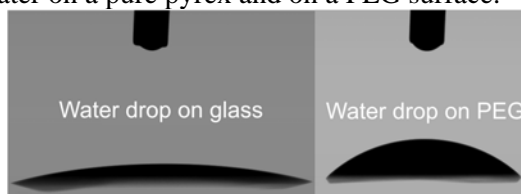


Figure 1. On a pure pyrex surface the water droplet perfectly wets the surface. When the surface is functionalised with PEG it becomes more hydrophobic.

The second obstacle towards C-TAS is the isolation of the WBCs. For this purpose the structure shown in figure 2 was designed, simulated and fabricated in PDMS. The system consists of two inlet channels, one for the blood sample containing the cells and one for a pure buffer solution, a pinched segment, where the particle solution and the buffer come into contact and the particles can be pressed towards the upper wall, and a separation chamber with several outlet channels. Through Comsol simulations on this structure and considering that we would like to separate WBCs (average diameter of 10  $\mu\text{m}$ ) from RBCs (average minimum dimension of 3  $\mu\text{m}$ ) it can be shown that for given dimensions of the pinched segment the most critical parameters for the separation are the inlet flow rate ratio as well as the relative hydraulic resistance of the channels. It was calculated that a flow rate ratio of 0.1 between the particle carrying flow (channel a) and the buffer carrying flow (channel b) is necessary for a 40  $\mu\text{m}$  wide pinched segment, as well as a hydraulic resistance which is 7 times larger for the first outlet (top left outlet E) than for the remaining five outlets.

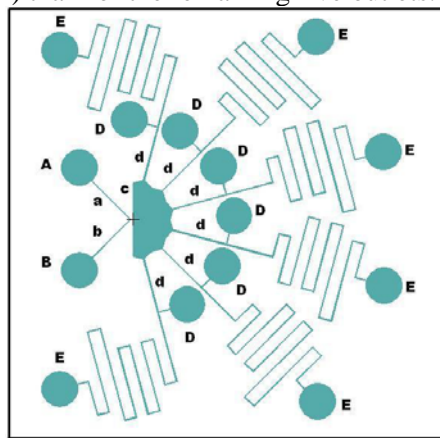


Figure 2. The chip design for the isolation of WBCs. A is the inlet for the blood, B is the inlet for the buffer, E are the long outlets (the hydraulic resistance from the separation chamber c to E is 7 times larger than the hydraulic resistance from c to the short outlets D) and d are the outlet channels. For the separation, outlet E is used for the first channel and outlets D are used for the remaining channels.

After the WBCs have been collected in the second from the top outlet D (s. figure 2) they need to be isolated and lysed. The isolation is necessary due to the inevitable changes in chromosome sizes between cells occurring when stopping the cell cycle at different points in time in the metaphase. Figure 3a shows the structure designed and simulated for the purpose. The cells entrance and exit is indicated by the two arrows. There are two different structures, a meander and a cell trap. At each intersection the cell has to choose whether to move into the trap or continue through the meander. The structure is designed in a way so that the cell will always choose to move through the trap and as it is bigger than the trap it will stop there and block access for the remaining cells. The next incoming cell will therefore pass through the first meander structure and go down the second trap instead and so on. It can be shown that the system will function best when more than 4 traps are included in the structure. Once the cells are captured, a voltage applied through electrodes placed on each side of the trap will provoke lysis, releasing the chromosomes from the cell.

The chromosomes will then be taken to the sorting part of the chip. Electrical forces (electrophoresis and/or dielectrophoresis) will be used for sorting the chromosomes. In order to find the optimal parameters an estimate of the chromosome dielectric constant, conductivity and dimensions is needed. The chromosomes were therefore imaged by AFM and the permittivity measurements were performed on several different chromosomes with cantilevers working at four different vibration frequencies. The results are shown in figure 3b and indicate that the permittivity is a constant independent on the chromosome height and the frequency of vibration, at least in the kHz range. The length of the chromosomes was in the range of 1 to 10  $\mu\text{m}$ .

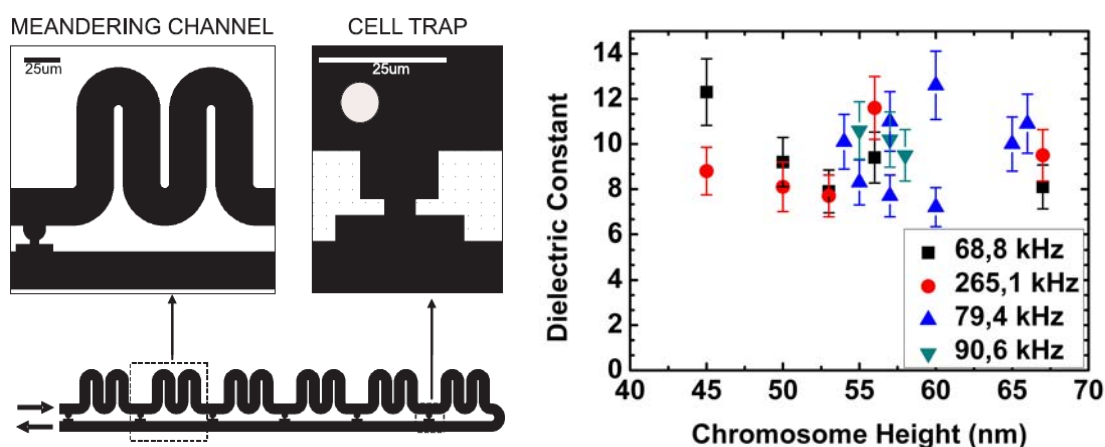


Figure 3. (a) The cell trapping structure. The cells enter and exit from the points indicated by arrows. Details of the meander and traps are also shown. (b) The measured dielectric constant of different chromosomes as a function of chromosome height for different vibration frequencies.

#### 4. Discussion and Conclusion

We have shown experimental and theoretical results relating to the fabrication of a total analysis system for chromosome translocations. By surface functionalisation with PEG, sticking of the biological matter on the channels is avoided. The sorting of the WBCs from blood can be achieved without centrifugation by a method called pinched flow fractionation. We have shown that effective separation is possible for a 40 μm wide pinched segment when the flow rate ratio is adjusted between the two inlets. A system where each outlet channel has two possible outlets has been designed and this makes it possible to tune the separation radius further.

After separation the cells are trapped in a special structure where they are lysed by help of electric fields generated by electrodes placed on each side of the traps. The extracted chromosomes are then led to the sorting chip. As electrical forces are going to be used for the sorting, it is necessary to measure the chromosomes dielectric constant and conductivity as well as their dimensions in order to be able to predict the correct parameters for the separation. The dielectric constant was measured for chromosomes of different heights and with cantilevers vibrating at different frequencies. It was shown that the dielectric constant is independent of the chromosome height as well as the frequency of the cantilever vibration (which corresponds to the frequency of the electric field for a dielectrophoresis experiment) in the range of ca. 60 – 300 kHz.

Future work will involve the experimental confirmation of our theoretical results as well as measurements of the conductivity and charge of the chromosomes.

#### References

- [1] P P. Métézeau, A A. Schmitz and G G. Frelat, *Biology of the Cell* 78, p. 31 (1993)
- [2] <http://www.nanoandmore.com>
- [3] C. Staii, A. T. Johnson and N. J. Pinto, *Nano Letters* 4 (5), p. 859, 2004
- [4] M. Bockrath, N. Markovic, A. Shepard, M. Tinkham, L. Gurevich, L.P. Kouwenhoven, M.W. Wu and L.L. Sohn, *Nano Letters*, 2(3), p. 187 (2002)
- [5] T.S. Jespersen and J. Nygaard, *Nano Letters* 5 (9), p. 1838 (2005)
- [6] W. Wray and E. Stubblefield, *Experimental Cell Research* 59, p. 469 (1970)
- [7] Masumi Yamada, Megumi Nakashima, and Minoru Seki, *Anal. Chem.* 76, p. 5465 (2004)
- [8] <http://www.comsol.com>
- [9] <http://www.microchem.com>
- [10] <http://www.dowcorning.com>
- [11] W. Tan and S. Takeuchi, *PNAS* 104 (4), p. 1146 (2007)

# Scanning conductance microscopy investigations on fixed human chromosomes

Casper Hyttel Clausen, Jacob Moresco Lange, Linda Boye Jensen, Pranjul Jaykumar Shah, Maria Ioannou Dimaki, and Winnie Edith Svendsen  
MIC—Department of Micro and Nanotechnology, Technical University of Denmark, Lyngby, Denmark

*BioTechniques* 44:225-228 (February 2008)  
doi 10.2144/000112676

*Scanning conductance microscopy investigations were carried out in air on human chromosomes fixed on pre-fabricated SiO<sub>2</sub> surfaces with a backgate. The point of the investigation was to estimate the dielectric constant of fixed human chromosomes in order to use it for microfluidic device optimization. The phase shift caused by the electrostatic forces, together with geometrical measurements of the atomic force microscopy (AFM) cantilever and the chromosomes were used to estimate a value for the dielectric constant of different human chromosomes.*

## INTRODUCTION

In recent years, the interest in micro total analysis systems ( $\mu$ -TAS) for the sorting and characterization of biological samples has increased. Considerable efforts have been put into realizing such a device, and several simple systems have already been produced (1). The devices of the current generation of  $\mu$ -TAS rely on everything from cleverly designed microfluidic flow to light or electrical fields for manipulation and detection of the samples (2). Systems that currently use electrical readout are not optimal because the physical properties (e.g., size, permittivity, conductivity) of biological samples are mostly unknown. In order to optimize these devices, the physical properties need to be measured. This limited knowledge may be due to the biological samples' rather complex structure compared with fabricated solid state samples (nanowires/nanotubes, etc.). In this context, chromosomes are interesting in that they contain a very complex architecture of DNA and proteins, and chromosomal abnormalities may result in diseases such as Turner Syndrome and leukemia among others (3,4). The physical properties of biological samples are important because they may be used in the design of micro systems that depend on electrotaxis

and subsequent analysis of biological samples. One method for the study of physical properties is scanning probe microscopy (SPM), which has proven to be a flexible method for studying different sample types, both biological as well as solid state. Several SPM methods have already been used on chromosomes. Atomic force microscopy (AFM) (topography) imaging of stained G band patterns of the chromosomes was used to investigate the possibility of obtaining better resolution of the bands (5). Other reports of SPM applications on chromosomes include near-field scanning optical microscopy measurements of the bands (6) and elasticity investigation of chromosome structure (7). One SPM method, scanning conductance microscopy (SCM), has in recent years been used to map out different properties of nano-sized particles, for example, the dielectric constant of nanoparticles of poly(ethylene oxide) (8), the conductance of carbon nanotubes and DNA (9), and trapped charges on a surface by carbon nanotubes (10). This makes SCM an interesting method for studying the electrical properties of small samples. As we have not been able to locate any reports of SCM used on chromosomes, we believe that this is the first time this method has been used on chromosomes.

## MATERIALS AND METHODS

### Principle of the Measurements

The principle and various applications of the SCM method have been well documented by M. Bockrath et al. (9), C. Staii et al. (8), and T.S. Jespersen et al. (10). The basic principle is that the tip of the AFM cantilever acts as a capacitor plate while a heavily doped Si layer with an insulating SiO<sub>2</sub> layer on top acts as the other plate. The change in phase as the tip scans the samples deposited on top of the SiO<sub>2</sub> is recorded. The data are used to estimate the dielectric constant of the sample. A sketch of the principle is shown in Figure 1.

The procedure of the SCM method used in this article is as follows: first a sample is dispersed on a SiO<sub>2</sub> surface with a backgate, as shown in Figure 1. The SPM system performs a line scan along the surface of the sample in the dynamic mode using a conducting AFM tip. The tip is then raised several tens of nanometers and a new line scan is made following the topography trace of the previous scan. During the second scan a potential is applied between the tip and the doped layer. Because of the potential the phase in the second scan is different from the phase in the first. The only external force change on the AFM tip is the change in electric force. The phase difference depends on the cantilever parameters as well as the dielectric properties of the scanned objects, as was shown by C. Staii et al. (8). It is further assumed that the tip of the AFM cantilever is a flat disk according to studies done by T.S. Jespersen et al. (10). The phase shift between the bare SiO<sub>2</sub> surface and sample is mapped out and, according to C. Staii et al. (8) and T.S. Jespersen et al., (10) is governed by

$$\Delta\phi \approx \frac{Q}{2k} \left( \frac{\partial^2 C_1}{\partial^2 z} - \frac{\partial^2 C_2}{\partial^2 z} \right) V^2,$$

(Eq. 1)



where  $\Delta f$  is the difference in the measured phase of the bare substrate and the fixed chromosomes,  $C_1$  is the capacitance between the tip and backgate without a sample lying on the  $\text{SiO}_2$ ,  $C_2$  is the capacitance between the tip and backgate with a sample lying on the  $\text{SiO}_2$ ,  $z$  is the distance between the tip and sample (lift-height),  $V$  is the potential difference between the tip and conducting layer,  $Q$  is the quality factor of the AFM cantilever, and  $k$  its spring constant. The second derivatives of the capacitances are given as

$$\frac{\partial^2 C_1}{\partial^2 z} = \frac{2 \times \pi \times r_{\text{tip}}^2 \times \epsilon_0}{(z + d / \epsilon_{\text{SiO}_2})^3} \quad (\text{Eq. 2})$$

and

$$\frac{\partial^2 C_2}{\partial^2 z} = \frac{2 \times \pi \times r_{\text{tip}}^2 \times \epsilon_0}{(z + d / \epsilon_{\text{SiO}_2} + h / \epsilon_p)^3}, \quad (\text{Eq. 3})$$

where  $r_{\text{tip}}$  is the radius of the tip,  $\epsilon_0$  the vacuum permittivity,  $d$  the thickness of the oxide layer,  $h$  the height of the particle,  $\epsilon_{\text{SiO}_2}$  the permittivity of the oxide layer, and  $\epsilon_p$  the permittivity of the particle. The value of the quality factor of the cantilever is estimated by a measurement of the resonance frequency. The tip radius is estimated by the scanning electron microscopy images, and the spring constant is estimated by measuring the deflection of the AFM cantilever caused by another cantilever with a well-defined spring constant.

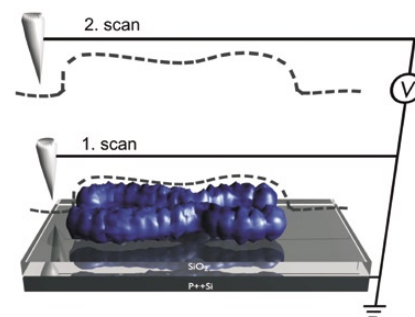
The lift-height  $z$  is estimated to be around a few tens of nanometers according to theoretical studies for optimal signal carried out by J. Colchero

et al. (11). Further, J. Colchero et al. (11) showed that the phase shift due to beam and cone of the AFM cantilever is almost constant compared to the contribution from the tip.

## Experimental Methods

Substrates were fabricated by the use of four-inch heavily p-doped silicon wafers. A 100 nm thick silicon oxide layer was grown on the substrates, the oxide on the back was removed by hydrofluoric acid (HF), and a 20 nm layer of titanium was evaporated on the backside followed by a 1000 nm layer of gold.

The suspension of chromosomes was prepared from human T-lymphocytes (Model no. ACC282; DSMZ, Braunschweig, Germany) by a variant of the method developed by Wray et al. (12). Briefly, the cells were grown in RPMI-1640 media (Model no. 61870010; Invitrogen, Taastrup, Denmark) supplemented with 10% fetal bovine serum (Model no. F9665; Sigma, Brøndby, Denmark) at 37°C and a 5%  $\text{CO}_2$  atmosphere. The cells were arrested in log-phase with 0.06  $\mu\text{g/mL}$  colcemide (Model no. D1925; Sigma) for 10 h and collected at 200 $\times g$  for 10 min. After removing the media the cells were washed once with serum-free media and collected at 200 $\times g$  for 10 min. The media was removed and the pellet was exposed to 75 mM KCl (Model no. P9327; Sigma) at 37°C, gently vortexed to resuspend the cells, and incubated at 37°C for 20 min. The cells were collected at 200 $\times g$  for 10 min and washed once with hexylene glycol buffer (1.0 M hexylene glycol [Model no. 112100; Sigma], 0.5 mM  $\text{CaCl}_2$  [Model no. 21115; Sigma], and 0.1 mM PIPES buffer at pH 6.7 [Model no. 80637; Sigma]) at 37°C before resuspending the cells in fresh hexylene glycol buffer. The final chromosome stock solution was obtained by forcing the suspension through a 23 G needle and purified by collecting unlysed cells at 200 $\times g$  for 10 min. To deposit chromosomes on a substrate, the chromosomes were collected at 7500 $\times g$  for 20 min and resuspended in fixative (3 volumes methanol [Model no. 179337; Sigma] + 1 volume acetic acid [Model no. 320099; Sigma]). The



**Figure 1. The principle of the SCM method.** First a topography line scan is made, then the tip is lifted and another line scan is made with a potential difference between the AFM tip and the backgate.

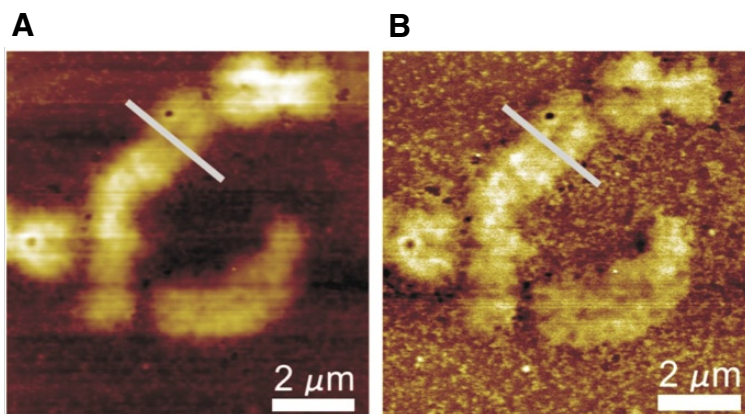
chromosomes were finally deposited on the substrate by droplets and allowed to dry out at room temperature. The final resuspension in methanol/acetic acid was necessary in order to get sufficient and even spreading of the chromosomes. Using droplets of the hexylene glycol buffer resulted in a “pile” of chromosomes with salt residues on top because of the slow evaporation of hexylene glycol.

The scanning probe microscopy system used was a CP-II SPM system from Veeco (Breda, The Netherlands). AFM cantilevers were obtained from Budgetsensors (either model BS-ElectriMulti75 or BS-ElectriTap300; Nanoandmore, Wetzlar, Germany) (13), which both have a platinum coating. Analysis of the obtained data from the SPM system was carried out using the “SPIP” software (Image Metrology, Horsholm, Denmark) (14).

## RESULTS AND DISCUSSION

The SPM images were obtained with a resolution of 512  $\times$  512 pixels, with a scan rate of 0.6 Hz, a potential difference of 2 V, and lift-height of 30 nm. The topography images were obtained by non-contact scans.

Topography and lift-mode phase images of different chromosomes were obtained under ambient conditions. The phase shift and the corresponding chromosome height for each chromosome were obtained by taking the average across the middle of two of the arms of the chromosome (10



**Figure 2. Topography and lift-mode phase images of different chromosomes.** (A) topography image of chromosomes dispersed on a SiO<sub>2</sub> surface with backgate; (B) phase shift image in lift-mode of the same chromosomes as in (A). The gray lines mark the line profiles across the chromosomes.

pixel to each side of the line profile [the gray line] in Figure 2, A and B). Using Equations 1, 2, and 3 the dielectric constant was estimated for each of the chromosomes. The chromosomes were investigated with different cantilevers with relative uniform resonance frequencies ( $\pm 15$  kHz). Five of the chromosomes were mapped out twice with a cantilever with a relative higher (around three times higher or 265.1 kHz) resonance frequency. This was done to check if the dielectric constant changed due to the frequency of the cantilever.

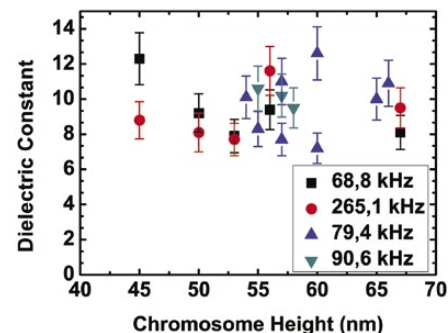
Figure 3 shows the different dielectric constant obtained for different chromosomes with respect to their height. The error bars are calculated on the background of measurement uncertainties of the spring constant, the quality factor, the tip radius, and the oxide thickness. These have been calculated to be  $\pm 5\%$  to  $\pm 8\%$ . Uncertainty values found for the lift-height and the sample height were  $\pm 1\%$ , and for the potential difference an uncertainty of  $\pm 5\%$  was chosen.

As Figure 3 shows, the value for the dielectric constant is  $10 (\pm 4)$ . Moreover the dielectric constant does not seem to vary with the chromosomes' height or the cantilever. Neither does the dielectric constant seem to vary with cantilever frequency. The flat curve of the dielectric constant for different chromosome height indicates that no artifacts influence the measurements. The spread in the values of the

dielectric constant can be contributed to different effects. First of all, a chromosome is not a uniform material, rather it is composed of a complex mixture of proteins and DNA, and the dielectric constant may depend on the DNA-protein ratio at the point of measurement. This could give rise to the variation in the dielectric constant. Another thing that will influence the result is that the tip is not exactly flat but rather a bit curved. But according to researchers C. Staii et al. (8) and T.S. Jespersen et al. (10), who have reported good agreement between this assumption (flat tip) and experimental observations when investigating nanoparticles, this does not seem to be the obvious case. Finally, the sample preparation may also affect the chromosomal integrity, which could influence the measured dielectric constant. For example, the chromosomes' suspension will contain other biological material; the layer is not uniform and the layer thickness of the material is small (around 5 nm) compared with the chromosomes, making it hard to make a good prediction of the impact on the measured data.

### Conclusion

We have used SCM to investigate electrical properties of chromosomes fixed on a surface. We have estimated a value of the dielectric constant of the fixed chromosomes to be around 10. This was done by estimating the



**Figure 3. Measured dielectric constant of different chromosomes as a function of the height of the chromosome in question.**

properties of the AFM cantilever (quality factor, spring constant, and tip radius) and from the measured phase shift. We also used the assumption that the tip and surface act as a parallel plate capacitor. By these assumptions we have estimated a value of the dielectric constant of the fixed chromosomes, which was found to be around 10. Future studies will compare the influence of different preparation methods on the dielectric constant and include tests of this method in liquid. This work was guided by our interest in automated microsystems for chromosome analysis, which has led us to estimate the dielectric constant of chromosomes for later electric manipulation. It is believed that this method in the future can be used to characterize different biological samples and that the result will be used in design of future devices for biological sample detection.

### ACKNOWLEDGMENTS

*The authors would like to thank our colleagues for stimulating discussions. This work is supported by the Lundbeck Foundation.*

### COMPETING INTERESTS STATEMENT

*The authors declare no competing interests.*



## Short Technical Reports

### REFERENCES

1. Breslauer, D.N., P.J. Lee, and L.P. Lee. 2006. Microfluidics-based systems biology. *Mol. Biosyst.* 2:97-112.
2. Dittrich, P.S., K. Tachikawa, and A. Manz. 2006. Micro total analysis systems. latest advancements and trends. *Anal. Chem.* 78:3887-3907.
3. C. E. Ford, K. W. Jones, P. E. Polani, J. C. Dealmeida, and J. H. Briggs. 1959. A sex-chromosome anomaly in a case of gonadal dysgenesis (Turner's syndrome). *Lancet* 1: 711-713.
4. Nowell, P.C. and D.A. Hungerford. 1960. Minute chromosome in human Chronic granulocytic leukemia. *Science* 132:1497.
5. Tamayo, J. 2003. Structure of human chromosomes studied by atomic force microscopy Part II. Relationship between structure and cytogenetic bands. *J. Struct. Biol.* 141:189-197.
6. Moers, M.H.P., W.H.J. Kalle, A.G.T. Ruiter, J.C.A.G. Wiegant, A.K. Raap, J. Greve, B.G. De Grooth, and N.F. Van Hulst. 1996. Fluorescence *in situ* hybridization on human metaphase chromosomes detected by near-field scanning optical microscopy. *J. Microsc.* 182:40-45.
7. Nomura, K., O. Hoshi, D. Fukushi, T. Ushiki, H. Haga, and K. Kawabata. 2005. Visualization of elasticity distribution of single human chromosomes by scanning probe microscopy. *Jpn. J. Appl. Phys.* 44:5421-5424.
8. Staii, C., A.T. Johnson, Jr., and N.J. Pinto. 2004. Quantitative analysis of scanning conductance microscopy. *Nano Lett.* 4:859-862.
9. Bockrath, M., N. Markovic, A. Shepard, M. Tinkham, L. Gurevich, L.P. Kouwenhoven, M.W. Wu, and L.L. Sohn. 2002. Scanned conductance microscopy of carbon nanotubes and 1-DNA. *Nano Lett.* 2:187-190.
10. Jespersen, T.S. and J. Nygård. 2005. Charge trapping in carbon nanotube loops demonstrated by electrostatic force microscopy. *Nano Lett.* 5:1838-1841.
11. Colchero, J., A. Gil, and A.M. Baró. 2001. Resolution enhancement and improved data interpretation in electrostatic force microscopy. *Phys. Rev. B* 64:245403-245414.
12. Wray, W. and E. Stubblefield. 1970. A new method for the rapid isolation of chromosomes, mitotic apparatus, or nuclei from mammalian fibroblasts at near neutral pH. *Exp. Cell Res.* 59:469-478.
13. www.nanoandmore.com
14. www.imagemet.com

Received 12 September 2007; accepted 16 October 2007.

Address correspondence to Casper Hyttel Clausen, MIC-Department of Micro and Nanotechnology, Technical University of Denmark, Building 345 East, DK-2800 Kgs. Lyngby, Denmark. e-mail: chc@mic.dtu.dk

To purchase reprints of this article, contact: Reprints@BioTechniques.com

THINK  
RECORD  
DEVELOP

#### NOTEBOOKS TO RECORD YOUR WORK FOR PATENT APPLICATION.

Scientific Notebook Co. offers the broadest line of high-quality laboratory notebooks. Available in a range of configurations to meet the requirements of any individual laboratory, engineering department or research facility.



Call **1-800-537-3028**  
or try our web site at **www.snco.com**

# ERRATA

# ERRATA

Figure 3.13 in the chapter doesn't contain scale bars and pointers to cells and pores. Since the figure in the chapter has already been published, we include this figure in the appendix to show the difference between cells and pores. We have also added scale bars to highlight the size of the cells. On day 3, typically the cells start clumping and they overlap as a result making them difficult to count via image analysis techniques. As a result, CFSE staining technique was used to quantify their growth and assess the proliferation quality. The cytoplasm of the cell highlight in the inset has expanded and can be clearly seen that the cell has reached the size of 18  $\mu\text{m}$ . This is visual confirmation that the cell is undergoing cell cycle and proliferating.

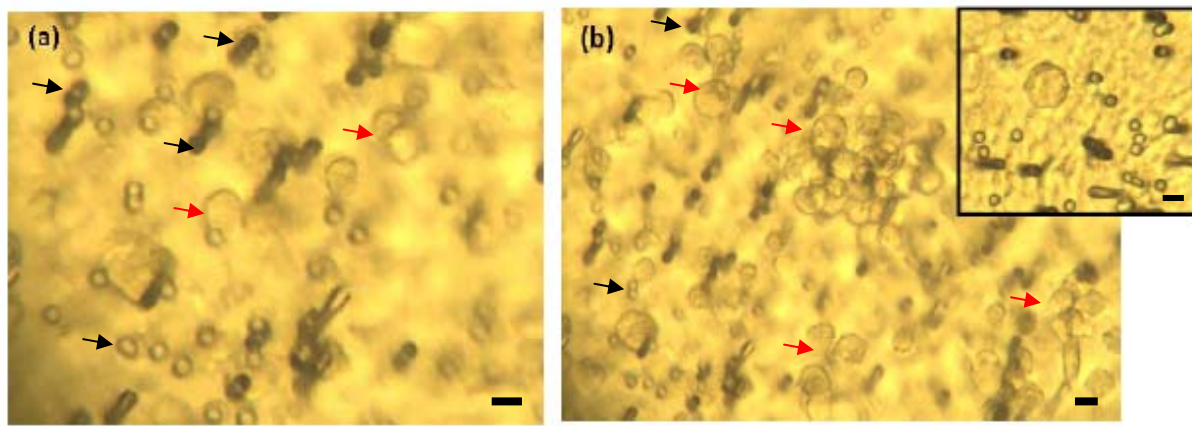


Figure 3.13: FISHprep culture (a) Day 0 (b) Day 3. (Red arrows point to cells, Black arrows indicate pores and all the scale bars are 10  $\mu\text{m}$ ). As can be seen in the inset picture, the diameter of the cell has expanded to 16  $\mu\text{m}$ , which happens when the cytoplasm expands during mitosis and cells also tend to grow in clumps as in (b).